

Site- and Stereo-selective Functionalization of Carbohydrate Hydroxyl Groups Using Chiral Catalysts

By

Daniel Abraham Glazier

A dissertation submitted in partial fulfillment of the requirements for the degree of

Doctor of Philosophy

(Chemistry)

at the

UNIVERSITY OF WISCONSIN-MADISON

2019

Date of final oral examination: 10/7/2019

The dissertation is approved by the following members of the Final Oral Committee:

Weiping Tang, Professor, Pharmacy

Jennifer Schomaker, Professor, Chemistry

Sandro Mecozzi, Professor, Pharmacy

Jennifer Golden, Assistant Professor, Pharmacy

Table of Contents

Chapter 1: The Chemical Synthesis and Stabilization of RNA For Therapeutic ASOs and siRNAs

1.1	Introduction.....	2
1.2	Solid Phase Oligonucleotide Synthesis.....	4
1.2.1	Phosphoramidate Coupling Cycle.....	4
1.2.2	Solid Support Chemistry and Linkers.....	6
1.2.3	Phosphoramidite Synthesis.....	7
1.3	Ribose Modifications.....	8
1.3.1	2' Functionality.....	8
1.3.2	Bridged and Locked Nucleic Acids (BNA and LNA).....	11
1.3.3	5' Methyl Modification.....	14
1.3.4	5' Phosphonates.....	15
1.4	Backbone Modifications.....	17
1.4.1	Phosphorothioate Diesters.....	17
1.4.2	Other Backbone Modifications.....	21
1.5	Conclusion.....	23
1.6	References.....	25

Chapter 2: Stereoselective Acylation of Lactols

2.1	Introduction.....	29
2.2	2,3,4,6-Tetra-deoxy-4-Amino Sugar Synthesis.....	31
2.3	Attempts to Develop a Dynamic Kinetic Enantioselective Acylation (DKEA) for Coumarin Derived Lactols.....	35
2.4	DKEA of 2-Chromanols.....	37
2.5	References.....	42

Chapter 2 Supporting Information.....	44
Chapter 3: Site-Selective Functionalization of Carbohydrates	
3.1 Introduction.....	102
3.2 Site-Selective Acylation of Carbohydrate <i>Trans</i>-1,2-Diols.....	104
3.3 Attempts to use Chiral Catalysts to Site-Selectively Functionalize Carbohydrate <i>Trans</i>-1,2-Diols.....	115
3.4 Site- and Stereo-Selective Phosphoramidation of Carbohydrate <i>Trans</i>-1,2-Diols.....	116
3.5 Conclusions and Future Work.....	122
3.6 References.....	123
Chapter 3 Supporting Information.....	125
Chapter 4: Density Functional Theory Investigation of a novel Hetero-[5+2] Cycloaddition of Oxidopyrylium Ylide with Cyclic Imines	
4.1 Introduction.....	192
4.1.1 Oxidopyrylium [5+2] Cycloadditions.....	192
4.1.2 Computational Investigations of Oxidopyrylium [5+2] Cycloadditions.....	196
4.2 Methods.....	198
4.2.1 A Qualitative Explanation of Density Functional Theory (DFT).....	198
4.2.2 DFT Investigation Work-Flow.....	199
4.3 Results.....	201
4.4 Conclusion.....	204
4.5 References.....	205
Chapter 4 Supporting Information.....	207

1. The Chemical Synthesis and Stabilization of RNA For Therapeutic ASOs and siRNAs

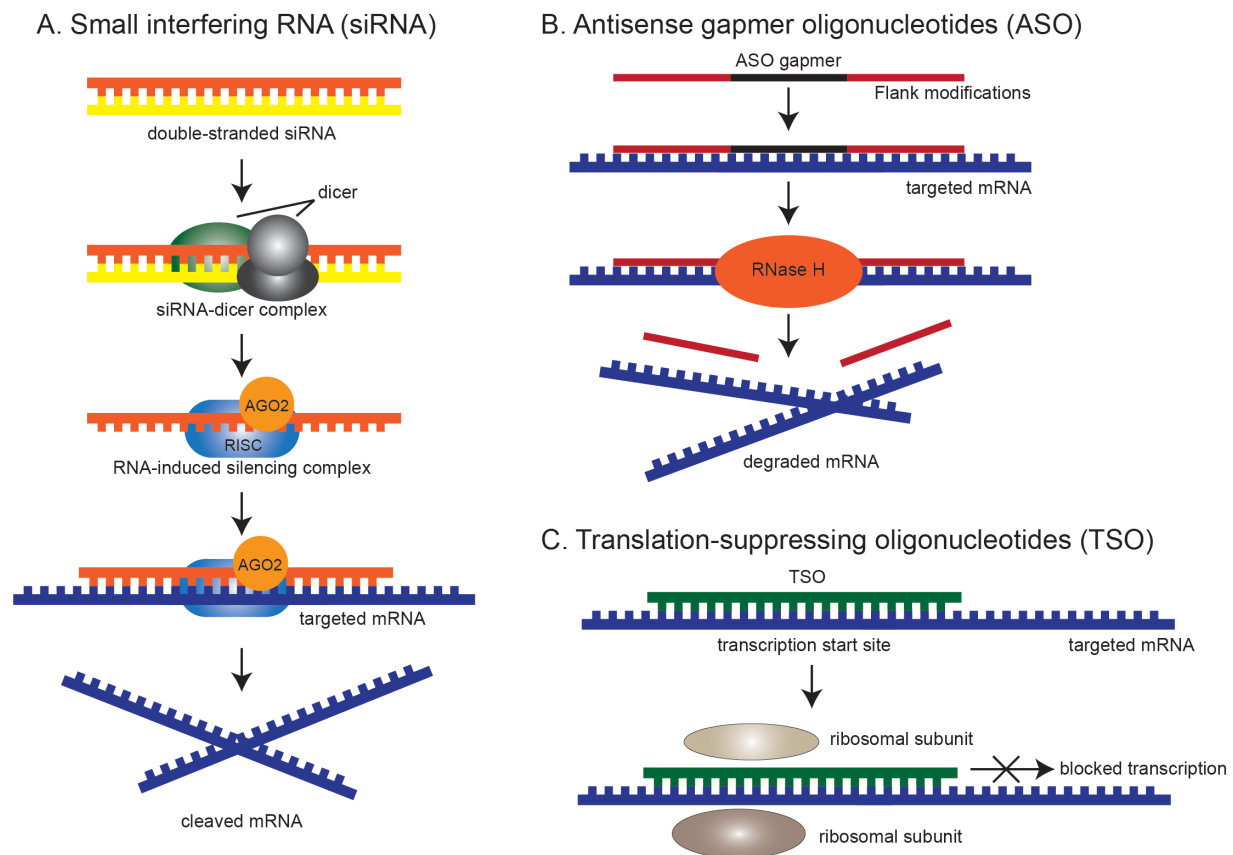
1.1. Introduction

RNA plays a myriad of roles in the body including the coding, decoding, regulation and expression of genes. More recently RNA oligonucleotides (ONs) have garnered significant interest as therapeutics via antisense ON RNA (ASO) or small interfering RNA (siRNA) strategies for the treatment of diseases ranging from hyperlipidemia to HCV and others. Since the first demonstration that ASOs could decrease protein translation in 1978, significant effort has been directed towards improving both the chemical synthesis of and desired therapeutic properties of ONs.^[1] The discovery of siRNA 20 years ago drove further interest in RNA chemistry and led to a Nobel prize. RNA presents numerous challenges as both a synthetic target and a potential therapeutic. RNA is inherently unstable, it is difficult to deliver into cells, and is potentially immunogenic by itself or upon modification. Despite these challenges, multiple RNA based drugs have been approved by the FDA, starting with the ASO Fomivirsen in 1998. The first siRNA drug, Patisiran, was approved for sale in 2018. Typically, these therapeutic ONs are ~22 nucleotides long, but there are exceptions. This review will focus on the chemical synthesis of RNA and how chemical modifications of the ribose units and of the phosphodiester (PO) backbone affect the hybridization ability, nuclease stability, and other properties of ONs.

First, however, some of the different mechanisms by which ASOs and siRNA act must be explained so that the differences in desired properties and tolerated modifications can be understood (**Scheme 1.1**). Both ASOs and siRNAs have the potential to function in a catalytic manner, which is a significant departure from the normal small molecule paradigm that acts in a stoichiometric manner.

siRNAs are double stranded or hairpin RNAs, 20-24 base pairs long, that silence genes via repression of transcription (**Scheme 1.1A**). Single stranded siRNAs (ss-siRNAs) have also recently been developed. Typically, in nature a long dsRNA or hairpin RNA is cut by Dicer into a siRNA duplex. Therapeutic siRNAs are not reliant on Dicer, but short hairpin RNAs (shRNAs) need Dicer to cleave them into active siRNA. The siRNA duplex is loaded into the RISC

complex and is unwound into a sense strand, which is discarded, and a guide strand, which is retained in the RISC complex. The guide strand needs to have a more flexible 5' end to be preferentially retained by RISC. When the guide strand in the RISC complex finds a mRNA strand that is perfectly complimentary, a component of the RISC complex named AGO2 cleaves the mRNA to silence the gene. Mammalian cells have receptors that recognize dsRNA, which is often a hallmark of viral infection and because siRNAs are double stranded they can elicit an immune response.^[2]



Scheme 1.1. siRNA and ASO mechanisms.

ASOs are single stranded ONs that modulate gene expression via multiple mechanisms. Gapmers are ASOs with an 8-10 nucleotide DNA or DNA mimic “gap” in-between RNA end caps (**Scheme 1.1B**). This motif binds to the target mRNA strand and then recruits RNase-H to cleave the target mRNA strand leading to reduced protein expression. Another ASO mechanism is to bind to target strands to sterically block translation or other cellular processes (**Scheme 1.1C**).

Via this mechanism they can regulate naturally occurring miRNA sequences by blocking the ability of Dicer and other required proteins to cleave pre-miRNA into the active miRNA. By regulating miRNA you can regulate the multiple proteins that miRNA regulates. ASOs can also modulate the splicing of pre-mRNA into mRNA, thereby altering the protein isomer expressed.

1.2 Solid Phase Oligonucleotide Synthesis

1.2.1 Phosphoramidate Coupling Cycle

Modern ON synthesis is completed via a four step cycle on solid support in an automated ON synthesizer column (**Scheme 1.2**).

Step 1: Deblocking

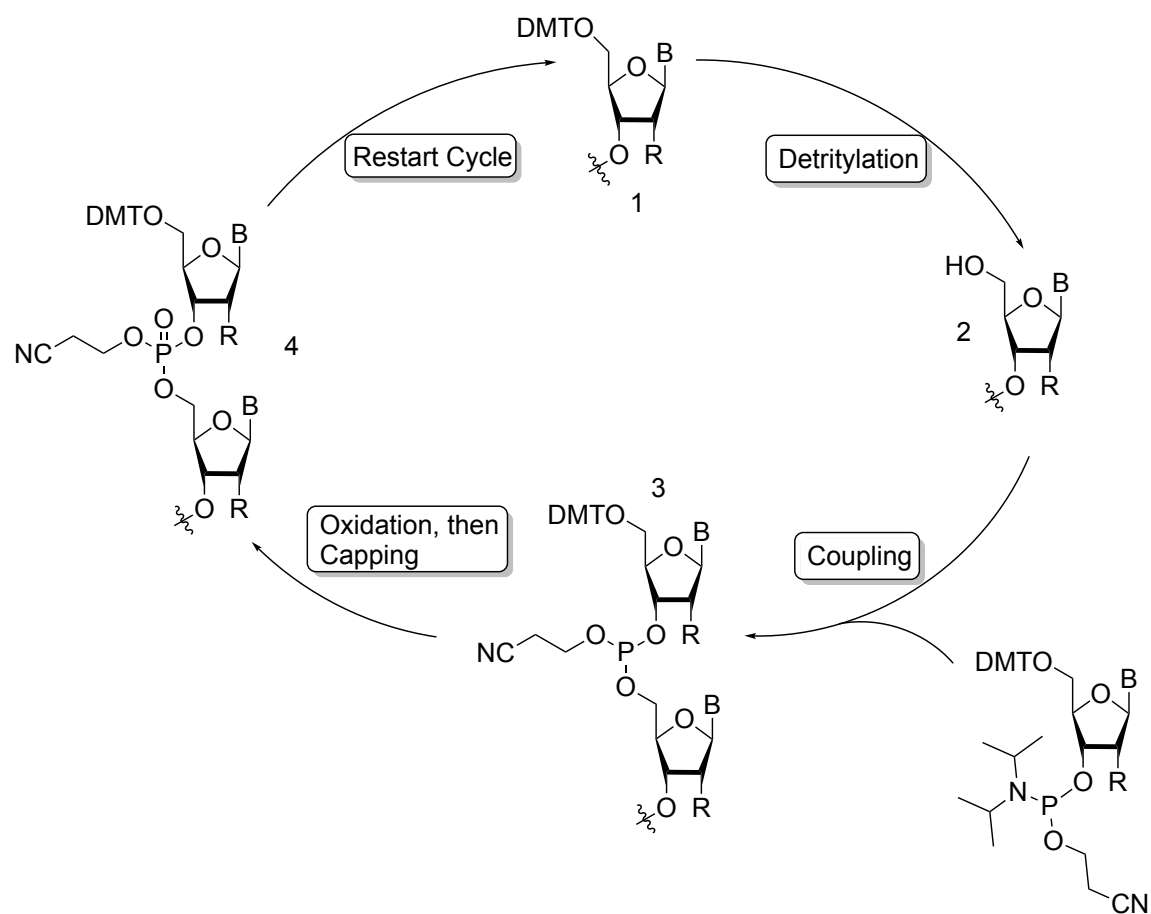
The cycle typically starts at position 1 in **Scheme 1.2** with a 5'OH tritylated nucleotide chain. The trityl group is removed, which deblocks the 5'OH. This deblocking step commonly uses dichloroacetic acid (DCA) or trichloroacetic acid (TCA) in DCM or another non-polar solvent (position 2 **Scheme 1.2**). Deblocking that uses strong acids or occurs for extended periods of time can lead to depurination, which is one of the limiting factors affecting the maximum length of oligonucleotides that can be chemically synthesized.^[3]

Step 2: Coupling

After deblocking, the free 5'OH is ready to be coupled to the next nucleotide in the desired sequence. Typically, a nucleoside bearing a 2-cyanoethyl protected phosphoramidite on the 3'OH is used as a coupling partner. Coupling is mediated by an activator, such as an acidic azole or a similar compound. The azoles and 2-cyanoethyl phosphoramidites are briefly mixed in the ON synthesizer tubing before entering the packed column to generate activated phosphoramidites. This mixing promotes protonation of the phosphoramidite nitrogen to generate a good leaving group. The activated phosphoramidate must be present in large excess compared to the number of growing ON chains in order to have a high coupling efficiency. Successful coupling yields an unstable phosphite triester (position 3, **scheme 1.2**).

Step 3: Capping

Following coupling, the chains that were not coupled successfully (0.1-1%) need to be capped so that their free 5'OH groups do not react with later phosphoramidate coupling partners, which would yield n-1 deletions that will be difficult to separate from the desired ON. Additionally, the O6 position of guanosine can rarely react with activated phosphoramidates. Oxidation with iodine and water can also lead to depurination at these sites.^[4] Capping is usually accomplished with NMI and acetic anhydride. These reagents acylate the remaining free 5'OHs, prevent those chains from growing and remove the O6 guanosine phosphoramidite modification.



Scheme

1.2. Modern solid supported ON synthesis cycle.

Step 4: Oxidation

The phosphitetriesters must be oxidized to phosphatetriesters. This is accomplished with iodine in water in the presence of a weak base. TBHP and other reagents can be used for the oxidation in anhydrous solvents.

Deprotection and Cleavage

The previous four steps are repeated until the desired sequence is achieved. The ONs can be left with DMT on the 5'OH or it can be capped with a non-nucleoside phosphoramidite. This phosphoramidite can be a hydrophilic, hydrophobic or UV active moiety, or even a biologically active one such as biotin depending on the desired properties. The oligonucleotides are cleaved from the solid support and the phosphatetriesters and any N-acyl protected bases are deprotected in the presence of a weak base, such as ammonium hydroxide or methyl amine to give the free ON. The ONs are then purified and characterized.

1.2.2 Solid Support Chemistry and Linkers

The two most frequently used solid supports are controlled pore glass and macroporous polystyrene. The pore size of these materials affects the overall length of the ONs that can be synthesized on them. These materials must be amine functionalized to react with the linkers.

Traditionally the linker used is a 3'O succinate functionalized 5'OH DMT protected nucleoside that also serves as the first nucleoside in the desired sequence (**Figure 1.1A**). While easy to synthesize with common reagents, this method requires the synthesis of a different linker for each possible nucleoside one would want at the beginning of the sequence. Considering the number of 2' modifications and base modifications that are commonly used, this can quickly expand the number of necessary linkers.

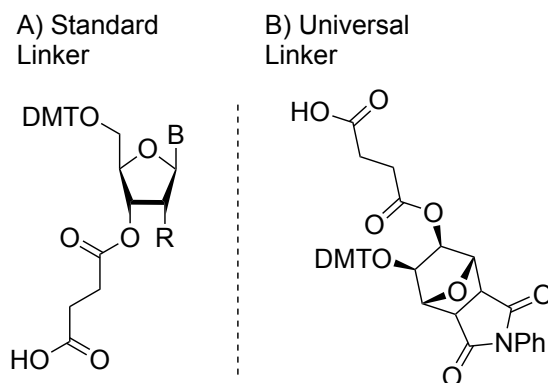
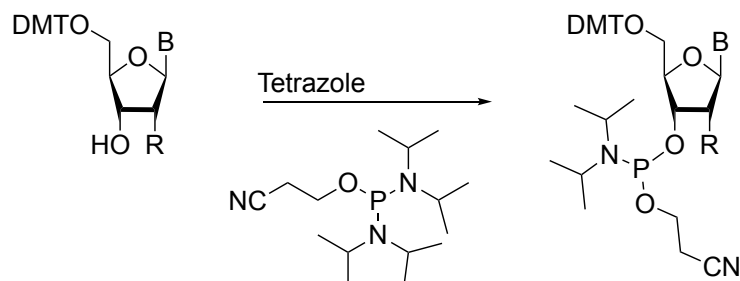


Figure 1.1. Linkers to anchor the ON chain to the solid support.

To overcome this problem, universal linkers have been developed. Universal linkers contain a DMT protected OH group that the ON can be grown off and are cleaved under conditions identical to traditional linkers to reveal a second OH group that attacks the 3' phosphate at the start of the ON and then falls off the chain (**Figure 1.1B**).^[5] Both linker types are commonly used today, along with other linkers, such as fluorophores, that impart functionality to the ON chain.

1.2.3 Phosphoramidite Synthesis

Phosphoramidites have become the chosen coupling partner for the solid-state synthesis of ONs because of their advantages over P(V) coupling reagents like chloro-phosphate diesters. These advantages arise from their stability under neutral and mild basic conditions, which makes them easy to store and handle, unlike chloro-phosphate diesters. At the same time, they become quite reactive in the presence of acid allowing chemists to turn them into reactive electrophiles on demand. Phosphoramidites can be prepared in a variety of ways from protected nucleosides, and common phosphoramidites are commercially available. The most tractable method for the synthesis phosphoramidites is shown in **Scheme 1.3**. A protected nucleoside reacts with a phosphordiamidite, typically 2-cyanoethyl N,N,N',N'-tetraisopropylphosphordiamidite, in the presence of a weak acid to yield a nucleoside phosphoramidite.^[6] This method is preferred because other methods typically involve unstable reagents, such as phosphorochloridites.



Scheme 1.3. Synthesis of 3' nucleoside phosphoramidites.

1.3 Ribose Modifications

With the general methods for the solid phase synthesis of ONs covered, it is now time to consider modifications to the ribosides. Modifications of ribose can increase the activity of ASOs and siRNAs in two primary ways. They can increase the binding to a target ligand, such as the target RNA strand for ASOs, or they can impart nuclease resistance to the ON allowing it to be active for a longer period of time.

1.3.1 2' Functionality

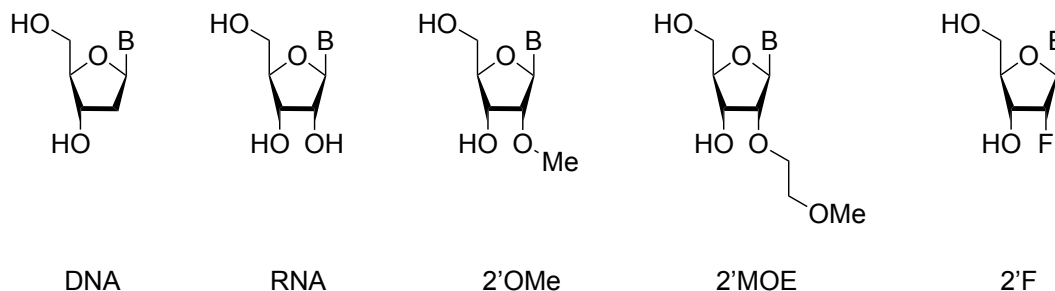


Figure 1.2 2' functionalities commonly found in ASOs and siRNA.

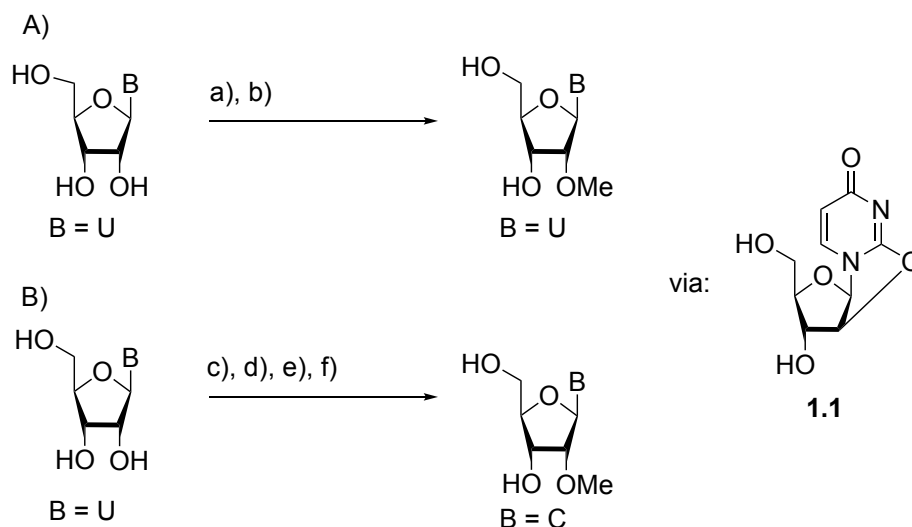
The synthesis of RNA is accomplished by using nucleoside phosphoramidites with 2'OTBS or 2'OTOM (TBSOCH₂O) can easily be removed in the presence of fluoride. Since RNA is too unstable to be used as a therapeutic agent for ASO or siRNA strategies, numerous ribose modifications have been developed (**Figure 1.2**). The first generation ASOs actually used unmodified DNA^[1b], but it became readily apparent that while DNA is more stable than RNA in the presence of endogenous exo- and endonucleases in the body, it is still rapidly degraded.

This realization led to the development of other ribose modifications to stabilize ONs. However, DNA is still used in some ASOs, such as ASO gapmers.^[7]

To further improve nucleotide stability and activity, other 2' modifications were developed. Like the 2-deoxy modification, the 2'OMe modification occurs naturally in the body. 2'OMe RNA has multiple advantages over RNA and DNA, such as improved ASO binding affinity, improved nuclease resistance and reduced immune stimulation.^[8] The stability is on the order of 0.2 °C - 0.8 °C ΔT_m per modified nucleotide 2'OMe:RNA duplex / DNA:RNA duplex of the same sequence for uridine.^[9] The appealing properties of 2'OMe RNA inspired researchers to extensively test 2'O-alkyl RNAs to determine the optimal alkyl substituent. ^[9, 10] Of the tested alkyl substituents, 2'-O-methoxyethyl (2'-MOE)^[11] proved to be one of the best modifications for increased nuclease resistance and higher binding affinities for ASOs (0.9 °C - 1.7 °C ΔT_m).^[12, 13] The approved antisense drug Kynamro and numerous candidates currently in clinical trials feature 2'MOE RNA, making it one of the most successful ribose modifications. 2'OMe and 2'MOE are somewhat interchangeable modifications in ASOs, however, 2'MOE is more common in ASOs than 2'OMe. 2'OMe is significantly more common in siRNAs compared to 2'MOE because the guide strand is considerably more sensitive to modification, and the 2'MOE modification is a greater deviation from natural RNA.^[14, 15] 2'MOE is also absent from the sense strands of siRNA. In fact, a full 2'MOE sense strand results in a completely inactive siRNA, whereas the full 2'OMe strand is active.^[13] This is thought to occur because the siRNA associates with the RISC complex before strand dissociation. If the sense strand is too difficult to remove, it can render the siRNA inactive.^[16] Interestingly, alternating DNA/2'MOE RNA motifs resulted in an active sense strand.^[13]

ON chemists do not usually need to concern themselves with the synthesis of 2'OMe and 2'MOE nucleosides because both the functionalized RNA monomers and the functionalized phosphoramidates are commercially available from various vendors. However, if the need arises to synthesize a 2'OMe or 2'MOE nucleoside that is not commercially available, these nucleosides are easily synthesized. For Adenine and Cytosine, protecting groups are not

needed for the ribose OHs, because the 2'OH is the most reactive hydroxyl of ribonucleosides in the presence of a strong base such as NaH or NaHMDS. Selectivities of up to 5:1 2'/3' have been reported with overall yields around ~25% using iodomethane as the methylating reagent.^[17] For guanosine disilyl protecting group MDPSCl₂ is needed to protect the 5' and 3' OHs to obtain the 2' functionalized product using chloromethane as the methylating reagent.^[18] Iodomethane can be used if the guanosine is protected. Carbonates can induce the urea O of uracil to attack the C2' position resulting in compound **1.1** (**Scheme 1.4A**). Mg(OCH₃)₂ can be used to ring open **1.1** to give 2'O methyl uridine.^[19] Uridine can be converted into 2'O methyl cytidine in four steps (**Scheme 1.4B**).^[20] 2'MOE nucleosides can be synthesized using similar strategies.



Scheme 1.4 Synthesis of 2'OMe nucleosides via uracil ring closure. a) (C₆H₅O)₂CO, NaHCO₃; b) Mg(OCH₃); c) (CH₃CO)₂O, DMAP, pyridine; d) tetrazole, TsCl, diphenylphosphate, pyridine; e) NH₄Cl, KOH, Et₃N, MeCN/H₂O; f) NH₃, MeOH.

2'F nucleosides also stabilize ASO binding ($\Delta T_m \sim 2.5$ °C per modified nucleotide).^[21] Additionally the 2'F modification is the best 2'OH mimic that's been developed, in terms of size and charge. This makes the 2'F a particularly useful modification for RNAi guide strands since it can help the ON bind to the RISC complex.^[22] The 2'F modification over winds the ON, resulting in more stacking and a higher T_m. This phenomena leads to full 2'F RNA guide strands having reduced activity.^[23] Fortuitously, the 2'OMe modification under winds the ON, resulting in less stacking

and a higher T_m . While full 2'OMe guide strands are inactive, strands that alternate 2'F and 2'OMe nucleotides are well tolerated.^[23, 24] However, more complex patterns, such as stretches of 2'OMe or 2'F, can lead to better structural tuning and many clinical compounds feature more complex patterns.^[25] It should be noted that the RNAi sense strands can be modified more extensively than the guide strand so the optimal modification pattern and density for the guide and sense strands will be different. ^[26]

Similar to the 2'OMe and 2'MOE modified nucleosides, 2'F modified nucleosides are commercially available from multiple vendors. Nonetheless, 2'F nucleosides are easily synthesized in 2-3 steps. 2'F uridine can be synthesized by ring opening intermediate **1.1** using HF in dioxanes.^[27] As with the 2'OMe nucleosides, 2'F uridine can be converted to 2'F cytidine in four steps.^[28] The Chemical synthesis of 2'F guanosine and adenosine is difficult, but 2'F uridine is easily converted to 2'F guanosine and adenosine using enzymatic catalysis.^[29]

1.3.2 Bridged and Locked Nucleic Acids (BNA and LNA)

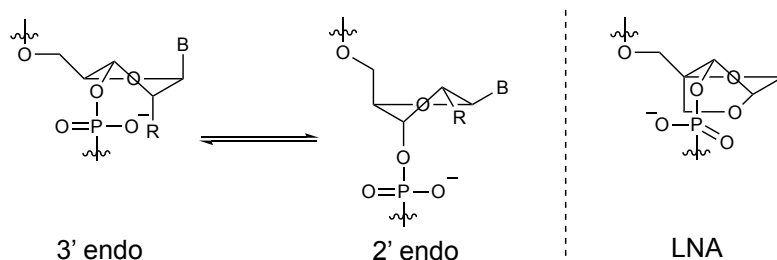


Figure 1.3 Ribose pucker. The 3' endo configuration favors the formation of α -helices. This configuration can be locked in by using a linker between the 4'C and 2'O.

Further modification of ribose can increase T_m more than simple 2' modifications. Both 2'OMe and 2'F favor the 3' endo conformation leading to α -helices (A-DNA) (**Figure 1.3**).^[30] By locking the ribose in the 3' endo configuration with a linker between the 4'C and 2'O T_m should increase even more. These locked nucleic acids (LNA, also called bridged nucleic acids or BNA) can significantly increase binding affinity to a target RNA (ΔT_m 1.5 - 6 °C typically per modified nucleotide RNA-RNA, but up to 10 °C has been reported), while also imparting nuclease resistance to the ON.^[31, 32] In general, LNAs are found in ASOs and not siRNAs because the

guide strand must be separated from the sense strand to function in the RISC complex. Thus, over stabilizing the siRNA double strand can lead to lower activity as mentioned previously. Additionally, the guide strand must be somewhat flexible, especially towards the 5' end, so modifications that rigidify the strand too much can be detrimental to RNAi activity.^[33] LNAs can increase binding affinity to such a high degree that ASOs shorter than 20-mers can be potent therapeutics if an appropriately specific sequence can be found; for instance, Miravirsen is a 15-mer ASO in phase II clinical trials with 8 LNA units and 7 DNA units. Additionally, it has been shown that an ASO 8-mer comprised of LNA can disrupt an entire family of miRNA by targeting a common seed sequence of the pre-miRNA, inhibiting their maturation.^[34]

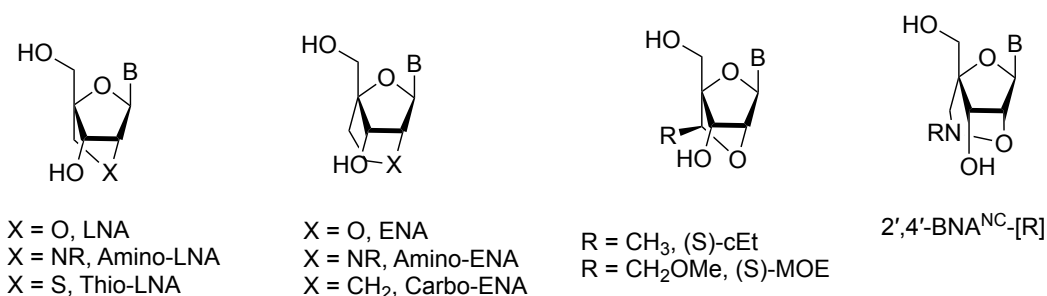
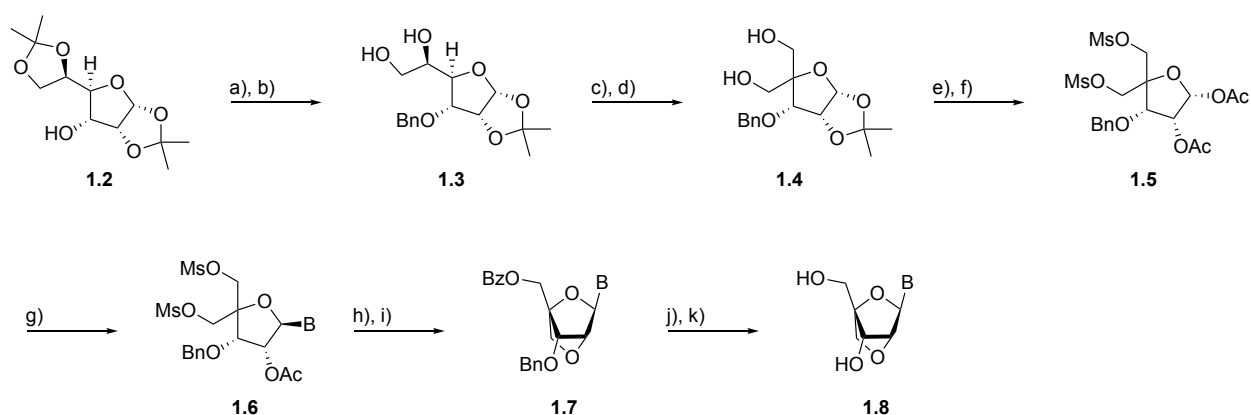


Figure 1.4 Selected BNA modifications.

The most common bridging chemistry is methylene, but a wide variety of linkers have been studied (**Figure 1.4**). The different linkers that have been tested feature different carbon chain lengths, up to propyl, hetero-atoms in place of C in the linkers, and branches at both the C4' and C2' ends. Additionally, some BNAs replace the C2'O with S, NR or CR₂. Most BNAs exhibit similar ΔT_m per BNA modification ($\Delta T_m \sim 5$ °C). However, this does not mean that all BNA modifications are interchangeable. For instance, ONs with one 2',4'-BNA^{NC}-[NMe] or -[NBn] modification exhibit increased T_m (+1 °C) for the binding to RNA strands and decreased ΔT_m (-1 and -2 °C respectively) for the binding to DNA when compared to native RNA strands. This indicates that these modifications can be used to synthesize RNA selective ONs. The standard methylene LNA modification increases the T_m for both RNA and DNA strands.^[35] Another noteworthy modification is the “constrained ethyl” (S)-cEt modification, because (S)-cEt modified ASOs display improved potency compared to standard methylene LNA without any increase in

toxicity.^[36] (S)-cEt is the only BNA modification other than the standard methylene LNA modification currently in the clinic or in clinical trials.^[14, 37]

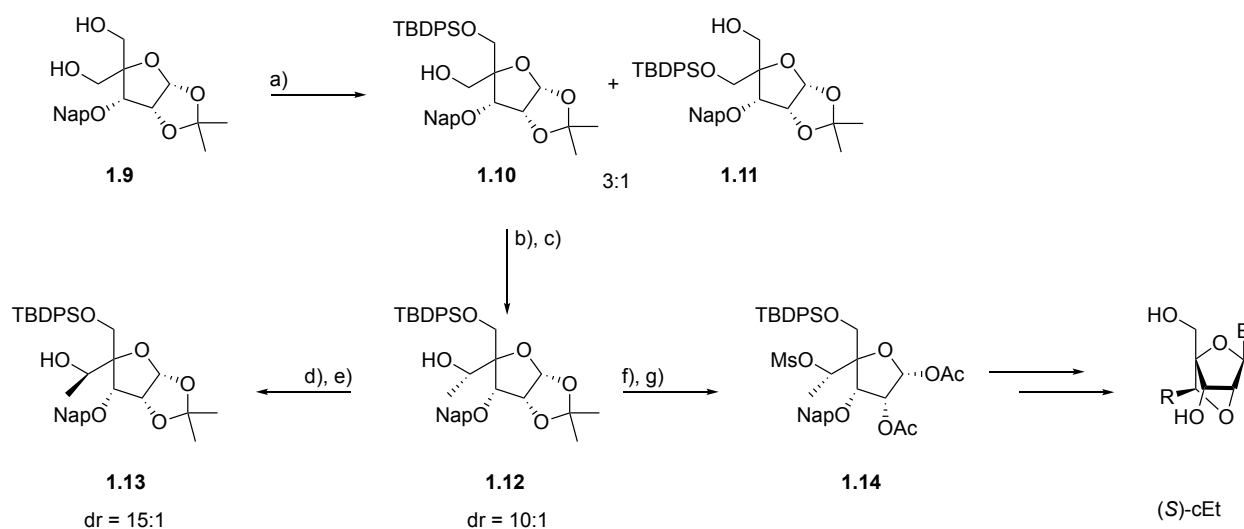
Like the 2' modified nucleosides, methylene LNAs are commercially available, although at significantly higher cost. LNA synthesis requires 11 steps from commercially available allofuranose **1.2** (**Scheme 1.5**). Protection of the 3'OH with BnBr and NaH followed by deprotection of the C5/C6 diol gives **1.3**. NaIO₄ oxidation gives an aldehyde on the 5' position. The treatment of this aldehyde with NaOH and formaldehyde gives diol **1.4** via a sequential aldol reaction followed by Cannizzaro reaction (**1.4** is commercially available). Mesylation of **1.4** with mesylchloride in pyridine and then deprotection followed by reprotection of the C1/C2 diol is accomplished with H₂SO₄, HOAc and Ac₂O to give **1.5**. Glycosylation with the desired nucleoside base is mediated by N,O-bis(TMS)acetamide to give nucleosides **1.6**. Ring closure to give the protected LNA is accomplished by treatment with base, either LiOH or NaH, depending on the nucleoside base. The mesyl group on C5' is displaced by NaOBz to give compound **1.7**. Deprotection of the 5'OBz and 3'OBn gives LNA **1.8** in 9% overall yield from **1.2** when adenine is used as the base.^[38, 39]



Scheme 1.5 LNA synthesis B = U. a) NaH, BnBr, DMF; b) 80% HOAc; c) NaIO₄, THF/H₂O 1:1; d) 37% Formaldehyde, NaOH, dioxane; e) MsCl, pyridine:DCM 3:2; f) HOAc, AC₂O, H₂SO₄; g) Nucleoside base, N,O-bis(trimethylsilyl)acetamide, TMSOTf, MeCN or 1,2-dichloroethane, reflux; h) NaOH or LiOH·H₂O, THF-H₂O; i) NaOBz, DMSO, 100 °C; j) NaOH or LiOH·H₂O, THF-H₂O; k) 20% Pd(OH)₂/C, HCO₂H or HCO₂NH₄, THF-MeOH, reflux.

(S)-cEt BNAs are synthesized in a similar fashion (**Scheme 1.6**). Compound **1.9** is synthesized following the same route as **1.4** and is protected using TBDPSCI to give **1.10** in a 3:1 ratio over

1.11. **1.10** is a crystalline solid, while **1.11** is not, so they are easily separable via crystallization. Swern oxidation of **1.10** followed by the treatment of MeMgBr gives **1.12** in 10:1 dr favoring the desired (*S*)-cEt diastereomer. The newly formed stereo center can be inverted by a second Swern oxidation followed by reduction with LiBH₄ to give **1.13** (*R*)-cEt in a 15:1 ratio. Mesylation of the free OH followed by a similar H₂SO₄, HOAc and Ac₂O deprotection/reprotection as seen in **Scheme 1.5** gives **1.14**. From there, glycosylation with the desired nucleobase, ring closure, and deprotection yields the (*S*)-cEt BNA.^[40]



Scheme 1.6 (*S*)-cEt BNA synthesis B = U. a) TBDPSCI, Et₃N; b) Swern oxidation; c) MeMgBr, CeCl₃; d) Swern oxidation; e) LiBH₄; f) MsCl, pyridine; g) HOAc, Ac₂O, H₂SO₄.

1.3.3 5' Methyl Modification

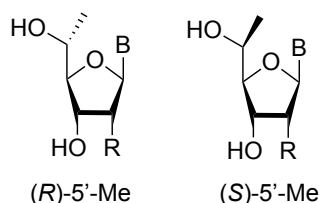


Figure 1.5 5'-Me modified RNA.

Modification of the 5' position of ribose can increase the nuclease stability of the resulting ON. Methylating the C5' of ribose gives (*R*)- and (*S*)-5'-C-methyl (C5'-Me) substituted nucleosides (**Figure 1.5**). This transformation is easily accomplished by oxidizing the C5'OH of a nucleoside with Dess-Martin periodinane and then treating the resulting aldehyde with methyl Grignard to

give the (*R*)- and (*S*)- diastereomers in a roughly 1:1 ratio and low yield (~45 % from the crude aldehyde).^[41] The diastereomers can be separated via chromatography followed by crystallization and then treated with 2-cyanoethyl *N,N,N',N'*-tetraisopropylphosphorodiamidite to give nucleoside phosphoramidites for use in solid supported ON synthesis. The pyrimidine (*R*)-5'-C-methyl nucleosides adopt the 2'-endo sugar pucker conformation, whereas the (*S*)-5'-C-methyl had a 3'-endo conformation. As mentioned in the previous section, the 3'-endo configuration leads to ONs with higher T_m . Consequently the use of (*R*)-5'-C-methyl nucleosides resulted in DNA ONs lower T_m for DNA/DNA and DNA/RNA duplexes, while the (*S*)-5'-C-methyl nucleosides exhibited higher T_m in those dimers. RNA ONs with either one of the two RNA/DNA and RNA/RNA duplexes.^[41] Having two 5'-C-methyl nucleosides at the 3' end of an ON can dramatically increase the $T_{1/2}$ of the ON in the presence of 3'-exonucleases (≤ 0.3 hours to >11 hours). It should be noted however that the (*S*)-5'-C-methyl diastereomer is more more nuclease resistant than the (*R*)-5'-C-methyl.^[41]

1.3.5 5' Phosphonates

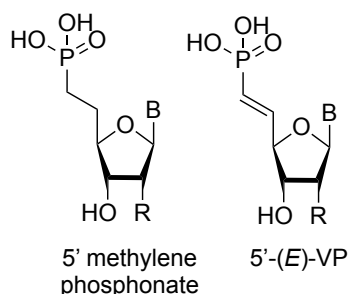
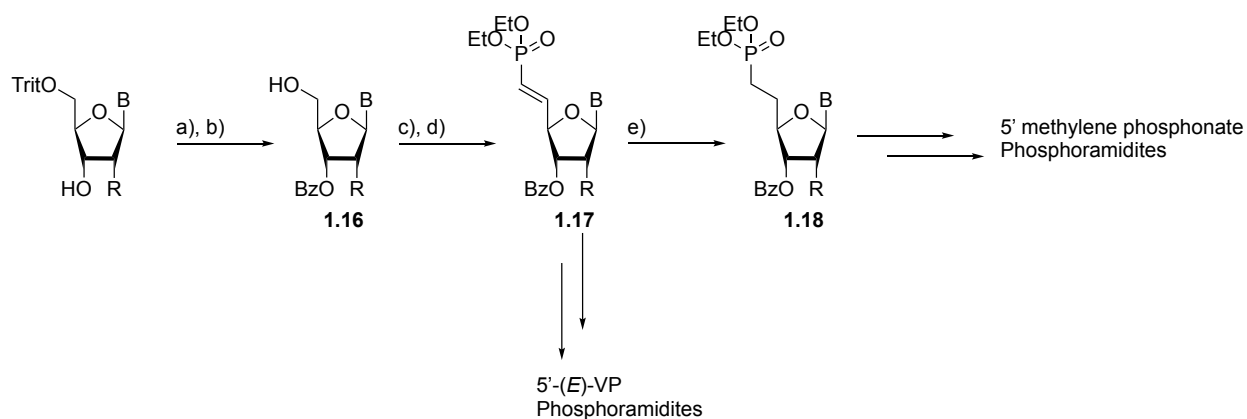


Figure 1.6 5'-phosphonate modified RNA.

ss-siRNAs require a 5' phosphate to be loaded into RISC.^[42] The 5' phosphate on RNA is rapidly cleaved to form the 5'OH in the body.^[42, 43] Indeed, a ss-siRNA targeting mutant HTT protein is completely inactive if administered with a 5'OH or a 5' phosphate.^[43] Stable 5' phosphate analogues have been developed to solve this problem; the most successful of these being 5' phosphonates (**Figure 1.6**). 5' methylene phosphonates mimic the charge and size of the 5' phosphate, but they cannot be cleaved by phosphatases.^[44] Further modifications, such as 5'-(*E*)-vinyl phosphonates (5'-(*E*)-VP) can further improve ss-siRNA activity by placing the

phosphonate in the appropriate orientation for RISC binding.^[44, 45] The same ss-siRNA sequence targeting mutant HTT protein mentioned previously is active with the 5'-(*E*)-VP modification. Because siRNA only cleaves exactly matching sequences, the guide strand of the ss-siRNA only targets the mutant allele, allowing the fibroblast cells to continue to make normal HTT protein.^[43]

Synthesis of 5' methylene phosphate and 5'-(*E*)-VP nucleosides is easily accomplished in 5 and 4 steps respectively from commercially available 2'OH functionalized 5'OH triylated nucleosides (**Scheme 1.7**). Protection of the 3'OH with BzCl followed by detritylation gives **1.16** with a free 5'OH. Oxidation of the 5'OH gives an aldehyde. The treatment of the resulting aldehyde with tetraethyl methylenediphosphonate to gives 5'-(*E*)-VP **1.17**. Reduction with Pd/C and H₂ gives 5' methylene phosphate **1.18**. The 3'OBz can be removed with ammonium methoxide and then the phosphoramidite can be installed using standard conditions.^[44]



Scheme 1.7 5'-Phosphonate RNA synthesis. a) BzCl, pyridine; b) TFA, DCM, TESCI; c) DCC, DMSO, pyridine•TFA; d) tetraethyl methylenediphosphonate, THF, KO^t-Bu' e) Pd/C, H₂.

1.4 Backbone Modifications

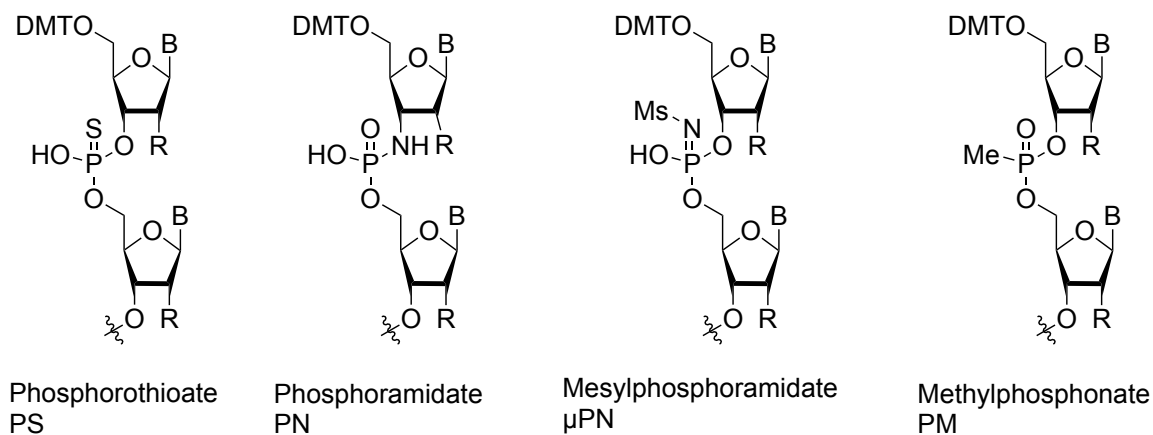


Figure 1.7 Selected ON backbone modifications.

Backbone modifications, just like the previously discussed ribose modifications, can modulate ON activity and nuclease resistance. Unlike ribose modifications, backbone modifications can require significant modification of the standard solid supported ON synthesis.

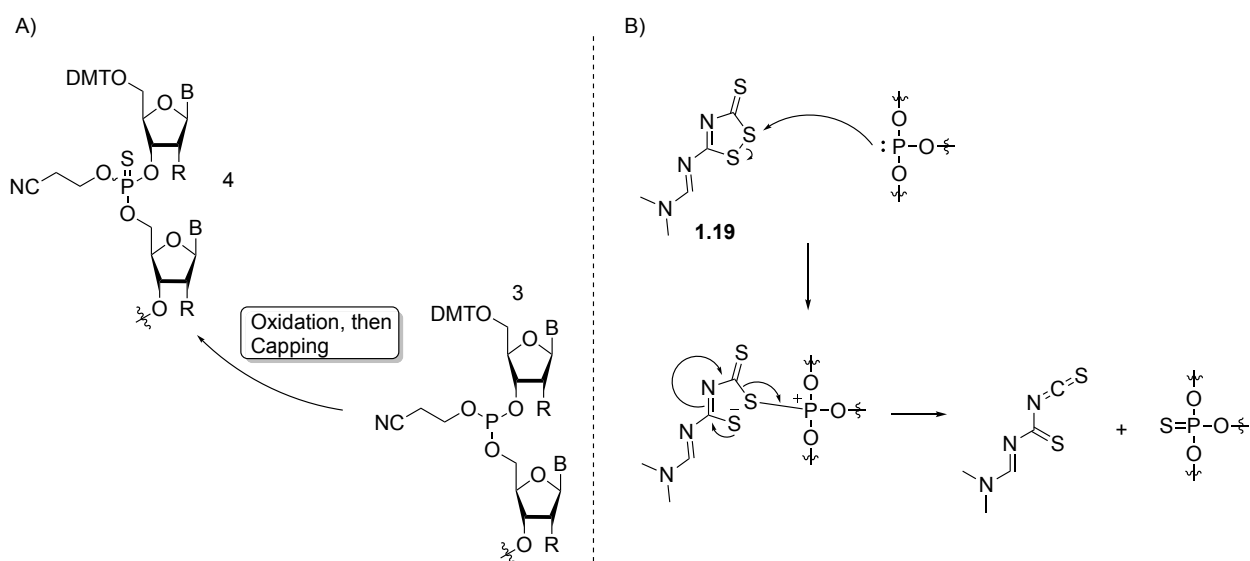
1.4.1 Phosphorothioate Diesters

The backbone modification that has proved to be the most advantageous, to the point of being the most common modification in clinical ASOs, is also the oldest; the phosphorothioate (PS) modification.^[46] Other backbone modifications have had little impact on the clinic. This clinical success comes despite the fact that the PS modification lowers T_m by 0.5 - 0.7 °C per modification and fully PS ONs are cytotoxic. The other properties PS modifications confer on ONs are beneficial enough to outweigh these drawbacks. Initially this modification was added to increase nuclease resistance of ASO DNA; it converts DNA or RNA strands with half-lives of minutes in to strands with half-lives of days.^[14] PS modifications were fortuitously found to increase ON bioavailability and cell uptake.^[46, 47] It is thought that this is due to the sulfur atom's increased hydrophobicity compared to the original oxygen. This change results in a more hydrophobic ON that interacts with serum proteins, such as heparin binding proteins or albumin, which protect the ON from nucleases.^[47b, 48] Additionally, PS modified ASOs can be diffused into

cells by gymnotic ('naked') uptake which means that no targeting chemistry or transfection agent is required.^[49] The first approved ASO drug, fomivirsen, is a PS-DNA 21-mer.

This PS modification is also commonly seen in siRNAs. Unlike ASOs, only the ends of siRNAs are typically modified. This minimal modification is due to the siRNA guide strand's being considerably more sensitive to modification than an ASO strand. By putting the PS modification on the ends, the siRNA is conferred some additional nuclease resistance without weakening the activity excessively.

The synthesis of PS ON differs slightly from PO ONs. The first two steps of the cycle, deblocking and coupling, are identical, but the sequence of capping and oxidation is switched (**Scheme 1.8A**). Chains are capped first because the capping reagents can interfere with the oxidation chemistry. Oxidation is accomplished with compounds like dithiazole **1.19** via the mechanism shown in **scheme 1.8B**.^[50] Although similar compounds with a carbonyl oxygen in place of the carbonyl sulfur can promote the same oxidation, they should be avoided, because the resulting byproduct is an isocyanate, which is far more reactive than the isothiocyanate resulting from **1.19**. The isocyanate can react with the growing ON chains and lower yields.

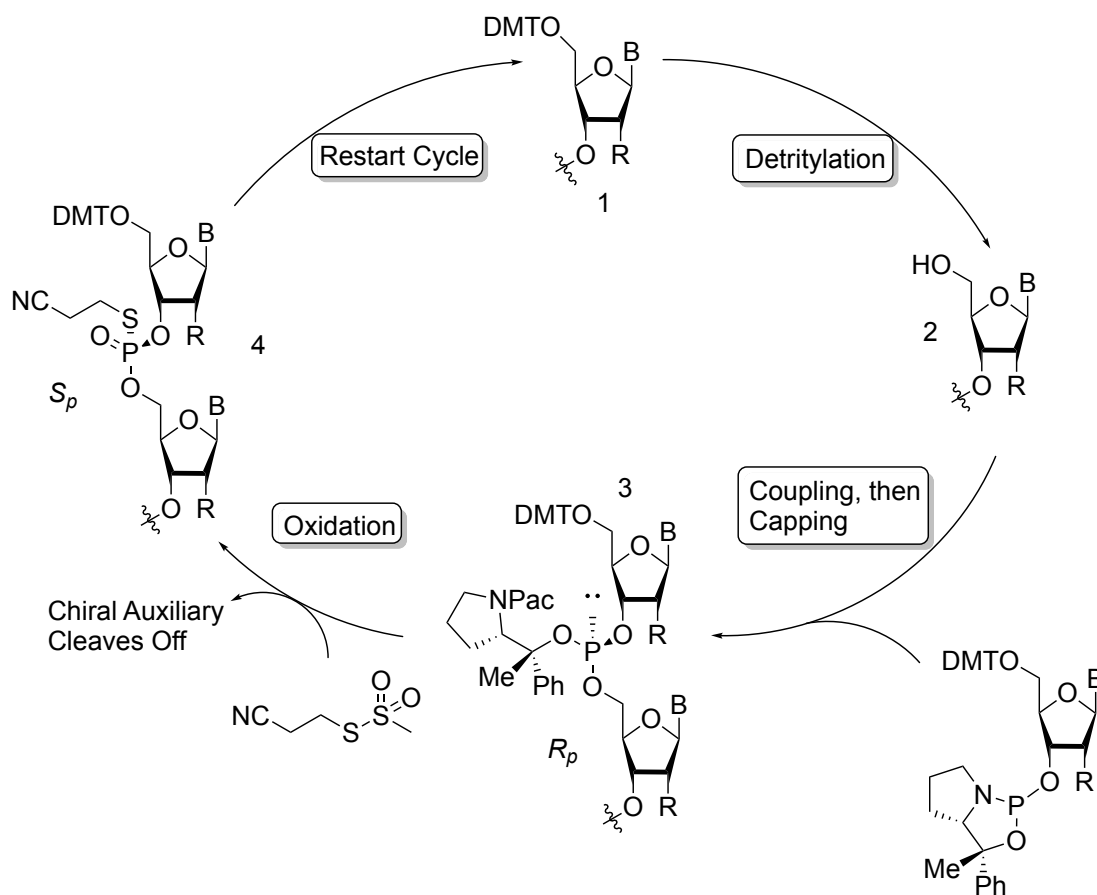


Scheme 1.8 PS ON backbone synthesis and mechanism.

The above synthesis yields diastereomeric mixtures of ONs because there is no control over the newly formed stereocenter at phosphorus. This can lead to a huge number of diastereomers present in the ON product. For example, fomivirsen has 2^{20} different diastereomers. Despite medicinal chemists' aversion to giving patients mixtures of stereoisomers, PS ON therapeutics are all diastereomeric mixtures because scaling stereoselective PS synthesis is challenging.

In spite of this, significant effort has been devoted to study the properties of stereoisomeric PS ONs. The *Sp* and *Rp* diastereomeric PS modifications have different properties: the *Rp* diastereomer binds with higher affinity and induces RNase-H activity better than the *Sp* diastereomer. However, the *Sp* diastereomer exhibits better nuclease resistance.^[51] Stereorandom PS ASOs tend to have a more desirable mix of properties than stereopure PS ASOs. Precise patterns of PS stereochemistry lead to improved mismatch discrimination and RNase-H activity that bests both stereopure and stereo random PS ASOs.^[52, 53]

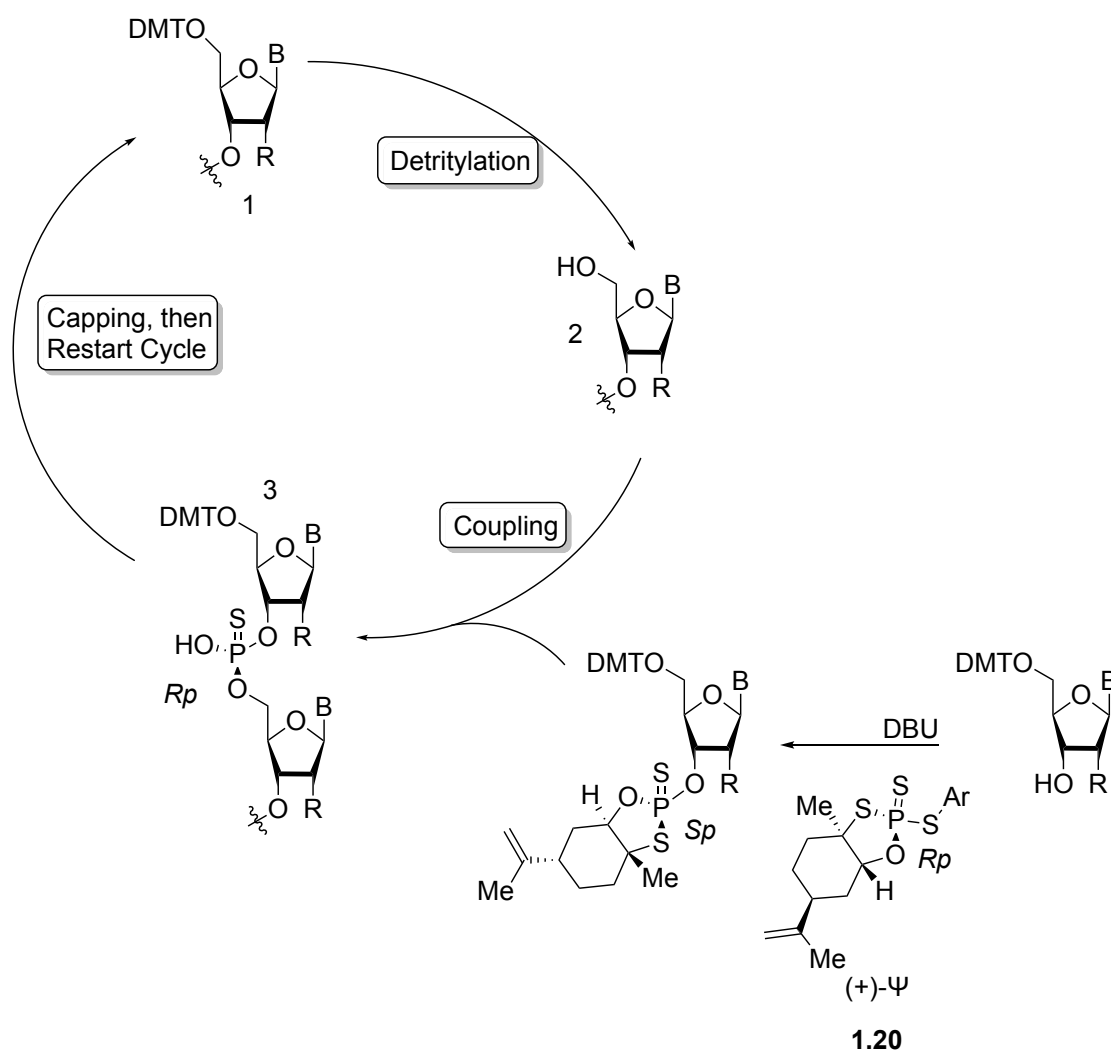
Two methods exist for the synthesis of stereopure PS ONs. The first method, like standard ON synthesis, uses a P(III) reagent as the coupling partner. Instead of a phosphoramidite, this method uses an oxazaphospholidine that acts as a chiral auxiliary. The synthetic cycle is similar to standard PO ON synthesis with capping done before oxidation (**Scheme 1.9**). Removal of the chiral auxiliary occurs spontaneously during the capping step or during the cleavage step at the end of ON synthesis, depending on what sulfurization reagent is used.^[5] Unfortunately, the synthesis of oxazaphospholidine nucleoside monomers requires the synthesis of 2-chloro-oxazaphospholidines which are unstable and difficult to handle, so scaling this approach can be challenging.



Scheme 1.9 Chiral PS backbone synthesis using tradition P(III) chemistry.

A recently reported a method for the synthesis of stereopure PS ONs uses a chiral P(V) reagent **1.20** (Scheme 1.10). This PSI (phosphorus-sulfur incorporation) reagent can be prepared at scale in three steps from commercial starting materials with the chirality coming from limonene oxide. The reagent, which is bench stable, is then coupled to a nucleoside using DBU to produce bench stable nucleosides ready for coupling. This modified nucleoside (**1.21**) is coupled on to the solid bound ON chain in the presence of DBU. Because the phosphorus is already oxidized, no oxidation step is needed, simplifying the synthetic cycle.^[54] Note that in the P(III) method the stereochemistry at phosphorus is retained throughout the cycle, in this P(V) strategy the stereochemistry at phosphorus undergoes double inversion. This method has the

potential to enable the synthesis of stereochemically defined PS ONs at the scale needed for clinical applications.



Scheme 1.10 Chiral PS backbone synthesis using novel P(V) chemistry.

1.4.2 Other Backbone Modifications

Other backbone modifications have been synthesized in an attempt to improve on the PS backbone such as phosphoramidate and methyl-phosphonate (**Figure 1.7**).

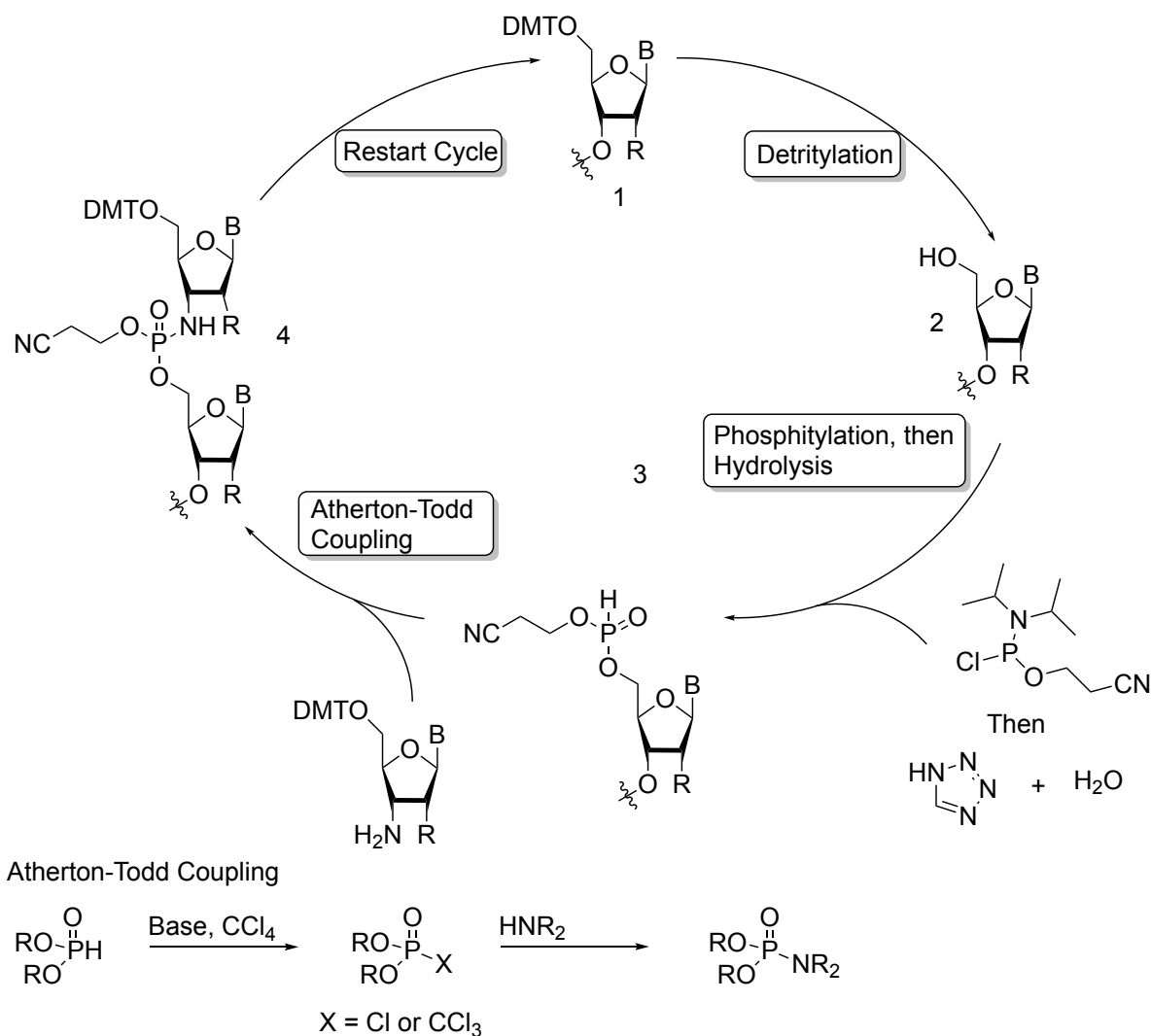
Achiral phosphoramidates (PN) ONs are significantly more nuclease resistant than their PO counterparts. Additionally they exhibit higher T_m than the natural PO ON for hybridization

towards both RNA and DNA.^[55] This higher T_m is thought to arise from the change of the 3'OH to 3'NH₂ resulting in the ribose adopting the 3'-endo configuration.^[55]

The synthesis of PN backbone RNA can be accomplished on solid support, but the cycle looks very different than a standard PO synthetic cycle (**Scheme 1.11**). Deblocking happens as normal, then 2-cyanoethyl-N,N-diisopropylchlorophosphine is coupled onto the free 5'OH to form a 5' phosphoramidate. Treatment with tetrazole and water gives the 5' H-phosphonate diester (position 3 **Scheme 1.11**). Atherton-Todd coupling of a 5'-DMT-3'-aminonucleoside with the 5'-H-phosphonate diester in the presence of CCl₄ yields the PN linkage. Cleavage and deprotection are accomplished under conditions identical to standard PO synthesis. Note that no capping step was performed. Average coupling yields for this method are 94-96%, which are significantly lower than traditional PO synthesis.^[55]

Racemic mesylphosphoramidate diester backbones (μ PN) have also been synthesized and tested for ASO activity. An anti-miR-22 (an oncogenic miRNA) μ PN DNA ON exhibited better RNA binding affinity, higher nuclease resistance, higher specificity, and lower cytotoxicity than the PS analogue.^[56] The μ PN decreases T_m for both DNA/DNA and DNA/RNA duplex compared to the natural PO linkage.^[57]

The synthesis of μ PN ONs is identical to PO ON synthesis, except the oxidation step is accomplished via a Staudinger reaction using MsN₃. Interestingly, this method seems amenable to chiral μ PN diester synthesis using a similar strategy as shown in the P(III) PS synthesis in **Scheme 1.9**.



Scheme 1.11 PN backbone ON synthesis.

Methyl phosphonate backbones (PM) have been tested as PS alternatives since the 80s.^[58] PM modified RNA is completely resistant to nucleases and results in lower T_m compared to DNA/RNA dimers with the natural PO linkage (roughly -1°C per PM modification), however it exhibits higher T_m than the equivalent PS ON.^[59] The synthesis of PM ONs is similar to PO ONs, differing only in the nucleoside coupling partner (methylphosphoramidite instead of a phosphoramidite).^[58]

1.5 Conclusion

Therapeutic ASOs and siRNA require significant chemical modifications to function, however the modifications discussed above have proven sufficient to get the field to the point where ASO

and siRNA drugs are on the market and feature in the clinical pipelines for multiple companies. Numerous other modifications have been tested in the literature, but they have not been able to make the jump into the clinic. Modifications need to be combined to yield active and safe compounds. There are few rules for the chemistry of ON therapeutics so the choice of what modifications and where to place them in the ON must be guided by empirical testing. Even with all of this success, there are still many unsolved problems with therapeutic ONs, such as cell type and tissue targeting, the inherent immunogenicity of dsRNA, and the challenge of synthesizing tons of ON if an ASO or siRNA drug takes off in the market.

1.6 References

- (1) a) P. C. Zamecnik, M. L. Stephenson, *Proc. Natl. Acad. Sci.* **1978**, 75, 280 LP – 284. b) M. L. Stephenson, P. C. Zamecnik, *Proc. Natl. Acad. Sci.* **1978**, 75, 285 LP – 288.
- (2) M. Robbins, A. Judge, I. MacLachlan, *Oligonucleotides* **2009**, 19, 89–102.
- (3) E. M. LeProust, B. J. Peck, K. Spirin, H. B. McCuen, B. Moore, E. Namsaraev, M. H. Caruthers, *Nucleic Acids Res.* **2010**, 38, 2522–2540.
- (4) R. T. Pon, N. Usman, M. J. Damha, K. K. Ogilvie, *Nucleic Acids Res.* **1986**, 14, 6453–6470.
- (5) V. T. Ravikumar, R. K. Kumar, P. Olsen, M. N. Moore, R. L. Carty, M. Andrade, D. Gorman, X. Zhu, I. Cedillo, Z. Wang, et al., *Org. Process Res. Dev.* **2008**, 12, 399–410.
- (6) J. Nielsen, M. Taagaard, J. E. Marugg, J. H. van Boom, O. Dahl, *Nucleic Acids Res.* **1986**, 14, 7391–7403.
- (7) B. P. Monia, E. A. Lesnik, C. Gonzalez, W. F. Lima, D. McGee, C. J. Guinosso, A. M. Kawasaki, P. D. Cook, S. M. Freier, *J. Biol. Chem.*, **268**, 14514–14522
- (8) a) S. Choung, Y. J. Kim, S. Kim, H.-O. Park, Y.-C. Choi, *Biochem. Biophys. Res. Commun.* **2006**, 342, 919–927. b) M. Robbins, A. Judge, L. Liang, K. McClintock, E. Yaworski, I. MacLachlan, *Mol. Ther.* **2007**, 15, 1663–1669. c) L. L. Cummins, S. R. Owens, L. M. Risen, E. A. Lesnik, S. M. Freier, D. McGee, C. J. Guinosso, P. D. Cook, *Nucleic Acids Res.* **1995**, 23, 2019–2024. d) B.P. Monia, J.F. Johnston, H. Sasmor, L.L. Cummins, *J. Biol. Chem.* **1996**, 271, 14533–14540.
- (9) S. M. Freier, K.-H. Altmann, *Nucleic Acids Res.* **1997**, 25, 4429–4443.
- (10) a) M. Manoharan, *Biochim. Biophys. Acta - Gene Struct. Expr.* **1999**, 1489, 117–130. b) M. M. Mangos, M. J. Damha, *Curr. Top. Med. Chem.* **2002**, 2, 1147–1171 c) T. P. Prakash, *Chem. Biodivers.* **2011**, 8, 1616–1641. d) M. Egli, G. Minasov, V. Tereshko, P. S. Pallan, M. Teplova, G. B. Inamati, E. A. Lesnik, S. R. Owens, B. S. Ross, T. P. Prakash, et al., *Biochemistry* **2005**, 44, 9045–9057.
- (11) a) C. Esau, X. Kang, E. Peralta, E. Hanson, E. G. Marcusson, L. V. Ravichandran et al. *J Biol Chem.* **2004**, 279, 52361–52365. b) P. Martin, *Helv. Chim. Acta* **1995**, 78, 486–504.
- (12) a) M. J. Damha, C. J. Wilds, A. Noronha, I. Brukner, G. Borkow, D. Arion, M. A. Parniak, *J. Am. Chem. Soc.* **1998**, 120, 12976–12977. b) J. K. Watts, M. J. Damha, *Can. J. Chem.* **2008**, 86, 641–656. c) T. P. Prakash, C. R. Allerson, P. Dande, T. A. Vickers, N. Sioufi, R. Jarres, B. F. Baker, E. E. Swayze, R. H. Griffey, B. Bhat, *J. Med. Chem.* **2005**, 48, 4247–4253. d) G. F. Deleavey, J. K. Watts, M. J. Damha, *Curr. Protoc. Nucleic Acid Chem.* **2009**, 39, 16.3.1-16.3.22.
- (13) S. Davis, B. Lollo, S. Freier, C. Esau, *Nucleic Acids Res.* **2006**, 34, 2294–2304.
- (14) X. Shen, D. R. Corey, *Nucleic Acids Res.* **2017**, 46, 1584–1600.
- (15) C. Matranga, Y. Tomari, C. Shin, D. P. Bartel, P. D. Zamore, *Cell* **2005**, 123, 607–620.
- (16) a) C. Matranga, Y. Tomari, C. Shin, D. P. Bartel, P. D. Zamore, *Cell* **2005**, 123, 607–620. b) T. P. Chendrimada, R. I. Gregory, E. Kumaraswamy, J. Norman, N. Cooch, K. Nishikura, R. Shiekhattar, *Nature* **2005**, 436, 740–744. c) R. I. Gregory, T. P. Chendrimada, N. Cooch, R. Shiekhattar, *Cell* **2005**, 123, 631–640. d) K. Miyoshi, H. Tsukumo, T. Nagami, H. Siomi, M. C. Siomi, *Genes Dev.* **2005**, 19, 2837–2848. e) E. Maniataki, Z. Mourelatos, *Genes Dev.* **2005**, 19, 2979–2990.
- (17) P. J. L. M. Quaedflieg, A. P. Van der Heiden, L. H. Koole, A. J. J. M. Coenen, S. Van der Wal, E. M. Meijer, *J. Org. Chem.* **1991**, 56, 5846–5859.
- (18) S. Chow, K. Wen, Y. S. Sanghvi, E. A. Theodorakis, *Bioorg. Med. Chem. Lett.* **2003**, 13, 1631–1634.
- (19) S. K. Roy, J. Tang, *Org. Process Res. Dev.* **2000**, 4, 170–171.
- (20) S. K. Mahto, C. S. Chow, *Bioorg. Med. Chem.* **2008**, 16, 8795–8800.
- (21) A. Khvorova, J. K. Watts, *Nat. Biotechnol.* **2017**, 35, 238.
- (22) a) M. Manoharan, A. Akinc, R. K. Pandey, J. Qin, P. Hadwiger, M. John, K. Mills, K. Charisse, M. A. Maier, L. Nechev, et al., *Angew. Chemie Int. Ed.* **2011**, 50, 2284–2288. b) T. L. Cuellar, D. Barnes, C. Nelson, J. Tanguay, S.-F. Yu, X. Wen, S. J. Scales, J. Gesch, D. Davis, A. van Brabant Smith, et al., *Nucleic Acids Res.* **2014**, 43, 1189–1203.

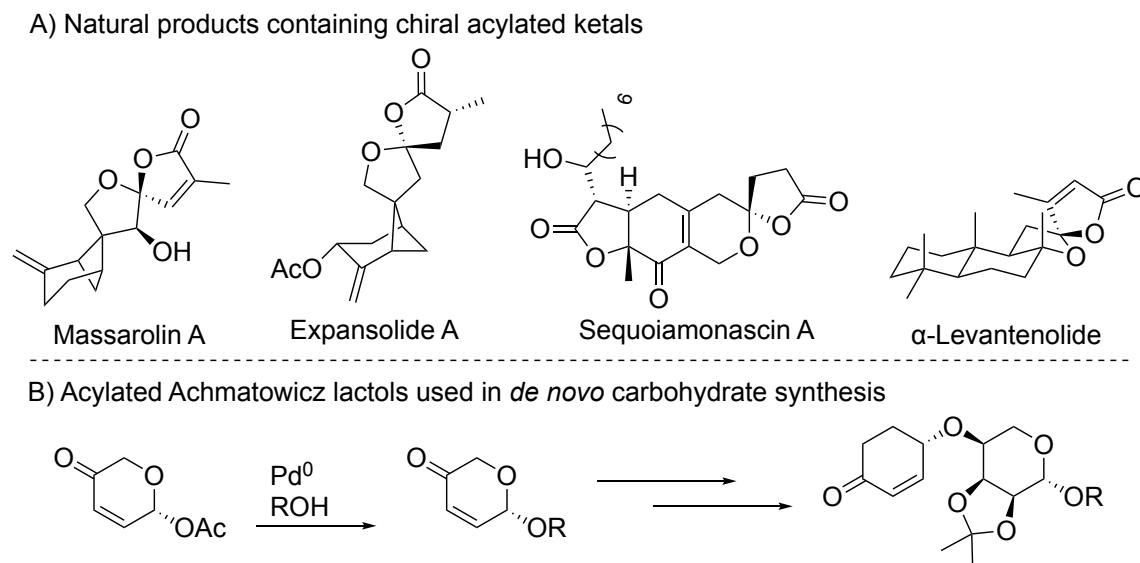
- (23) G. F. Deleavey, J. K. Watts, T. Alain, F. Robert, A. Kalota, V. Aishwarya, J. Pelletier, A. M. Gewirtz, N. Sonenberg, M. J. Damha, *Nucleic Acids Res.* **2010**, 38, 4547–4557.
- (24) C. R. Allerson, N. Sioufi, R. Jarres, T. P. Prakash, N. Naik, A. Berdeja, L. Wanders, R. H. Griffey, E. E. Swayze, B. Bhat, *J. Med. Chem.* **2005**, 48, 901–904.
- (25) a) H. Addepalli, Meena, C. G. Peng, G. Wang, Y. Fan, K. Charisse, K. N. Jayaprakash, K. G. Rajeev, R. K. Pandey, G. Lavine, et al., *Nucleic Acids Res.* **2010**, 38, 7320–7331. b) Rajeev, K.G. et al. US patent 9,399,775. **2016**.
- (26) J. K. Watts, G. F. Deleavey, M. J. Damha, *Drug Discov. Today* **2008**, 13, 842–855.
- (27) J. R. Mercer, E. E. Knaus, L. I. Wiebe, *J. Med. Chem.* **1987**, 30, 670–675.
- (28) A. Krug, S. Schmidt, J. Lekschas, K. Lemke, D. Cech, *J. für Prakt. Chemie* **1989**, 331, 835–842.
- (29) J. V Tuttle, M. Tisdale, T. A. Krenitsky, *J. Med. Chem.* **1993**, 36, 119–125.
- (30) N. T. Schirle, J. Sheu-Gruttadauria, I. J. MacRae, *Science* (80-.). **2014**, 346, 608 LP – 613.
- (31) K. A. Lennox, M. A. Behlke, *Gene Ther.* **2011**, 18, 1111–1120.
- (32) a) K. A. Lennox, M. A. Behlke, *Gene Ther.* **2011**, 18, 1111–1120. b) S. Obika, D. Nanbu, Y. Hari, J. Andoh, K. Morio, T. Doi, T. Imanishi, *Tetrahedron Lett.* **1998**, 39, 5401–5404. e) D. A. Braasch, D. R. Corey, *Chem. Biol.* **2001**, 8, 1–7. d) E. M. Straarup, N. Fisker, M. Hedtjörn, M. W. Lindholm, C. Rosenbohm, V. Aarup, H. F. Hansen, H. Ørum, J. B. R. Hansen, T. Koch, *Nucleic Acids Res.* **2010**, 38, 7100–7111.
- (33) a) A. Khvorova, A. Reynolds, S. D. Jayasena, *Cell* **2003**, 115, 209–216. b) A. L. Jackson, et al. *RNA* **2006**, 12, 1197–1205.
- (34) a) L. F. R. Gebert, M. A. E. Rebhan, S. E. M. Crivelli, R. Denzler, M. Stoffel, J. Hall, *Nucleic Acids Res.* **2013**, 42, 609–621. b) S. Obad, C. O. dos Santos, A. Petri, M. Heidenblad, O. Broom, C. Ruse, C. Fu, M. Lindow, J. Stenvang, E. M. Straarup, et al., *Nat. Genet.* **2011**, 43, 371–378.
- (35) S. M. Abdur Rahman, S. Seki, S. Obika, H. Yoshikawa, K. Miyashita, T. Imanishi, *J. Am. Chem. Soc.* **2008**, 130, 4886–4896.
- (36) P. P. Seth, A. Siwkowski, C. R. Allerson, G. Vasquez, S. Lee, T. P. Prakash, E. V Wancewicz, D. Witchell, E. E. Swayze, *J. Med. Chem.* **2009**, 52, 10–13.
- (37) J. K. Watts, *Chem. Commun.* **2013**, 49, 5618–5620.
- (38) C. Chapron, R. Glen, M. La Colla, B. A. Mayes, J. F. McCarville, S. Moore, A. Moussa, R. Sarkar, M. Seifer, I. Serra, et al., *Bioorg. Med. Chem. Lett.* **2014**, 24, 2699–2702.
- (39) H. M. Pfundheller, C. Lomholt, *Curr. Protoc. Nucleic Acid Chem.* **2002**, 8, 4.12.1-4.12.16.
- (40) P. P. Seth, G. Vasquez, C. A. Allerson, A. Berdeja, H. Gaus, G. A. Kinberger, T. P. Prakash, M. T. Migawa, B. Bhat, E. E. Swayze, *J. Org. Chem.* **2010**, 75, 1569–1581.
- (41) A. V Kel'in, I. Zlatev, J. Harp, M. Jayaraman, A. Bisbe, J. O'Shea, N. Taneja, R. M. Manoharan, S. Khan, K. Charisse, et al., *J. Org. Chem.* **2016**, 81, 2261–2279.
- (42) W. F. Lima, T. P. Prakash, H. M. Murray, G. A. Kinberger, W. Li, A. E. Chappell, C. S. Li, S. F. Murray, H. Gaus, P. P. Seth, et al., *Cell* **2012**, 150, 883–894.
- (43) D. Yu, H. Pendergraff, J. Liu, H. B. Kordasiewicz, D. W. Cleveland, E. E. Swayze, W. F. Lima, S. T. Crooke, T. P. Prakash, D. R. Corey, *Cell* **2012**, 150, 895–908.
- (44) T. P. Prakash, W. F. Lima, H. M. Murray, W. Li, G. A. Kinberger, A. E. Chappell, H. Gaus, P. P. Seth, B. Bhat, S. T. Crooke, et al., *Nucleic Acids Res.* **2015**, 43, 2993–3011.
- (45) a) R. Parmar, J. L. S. Willoughby, J. Liu, D. J. Foster, B. Brigham, C. S. Theile, K. Charisse, A. Akinc, E. Guidry, Y. Pei, et al., *ChemBioChem* **2016**, 17, 985–989. b) N. T. Schirle, G. A. Kinberger, H. F. Murray, W. F. Lima, T. P. Prakash, I. J. MacRae, *J. Am. Chem. Soc.* **2016**, 138, 8694–8697.
- (46) F. Eckstein, *Nucleic Acid Ther.* **2014**, 24, 374–387.
- (47) a) R. S. Geary, D. Norris, R. Yu, C. F. Bennett, *Adv. Drug Deliv. Rev.* **2015**, 87, 46–51. b) E. Koller, T. M. Vincent, A. Chappell, S. De, M. Manoharan, C. F. Bennett, *Nucleic Acids Res.* **2011**, 39, 4795–4807. c) K. Fluiter, *ChemMedChem* **2009**, 4, 879.
- (48) S. F. Dowdy, *Nat. Biotechnol.* **2017**, 35, 222.

- (49) a) C. A. Stein, J. B. Hansen, J. Lai, S. Wu, A. Voskresenskiy, A. Høg, J. Worm, M. Hedtjärn, N. Souleimanian, P. Miller, et al., *Nucleic Acids Res.* **2009**, 38, e3–e3. b) Z. Chen, B. P. Monia, D. R. Corey, *J. Med. Chem.* **2002**, 45, 5423–5425.
- (50) A. P. Guzaev, *Tetrahedron Lett.* **2011**, 52, 434–437.
- (51) a) M. Koziolkiewicz, A. Krakowiak, M. Kwinkowski, M. Boczkowska, W. J. Stec, *Nucleic Acids Res.* 1995, 23, 5000–5005. b) W. J. STEC, C. S. CIERNIEWSKI, A. OKRUSZEK, A. KOBYLAŃSKA, Z. PAWŁOWSKA, M. KOZIOŁKIEWICZ, E. PLUSKOTA, A. MACIASZEK, B. REBOWSKA, M. STASIAK, *Antisense Nucleic Acid Drug Dev.* 1997, 7, 567–573. c) M. Boczkowska, P. Guga, W. J. Stec, *Biochemistry* 2002, 41, 12483–12487.
- (52) K. T. Gagnon, J. K. Watts, *Nucleic Acid Ther.* **2014**, 24, 428–434.
- (53) N. Iwamoto, D. C. D. Butler, N. Svrzikapa, S. Mohapatra, I. Zlatev, D. W. Y. Sah, Meena, S. M. Standley, G. Lu, L. H. Apponi, et al., *Nat. Biotechnol.* **2017**, 35, 845.
- (54) K. W. Knouse, J. N. deGruyter, M. A. Schmidt, B. Zheng, J. C. Vantourout, C. Kingston, S. E. Mercer, I. M. McDonald, R. E. Olson, Y. Zhu, et al., *Science* (80-). **2018**, 361, 1234 LP – 1238.
- (55) S. Gryaznov, J.-K. Chen, *J. Am. Chem. Soc.* **1994**, 116, 3143–3144.
- (56) S. K. Miroshnichenko, O. A. Patutina, E. A. Burakova, B. P. Chelobanov, A. A. Fokina, V. V. Vlassov, S. Altman, M. A. Zenkova, D. A. Stetsenko, *Proc. Natl. Acad. Sci.* **2019**, 116, 1229 LP – 1234.
- (57) B. P. Chelobanov, E. A. Burakova, D. V Prokhorova, A. A. Fokina, D. A. Stetsenko, *Russ. J. Bioorganic Chem.* **2017**, 43, 664–668.
- (58) S. Agrawal, J. Goodchild, *Tetrahedron Lett.* **1987**, 28, 3539–3542.
- (59) L. Kibler-Herzog, G. Zon, B. Uznanski, G. Whittier, W. D. Wilson, *Nucleic Acids Res.* **1991**, 19, 2979–2986.

2. Stereoselective Acylation of Lactols

Portions of this chapter were previously published in: H.-Y. Wang, K. Yang, D. Yin, C. Liu, D. A. Glazier, W. Tang, *Org. Lett.* **2015**, 17, 5272–5275.; Z. Zhu, D. A. Glazier, D. Yang, W. Tang, *Adv. Synth. Catal.* **2018**, 360, 2211–2215.; D. A. Glazier, J. M. Schroeder, J. Liu, W. Tang, *Adv. Synth. Catal.* **2018**, 360, 4646–4649.

2.1. Introduction



Scheme 2.1. Chiral acyl acetals and ketals are present in numerous natural products and are useful intermediates in the *de novo* synthesis of carbohydrates.

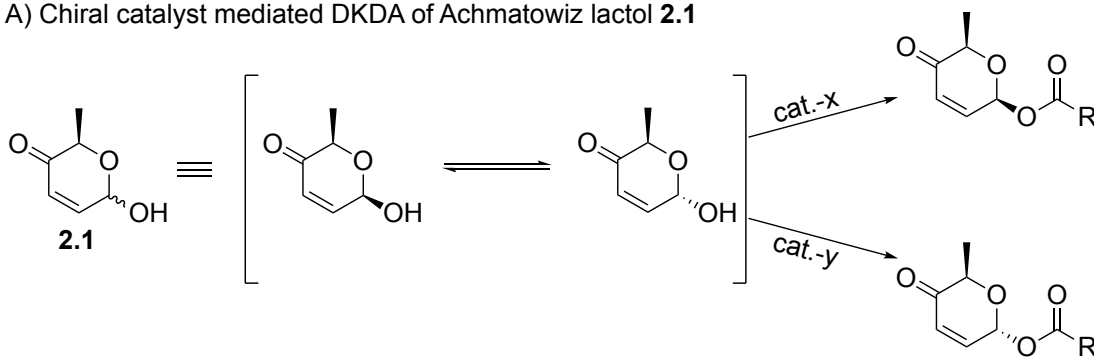
Chiral acyl acetals and ketals are present in numerous bioactive natural products and pharmaceutical reagents, such as massarolinol A,^[1] expansolides A and B^[2] sequoiamonascins,^[3] and levantenolides (**Scheme 2.1A**).^[4] Chiral acyl lactols that are derived from the acylation of Achmatowicz rearrangement products (**Scheme 2.1B**)^[5] are also useful intermediates in the *de novo* synthesis of various mono- and oligosaccharides.^[6] This has led to the development of methods for the stereoselective acylation of lactols. The achiral catalyst DMAP has been used to acylate chiral Achmatowicz lactols and then the diastereomers could be easily separated by column chromatography for the use in the *de novo* synthesis of carbohydrates.^[7] Previous methods to synthesize chiral acylated lactols use enzymes to affect a dynamic kinetic stereoselective acylation (DKSA) or HKR of the lactol, but the scope of the acyl group is limited and reaction times can be excessive.^[8]

We envisioned that chiral catalysts could either reinforce or override the intrinsic diastereoselectivity for the acylation of lactol **2.1** and provide a general solution for the synthesis of either *trans*-**2.2** or *cis*-**2.2** via a chiral catalyst-directed dynamic kinetic diastereoselective acylation (DKDA) (**Scheme 2.2A**). The advantage of using a chiral catalyst over previously

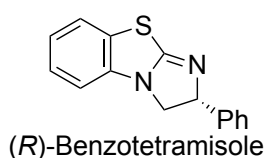
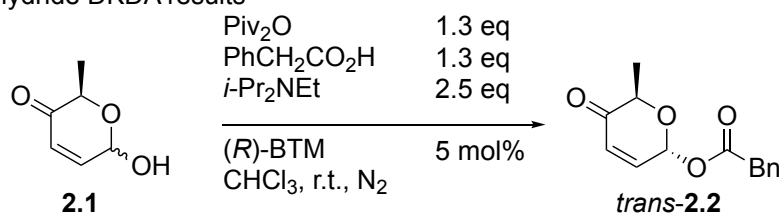
attempted enzymatic methods is that both enantiomers of the catalyst can be used to obtain both stereoisomers of the acylated lactol. After we analyzed chiral organocatalysts that are known to mediate the enantioselective acylation of alcohols,^[9] we chose to move forward with commercially available benzotetramisole (BTM). This catalyst has been extensively used by Birman and co-workers for the kinetic resolution of secondary alcohols,^[10] azlactones,^[11] and α -thiolcarboxylic acids.^[12] Wiskur and co-workers also applied them to the asymmetric silylation of alcohols.^[13]

Chiral lactol **2.1** was prepared enantioselectively in two steps from 2-acetylfuran via catalytic asymmetric hydrogenation (98% ee) and Achmatowicz rearrangement according to known protocols.^[14] Working with Hao-yuan Wang, I helped develop a novel BTM catalyzed mixed anhydride DKDA that gives acylated lactols in excellent dr and high yields (**Scheme 2.2B**).

A) Chiral catalyst mediated DKDA of Achmatowicz lactol **2.1**



B) Mixed anhydride DKDA results

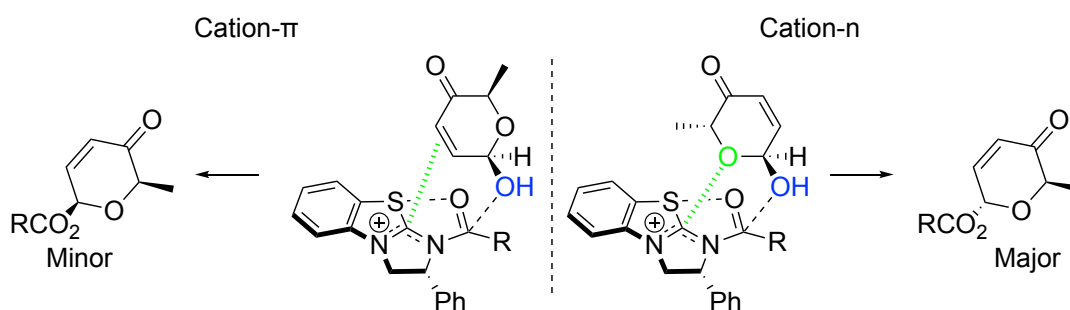


Catalyst	Yield (%)	dr
(<i>R</i>)-BTM	76	>20:1
(<i>S</i>)-BTM	73	1:16

Scheme 2.2. BTM catalyzed mixed anhydride DKDA of Achmatowicz lactol **2.1**.

We noticed that when we applied Birman and Houk's cation- π interaction^[15] model to substrate **2.1** the model predicts that the wrong stereoisomer will be favored (**Scheme 2.3**). If the

substrate is flipped around, the *endo*-O points at the cationic acylated catalyst, suggesting that the origin of the stereoselectivity for this reaction is a cation-*n* interaction, not a cation- π interaction. The alkene in **2.1** is electron deficient which should help the selectivity by decreasing the ability for the alkene to interact with the cationic catalyst. This cation-*n* interaction was then used to predict and rationalize the acylation of different types of carbohydrate substrates.^[16]



Scheme 2.3. Analyzing the selectivity of the DKDA suggests that it is controlled by a cation-*n* interaction, not a cation- π interaction as in previously reported kinetic resolutions with this catalyst. This is a novel mode of catalyst substrate interaction.

2.2 2,3,4,6-Tetraoxy-4-Amino Sugar Synthesis

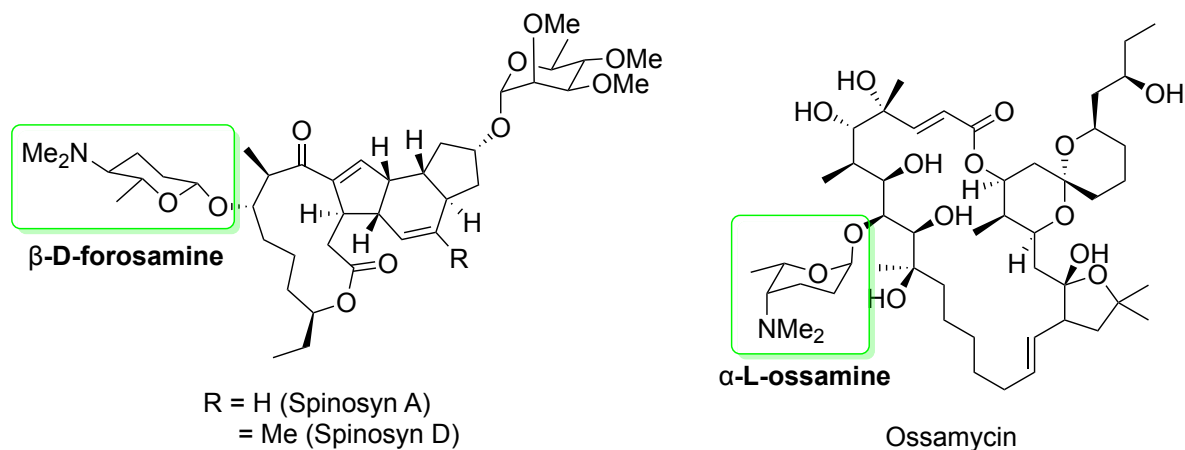


Figure 2.1. Selected 2,3,4,6-tetraoxy-4-amino pyranoside containing natural products. The glycones are highlighted in green.

Having developed a BTM catalyzed mixed anhydride DKDA for Achmatowicz lactols I wanted to evince the utility of this method for the *de novo* synthesis of carbohydrates. My lab mate

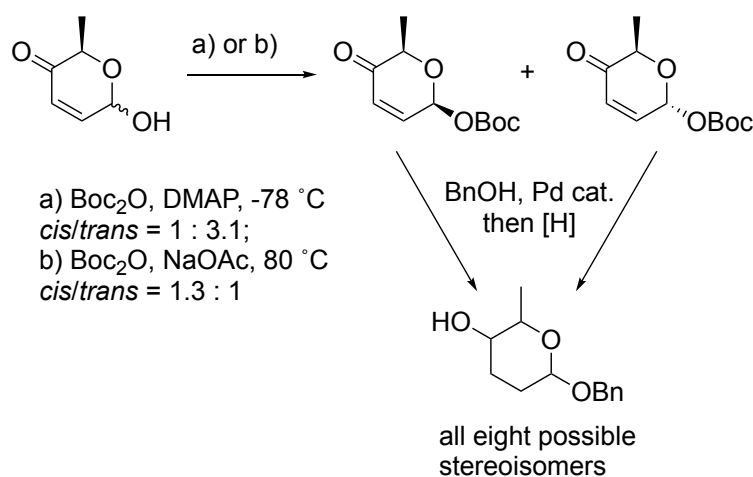
Zhongpeng Zhu and I decided to develop a systematic synthesis of all eight stereoisomers of the 2,3,4,6-tetra-deoxy-4-amino sugars.

Deoxyamino sugars are frequently found in natural products, such as aminoglycosides, macrolides, and anthracyclines, and the sugar units are often essential to the pharmacological activities of the natural products.^[17] Some examples of 2,3,4,6-tetra-deoxy-4-amino-pyranoside-containing natural products are shown in **Figure 2.1**. These natural products have a broad range of biological activities, such as cytotoxic agent grecoycline A,^[18] protein tyrosine phosphatase 1B inhibitor grecoycline B,^[19] insecticide spinosyns, and oxidative phosphorylation inhibitor ossamycin.^[20] Derivatives of griseusins also have potent antibiotic, antifungal, and anticancer activities.^[21]

Not surprisingly, significant efforts have been devoted to the synthesis of deoxyamino sugars.^[22] For example, both O-ethyl ossaminide and ossamine were synthesized from glucose or its derivatives in over 10 steps.^[20c,23] More recent efforts on the synthesis of ossamine and its analogues were also realized from chiral starting materials.^[24]

Forosamine is a diastereoisomeric isomer of ossamine. Both α/β and D/L forms of forosamines are found in natural products as shown in Figure 1. Since the structure and stereochemistry of forosamine was discovered in 1966, a number of synthetic routes have been developed.^[23a,25] Two *de novo* syntheses of forosamine involved either the epoxidation of sorbic acid followed by kinetic resolution of the resulting acid or chemoenzymatic resolution of the epoxide derived from methyl sorbate.^[26] In Evans's synthesis of lepicidin A, the L-forosamine glycone was prepared from an oxazolidinone chiral auxiliary in nearly ten steps.^[27] Racemic forosamine was synthesized by Tietze's group via a domino Knoevenagel-Hetero-Diels-Alder reaction and resolved by chiral HPLC.^[28] A Ru-catalyzed cycloisomerization was employed by Merck for the synthesis of L-forosamine from an acyclic chiral amino alcohol.^[29] Dai's group recently accomplished a concise synthesis of spinosyn A and observed a 1:1 α/β stereoselectivity.^[30] Prior to Dai's work, the undesired α -isomer was the major product^[27,31] with the exception of Roush's strategy.^[32] In Roush's synthesis of spinosyn A, a deoxyamino sugar with a C(2)-OAc

directing group was introduced to the macrocyclic aglycone with β -selectivity by Schmidt glycosylation, and the C(2)-OAc was later removed by deoxygenation.^[33] The synthesis of Roush's glycosyl donor, however, requires more than ten steps and another five steps are necessary for the removal of the C(2)-OAc group after the glycosylation. We devised a route to these rare amino sugars by streamlining and expanding upon our group's previously reported divergent strategy for the synthesis of all possible stereoisomers of 2,3,6-trideoxypyranosides (**Scheme 2.4**).^[33]

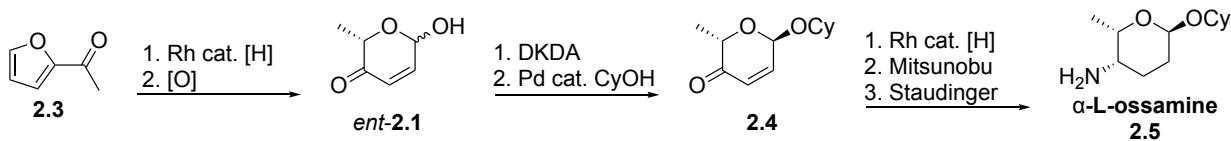


Scheme 2.4. Previously published route to all eight stereoisomers of 2,3,6-trideoxypyranosides.

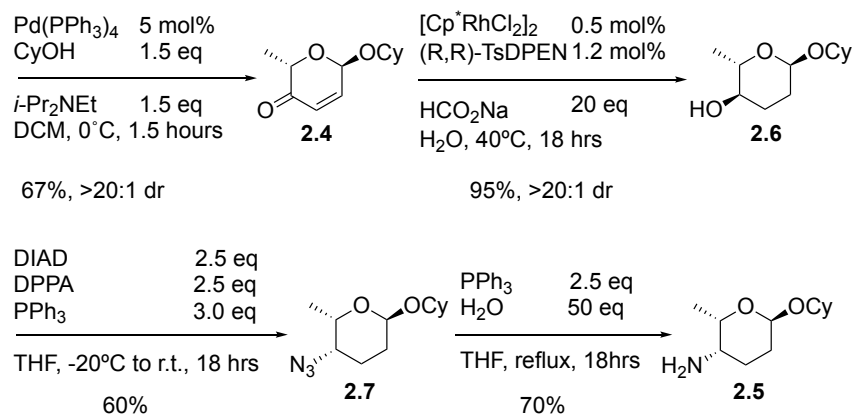
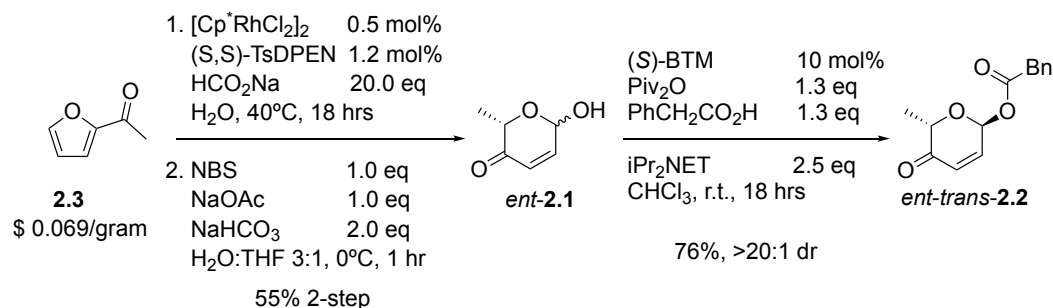
I focused on the synthesis of L-ossamine (**Figure 2.1**). As with our previous strategy I intended to begin my synthesis by using a chiral Rh catalyst to perform an asymmetric reduction of the inexpensive starting material 2-Acetylfuran. An Achmatowicz rearrangement will give the lactol *ent-2.1*. Our DKDA followed by a stereo-retentive Tsuji-Trost reaction should give the glycosylated lactol **2.3** in high yield and excellent dr. This is in contrast with our previous work towards the synthesis of 2,3,6-trideoxypyranosides (**Scheme 2.4**) where we used the achiral catalyst DMAP to acylate the lactol and then separated the diastereomers via column chromatography. The DKDA approach is much more efficient. After I obtain **2.3**, a second Rh catalyzed asymmetric reduction will give the 2,3,6-trideoxypyranoside as with our previous work. Then a Mitsunobu inversion and Staudinger reduction should yield L-ossamine after 7 steps and 6 purifications (**Scheme 2.5A**).

Following the route described above, I synthesized L-ossamine in 11% overall yield (**Scheme 2.5B**). Zhongpeng, following the same route, was able to synthesize all 8 stereoisomers of the 2,3,6-trideoxy and 2,3,4,6-tetradeoxy-4-amino pyranosides and their dimethyl amino variants using only two pairs of chiral catalysts (**Scheme 2.6**). This route is not only the most efficient route to 2,3,6-trideoxy and 2,3,4,6-tetradeoxy-4-amino pyranosides, but also the only systematic route to all members of the class and should simplify the synthesis of natural products and

A) Proposed route to α -Lossamine



B) *De novo* synthesis of α -Lossamine

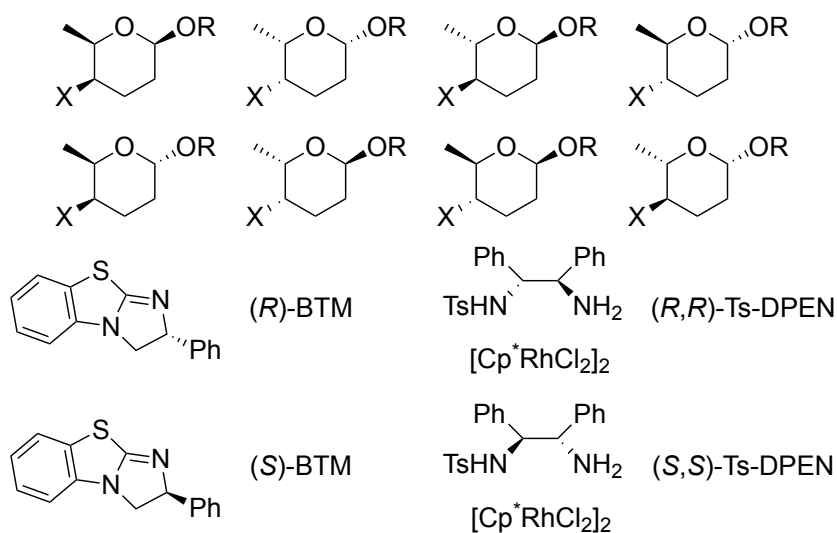


enable more complete SAR studies of biologically active compounds containing these sugars.

Scheme 2.5. *De novo* synthesis of α -Lossamine.

The Tang lab has continued to develop methods for the *de novo* synthesis of rare amino sugars using the DKDA as a key synthetic step. Most recently Peng Wen has developed an

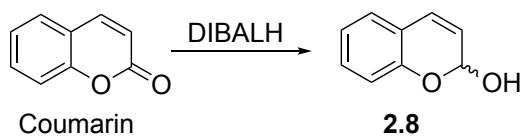
unpublished route to 2,3,6-trideoxy-3-aminopyranosides by using a late stage Rh catalyzed C-H nitrene insertion reaction.



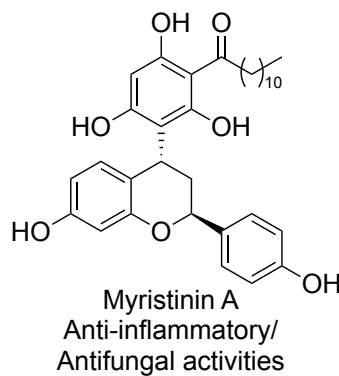
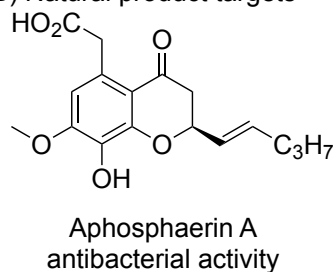
Scheme 2.6. All 8 stereoisomers of the 2,3,4,6-tetradeoxy-4-aminopyranosides synthesized using two pairs of chiral catalysts. X = OH, NH₂, and NMe₂

2.3 Attempts to Develop a Dynamic Kinetic Enantioselective Acylation (DKEA) for Coumarin Derived Lactols

A) Coumarin lactol synthesis



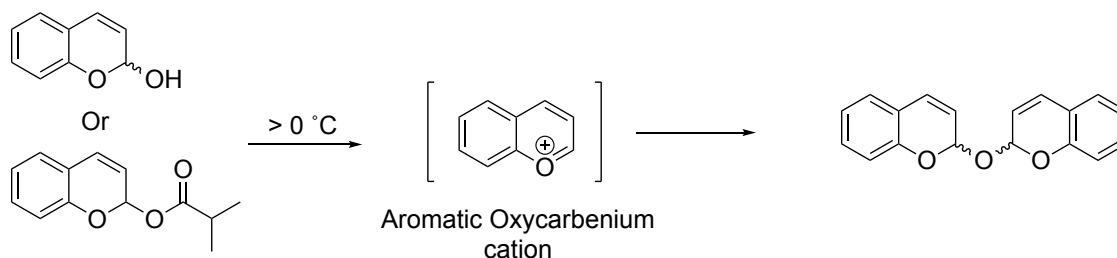
B) Natural product targets



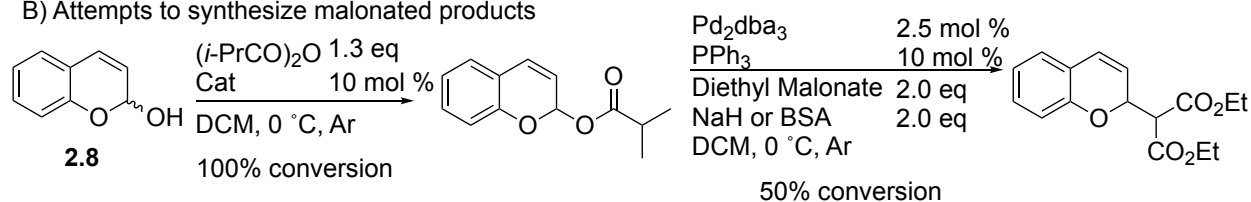
Scheme 2.7. Coumarin lactol synthesis and natural product synthetic targets.

I wanted to extend our BTM catalyzed DKEA chemistry beyond Achmatowicz lactols. I decided to focus on coumarin derived lactols because they are easy to synthesize from coumarins, many of which are commercially available (**Scheme 2.7A**), If they can be stereoselectively acylated then Tsuji-Trost reactions with C-nucleophiles should yield biologically interesting natural products^[34] (**Scheme 2.7B**), and there is a a question of selectivity because these lactols have π -systems on both sides of the hydroxyl group.

A) Dimer formation via an aromatic oxycarbenium cation



B) Attempts to synthesize malonated products

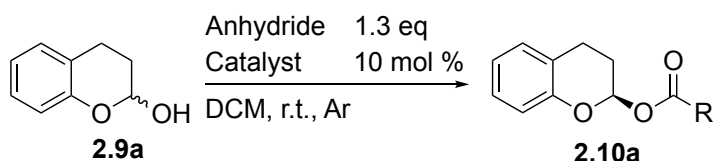


Scheme 2.8. Problems with coumarin derived lactols.

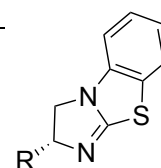
Following a literature procedure, I reduced coumarin to lactol **2.8**.^[35] I noticed that after a few hours on the bench top, the lactol, which is a clear colorless oil, had developed a white crystalline precipitate. I decided to attempt the DKEA reaction with this sample and planned to keep the lactol in the freezer in the future. Subjecting **2.8** to acylation conditions yielded no acylated product. Taking a closer look at the white precipitate, I determined that the precipitate is a dimer of the lactol that forms via an aromatic oxycarbenium cation (**Scheme 2.8A**). Obviously putting an acyl group on the lactol results in an even more unstable product. I attempted to run the DKEA reaction at $0\text{ }^\circ\text{C}$ and then take that crude reaction mixture and subject it to Tsuji-Trost conditions. I was able to get complete conversion to crude acylated products, but observed poor conversion to malonated products via the Tsuji-Trost reaction (**Scheme 2.8B**). The conversion is limited because the DMAP or BTM from the acylation binds

to and deactivates the Pd catalyst and there are no conditions that will remove the nucleophilic catalysts that are mild enough to leave the acylated lactol intact. I determined that this DKEA reaction was not worth pursuing further as both the substrates and products are difficult to purify and store. If the alkene in the coumarins is reduced before the lactone, the resulting lactol, a 2-chromanol, cannot form an aromatic oxycarbenium cation and should be a more stable substrate.

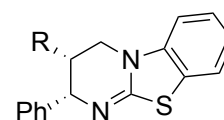
2.4 DKEA of 2-Chromanols



Entry	Catalyst	Anhydride	ee (%)	Yield (%)
1	(<i>R</i>)-BTM	(<i>i</i> -PrCO) ₂ O	96	95
2	(<i>R</i>)-BTM	Ac ₂ O	89	86
3	(<i>R</i>)-BTM	(EtCO) ₂ O	-	87
4	(<i>R</i>)-BTM	Piv ₂ O	-	-
5	(<i>R</i>)- <i>i</i> -Pr-BTM	(<i>i</i> -PrCO) ₂ O	93	90
6	(<i>R</i>)-Bn-BTM	(<i>i</i> -PrCO) ₂ O	82	84
7	(<i>R</i>)-HBTM	(<i>i</i> -PrCO) ₂ O	-92	79
8	(<i>S</i>)-HBTM-2.1	(<i>i</i> -PrCO) ₂ O	96	88
9	(<i>S</i>)-Tetramisole	(<i>i</i> -PrCO) ₂ O	-85	75



R = Ph: (*R*)-BTM
 R = *i*-Pr: (*R*)-*i*-Pr-BTM
 R = Bn: (*R*)-Bn-BTM



R = H: (*S*)-HBTM
 R = *i*-Pr: (*S*)-HBTM-2.1

Table 2.1. Condition screening for the DKSA of 2-chromanols.

Chromanol is a prevalent structural motif in bioactive natural products and pharmaceutical agents.^[36] Various chromanol derivatives can also be used as intermediates for the synthesis of other bioactive compounds. For example, Maguire and co-workers recently screened a variety of hydrolase enzymes for the DKEA of 2-chromanols in an attempt to develop a more practical synthesis of the anti-muscarinic drugs tolterodine and fesoterodine.^[37] Although up to 88%

conversion and 92% ee could be achieved in two model systems, 2-chromanol and 3-methyl-2-chromanol, the substrate scope was very limited. They were not able to achieve high enantioselectivity together with efficient conversion for other substituted 2-chromanols using the same panel of enzymes. I was able to obtain high yields and enantioselectivity for a broad range of 2-chromanols. This represents the first example of small molecule-mediated DKEA of lactols beyond dihydropyranone-type Achmatowicz rearrangement products.

2-Chromanol (**2.9a**) was chosen as the model substrate for the DKEA reaction. Much to my surprise, the initial conditions I tried (entry 1, **Table 2.1**) using (*R*)-BTM as a catalyst and isobutyric anhydride as the acylating reagent produced both high enantioselectivity and high yields. Stereochemistry of the product was tentatively assigned based on our previous results on the DKDA of dihydropyranones. Next, anhydride acylating reagents were screened (entries 2–4). While acetic and propionic anhydride could achieve similar yields to isobutyric anhydride, they gave lower enantioselectivities. Fortunately, I found that pivalic anhydride showed no reactivity, which implied that it should be possible to use a mixed anhydride method to acylate 2-chromanols. Catalysts were then screened. (*R*)-*i*-Pr-BTM and (*R*)-Bn-BTM both showed small decreases in activity and selectivity when compared to (*R*)-BTM (entries 5 and 6). HBTM ((*R*)-homo-BTM) and H-*i*-Pr-BTM can achieve similar ees to (*R*)-BTM, however, they give slightly lower yields (entries 7 and 8). (*R*)-homo-BTM (HBTM) catalyst yields the opposite enantiomer comparing to (*R*)-BTM. Finally, (*S*)-tetramisole provides a lower yield and selectivity than BTM catalyst (entry 9).

I then applied our optimized conditions to a variety of substituted 2-chromanols (**Table 2.2**). The enantiomeric product (*ent*-**2.10a**) was prepared in high optical purity by switching the catalyst to (*S*)-BTM (entry 2). The DKEA reaction tolerates a variety of substituents such as the 6-methoxy group in **2.10b**, 5-acyloxy group in **2.10c**, 5-benzyloxy group in **2.10d**, and 4-aryl group in **2.10e**. Fused benzene or cyclohexane motifs are also well tolerated (**2.10f** and **2.10g**). Both electron donating methoxy and electron withdrawing fluorine atoms can be tolerated on the 4-position, as shown in products **2.10h** and **2.10i**. Lastly, the corresponding free lactol of

compound **2.10j** was an intermediate used as a racemic mixture of four stereoisomers in the synthesis of antimuscarinic drugs tolterodine and fesoterodine.^[38] The 4-phenyl stereogenic center was resolved at the end of the synthesis. To develop a more practical synthesis, Maguire and co-workers attempted to synthesize and resolve the two acylated lactol diastereomers such as **2.10j**, but the enzymatic approach could not tolerate the necessary 4-phenyl motif.^[37] It is well tolerated by BTM type catalysts in my DKDA.

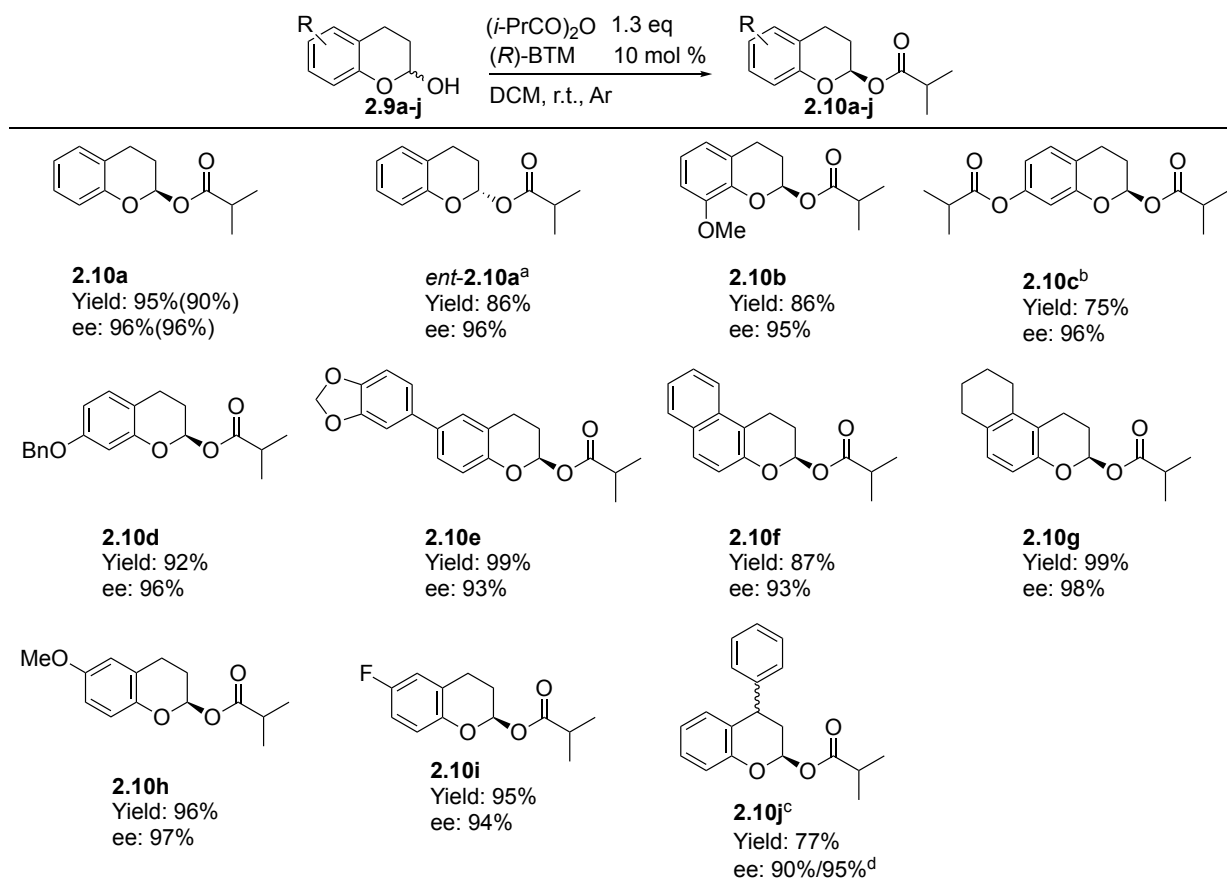
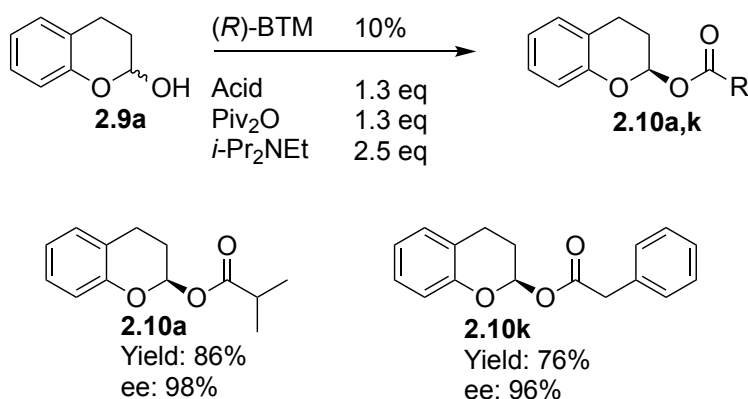


Table 2.2. Substrate scope of the DKEA. Conditions: 0.1 mmol of substrate in 1 mL of DCM. Reaction was monitored via TLC and quenched when complete. Typical reaction time was 1-1.5 hours. a: Reaction run with S-BTM in place of R-BTM. b: Reaction run with 2.6 equivalents of anhydride. c: Reaction run in amylene stabilized chloroform instead of DCM. d: cis/trans % ee.

Next, I tested the mixed anhydride conditions using compound **2.9a** as a substrate as shown in **Scheme 2.9**. Both isobutyric acid and phenylacetic acid gave acylated products in high yield and ee. This allows for the use of acyl groups, not commercially available as anhydrides, to be used in the acylation of chiral lactols.



Scheme 2.9. Mixed anhydride DKDA of 2-chromanols.

I was intrigued by the exceptional enantioselectivity of the DKEA and performed DFT calculations to identify the source of this selectivity. We have previously shown that a cation-*n* interaction dictates the BTM-catalyzed site-selective acylation of carbohydrate hydroxyl groups.^[16] I hypothesized that the stereoselectivity of the DKEA of 2-chromanols is also dictated by a similar of cation-*n* interaction.

The lowest energy transition state for the (*R*)-BTM catalyzed DKEA of **2.9a**, **2.9a-TS1**, leads to the experimentally observed (*R*)-product (**Figure 2.2**). As I hypothesized, it features a cation-*n* interaction with the endo-oxygen of **2.9a** pointing at the catalyst. The lowest energy transition state leading to the (*S*) product, **2.9a-TS2**, lacks this cation-*n* interaction. The $\Delta\Delta G^\ddagger$ for **2.9a-TS1** and **2.9a-TS2** is 3.4 Kcal/mol, which agrees with the high degree of ee obtained experimentally.

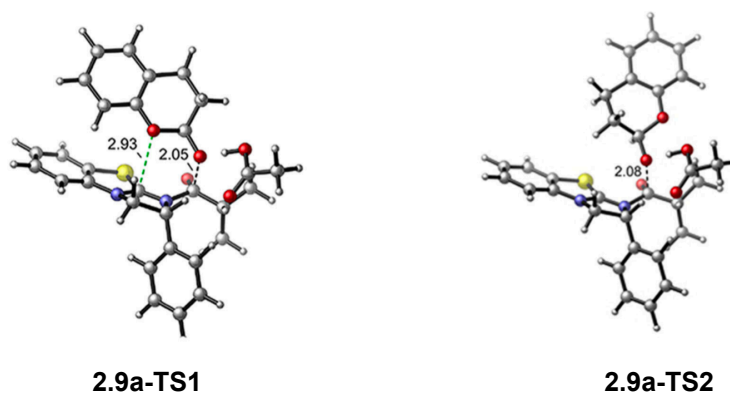


Figure 2.2. Transition States for the DKFA of **2.9a**. (The cation-*n* interaction in **2.9a-TS1** is highlighted as the green dotted line. Structures were optimized using the m062x/6-31G(d) level of theory. Single point energies were calculated using the m062x/6-311++G(d,p)/SMD level of theory.)

In summary, I have developed a practical and general method for the DKFA of 2-chromanols using BTM catalysts with high yields and ees. I propose that the high enantioselectivity is controlled by a cation-*n* interaction between the acylated catalyst and the endo-oxygen of the 2-chromanol. This method can be potentially used for the synthesis of various bioactive chiral compounds, such as antimuscarinic drugs tolterodine and fesoterodine.

2.5 References

- (1) H. Oh, J. B. Gloer, C. A. Shearer, *J. Nat. Prod.* **1999**, 62, 497
- (2) M. Massias, S. Rebuffat, L. Molho, A. Chiaroni, C. Riche, B. Bodo, *J. Am. Chem. Soc.* **1990**, 112, 8112.
- (3) D. B. Stierle, A. A. Stierle, T. Bugni, *J. Org. Chem.* **2003**, 68, 4966.
- (4) a) J. A. Giles, J. N. Schumacher, *Tetrahedron* **1961**, 14, 246; b) A. G. Gonzalez, C. G. Francisco, R. Freire, R. Hernandez, J. A. Salazar, E. Suarez, *Tetrahedron Lett.* **1976**, 1897.
- (5) O. Achmatowicz, P. Bukowski, B. Szechner, Z. Zwierzch, A. Zamojski, *Tetrahedron* **1971**, 27, 1973.
- (6) a) A. Z. Aljahdali, P. Shi, Y. S. Zhong, G. A. O'Doherty, in *Advances in Carbohydrate Chemistry and Biochemistry, Vol 69, Vol. 69* (Ed.: D. Horton), **2013**, pp. 55; b) M. F. Cuccarese, J. J. Li, G. A. O'Doherty, in *Modern Synthetic Methods in Carbohydrate Chemistry: From Monosaccharides to Complex Glycoconjugates* (Eds.: D. B. Werz, S. Vidal), **2014** Wiley-VCH Verlag GmbH & Co. KGaA, Weinheim, **2014**, pp. 1; c) W. Song, S. Wang, W. Tang, *Chem. Asian J.* **2017**, 12, 1027.
- (7) a) R. S. Babu, G. A. O'Doherty, *J. Am. Chem. Soc.* **2003**, 125, 12406–12407.; b) R. S. Babu, M. Zhou, G. A. O'Doherty, *J. Am. Chem. Soc.* **2004**, 126, 3428.; c) M. Zhou, G. A. O'Doherty, *Org. Lett.* **2006**, 8, 4339.
- (8) a) M. van den Heuvel, A. D. Cuiper, H. van der Deen, R. M. Kellogg, B. L. Feringa, *Tetrahedron Lett.* **1997**, 38, 1655–1658.; b) T. Benkovics, A. Ortiz, Z. Guo, A. Goswami, P. Deshpande, *Org. Synth.* **2014**, 91, 293 – 306.
- (9) a) G. C. Fu, *Acc. Chem. Res.* **2004**, 37, 542.; b) C. E. Mueller, P. R. Schreiner, *Angew. Chem., Int. Ed.* **2011**, 50, 6012.
- (10) a) V. B. Birman, X. Li, *Org. Lett.* 2006, 8, 1351–1354.; b) X. Li, H. Jiang, E. W. Uffman, L. Guo, Y. Zhang, X. Yang, V. B. Birman, *J. Org. Chem.* **2012**, 77, 1722.
- (11) X. Yang, G. Lu, V. B. Birman, *Org. Lett.* **2010**, 12, 892.
- (12) G. Lu, V. B. Birman, *Org. Lett.* 2011, 13, 356.
- (13) a) C. I. Sheppard, J. L. Taylor, S. L. Wiskur, *Org. Lett.* **2011**, 13, 3794.; b) L. Wang, R. K. Akhiani, S. L. Wiskur, *Org. Lett.* **2015**, 17, 2408.
- (14) a) H. -y. Wang, K. Yang, S. R. Bennett, S. -r. Guo, W. Tang, *Angew. Chem., Int. Ed.* **2015**, 54, 8756.; b) X. Wu, X. Li, A. Zanotti-Gerosa, A. Pettman, J. Liu, A. J. Mills, J. Xiao, *Chem. - Eur. J.* **2008**, 14, 2209.; c) M. P. Croatt, E. M. Carreira, *Org. Lett.* **2011**, 13, 1390.
- (15) a) Yang, X.; Liu, P.; Houk, K. N.; Birman, V. B. *Angew. Chem., Int. Ed.* **2012**, 5, 9638.; b) Li, X.; Liu, P.; Houk, K. N.; Birman, V. B. *J. Am. Chem. Soc.* **2008**, 130, 13836. c) Liu, P.; Yang, X.; Birman, V. B.; Houk, K. N. *Org. Lett.* **2012**, 14, 3288.
- (16) G. Xiao, G. A. Cintron-Rosado, D. A. Glazier, B.-M. Xi, C. Liu, P. Liu, W. Tang, *J. Am. Chem. Soc.* **2017**, 139, 4346.
- (17) S. I. Elshahawi, K. A. Shaaban, M. K. Kharel, J. S. Thorson, *Chem. Soc. Rev.* **2015**, 44, 7591–7697.
- (18) T. Paululat, A. Kulik, H. Hausmann, A. D. Karagouni, H. Zinecker, J. F. Imhoff, H. P. Fiedler, *Eur. J. Org. Chem.* **2010**, 2344.
- (19) a) T. C. Sparks, G. D. Crouse, G. Durst, *Pest Manage. Sci.* **2001**, 57, 896; b) H. A. Kirst, *J. Antibiot.* **2010**, 63, 101.
- (20) a) H. Schmitz, S. D. Juninski, I. R. Hooper, K. E. Crook, K. E. Price, J. Lein, *J. Antibiot.* **1965**, 18, 82; b) P. Walter, H. A. Lardy, D. Johnson, *J. Biol. Chem.* **1967**, 242, 5014; c) C. L. Stevens, G. E. Gutowski, C. P. Bryant, R. P. Glinski, *Tetrahedron Lett.* **1969**, 15, 1181; d) M. Galanis, J. R. Mattoon, P. Nagley, *FEBS Lett.* **1989**, 249, 333; e) H. A. Kirst, J. S. Mynderse, J. W. Martin, P. J. Baker, J. W. Paschal, J. L. R. Steiner, E. Lobkovsky, J. Clardy, *J. Antibiot.* **1996**, 49, 162.
- (21) a) M. Maruyama, C. Nishida, Y. Takahashi, H. Nagana- wa, M. Hamada, T. Takeuchi, *J. Antibiot.* **1994**, 47, 952; b) Y. Zhang, Q. Ye, X. Wang, Q.-B. She, J. S. Thorson, *Angew. Chem. Int. Ed.* **2015**, 54, 11219.

- (22) a) A. F. G. Bongat, A. V. Demchenko, *Carbohydr. Res.* **2007**, 342, 374; b) L. Zhang, N. Ding, W. Zhang, P. Wang, Y. Li, *Chinese Journal of Organic Chemistry*, **2011**, 31, 1553; c) S. Mirabella, F. Cardona, A. Goti, *Org. Biomol. Chem.* **2016**, 14, 5186.
- (23) a) E. L. Albano, D. Horton, *Carbohydr. Res.* **1969**, 11, 485; b) A. Malik, N. Afza, W. Voelter, *Liebigs Ann. Chem.* **1984**, 636.
- (24) a) S. Inuki, K. Sato, T. Fukuyama, I. Ryu, Y. Fujimoto, *J. Org. Chem.* **2017**, 82, 1248; b) A. M. P. Koskinen, L. A. Otsomaa, *Tetrahedron* **1997**, 53, 6473; c) N. Kutsumura, S. Nishiyama, *J. Carbohydr. Chem.* **2006**, 25, 377.
- (25) a) C. L. Stevens, G. E. Gutowski, C. P. Bryant, R. P. Glinski, O. E. Edwards, G. M. Sharma, *Tetrahedron Lett.* **1969**, 10, 1181–1184.; b) H. H. Baer, Z. S. Hanna, *Carbohydr. Res.* **1981**, 94, 43–55.; c) A. Malik, N. Afza, W. Voelter, *J. Chem. Soc. Perkin Trans. 1* **1983**, 0, 2103.
- (26) a) I. Dyong, R. Knollmann, N. Jersch, *Angew. Chem. Int. Ed.* **1976**, 15, 302; b) M. Ono, C. Saotome, H. Akita, *Heterocycles* **1999**, 51, 1503; c) C. Saotome, M. Ono, H. Akita, *Chem. Pharm. Bull.* **2001**, 49, 849.
- (27) D. A. Evans, W. C. Black, *J. Am. Chem. Soc.* **1993**, 115, 4497.
- (28) a) L. F. Tietze, N. Bohnke, S. Dietz, *Org. Lett.* **2009**, 11, 2948; b) L. F. Tietze, S. Dietz, N. Boehnke, M. A. Duefert, I. Objartel, D. Stalke, *Eur. J. Org. Chem.* **2011**, 2011, 6574; c) L. F. Tietze, S. Dietz, N. Schutzenmeister, S. Biller, J. Hierold, T. Scheffer, M. M. Baag, *Eur. J. Org. Chem.* **2013**, 7305.
- (29) M. J. Zacuto, D. Tomita, Z. Pirzada, F. Xu, *Org. Lett.* **2010**, 12, 684.
- (30) Y. Bai, X. Shen, Y. Li, M. Dai, *J. Am. Chem. Soc.* **2016**, 138, 10838.
- (31) a) L. A. Paquette, Z. L. Gao, Z. J. Ni, G. F. Smith, *J. Am. Chem. Soc.* **1998**, 120, 2543; b) L. A. Paquette, I. Collado, M. Purdie, *J. Am. Chem. Soc.* **1998**, 120, 2553.
- (32) D. J. Mergott, S. A. Frank, W. R. Roush, *Proc. Natl. Acad. Sci. USA* **2004**, 101, 11955.
- (33) W. Song, Y. Zhao, J. C. Lynch, H. Kim, W. Tang, *Chem. Commun.* **2015**, 51, 17475.
- (34) F. Li, Z. Meng, J. Hua, W. Li, H. Lou, L. Liu, *Org. Biomol. Chem.* **2015**, 13, 5710–5715.
- (35) B. Padhi, D. S. Reddy, D. K. Mohapatra, *European J. Org. Chem.* **2015**, 2015, 542–547.
- (36) M. Birringer, K. Siems, A. Maxones, J. Frank, S. Lorkowski, *RSC Adv.* **2018**, 8, 4803.
- (37) D. P. Gavin, A. Foley, T. S. Moody, U. B. R. Khandavilli, S. E. Lawrence, P. O'Neill, A. R. Maguire, *Tetrahedron: Asymmetry* **2017**, 28, 577.
- (38) a) C. Botteghi, T. Corrias, M. Marchetti, S. Paganelli, O. Piccolo, *Org. Process Res. Dev.* **2002**, 6, 379; b) O. Dirat, A. J. Bibb, C. M. Burns, G. D. Checksfield, B. R. Dillon, S. E. Field, S. J. Fussell, S. P. Green, C. Mason, J. Mathew, S. Mathew, I. B. Moses, P. I. Nikiforov, A. J. Pettman, F. Susanne, *Org. Process Res. Dev.* **2011**, 15, 1010.

Supporting Information

Chapter 2: Stereoselective Acylation of Lactols

Table of Contents

General remarks.....	45
Procedures for the DKDA of Achmatowicz derived lactols.....	46
Characterization of acylated Achmatowicz derived lactols.....	46
Procedures for the reduction of dihydrocoumarins.....	49
Characterization of 2-chromanols.....	49
Procedures for the DKEA of 2-chromanols.....	53
Characterization of acylated 2-chromanols.....	53
Computational Details.....	59
References	68
Copy of NMR spectra	69
Copy of HPLC traces.....	91

General remarks:

All reactions in non-aqueous media were conducted under a positive pressure of dry argon in glassware that had been oven dried prior to use unless noted otherwise. Anhydrous solutions of reaction mixtures were transferred via an oven dried syringe or cannula. All solvents were dried prior to use unless noted otherwise. Thin layer chromatography was performed using precoated silica gel plates. Flash column chromatography was performed with silica gel (40-63 μm). Infrared spectra (IR) were obtained on a Bruker Equinox 55 Spectrophotometer. ^1H and ^{13}C nuclear magnetic resonance spectra (NMR) were obtained on a Bruker Ascend 400 MHz recorded in ppm (δ) downfield of TMS ($\delta = 0$) in CDCl_3 unless noted otherwise. Signal splitting patterns were described as singlet (s), doublet (d), triplet (t), quartet (q), quintet (quint), or multiplet (m), with coupling constants (J) in hertz. High resolution mass spectra (HRMS) were performed by Analytical Instrument Center at the School of Pharmacy or Department of Chemistry on an Electron Spray Injection (ESI) mass spectrometer. (RT = room temperature.)

Compounds **2.1** and *ent*-**2.1** were prepared according to our previously reported procedures and their spectra are in accordance with literature.^[1]

Compound **2.4** was prepared accordingly to previously reported procedures.^[2]

2,3,6-Trideoxy-hexopyranoside **2.6** was prepared stereoselectively from **2.4** and according to previously reported procedures.^[3]

We adapted a literature procedure for the Mitsunobu reaction and the following reduction.^[4]

General Synthesis of Dihydrocoumarins

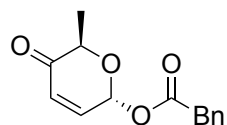
Coumarins were synthesized from substituted salicylaldehydes following two different methods from the literature. The first used dimethylacetamide (DMAc) and phosphorus(V) oxychloride,^[5] while the second employed sodium acetate and acetic anhydride.^[6] Hydrogenation of the

coumarins was accomplished by using palladium on carbon in acetic acid. The 4-phenyl dihydrocoumarin was synthesized from cinnamic acid and phenol following a known procedure.^[7]

Procedure A for BTM-catalyzed DKDA of 2.1 and *ent*-2.1 using mixed anhydride:

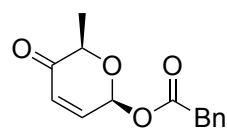
To an oven-dried flask was added **2.1** (25.6 mg, 0.2 mmol), (*R*)-BTM or (*S*)-BTM (5 mg, 0.02 mmol), *i*-Pr₂NEt (82.7 μ L, 0.5 mmol) and anhydrous CHCl₃ (1.2 mL) under Ar. The mixture was stirred at RT for 5 min before Piv₂O (52.7 μ L, 0.26 mmol) and phenyl acetic acid (35.4 mg, 0.26 mmol) were added. The reaction was stirred at RT for 12 h and monitored by TLC. After the reaction was completed, the solvent was evaporated and the residue was purified by flash column chromatography.

(2*R*,6*R*)-6-methyl-5-oxo-5,6-dihydro-2H-pyran-2-yl 2-phenylacetate (*trans*-2.2)



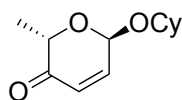
2.1 and (*R*)-BTM were used according to procedure A. 37.4 mg, The product was isolated by column chromatography on silica gel (Hexane/ethyl acetate=8:1) as a yellow oil (37.4 mg, 76%). $[\alpha]_{25} = -100.8^\circ$ (CHCl₃, *c* = 1.0). ¹H NMR (500 MHz, CDCl₃): δ 7.37 - 7.32 (m, 2H), 7.32 - 7.28 (m, 3H), 6.85 (dd, *J* = 10.0, 3.5 Hz, 1H), 6.49 (d, *J* = 3.5 Hz, 1H), 6.19 (d, *J* = 10.0 Hz, 1H), 4.45 (q, *J* = 7.0 Hz, 1H), 3.69 (s, 2H), 1.35 (d, *J* = 7.0 Hz, 3H). ¹³C NMR (126 MHz, CDCl₃): δ 196.0, 170.4, 141.6, 133.5, 129.4, 129.0, 128.6, 127.7, 87.6, 72.6, 41.6, 15.5. IR: ν 3021, 1749, 1703, 1216, 756 cm⁻¹. HRMS (ESI) *m/z* calcd. for C₁₄H₁₄O₄ + Na = 269.0784, found 269.0783.

(2*S*,6*R*)-6-methyl-5-oxo-5,6-dihydro-2H-pyran-2-yl 2-phenylacetate (*cis*-2.2)



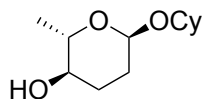
2.1 and (*S*)-BTM were used according to procedure A. The product was isolated by column chromatography on silica gel (Hexane/ethyl acetate=8:1) as a yellow oil (36.0 mg, 73%). $[\alpha]_{25} = 107.2^\circ$ (CHCl₃, *c* = 0.5). ¹H NMR (500 MHz, CDCl₃): δ 7.37 - 7.31 (m, 2H), 7.31 – 7.27 (m, 3H), 6.84 (dd, *J* = 10.0, 2.0 Hz, 1H), 6.58 – 6.55 (m, 1H), 6.20 (d, *J* = 10.0 Hz, 1H), 4.34 (q, *J* = 7.0 Hz, 1H), 3.69 (s, 2H), 1.36 (d, *J* = 7.0 Hz, 3H). ¹³C NMR (126 MHz, CDCl₃): δ 196.1, 170.2, 143.2, 133.2, 129.6, 129.0, 128.4, 127.7, 88.2, 76.1, 41.6, 18.8. IR: ν 3020, 1753, 1699, 1217, 764 cm⁻¹. HRMS (ESI) *m/z* calcd. for C₁₄H₁₄O₄ + Na = 269.0784, found 269.0784.

(2*S*,6*R*)-6-(cyclohexyloxy)-2-methyl-2H-pyran-3(6H)-one (2.4)



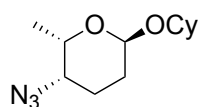
2.4 was synthesized according to our published procedure except Pd(PPh₃)₄ was used in place of Pd₂dba₃ because the dba co-eluted with the product. [site] The product was isolated by column chromatography on silica gel (pentane/ethyl acetate=9:1) as a colorless oil (185 mg, 67%). $[\alpha]_{22} = 0.62^\circ$ (CHCl₃, *c* = 0.1). ¹H NMR (400 MHz, CDCl₃) δ 6.81 (dd, *J* = 10.2, 3.5 Hz, 1H), 6.05 (d, *J* = 10.2 Hz, 1H), 5.32 (d, *J* = 3.5 Hz, 1H), 4.59 (q, *J* = 6.8 Hz, 1H), 3.70 (tt, *J* = 9.3, 3.9 Hz, 1H), 2.00 – 1.84 (m, 2H), 1.75 (ddd, *J* = 12.6, 5.7, 2.5 Hz, 2H), 1.58 – 1.51 (m, 1H), 1.49 – 1.06 (m, 8H). ¹³C NMR (101 MHz, CDCl₃) δ 197.54, 144.41, 127.34, 91.64, 77.14, 70.48, 33.68, 32.20, 25.71, 24.47, 24.30, 15.45. IR: 3019, 2936, 2859, 1699, 1451, 1398, 1374, 1233, 1217, 1157, 1127, 1103, 1082, 1029, 990, 973, 953, 890, 808, 753, 667 cm⁻¹. HRMS (ESI) *m/z* calcd. for C₁₂H₁₈O₃ + Na = 233.1148, found 233.1145.

(2*S*,3*R*,6*R*)-6-(cyclohexyloxy)-2-methyltetrahydro-2H-pyran-3-ol (2.6)



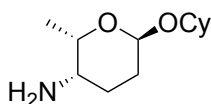
2.6 was synthesized according to a published procedure. [site] The product was isolated by column chromatography on silica gel (pentane/ethyl acetate=4:1) as a colorless oil (102 mg, 95%). $[\alpha]_{22} = -7.26^\circ$ (CHCl_3 , $c = 1.1$). $^1\text{H NMR}$ (400 MHz, CDCl_3) δ 4.89 (t, $J = 2.0$ Hz, 1H), 3.66 (dq, $J = 9.2, 6.3$ Hz, 1H), 3.55 (tt, $J = 9.1, 4.0$ Hz, 1H), 3.25 (dq, $J = 9.4, 4.2$ Hz, 1H), 2.03 – 1.62 (m, 8H), 1.62 – 1.45 (m, 2H), 1.46 – 1.00 (m, 8H). $^{13}\text{C NMR}$ (101 MHz, CDCl_3) δ 93.84, 74.20, 72.52, 69.62, 33.75, 31.85, 30.34, 27.86, 25.93, 24.61, 24.30, 18.08. IR: 3409, 2932, 2857, 1649, 1451, 1360, 1261, 1228, 1195, 1118, 1048, 1026, 991, 976, 935, 890, 870, 851, 799, 755, 666 cm^{-1} . HRMS (ESI) m/z calcd. for $\text{C}_{12}\text{H}_{22}\text{O}_3 + \text{Na} = 237.1461$, found 237.1457.

(2S,3S,6R)-3-azido-6-(cyclohexyloxy)-2-methyltetrahydro-2H-pyran (2.7)



2.7 was synthesized from **2.6** according to an adapted literature procedure. The product was isolated by column chromatography on silica gel (pentane/ethyl acetate=19:1) as a colorless oil (31.6 mg, 60%). $[\alpha]_{22} = -6.07^\circ$ ($c = 0.8$, CHCl_3) $^1\text{H NMR}$ (400 MHz, CDCl_3) δ 4.96 (d, $J = 3.4$ Hz, 1H), 4.08 (qd, $J = 6.6, 1.8$ Hz, 1H), 3.54 (tt, $J = 9.0, 4.0$ Hz, 1H), 3.44 (dt, $J = 3.9, 2.4$ Hz, 1H), 2.25 – 2.07 (m, 1H), 2.02 – 1.79 (m, 4H), 1.79 – 1.65 (m, 2H), 1.63 – 1.48 (m, 2H), 1.43 – 1.06 (m, 8H). $^{13}\text{C NMR}$ (101 MHz, CDCl_3) δ 94.64, 74.54, 65.35, 60.39, 33.76, 31.92, 25.90, 24.85, 24.57, 24.27, 23.24, 18.18. IR: 2933, 2858, 2098, 1450, 1383, 1258, 1344, 1320, 1271, 1236, 1215, 1117, 1084, 1062, 1050, 1021, 994, 978, 936, 890, 790, 760 cm^{-1} . HRMS (ESI) m/z calcd. for $\text{C}_{12}\text{H}_{21}\text{N}_3\text{O}_2 + \text{Na} = 262.1525$, found 262.1522.

(2S,3S,6R)-6-(cyclohexyloxy)-2-methyltetrahydro-2H-pyran-3-amine (2.5)

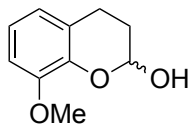


2.5 was synthesized from **2.7** according to an adapted literature procedure. The product was isolated by column chromatography on silica gel (DCM/MeOH=15:1) as an off white solid (19.4 mg, 70%). $[\alpha]_D^{25} = -20.1^\circ$ ($c = 0.6$, CHCl_3) $^1\text{H NMR}$ (400 MHz, CDCl_3) δ 4.86 (d, $J = 3.7$ Hz, 1H), 4.01 (qd, $J = 6.6, 1.7$ Hz, 1H), 3.48 (dp, $J = 9.1, 4.1$ Hz, 1H), 2.67 (t, $J = 3.3$ Hz, 1H), 2.04 (tt, $J = 13.6, 4.1$ Hz, 1H), 1.86 (dtt, $J = 32.8, 8.9, 4.5$ Hz, 6H), 1.74 – 1.58 (m, 2H), 1.57 – 1.35 (m, 2H), 1.35 – 1.08 (m, 5H), 1.05 (d, $J = 6.6$ Hz, 3H). $^{13}\text{C NMR}$ (101 MHz, CDCl_3) δ 94.92, 74.31, 66.07, 48.85, 33.79, 31.95, 26.66, 25.93, 24.65, 24.35, 24.17, 17.81. IR: ν 3390, 2932, 2857, 2099, 1569, 1477, 1450, 1388, 1357, 1328, 1273, 1222, 1206, 1162, 1110, 1083, 1017, 995, 972, 918, 890, 816, 756, 687, 668 cm^{-1} . HRMS (ESI) m/z calcd. for $\text{C}_{12}\text{H}_{23}\text{NO}_2 + \text{Na} = 236.1621$, found 236.1615.

Procedure B for the DIBAL-H reduction of dihydrocoumarins to 2-chromanols:

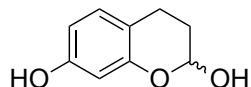
Dihydrocoumarin (148 mg, 1 mmol) was dissolved in dry DCM (1.5 mL) and the mixture was stirred under argon and cooled to -78°C . DIBAL-H (1.0M in hexanes, 1.05 mL, 1.05 mmol) was added dropwise and the reaction was let stir for a half hour. A drop of water was added to the reaction to quench and the reaction was allowed to warm to room temperature. TLC in DCM was performed to check conversion to the desired product. TLC in hexanes/ethyl acetate 2:1 was performed to determine if any over over-reduction had taken place (the product and starting material are separable in DCM, but not EA/hex. The reverse is true for the desired product and the over-reduced product.) The quenched reaction mixture was filtered through a pad of celite and the solvent was removed under reduced pressure. Purification of the crude product by column chromatography on silica gel using DCM afforded the desired product.

2-Hydroxy-8-methoxy-chroman (2.9b)



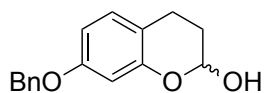
Synthesized according to procedure B. The product was isolated by column chromatography on silica gel (DCM) as an amorphous solid (31.3 mg, 87%). ¹H NMR (400 MHz, CDCl₃) δ 6.84 (t, J = 7.8 Hz, 1H), 6.72 (dd, J = 16.0, 7.9 Hz, 2H), 5.76 (q, J = 3.3 Hz, 1H), 3.87 (s, 3H), 3.34 (dd, J = 3.7, 1.7 Hz, 1H), 3.18 – 2.90 (m, 1H), 2.69 (ddd, J = 16.3, 5.7, 4.1 Hz, 1H), 2.15 – 1.83 (m, 2H). ¹³C NMR (101 MHz, CDCl₃) δ 148.3, 141.2, 122.9, 121.3, 120.3, 109.2, 92.0, 55.8, 26.6, 19.9. IR: 3450, 3017, 2939, 1615, 1587, 1482, 1463, 1441, 1336, 1263, 1210, 1186, 1146, 1098, 1078, 1005, 957, 945, 868, 846, 750 cm⁻¹. HRMS (ESI): calcd. for C₁₀H₁₂O₃ + Na = 203.0679, found 203.0676.

2,7-Dihydroxy-chroman (2.9c)



Synthesized according to a modified procedure B. DIBAL-H (1.0M hexanes, 2.1 mL, 2.1 mmol) was used. The product was isolated by column chromatography on silica gel (DCM) as an amorphous solid (82.9 mg, 50%). ¹H NMR (400 MHz, DMSO-d₆) δ 9.07 (s, 1H), 6.90 (d, J = 5.0 Hz, 1H), 6.80 (d, J = 8.2 Hz, 1H), 6.25 (dd, J = 8.2, 2.4 Hz, 1H), 6.12 (d, J = 2.4 Hz, 1H), 5.39 (dd, J = 8.0, 3.0 Hz, 1H), 3.32 (s, 1H), 2.70 (dt, J = 15.7, 7.8 Hz, 1H), 1.79 (td, J = 7.9, 6.8, 3.9 Hz, 2H). ¹³C NMR (101 MHz, DMSO-d₆) δ 159.1, 155.9, 132.1, 115.1, 110.3, 105.6, 94.1, 30.4, 22.4. IR: 3374, 2937, 2854, 1625, 1599, 1510, 1463, 1352, 1296, 1260, 1241, 1211, 1152, 1117, 1093, 1057, 1042, 1002, 967, 929, 914, 887 cm⁻¹. HRMS (ESI): calcd. for C₉H₁₀O₃ + Na = 189.0522, found 187.0363 = C₉H₈O₃ + Na

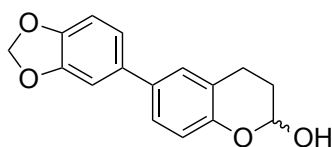
2-Hydroxy-7-benzyloxy-chroman (2.9d)



Synthesized according to procedure B. The product was isolated by column chromatography on silica gel (DCM) as an amorphous solid (165.9 mg, 65%). ¹H NMR (400 MHz, CDCl₃) δ 7.55 – 7.30 (m, 5H), 6.96 (d, J = 8.4 Hz, 1H), 6.55 (dd, J = 8.4, 2.6 Hz, 1H), 6.46 (d, J = 2.5 Hz, 1H),

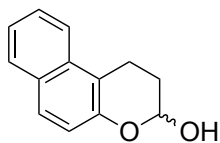
5.58 (td, $J = 4.2, 2.6$ Hz, 1H), 5.01 (s, 2H), 2.97 (dd, $J = 4.5, 1.3$ Hz, 1H), 2.90 (ddd, $J = 16.3, 10.3, 6.2$ Hz, 1H), 2.64 (dt, $J = 16.0, 5.3$ Hz, 1H), 2.15 – 1.85 (m, 2H). ^{13}C NMR (101 MHz, CDCl_3) δ 152.7, 137.1, 129.7, 128.6, 127.9, 127.4, 114.3, 108.4, 103.1, 100.0, 92.2, 70.1, 27.2, 19.6. IR: 3410, 3029, 2939, 1877, 1621, 1584, 1505, 1454, 1380, 1351, 1301, 1254, 1214, 1154, 1124, 1092, 1055, 1042, 1025, 1003, 961, 911, 888, 836, 753 cm^{-1} . HRMS (ESI): calcd. for $\text{C}_{16}\text{H}_{16}\text{O}_3 + \text{H} = 257.1172$, found 257.1167.

2-Hydroxy-6-(benzo-1,3-dioxole)-chroman (2.9e)



Synthesized according to procedure B. The product was isolated by column chromatography on silica gel (DCM) as an amorphous solid (41.4 mg, 50%). ^1H NMR (400 MHz, CDCl_3) δ 7.27 (d, $J = 6.8$ Hz, 1H), 7.23 – 7.21 (m, 1H), 7.06 – 6.92 (m, 2H), 6.85 (dd, $J = 8.2, 5.3$ Hz, 2H), 5.98 (s, 2H), 5.65 (d, $J = 2.7$ Hz, 1H), 3.13 – 2.91 (m, 2H), 2.75 (dt, $J = 16.4, 5.2$ Hz, 1H), 2.22 – 1.92 (m, 2H). ^{13}C NMR (101 MHz, CDCl_3) δ 151.3, 148.0, 146.6, 135.4, 133.9, 127.7, 126.0, 122.2, 120.1, 117.3, 108.5, 107.4, 101.1, 92.2, 27.0, 20.3. IR: 3400, 3018, 2958, 1609, 1583, 1500, 1479, 1448, 1344, 1225, 1169, 1126, 1097, 1040, 999, 954, 916, 866, 808, 750 cm^{-1} . HRMS (ESI): calcd. for $\text{C}_{16}\text{H}_{14}\text{O}_4 = 270.0892$, found 270.0877.

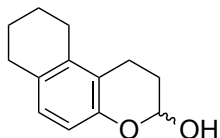
2,3-Dihydro-1H-benzo[f]chromen-3-ol (2.9f)



Synthesized according to procedure B. The product was isolated by column chromatography on silica gel (DCM) as an amorphous solid (123 mg, 71%). ^1H NMR (400 MHz, CDCl_3) δ 7.85 (dd, $J = 8.5, 1.0$ Hz, 1H), 7.76 (dt, $J = 8.2, 0.9$ Hz, 1H), 7.65 (d, $J = 8.8$ Hz, 1H), 7.50 (ddd, $J = 8.4,$

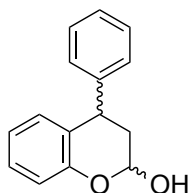
6.8, 1.4 Hz, 1H), 7.36 (ddd, $J = 8.0, 6.8, 1.2$ Hz, 1H), 7.05 (d, $J = 8.9$ Hz, 1H), 5.68 (td, $J = 4.4, 2.5$ Hz, 1H), 3.27 – 3.07 (m, 2H), 3.04 (dd, $J = 4.7, 1.3$ Hz, 1H), 2.39 – 2.08 (m, 2H). ^{13}C NMR (101 MHz, CDCl_3) δ 149.2, 132.7, 129.2, 128.4, 128.0, 126.4, 123.5, 122.0, 118.9, 113.8, 92.0, 27.0, 17.2. HRMS (ESI): calcd. for $\text{C}_{13}\text{H}_{12}\text{O}_2 + \text{Na} = 223.0730$, found 223.0727.

1H-Naphtho[2,1-b] pyran-3-ol,2,3,7,8,9,10-hexahydro- (2.9g)



Synthesized according to procedure B. The product was isolated by column chromatography on silica gel (DCM) as an amorphous solid (70.0 mg, 69%). ^1H NMR (400 MHz, CDCl_3) δ 6.87 (d, $J = 8.3$ Hz, 1H), 6.64 (d, $J = 8.3$ Hz, 1H), 5.56 (td, $J = 4.2, 2.4$ Hz, 1H), 2.96 (dd, $J = 4.4, 1.4$ Hz, 1H), 2.85 – 2.66 (m, 4H), 2.66 – 2.43 (m, 3H), 2.16 – 1.92 (m, 2H), 1.91 – 1.65 (m, 3H). ^{13}C NMR (101 MHz, CDCl_3) δ 149.5, 135.6, 129.7, 128.0, 120.0, 114.5, 91.5, 29.5, 27.0, 26.2, 23.2, 22.9, 17.7. IR: 3409, 3017, 2932, 2858, 1598, 1480, 1417, 1323, 1301, 1240, 1215, 1104, 1074, 1054, 987, 959, 891, 829, 802, 753 cm^{-1} . HRMS (ESI): calcd. for $\text{C}_{13}\text{H}_{16}\text{O}_2 + \text{Na} = 227.1043$, found 227.1038.

(±)-4-phenylchroman-2-ol (2.9j)



Synthesized according to procedure B. The product was isolated by column chromatography on silica gel (DCM) as an amorphous solid (138.5 mg, 70%) as a 3:1 mixture of diastereomers. Proton NMR data is tabulated for the major isomer. ^1H NMR (400 MHz, CDCl_3) δ 7.30 (dd, $J = 8.1, 6.5$ Hz, 3H), 7.21 – 7.15 (m, 3H), 6.83 – 6.74 (m, 3H), 5.63 (q, $J = 3.3$ Hz, 1H), 4.32 (dd, $J =$

11.1, 5.8 Hz, 1H), 3.90 – 3.76 (m, 1H), 2.26 (ddd, $J = 13.5, 5.8, 3.6$ Hz, 1H), 2.18 – 2.08 (m, 1H). ^{13}C NMR (101 MHz, CDCl_3) δ 153.4, 151.9, 144.3, 143.9, 129.7, 129.5, 128.9, 128.9, 128.8, 128.8, 128.7, 128.6, 128.1, 128.0, 127.0, 126.8, 125.5, 125.3, 121.1, 121.1, 117.0, 116.9, 94.5, 91.4, 41.5, 38.7, 36.9, 36.2. IR: 3416, 3062, 3030, 2962, 1725, 1604, 1488, 1453, 1299, 1221, 1055, 1016, 944, 917, 895, 754, 737, 701 cm^{-1} . HRMS (ESI): calcd. for $\text{C}_{15}\text{H}_{14}\text{O}_2 + \text{Na} = 249.0886$, found 249.0891.

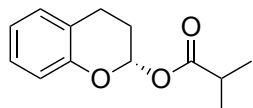
Procedure C for the DKEA of 2-chromanols using anhydride:

(*R*)- or (*S*)-BTM (2.5 mg, 0.01 mmol) and 2-chromanol (0.1 mmol) were dissolved in DCM (1 mL). Isobutyric anhydride (0.019 mL, 0.115 mmol) was added and the reaction was capped and stirred under argon. The reaction was monitored via TLC. When the reaction was deemed complete (usually 1.5-2 h) 0.5 mL of MeOH was added and the reaction was stirred for another 30 min. The solvent was removed under vacuum. Purification of the crude product by column chromatography on silica gel using DCM afforded the desired product. The ee of the isolated products were determined via chiral HPLC.

Procedure D for the DKEA of 2-chromanols used mixed anhydride:

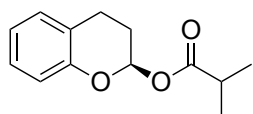
(*R*)- or (*S*)-BTM (2.5 mg, 0.01 mmol) and 2-chromanol (0.1 mmol) were dissolved in amylene stabilized chloroform (1 mL). Pivalic anhydride (0.026 mL, 0.13 mmol), *i*- Pr_2NEt (0.042 mL, 0.25 mmol) and acid (0.13 mmol) were added and the reaction was capped and stirred under argon. The reaction was monitored via TLC. After 18 hours 0.5 mL of MeOH was added and the reaction was stirred for another 30 min. The solvent was removed under vacuum. Purification of the crude product by column chromatography on silica gel using DCM afforded the desired product. The ee of the isolated products were determined via chiral HPLC.

2H-1-Benzopyran-2-ol, 3, 4-dihydro-, 2-isobutylate, (2*S*)- (*ent*-2.10a)



2.9a and (*S*)-BTM were used according to procedure C. The product was isolated by column chromatography on silica gel (DCM) as a colorless oil (18.9 mg, 86%). ¹H NMR (400 MHz, CDCl₃) δ 7.20 – 7.02 (m, 2H), 7.02 – 6.81 (m, 2H), 6.53 (t, J = 2.7 Hz, 1H), 2.98 (ddd, J = 16.4, 12.4, 6.1 Hz, 1H), 2.71 (ddd, J = 16.3, 5.8, 2.9 Hz, 1H), 2.53 (hept, J = 7.0 Hz, 1H), 2.15 – 1.98 (m, 2H), 1.15 (d, J = 7.0 Hz, 3H), 1.12 (d, J = 7.0 Hz, 3H). ¹³C NMR (101 MHz, CDCl₃) δ 175.8, 151.6, 129.2, 127.6, 121.7, 121.3, 117.1, 90.1, 34.1, 25.1, 19.7, 18.8, 18.7. IR: 2976, 2983, 1745, 1613, 1585, 1492, 1459, 1388, 1351, 1326, 1302, 1277, 1227, 1191, 1177, 1143, 1111, 1047, 1013, 950, 921, 898, 844, 815, 755 cm⁻¹. [α]_D²⁵ = -153.1° (c 0.995, CHCl₃). HRMS (ESI): calcd. for C₁₃H₁₆O₃ + Na = 243.0992, found 243.0989. HPLC Column: OD-H, 1:99 IPA/Hex, 1 mL/min, 220 nm, ee = 96 %

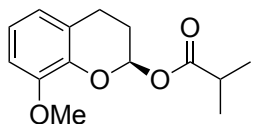
2H-1-Benzopyran-2-ol, 3, 4-dihydro-, 2-isobutylate, (2*R*)- (2.10a)



2.9a and (*R*)-BTM were used according to procedure C. The product was isolated by column chromatography on silica gel (DCM) as a colorless oil (20.9 mg, 95%). Spectroscopic data are identical to *ent*-**2.10a**. [α]_D²⁵ = 150.8° (c 1.07, CHCl₃). HPLC Column: OD-H, 1:99 IPA/Hex, 1 mL/min, 220 nm, ee = 96 %. Synthesis via mixed anhydride procedure D: Yield 86%, ee = 98%.

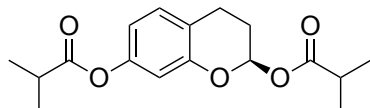
Large scale synthesis: Catalyst ((*R*)-BTM, 61.2 mg, 0.243 mmol) and **2.9a** (365 mg, 2.43 mmol) were dissolved in DCM (24.3 mL). Isobutyric anhydride (0.527 mL, 3.17 mmol) was added and the reaction was capped and stirred under argon. Obtained 480 mg of a colorless oil. Yield 90%, ee = 96%

2H-1-Benzopyran-2-ol, 3, 4-dihydro-8-methoxy, 2-isobutylate, (2*R*) - (2.10b)



2.9b and (*R*)-BTM were used according to procedure C. The product was isolated by column chromatography on silica gel (DCM) as a colorless oil (21.5 mg, 86%). ¹H NMR (400 MHz, CDCl₃) δ 6.80 (t, *J* = 7.9 Hz, 1H), 6.69 (d, *J* = 8.0 Hz, 1H), 6.63 (d, *J* = 7.6 Hz, 1H), 6.57 (d, *J* = 2.6 Hz, 1H), 3.78 (s, 3H), 2.88 (ddd, *J* = 16.5, 12.7, 6.0 Hz, 1H), 2.63 (ddd, *J* = 16.3, 5.9, 2.7 Hz, 1H), 2.47 (hept, *J* = 7.0 Hz, 1H), 2.12 – 2.04 (m, 1H), 2.02 – 1.92 (m, 1H), 1.08 (d, *J* = 7.1 Hz, 3H), 1.06 (d, *J* = 7.0 Hz, 3H). ¹³C NMR (101 MHz, CDCl₃) δ 174.5, 147.4, 140.1, 121.5, 120.1, 119.8, 108.9, 89.6, 55.0, 33.0, 24.0, 18.5, 17.9, 17.5. IR: 3024, 2976, 2940, 2839, 1744, 1615, 1589, 1485, 1442, 1389, 1329, 1267, 1221, 1198, 1183, 1144, 1103, 1046, 1018, 964, 942, 899, 869, 841, 800, 757 cm⁻¹. [α]_D²⁵ = 87.6° (c 0.94, CHCl₃). HRMS (ESI): calcd. for C₁₄H₁₈O₄ + Na = 273.1097, found 273.1092. HPLC Column: OD-H, 5:95 IPA/Hex, 1 mL/min, 220 nm, ee = 95%.

2H-1-Benzopyran-2-ol, 3, 4-dihydro-7, 2-isobutylate, (2*R*) - (2.10c)

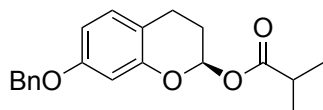


2.9c and (*R*)-BTM were used according to a modified procedure C. Isobutyric anhydride (0.038 mL, 0.26 mmol) was used. The product was isolated by column chromatography on silica gel (DCM) as a colorless oil (23.0 mg, 86%). ¹H NMR (400 MHz, CDCl₃) δ 7.06 (d, *J* = 8.2 Hz, 1H), 6.64 (dd, *J* = 8.2, 2.3 Hz, 1H), 6.60 (d, *J* = 2.3 Hz, 1H), 6.51 (t, *J* = 2.8 Hz, 1H), 2.94 (ddd, *J* = 15.7, 12.4, 6.0 Hz, 1H), 2.84 – 2.64 (m, 2H), 2.53 (hept, *J* = 7.0 Hz, 1H), 2.15 – 1.97 (m, 2H), 1.29 (d, *J* = 7.0 Hz, 6H), 1.15 (d, *J* = 7.0 Hz, 3H), 1.13 (d, *J* = 7.0 Hz, 3H). ¹³C NMR (101 MHz, CDCl₃) δ 175.7, 175.6, 152.0, 150.0, 129.5, 119.1, 114.6, 110.4, 89.8, 34.1, 34.0, 25.0, 19.3, 18.92, 18.93, 18.8, 18.6. IR: 2977, 2937, 2878, 1752, 1620, 1594, 1501, 1470, 1429, 1388, 1345, 1301, 1242, 1217, 1187, 1136, 1108, 1047, 1014, 952, 922, 893, 838, 754 cm⁻¹. [α]_D²⁵ =

92.1° (c 0.635, CHCl₃). HRMS (ESI): calcd. for C₁₇H₂₂O₅ + Na = 329.1359, found 329.1348.

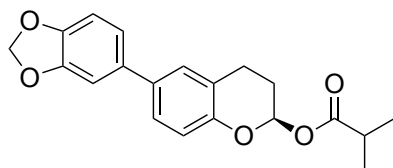
HPLC Column: OD-H, 1:99 IPA/Hex, 1 mL/min, 220 nm, ee = 96 %.

2H-1-Benzopyran-2-ol, 3, 4-dihydro-7-benzyloxy-2-isobutylate, (2R) - (2.10d)



2.9d and (*R*)-BTM were used according to procedure C. The product was isolated by column chromatography on silica gel (DCM) as an amorphous solid (30.0 mg, 92%). ¹H NMR (400 MHz, CDCl₃) δ 7.46 – 7.19 (m, 5H), 6.89 (d, *J* = 8.4 Hz, 1H), 6.51 (dd, *J* = 8.3, 2.6 Hz, 1H), 6.43 (dd, *J* = 9.7, 2.6 Hz, 2H), 4.93 (s, 2H), 2.82 (ddd, *J* = 16.0, 12.4, 5.9 Hz, 1H), 2.57 (ddd, *J* = 16.0, 5.9, 2.9 Hz, 1H), 2.46 (hept, *J* = 7.0 Hz, 1H), 2.07 – 1.86 (m, 2H), 1.08 (d, *J* = 7.0 Hz, 3H), 1.05 (d, *J* = 7.0 Hz, 3H). ¹³C NMR (101 MHz, CDCl₃) δ 175.9, 158.4, 152.2, 137.0, 129.6, 128.6, 127.9, 127.5, 114.0, 109.1, 103.0, 90.1, 70.1, 34.1, 25.3, 19.1, 18.9, 18.7. IR: 2975, 2936, 2360, 1741, 1624, 1586, 1506, 1469, 1455, 1385, 1329, 1309, 1254, 1216, 1203, 1162, 1141, 1106, 1045, 1012, 951, 921, 891, 835, 803, 752 cm⁻¹. [α]_D²⁵ = 79.4° (c 1.51, CHCl₃). HRMS (ESI): calcd. for C₂₀H₂₂O₄ + Na = 349.1410, found 349.1405. HPLC Column: OD-H, 1:99 IPA/Hex, 1 mL/min, 220 nm, ee = 96 %.

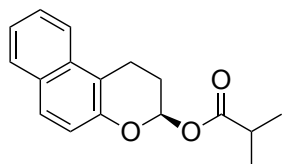
2-isobutyrate-6-(benzo-1,3-dioxole)- chroman-(2R) (2.10e)



2.9e and (*R*)-BTM were used according to procedure C. The product was isolated by column chromatography on silica gel (DCM) as an amorphous solid (33.6 mg, 99%). ¹H NMR (400 MHz, CDCl₃) δ 7.27 (dd, *J* = 8.5, 2.3 Hz, 1H), 7.22 (d, *J* = 2.3 Hz, 1H), 7.04 – 6.96 (m, 2H), 6.91 (d, *J* = 8.5 Hz, 1H), 6.85 (d, *J* = 8.0 Hz, 1H), 6.57 – 6.53 (m, 1H), 5.98 (d, *J* = 0.9 Hz, 2H), 3.03

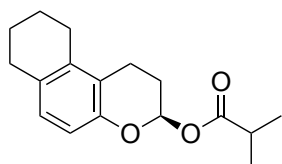
(ddd, $J = 17.7, 12.5, 6.1$ Hz, 1H), 2.75 (ddd, $J = 16.3, 5.8, 2.8$ Hz, 1H), 2.55 (hept, $J = 7.0$ Hz, 1H), 2.18 – 2.01 (m, 2H), 1.16 (d, $J = 7.1$ Hz, 3H), 1.13 (d, $J = 7.0$ Hz, 3H). ^{13}C NMR (101 MHz, CDCl_3) δ 175.8, 150.9, 148.1, 146.7, 135.2, 134.3, 127.6, 126.1, 121.8, 120.1, 117.4, 108.5, 107.4, 101.1, 90.1, 34.1, 25.2, 19.9, 18.9, 18.7. IR: 2975, 1741, 1609, 1586, 1501, 1479, 1448, 1422, 1388, 1340, 1277, 1227, 1195, 1172, 1145, 1122, 1100, 1040, 1011, 952, 921, 903, 891, 862, 806, 751 cm^{-1} . $[\alpha]_{\text{D}25} = 130.8^\circ$ (c 1.47, CHCl_3). HRMS (ESI): calcd. for $\text{C}_{20}\text{H}_{20}\text{O}_5 + \text{Na} = 363.1185$, found 363.1189. HPLC Column: OD-H, 1:99 IPA/Hex, 1 mL/min, 220 nm, ee = 93 %

2,3-Dihydro-1H-3-isobutyrate-benzo[f]chroman (2.10f)



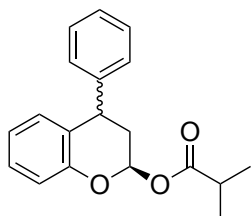
2.9f and (*R*)-BTM were used according to procedure C. The product was isolated by column chromatography on silica gel (DCM) as an amorphous solid (23.5 mg, 87%). ^1H NMR (400 MHz, CDCl_3) δ 7.86 (d, $J = 8.4$ Hz, 1H), 7.78 (d, $J = 8.1$ Hz, 1H), 7.65 (d, $J = 8.9$ Hz, 1H), 7.52 (ddd, $J = 8.4, 6.8, 1.3$ Hz, 1H), 7.38 (t, $J = 7.5$ Hz, 1H), 7.09 (d, $J = 8.9$ Hz, 1H), 6.60 (d, $J = 2.7$ Hz, 1H), 3.25 – 3.00 (m, 2H), 2.51 (hept, $J = 7.0$ Hz, 1H), 2.34 – 2.26 (m, 1H), 2.23 – 2.11 (m, 1H), 1.13 (d, $J = 7.0$ Hz, 3H), 1.09 (d, $J = 7.0$ Hz, 3H). ^{13}C NMR (101 MHz, CDCl_3) δ 174.9, 147.9, 131.5, 128.4, 127.5, 127.0, 125.4, 123.0, 121.0, 117.8, 112.7, 88.7, 33.0, 23.9, 17.8, 17.6, 15.4. IR: 2973, 2936, 1745, 1626, 1600, 1516, 1469, 1435, 1401, 1388, 1336, 1260, 1240, 1220, 1200, 1177, 1142, 1104, 1083, 1006, 977, 933, 904, 880 811, 751 cm^{-1} . $[\alpha]_{\text{D}25} = 213.0^\circ$ (c 1.10, CHCl_3). HRMS (ESI): calcd. for $\text{C}_{17}\text{H}_{18}\text{O}_3 + \text{Na} = 293.1148$, found 293.1140. HPLC Column: OD-H, 1:99 IPA/Hex, 1 mL/min, 220 nm, ee = 93 %.

1H-Naphtho[2, 1- b] pyran- 3- isobutyrate, 2, 3, 7, 8, 9, 10- hexahydro- (2.10g)



2.9i and (*R*)-BTM were used according to procedure C. The product was isolated by column chromatography on silica gel (DCM) as a colorless solid (27.1 mg, 99%). ¹H NMR (400 MHz, CDCl₃) δ 6.87 (d, *J* = 8.3 Hz, 1H), 6.68 (d, *J* = 8.3 Hz, 1H), 6.49 (t, *J* = 2.7 Hz, 1H), 2.77 – 2.46 (m, 7H), 2.20 – 2.10 (m, 1H), 2.07 – 1.96 (m, 1H), 1.92 – 1.67 (m, 4H), 1.15 (d, *J* = 7.0 Hz, 3H), 1.11 (d, *J* = 7.0 Hz, 3H). ¹³C NMR (101 MHz, CDCl₃) δ 176.0, 149.2, 135.4, 130.1, 128.0, 119.7, 114.5, 89.8, 34.0, 29.5, 26.1, 25.1, 23.1, 22.9, 19.0, 18.6, 16.9. IR: 2931, 2859, 1741, 1599, 1479, 1448, 1388, 1319, 1301, 1244, 1232, 1205, 1181, 1143, 1108, 1078, 1038, 1006, 976, 958, 931, 902, 881, 828, 806, 752 cm⁻¹. [α]_D²⁵ = 146.0° (c 1.37, CHCl₃). HRMS (ESI): calcd. for C₁₇H₂₂O₃ + Na = 297.1461, found 297.1452. HPLC Column: OD-H, 10:90 IPA/Hex, 1 mL/min, 220 nm, ee = 98 %.

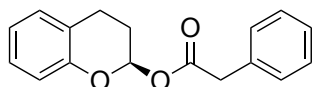
(±)-4-phenylchroman-2-(*R*)-isobutyrate (2.10j)



2.9j and (*R*)-BTM were used according to procedure C. The product was isolated by column chromatography on silica gel (DCM) as a colorless oil (22.9 mg, 77%) as a 1:1 mixture of diastereomers. ¹H NMR (400 MHz, CDCl₃) δ 7.41 – 7.08 (m, 12H), 6.99 – 6.80 (m, 5H), 6.74 (dt, *J* = 7.8, 1.4 Hz, 1H), 6.57 (t, *J* = 2.7 Hz, 1H), 6.49 (dd, *J* = 6.4, 3.0 Hz, 1H), 4.33 – 4.16 (m, 2H), 2.67 – 2.44 (m, 2H), 2.43 – 2.22 (m, 4H), 1.19 (d, *J* = 7.0 Hz, 3H), 1.15 (d, *J* = 7.0 Hz, 3H), 1.06 (d, *J* = 7.0 Hz, 3H), 0.96 (d, *J* = 7.0 Hz, 3H). ¹³C NMR (101 MHz, CDCl₃) δ 175.8, 175.7, 152.6, 151.5, 144.1, 143.4, 130.0, 129.3, 128.8, 128.8, 128.4, 128.2, 128.0, 127.0, 126.6, 125.4, 124.1, 121.5, 121.5, 117.3, 117.0, 91.4, 89.8, 38.9, 36.9, 34.8, 34.5, 34.1, 33.8, 18.8, 18.7, 18.6, 18.5. IR: 3030, 2973, 2877, 1747, 1604, 1585, 1488, 1455, 1182, 1140, 1105, 1031, 1007, 920, 754, 737, 700 cm⁻¹. HRMS (ESI): calcd. for C₁₉H₂₀O₃ + Na = 319.1305, found 319.1300. HPLC Col-

umn: OD-H, 1:99 IPA/Hex, 1 mL/min, 230 nm, for cis-isomer, ee = 90 %, for trans-isomer, ee = 95%.

2H- 1- Benzopyran- 2- ol, 3, 4- dihydro- , 2-phenylacetate, (2R) - (2.10k)



2.9a and (*R*)-BTM were used according to procedure D. The product was isolated by column chromatography on silica gel (DCM) as a colorless oil (20.3 mg, 76%). ¹H NMR (400 MHz, CDCl₃) δ 7.30 – 7.18 (m, 6H), 7.17 – 7.09 (m, 1H), 7.06 (d, J = 7.4 Hz, 1H), 6.92 (td, J = 7.4, 1.2 Hz, 1H), 6.85 (d, J = 8.2 Hz, 1H), 3.62 (s, 2H), 2.91 (ddd, J = 16.2, 12.3, 6.3 Hz, 1H), 2.68 (ddd, J = 16.2, 5.7, 2.8 Hz, 1H), 2.12 – 1.96 (m, 2H). ¹³C NMR (101 MHz, CDCl₃) δ 170.3, 151.5, 133.5, 129.2, 129.2, 128.5, 127.6, 127.1, 121.7, 121.4, 117.1, 90.6, 41.4, 25.0, 19.6. IR: 2975, 2935, 2878, 1737, 1626, 1596, 1511, 1468, 1388, 1352, 1328, 1300, 1213, 1191, 1142, 1109, 1045, 1014, 952, 921, 892, 848, 803, 755 cm⁻¹. [α]_D²⁵ = 39.27° (c 0.62, CHCl₃). HRMS (ESI): calcd. for C₁₇H₁₆O₃ + Na = 291.0992, found 291.0988. HPLC Column: OD-H, 10:90 IPA/Hex, 1 mL/min, 230 nm, ee = 96 %

Supporting Information for DFT Calculations

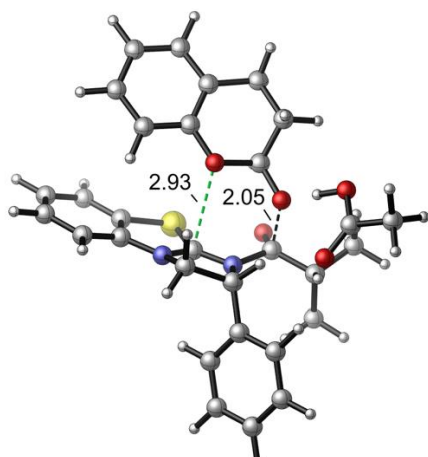
All DFT calculations were performed using Gaussian 09^[8]. The transition state geometries were optimized using the M06-2X^[9,10] density functional and the 6-31G(d) basis set in the gas phase. Single-point energies were calculated using M06-2X with the 6-311++G(d,p) basis set and include solvation energy corrections calculated using the SMD^[11] model.

I was interested in identifying the structures of four transition states: the (*R*) and (*S*) transition states with the 2-chromanol hydroxyl group in the equatorial orientation, and the analogous transition states with the hydroxyl group in the axial orientation. In both the (*R*) and (*S*) cases the equatorial transition state was lower in energy. Both transition states that lead to the (*R*) product, **2.9a-TS1** and **2.9a-TS3**, exhibit a cation-*n* interaction and are lower in energy than the

transition states that lead to the (*S*) product, **2.9a-TS2** and **2.9a-TS4**. Neither **2.9a-TS2** nor **2.9a-TS4** exhibit a cation-*n* interaction.

Cartesian Coordinates of All Optimized Structures

2.9a-TS1: (*R*) equatorial confirmation

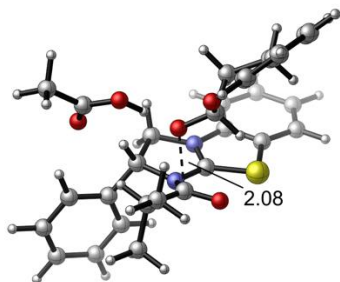


M06-2X/6-31G(d) SCF energy: -2045.60207069 a.u.
 M06-2X/6-31G(d) enthalpy: -2044.990409 a.u.
 M06-2X/6-31G(d) free energy: -2045.093453 a.u.
 M06-2X/6-311++G(d,p) SCF energy in solution: -2046.13543092 a.u.
 M06-2X/6-311++G(d,p) enthalpy in solution: -2045.523769 a.u.
 M06-2X/6-311++G(d,p) free energy in solution: -2045.626813 a.u.
 Three lowest frequencies (cm⁻¹): -126.79, 14.19, 20.31
 Imaginary frequency: -126.79 cm⁻¹

Cartesian coordinates

ATOM	X	Y	Z
C	2.40756000	-2.31174800	0.74573300
C	1.75208200	-2.47335700	-0.48131800
C	2.35588500	-3.12177800	-1.55227700
C	3.65400900	-3.58934500	-1.37286600
C	4.31916600	-3.42257200	-0.15521300
C	3.70135800	-2.78433700	0.91730900
C	0.19489100	-1.27747300	0.70307500
H	1.83566900	-3.23776200	-2.49751300
H	4.15585300	-4.08951300	-2.19433600
H	5.33224300	-3.79290100	-0.04176900
H	4.22293400	-2.64434400	1.85832800
C	-0.40942300	-1.42096500	-1.50683600
H	0.12098300	-0.67148700	-2.10222200
H	-0.75167900	-2.24925000	-2.12976900
C	-1.57150300	-0.79223300	-0.68376100
H	-1.79716300	0.21640700	-1.04077400
N	-0.97217800	-0.66791300	0.67653900
N	0.49217900	-1.89003800	-0.44932500

S	1.42623600	-1.38907300	1.90113600
C	-1.26688700	0.38701900	1.65339600
O	-0.53326200	0.40703000	2.62670200
C	-2.69261300	0.89339200	1.64240000
H	-3.02786900	0.99474300	0.60433100
C	-2.81694900	-1.64931600	-0.65065700
C	-4.02517200	-1.13775300	-1.12202600
C	-2.76721900	-2.94863200	-0.13695200
C	-5.17660900	-1.92355300	-1.07141300
H	-4.05646500	-0.12353400	-1.51280200
C	-3.91682000	-3.72789800	-0.08572500
H	-1.82728700	-3.34703700	0.24226300
C	-5.12613700	-3.21320000	-0.55319300
H	-6.11703800	-1.52061100	-1.43473700
H	-3.87223300	-4.73339400	0.32139400
H	-6.02600800	-3.81921400	-0.51122700
O	-0.59074600	1.77771400	0.30742000
C	0.71510400	2.00426100	0.50441400
C	1.15192900	3.43932500	0.24003400
H	1.02234700	1.70396700	1.52620500
O	1.47507000	1.11326900	-0.39730300
C	2.61977800	3.59787600	0.62194300
H	0.51110600	4.10812700	0.82234600
H	0.98951800	3.65862500	-0.82157200
C	2.82023200	1.31841300	-0.46272500
C	3.44216500	2.47654500	0.03006100
H	2.71490200	3.58997200	1.71594600
H	3.01328600	4.56203400	0.28172800
C	3.58917100	0.32407300	-1.07754900
C	4.83067200	2.57907400	-0.07509400
C	4.96758000	0.45088300	-1.17080400
H	3.08353500	-0.54354100	-1.48766000
C	5.60203800	1.58059800	-0.65679700
H	5.30851300	3.47942500	0.30604400
H	5.54333300	-0.33678600	-1.64863700
H	6.67977800	1.68908700	-0.72397700
C	-2.84942500	3.04940200	-1.56747600
O	-1.88670800	3.54527600	-0.83620200
O	-3.06766300	1.85225700	-1.71142700
C	-3.69198100	4.10963000	-2.23921100
H	-4.49003400	3.64410500	-2.81621500
H	-4.11175000	4.77662900	-1.48182400
H	-3.05946500	4.71632500	-2.89264400
H	-1.32162100	2.76583000	-0.37775100
C	-2.75713400	2.25249100	2.33368900
H	-2.19629800	2.99913700	1.76870700
H	-3.79856700	2.57821100	2.41594600
H	-2.33310000	2.17945900	3.33952100
C	-3.56078800	-0.13841800	2.37785300
H	-3.49640100	-1.13338300	1.92620300
H	-3.24555200	-0.21051800	3.42400700
H	-4.60853900	0.17520400	2.35217000

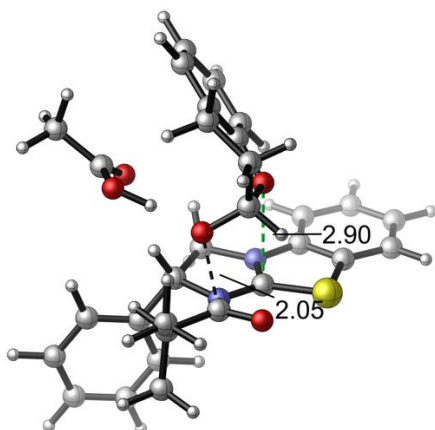
2.9a-TS2: (S) equatorial conformation

M06-2X/6-31G(d) SCF energy: -2045.58929411 a.u.
 M06-2X/6-31G(d) enthalpy: -2044.977700 a.u.
 M06-2X/6-31G(d) free energy: -2045.082621 a.u.
 M06-2X/6-311++G(d,p) SCF energy in solution: -2046.12805122 a.u.
 M06-2X/6-311++G(d,p) enthalpy in solution: -2045.516457 a.u.
 M06-2X/6-311++G(d,p) free energy in solution: -2045.621378 a.u.
 Three lowest frequencies (cm⁻¹): -115.48, 10.11, 17.50
 Imaginary frequency: -115.48 cm⁻¹

Cartesian coordinates

ATOM	X	Y	Z
C	-0.30863700	3.77520300	-0.41177200
C	-1.09200100	3.37114200	0.67785900
C	-1.36984200	4.22927600	1.73574900
C	-0.84243700	5.51462200	1.67664600
C	-0.06393000	5.92797500	0.59161700
C	0.21311700	5.06170000	-0.46211800
C	-1.06189600	1.45476300	-0.58832400
H	-1.97456600	3.90140600	2.57491500
H	-1.04018200	6.20664900	2.48825100
H	0.33339300	6.93689800	0.56931000
H	0.82277000	5.38039500	-1.30133900
C	-2.14040400	1.08451200	1.41580700
H	-1.52863500	0.96463800	2.31437800
H	-3.14680000	1.41318700	1.68598600
C	-2.16490800	-0.20913200	0.54153000
H	-1.59335400	-1.00081500	1.03294200
N	-1.42877700	0.19244500	-0.69242900
N	-1.50500800	2.05350100	0.52091100
S	-0.08069200	2.46367800	-1.58500400
C	-0.55503000	-0.69938900	-1.48177700
O	0.08246700	-0.14547200	-2.35877000
C	-0.95470600	-2.15677700	-1.50050600
H	-1.27450300	-2.45422800	-0.49588100
C	-3.56188800	-0.67815200	0.20979700

C	-3.99571200	-1.93240800	0.63612400
C	-4.41624800	0.13580000	-0.53952500
C	-5.27865800	-2.36838300	0.30569600
H	-3.32115800	-2.55889000	1.21484100
C	-5.69244800	-0.30280500	-0.86979800
H	-4.07022500	1.10827500	-0.88719900
C	-6.12455100	-1.56002300	-0.44684700
H	-5.61379100	-3.34734500	0.63418200
H	-6.34758200	0.32906100	-1.46157600
H	-7.11946300	-1.90691300	-0.70868500
O	0.66139700	-0.83316900	0.20151700
C	1.87194400	-0.29079500	-0.04540600
C	2.31458600	0.69901400	1.03052800
H	1.89409100	0.20195300	-1.03813900
O	2.84619900	-1.36206400	-0.11566900
C	3.64369600	1.33491100	0.63410500
H	2.40227600	0.14726500	1.97408800
H	1.53132100	1.45748800	1.15610700
C	4.15549900	-1.00861700	-0.16481200
C	4.61596100	0.27166500	0.17537000
H	3.47307800	2.05617300	-0.17789000
H	4.07719900	1.90096800	1.46644400
C	5.05896600	-2.00157000	-0.55768000
C	5.98720800	0.52331200	0.09877100
C	6.41613400	-1.72559700	-0.62362000
H	4.66127300	-2.98015900	-0.80629100
C	6.89031700	-0.45404000	-0.29920500
H	6.34594100	1.51482100	0.36882900
H	7.10716700	-2.50468400	-0.93202900
H	7.95141800	-0.23178900	-0.34909700
H	0.79733700	-2.08064600	0.94685000
C	-0.17825600	-3.40327800	2.02115800
O	-1.24367000	-2.79461000	2.00187500
O	0.91908700	-3.00353900	1.44295900
C	-0.01831400	-4.72263500	2.74138200
H	0.75061400	-4.62295300	3.51196300
H	-0.96402300	-5.02326500	3.19071200
H	0.32570100	-5.48294400	2.03554600
C	0.24526600	-2.99934900	-1.92639200
H	0.58331800	-2.69090300	-2.92009800
H	1.07248500	-2.87799100	-1.22407000
H	-0.04119100	-4.05477000	-1.96657300
C	-2.12065100	-2.31238400	-2.48885700
H	-2.45178100	-3.35497500	-2.50600700
H	-2.98034400	-1.68951300	-2.22208900
H	-1.79111900	-2.03740200	-3.49598100

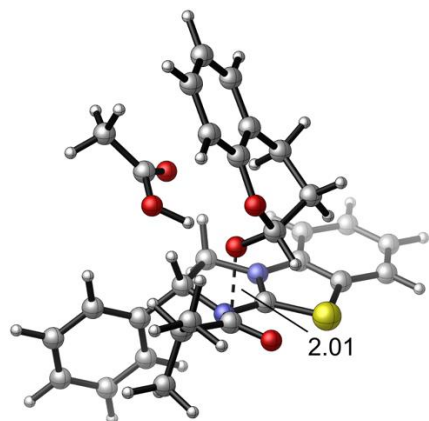
2.9a-TS3: (*R*) axial conformation

M06-2X/6-31G(d) SCF energy: -2045.60151882 a.u.
 M06-2X/6-31G(d) enthalpy: -2044.989817 a.u.
 M06-2X/6-31G(d) free energy: -2045.090789 a.u.
 M06-2X/6-311++G(d,p) SCF energy in solution: -2046.13330957 a.u.
 M06-2X/6-311++G(d,p) enthalpy in solution: -2045.521607 a.u.
 M06-2X/6-311++G(d,p) free energy in solution: -2045.622580 a.u.
 Three lowest frequencies (cm⁻¹): -120.42, 25.24, 33.22
 Imaginary frequency: -120.42 cm⁻¹

Cartesian coordinates

ATOM	X	Y	Z
C	2.00072800	-3.17147600	0.52415500
C	1.67450400	-2.62766300	-0.72502400
C	2.43519500	-2.89333700	-1.85874300
C	3.54195100	-3.72179700	-1.71140100
C	3.87360000	-4.27025800	-0.46917400
C	3.10784400	-3.99894200	0.66128900
C	0.01684100	-1.74587400	0.58773300
H	2.17081000	-2.45838700	-2.81749300
H	4.15671100	-3.94466900	-2.57694700
H	4.74208400	-4.91416400	-0.38215700
H	3.37081500	-4.41973400	1.62638200
C	-0.12796100	-0.91889400	-1.56271400
H	0.55014800	-0.10968000	-1.84931400
H	-0.48806300	-1.45781500	-2.44260700
C	-1.29808900	-0.37316500	-0.69401900
H	-1.17583100	0.70284100	-0.59622200
N	-1.05820800	-0.97563500	0.64379500
N	0.53404700	-1.84312500	-0.63713900
S	0.87421900	-2.63855300	1.78537800
C	-1.43288800	-0.36168600	1.92901300
O	-0.98105800	-0.92287000	2.91350600

C	-2.72590300	0.42694600	1.92276800
H	-2.76883200	1.02983700	1.00921100
C	-2.66192000	-0.71649500	-1.23922400
C	-3.53157900	0.30266200	-1.61863600
C	-3.06200600	-2.04852800	-1.36991700
C	-4.79760500	-0.00431900	-2.11365400
H	-3.21125100	1.33740200	-1.51964000
C	-4.32476100	-2.35656500	-1.86177500
H	-2.38716100	-2.84643900	-1.06335000
C	-5.19579100	-1.33204500	-2.23248300
H	-5.47269900	0.79521700	-2.40234900
H	-4.63383100	-3.39337400	-1.95189900
H	-6.18415100	-1.57147300	-2.61248100
O	-0.27287600	1.28340900	1.55198300
C	0.96787300	1.02164300	2.01652200
C	1.66389100	2.22298800	2.64966400
O	1.82978700	0.49158600	0.95476000
H	0.94301700	0.18803000	2.73448500
C	1.81060500	3.34244500	1.62537600
H	2.64758200	1.90118700	3.01125500
H	1.07419700	2.54863700	3.51136100
C	2.30828700	1.40659500	0.06606300
C	2.30964500	2.78846600	0.31133500
H	0.84356200	3.83369900	1.47233700
H	2.50522100	4.10884400	1.98764400
C	2.84106000	0.90458700	-1.12506100
C	2.78673400	3.63239200	-0.69406000
C	3.30747000	1.76549500	-2.10793500
H	2.88178700	-0.17449400	-1.25054100
C	3.26679400	3.14350900	-1.90335900
H	2.78630000	4.70499100	-0.50565800
H	3.70589800	1.36079300	-3.03376600
H	3.62583500	3.82601700	-2.66691600
H	-0.56917400	2.35339900	0.55034900
C	-0.48170200	3.12109600	-1.28958100
O	-0.85423700	3.17859900	-0.02364500
O	-0.14364700	2.10567300	-1.87194400
C	-0.53589200	4.47125400	-1.96351700
H	0.23515600	5.11186600	-1.52557200
H	-0.35822500	4.36118100	-3.03253900
H	-1.50326400	4.94486500	-1.77857600
C	-3.89600300	-0.56575200	1.95346500
H	-4.84443500	-0.02128200	1.92042900
H	-3.87649300	-1.26177100	1.10989200
H	-3.86179600	-1.14559000	2.88155400
C	-2.76231800	1.34925600	3.13792400
H	-2.64210600	0.76234200	4.05330300
H	-1.95286700	2.07768600	3.07850700
H	-3.72270700	1.87179100	3.18121000

2.9a-TS4: (S) axial conformation

M06-2X/6-31G(d) SCF energy: -2045.59644454 a.u.
 M06-2X/6-31G(d) enthalpy: -2044.984371 a.u.
 M06-2X/6-31G(d) free energy: -2045.084875 a.u.
 M06-2X/6-311++G(d,p) SCF energy in solution: -2046.13066653 a.u.
 M06-2X/6-311++G(d,p) enthalpy in solution: -2045.516457 a.u.
 M06-2X/6-311++G(d,p) free energy in solution: -2045.619097 a.u.
 Three lowest frequencies (cm⁻¹): -116.54, 19.71, 20.62
 Imaginary frequency: -116.54 cm⁻¹

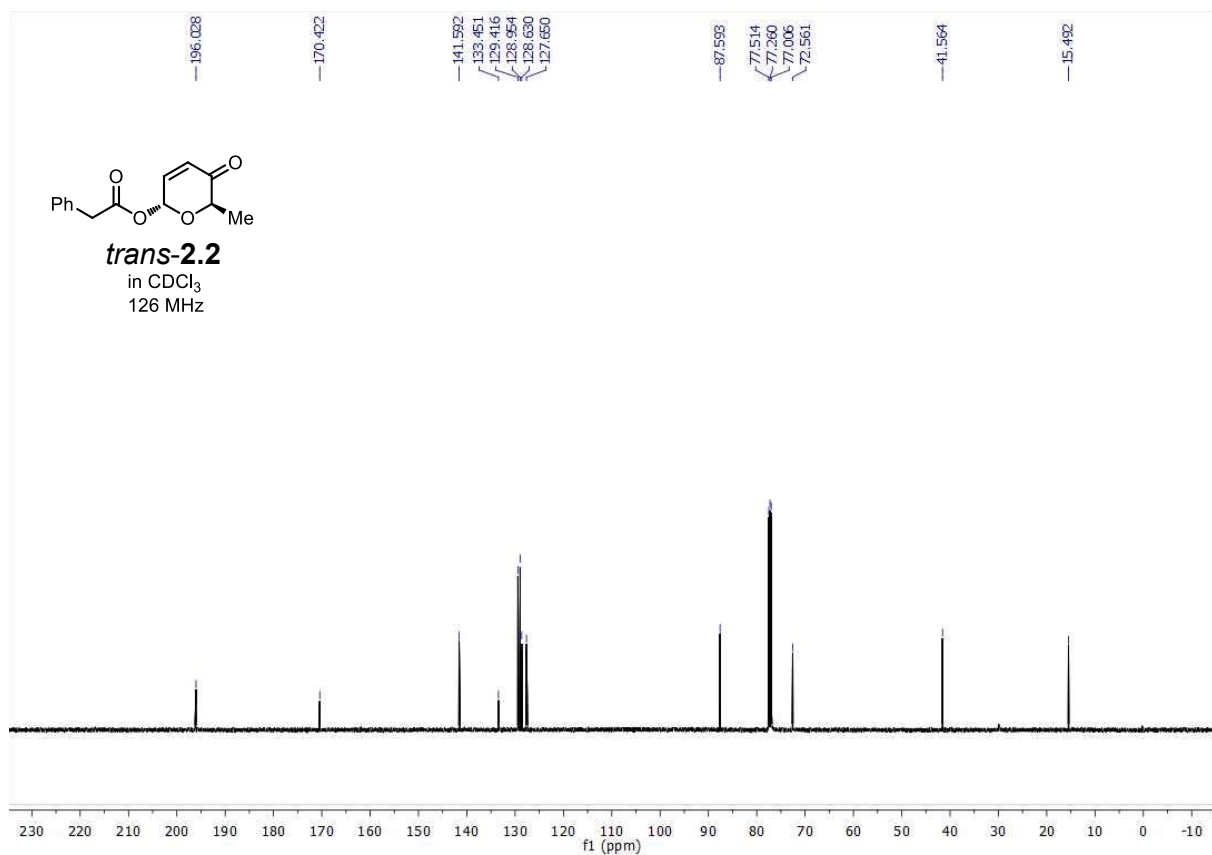
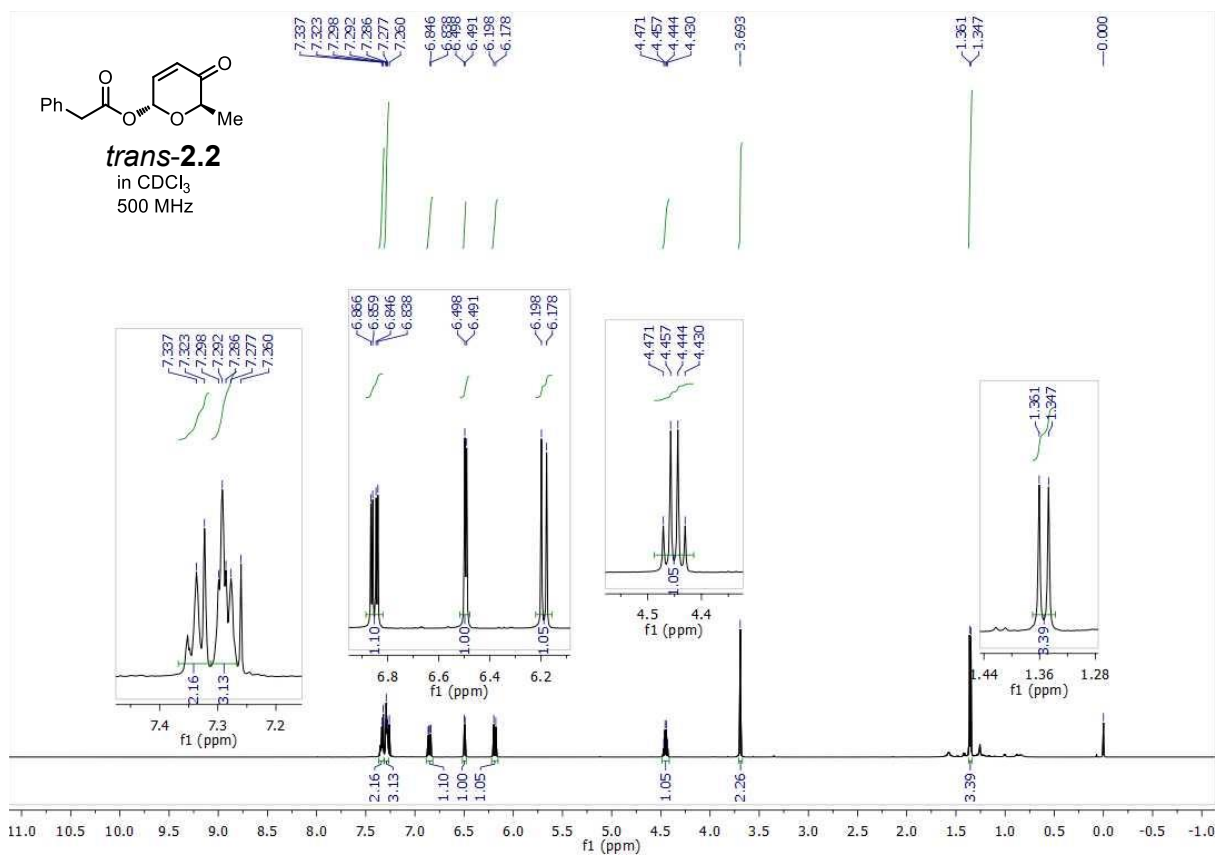
Cartesian coordinates

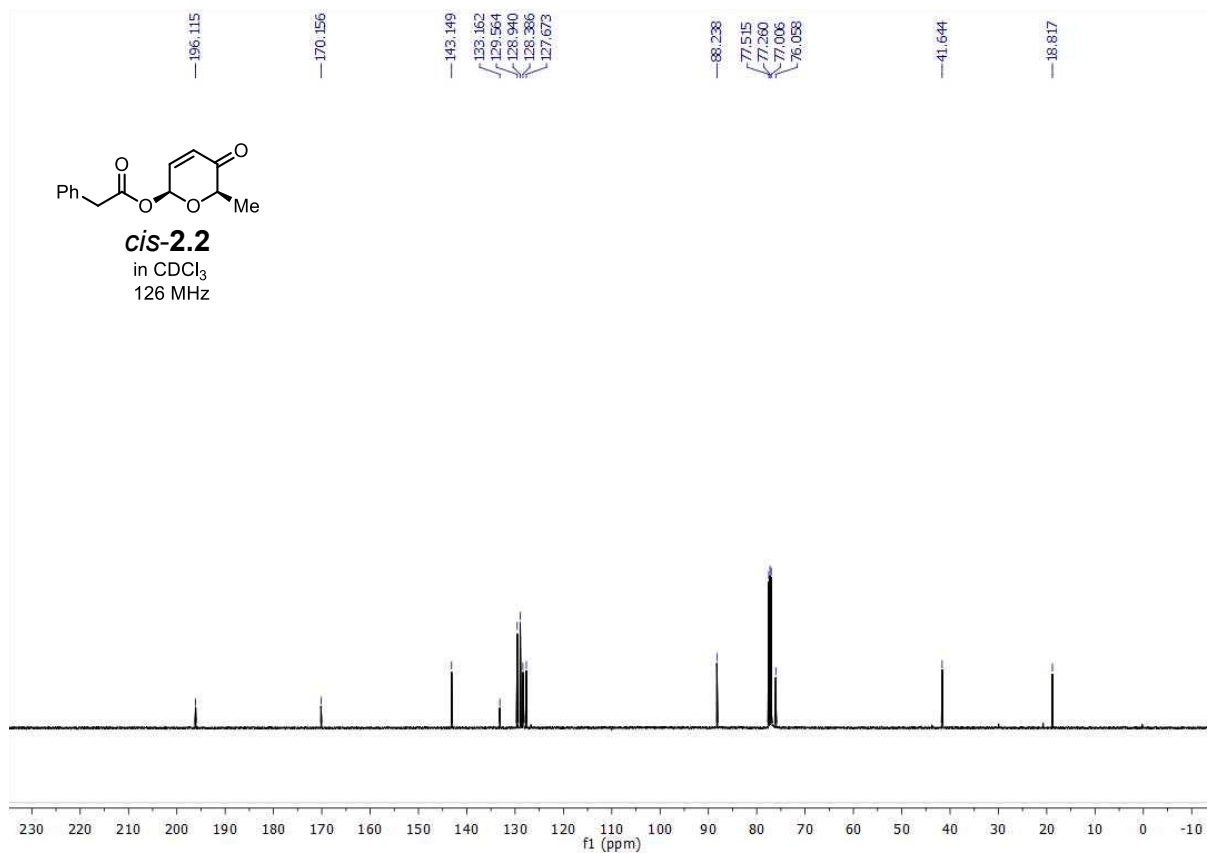
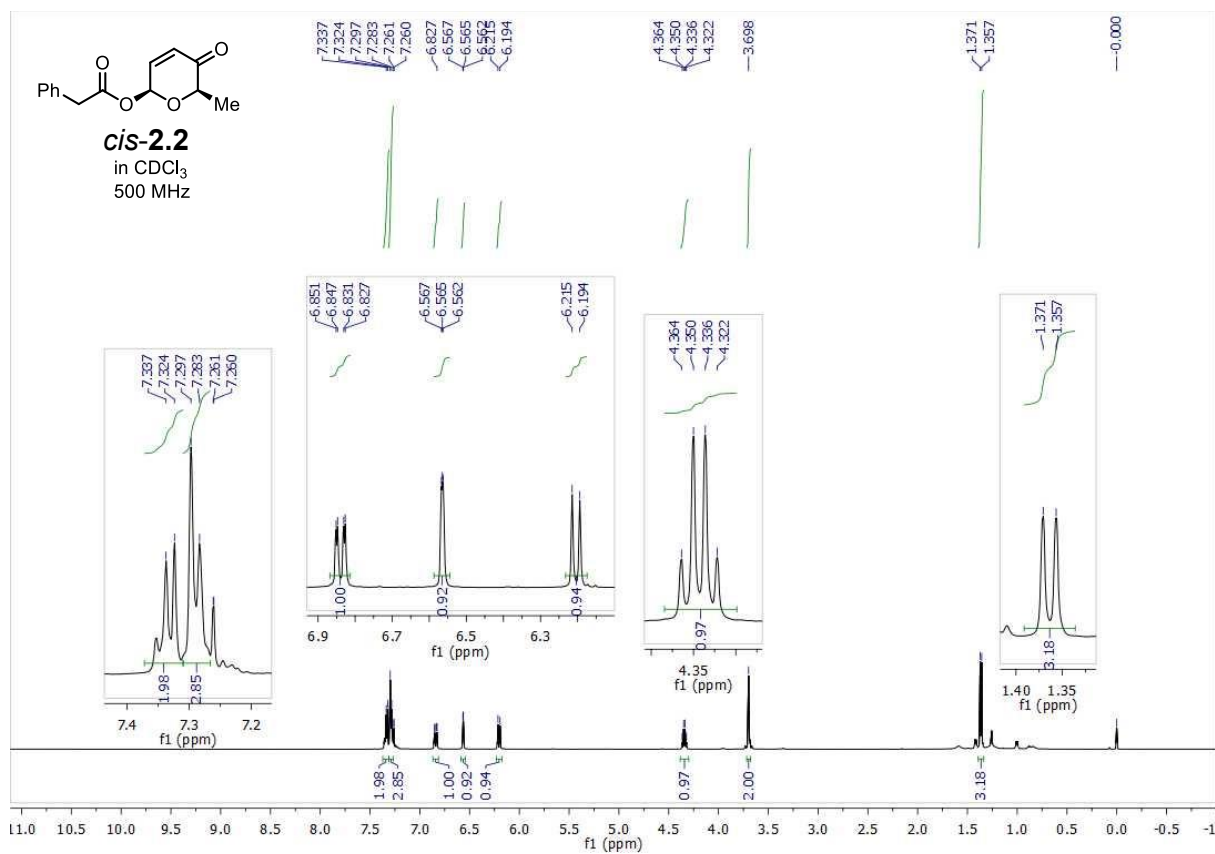
ATOM	X	Y	Z
C	-2.65784700	-3.02242700	0.40946800
C	-2.54478300	-2.39057200	-0.83635100
C	-2.81427700	-3.06150300	-2.02409400
C	-3.20579600	-4.39229800	-1.93448600
C	-3.32436400	-5.03071400	-0.69599900
C	-3.04824600	-4.35373800	0.48806000
C	-1.93757100	-0.69588100	0.58315200
H	-2.71350100	-2.56036000	-2.98113100
H	-3.42147800	-4.94331600	-2.84361500
H	-3.63317900	-6.06967100	-0.65556700
H	-3.13487100	-4.85104000	1.44869300
C	-1.75642200	-0.01037900	-1.61240900
H	-0.93067400	-0.33846200	-2.24908000
H	-2.62024300	0.29277500	-2.21028900
C	-1.27841900	1.11458300	-0.64673000
H	-0.20080900	1.21495500	-0.76321200
N	-1.53590900	0.55995800	0.71433100
N	-2.13875300	-1.07175900	-0.67820800
S	-2.21183700	-1.93885300	1.74203900
C	-0.65890900	0.82444500	1.88351700
O	-0.89172100	0.14661000	2.87109600

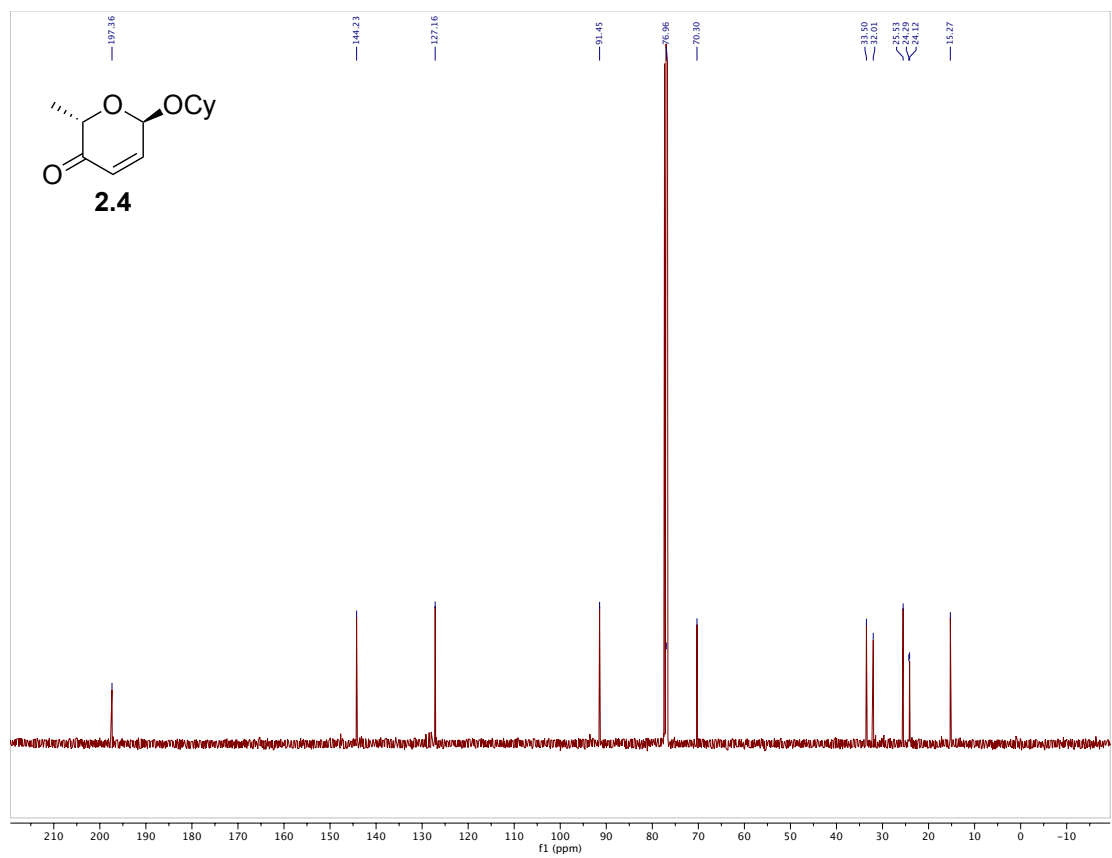
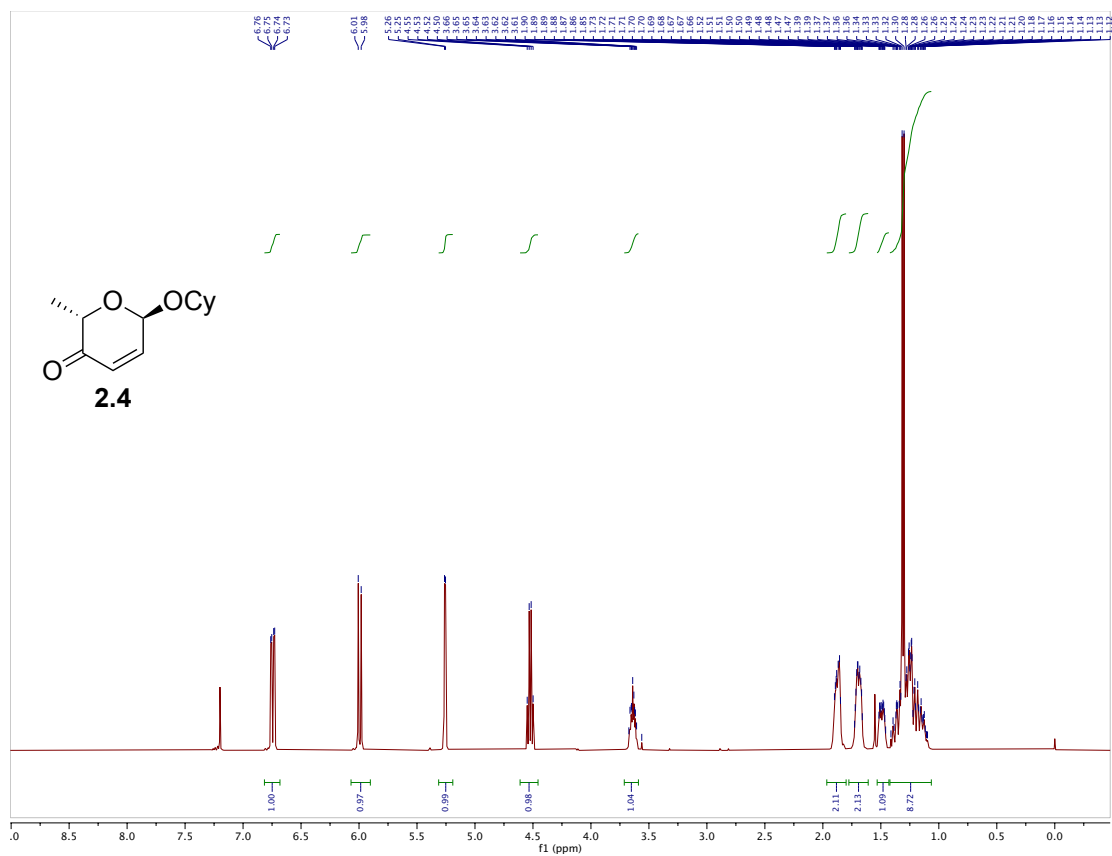
C	-0.08159000	2.22429400	1.94232400
H	0.24014600	2.53036600	0.94230800
C	-1.96141700	2.44164200	-0.85582500
C	-1.20670900	3.55642600	-1.21454500
C	-3.34045000	2.56981600	-0.67678000
C	-1.82491200	4.79304000	-1.39023800
H	-0.13087800	3.45185600	-1.34048600
C	-3.95772800	3.80326400	-0.84877500
H	-3.92771100	1.70281700	-0.37903400
C	-3.19818500	4.91755700	-1.20557300
H	-1.23117600	5.65914500	-1.66485700
H	-5.02871500	3.89957700	-0.69952400
H	-3.67862300	5.88220500	-1.33608100
O	0.82468200	-0.08006500	0.86821600
C	1.55368700	-0.95020100	1.62663600
C	1.57119700	-2.34917200	1.00692700
O	2.91526500	-0.49528900	1.78388200
H	1.16986500	-0.97600700	2.65787300
C	2.13984300	-2.24427900	-0.40391400
H	0.55066100	-2.74599800	0.99145100
H	2.18453200	-3.01098900	1.62965700
C	3.75554300	-0.67214400	0.72519100
C	3.45129000	-1.49925000	-0.36601900
H	1.43180300	-1.69242000	-1.03501600
H	2.28444000	-3.23403500	-0.85067900
C	4.97080300	0.01515500	0.77555900
C	4.38863700	-1.60357900	-1.39580600
C	5.88978900	-0.11389300	-0.25613600
H	5.16476800	0.64865100	1.63499300
C	5.60200200	-0.92590200	-1.35440400
H	4.15069700	-2.24147800	-2.24456300
H	6.83262300	0.42296000	-0.20450600
H	6.31660600	-1.03111200	-2.16469900
H	1.58103400	0.82896900	0.05319400
C	1.12484800	2.23843600	2.87671500
H	1.93417500	1.62137800	2.47887800
H	1.48857800	3.26365700	2.99393400
H	0.83984800	1.85422200	3.86083300
C	-1.18577600	3.16630800	2.44154600
H	-0.80732800	4.19218600	2.47832100
H	-2.06719000	3.15378800	1.79224900
H	-1.49334900	2.87294600	3.45028100
C	2.12832300	1.13699400	-1.80399400
O	2.11916600	1.52011800	-0.54163500
O	1.31125000	0.37031900	-2.29392300
C	3.25798600	1.75119500	-2.59125600
H	3.14045900	1.53550000	-3.65267300
H	3.29242600	2.82953900	-2.41652500
H	4.19666900	1.32476800	-2.22226600

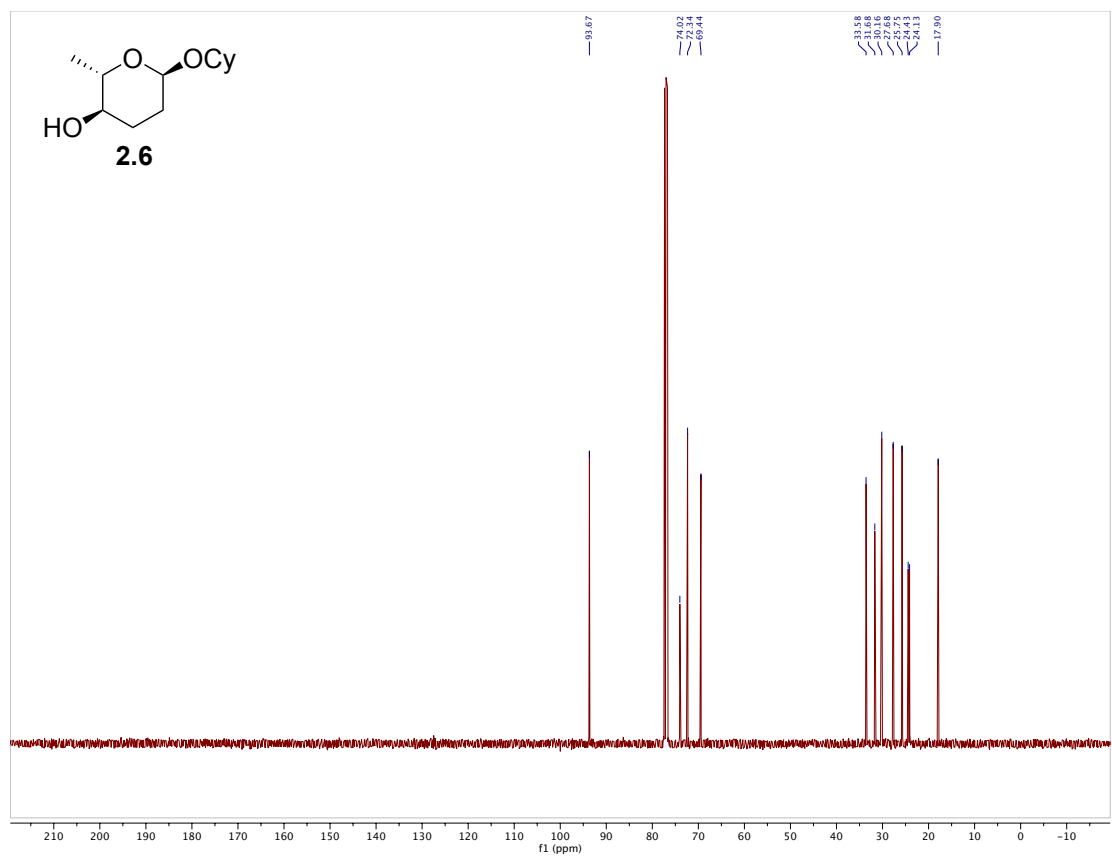
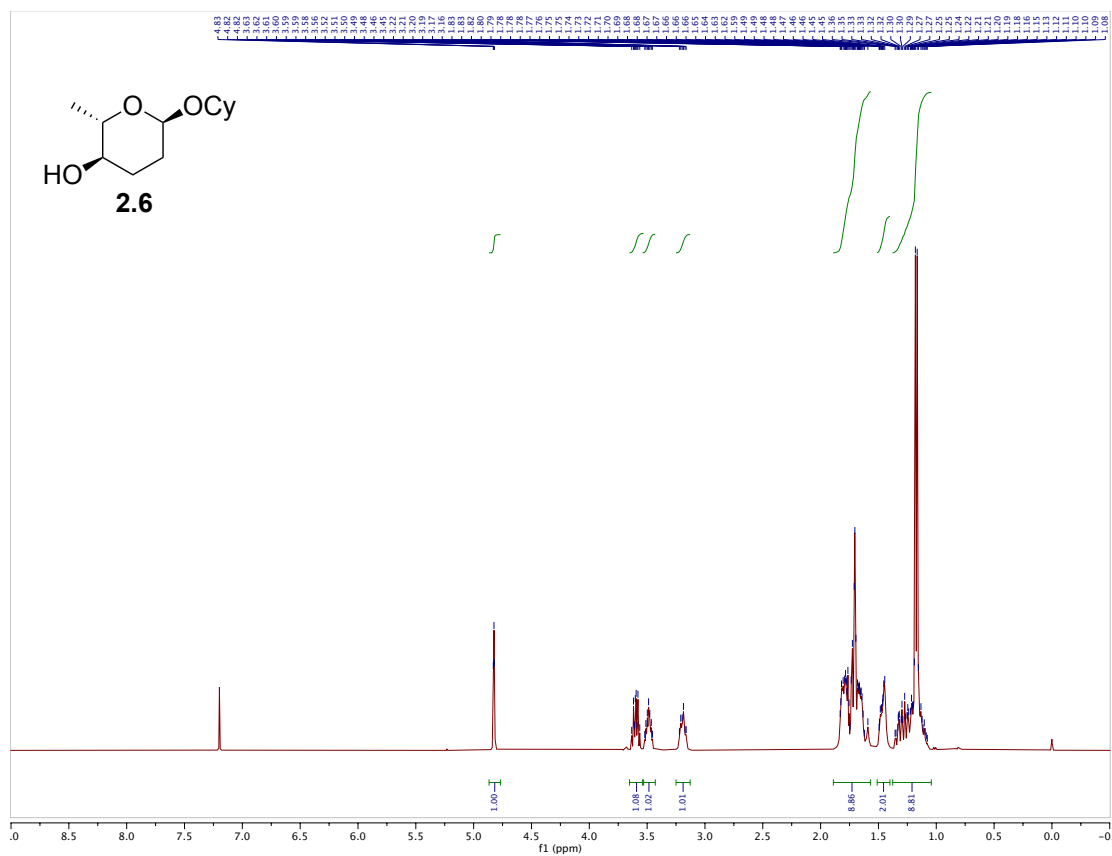
References:

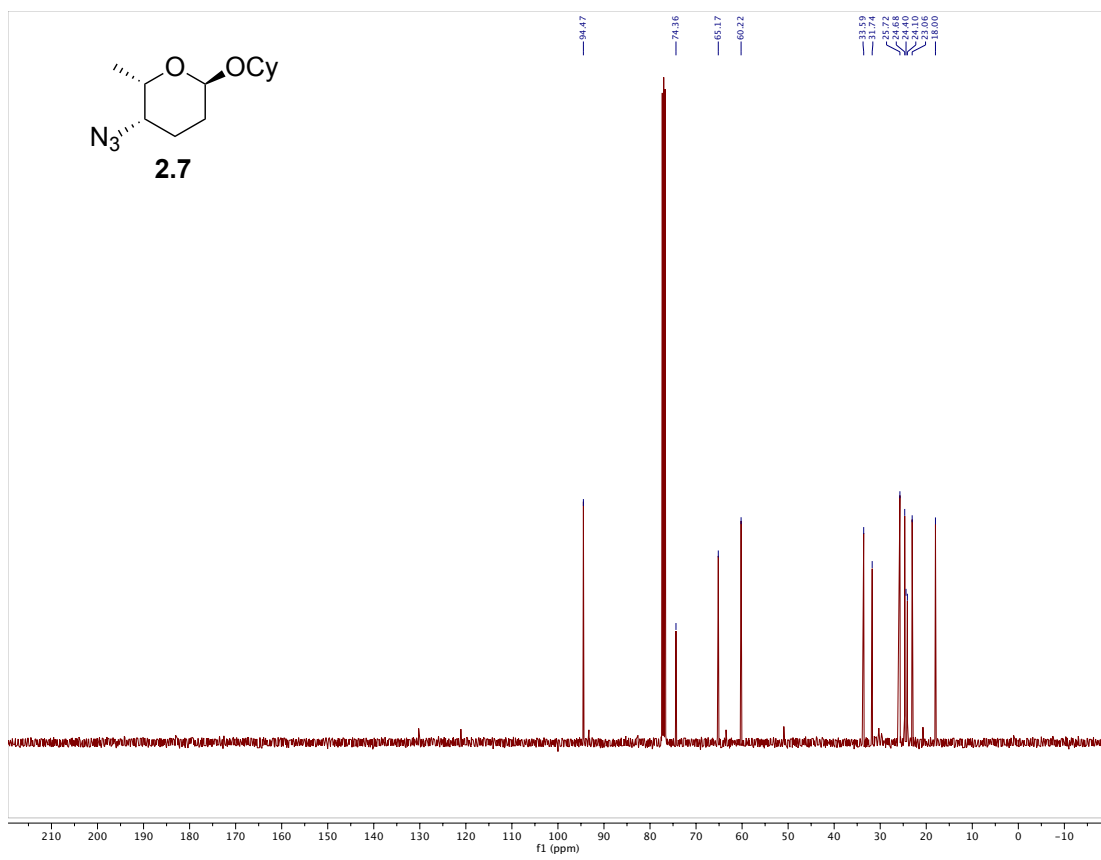
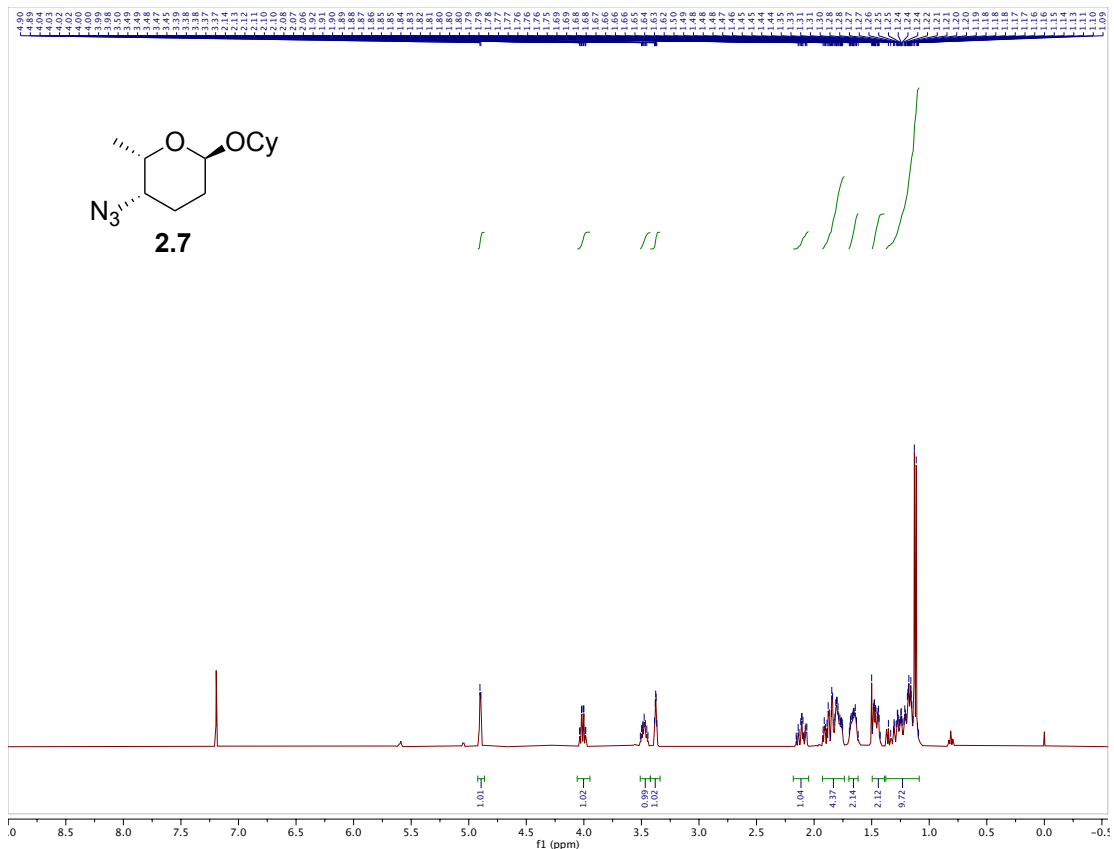
- 1) a) Wang, H.-Y.; Yang, K.; Bennett, S. R.; Guo, S.-r.; Tang, W. *Angew. Chem. Int. Ed.* **2015**, 54, 8756; b) Wu, X.; Li, X.; Zanotti-Gerosa, A.; Pettman, A.; Liu, J.; Mills, A. J.; Xiao, J. *Chem. Eur. J.* **2008**, 14, 2209; c) Croatt, M. P.; Carreira, E. M. *Org. Lett.* **2011**, 13, 1390.
- 2) H.-Y. Wang, K. Yang, D. Yin, C. Liu, D. A. Glazier and W. Tang, *Org. Lett.*, **2015**, 17, 5272.
- 3) W. Song, Y. Zhao, J. C. Lynch, H. Kim and W. Tang, *Chem. Commun.*, **2015**, 51, 17475.
- 4) a) W. Shi and T. L. Lowary, *Bioorg. Med. Chem.*, **2011**, 19, 1779.; b) M. Tajbakhsh, R. Hosseinzadeh, H. Alinezhad, S. Ghahari, A. Heydari and S. Khaksar, *Synthesis*, **2013**, 490.
- 5) S. G. Das, B. Srinivasan, D. L. Hermanson, N. P. Bleeker, J. M. Doshi, R. Tang, W. T. Beck and C. Xing, *J. Med. Chem.*, **2011**, 54, 5937.
- 6) B. Padhi, D. S. Reddy and D. K. Mohapatra, *Eur. J. Org. Chem.*, **2015**, 542.
- 7) M. M. Naik, D. P. Kamat, S. G. Tilve and V. P. Kamat, *Tetrahedron*, **2014**, 70, 5221.
- 8) Frisch, M. J., Trucks, G. W., Schlegel, H. B., Scuseria, G. E., Robb, M. A., Cheeseman, J. R., Scalmani, G., Barone, V., Mennucci, B., Petersson, G. A., Nakatsuji, H., Caricato, M., Li, X., Hratchian, H. P., Izmaylov, A. F., Bloino, J., Zheng, G., Sonnenberg, J. L., Hada, M., Ehara, M., Toyota, K., Fukuda, R., Hasegawa, J., Ishida, M., Nakajima, T., Honda, Y., Kitao, O., Nakai, H., Vreven, T., Montgomery, J. A. Jr., Peralta, J. E., Ogliaro, F., Bearpark, M., Heyd, J. J., Brothers, E., Kudin, K. N., Staroverov, V. N., Kobayashi, R., Normand, J., Raghavachari, K., Rendell, A., Burant, J. C., Iyengar, S. S., Tomasi, J., Cossi, M., Rega, N., Millam, N. J., Klene, M., Knox, J. E., Cross, J. B., Bakken, V., Adamo, C., Jaramillo, J., Gomperts, R., Stratmann, R. E., Yazyev, O., Austin, A. J., Cammi, R., Pomelli, C., Ochterski, J. W., Martin, R. L., Morokuma, K., Zakrzewski, V. G., Voth, G. A., Salvador, P., Dannenberg, J. J., Dapprich, S., Daniels, A. D., Farkas, Ö., Foresman, J. B., Ortiz, J. V., Cioslowski, J., Fox, D. J. Gaussian 09, Revision D.01; Gaussian, Inc.: Wallingford, CT, **2009**.
- 9) Grimme, S., Antony, J., Ehrlich, S., Krieg, H. *J. Chem. Phys.* **2010**, 132, 154104
- 10) Grimme, S. *J. Comput. Chem.* **2006**, 27, 1787.
- 11) Marenich, A. V., Cramer, C. J., Truhlar, D. G. *J. Phys. Chem. B*, **2009**, 113, 6378.

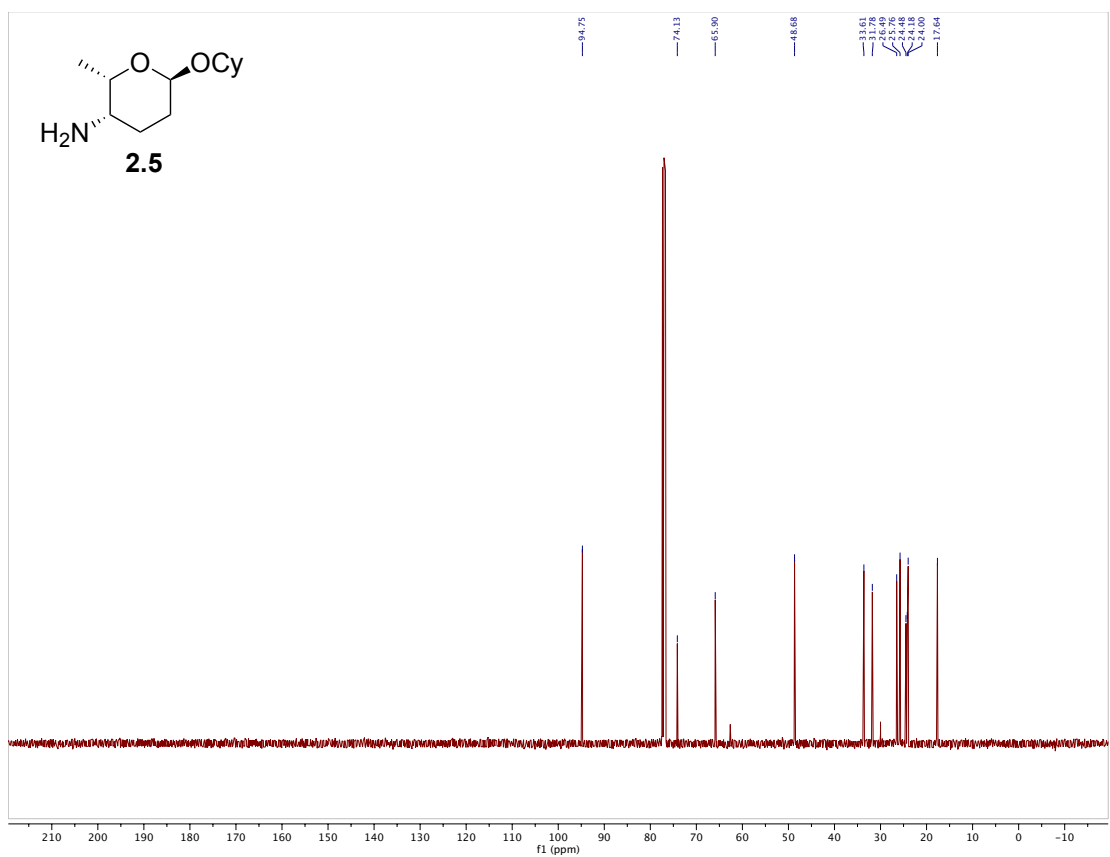
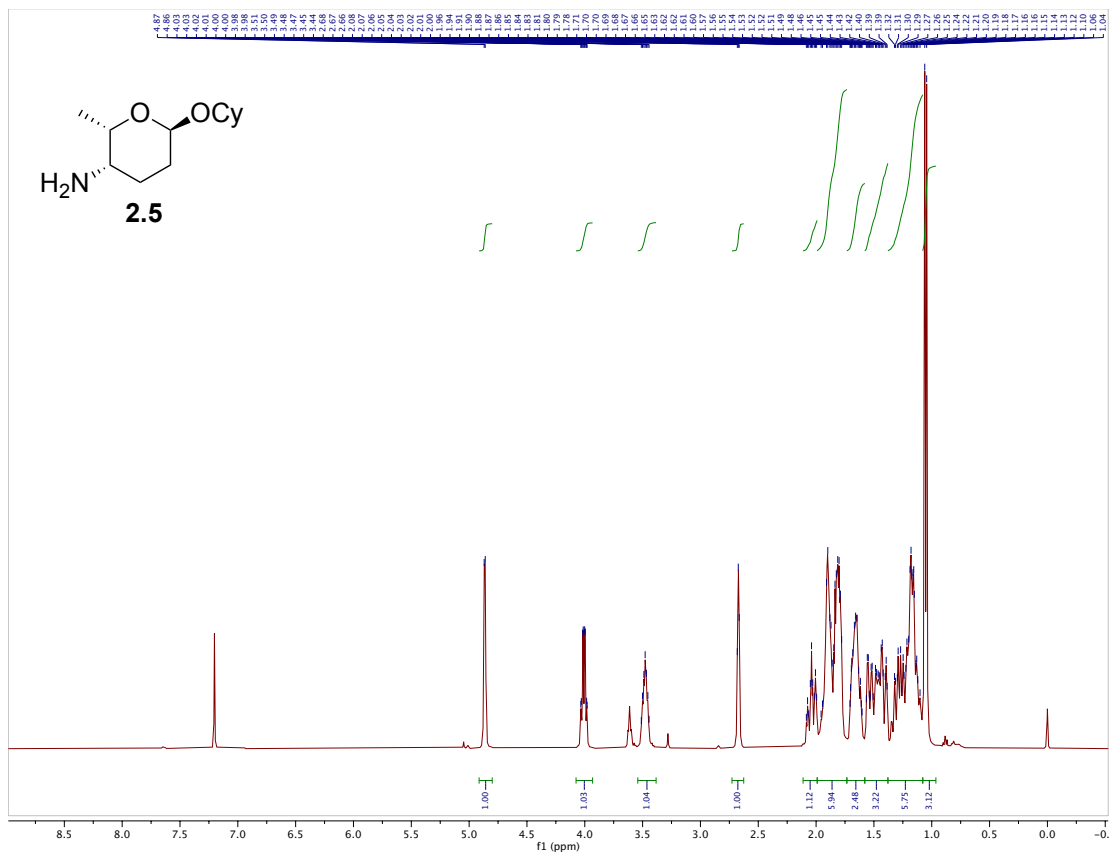


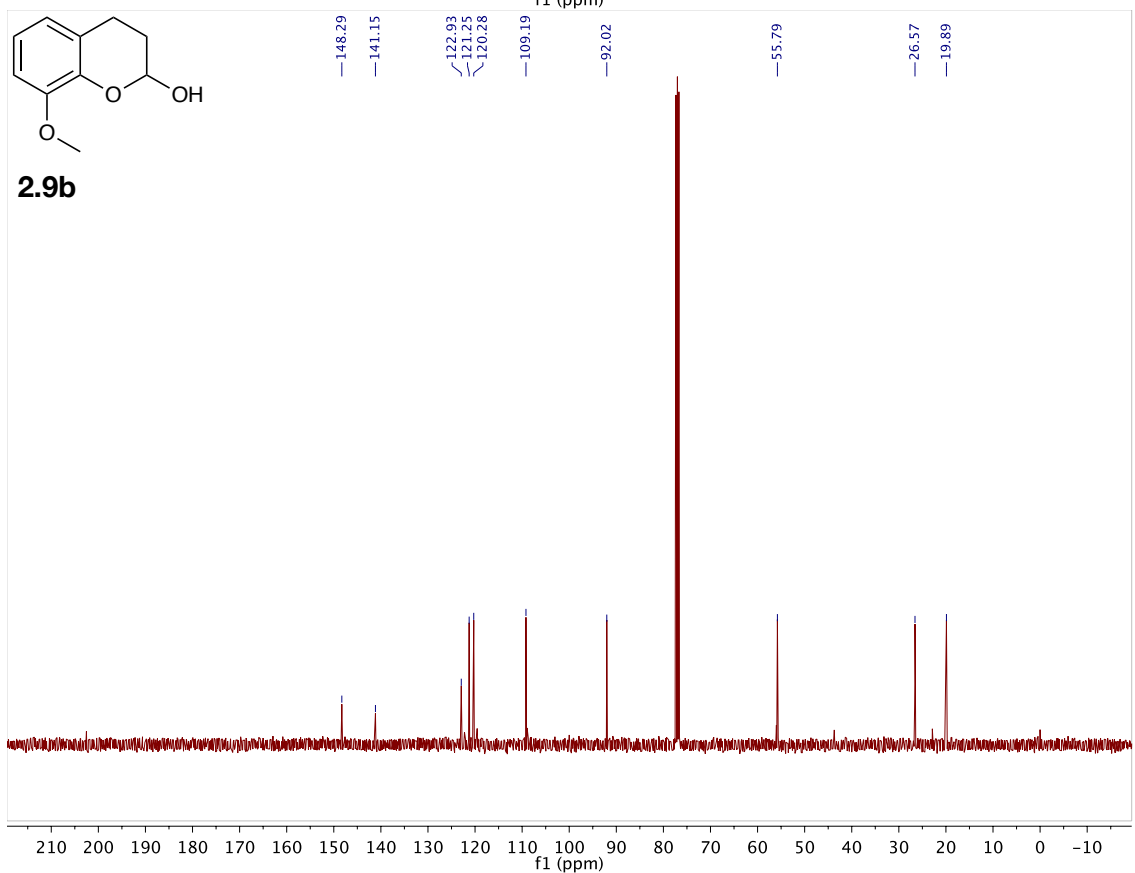
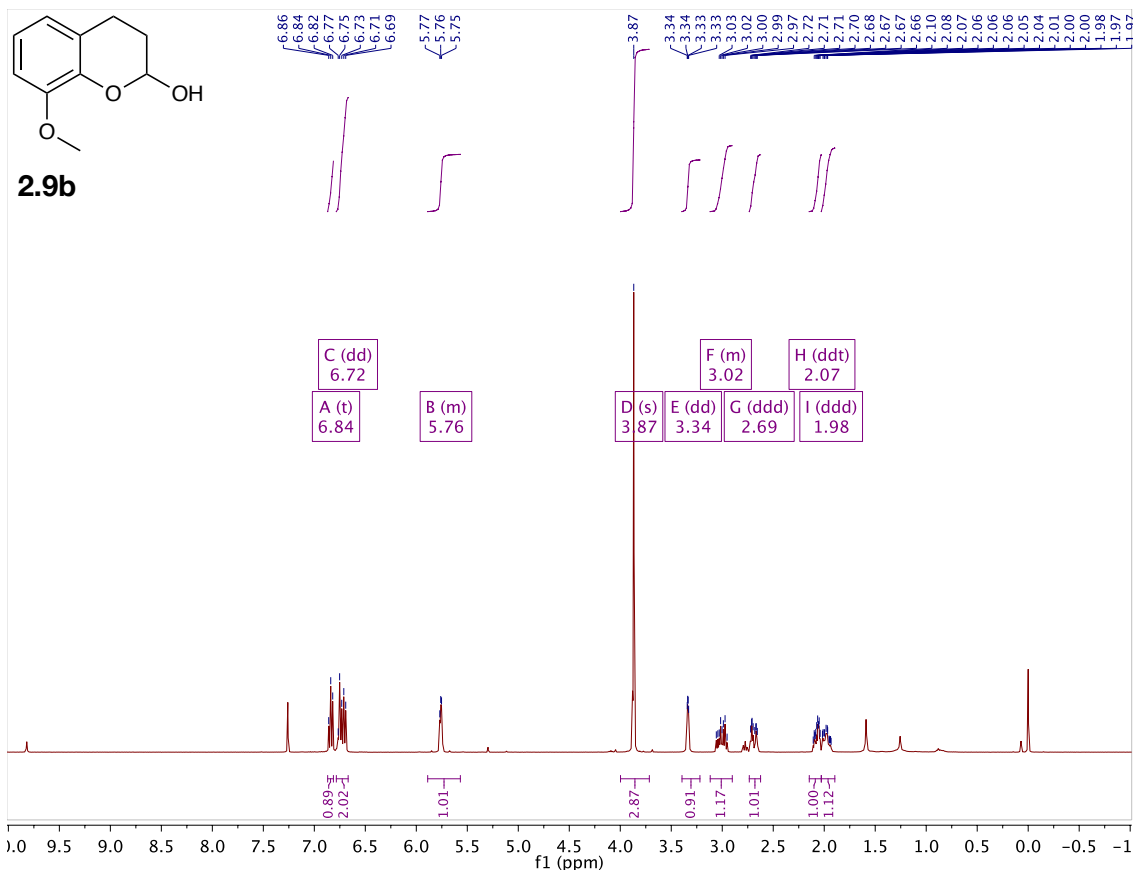


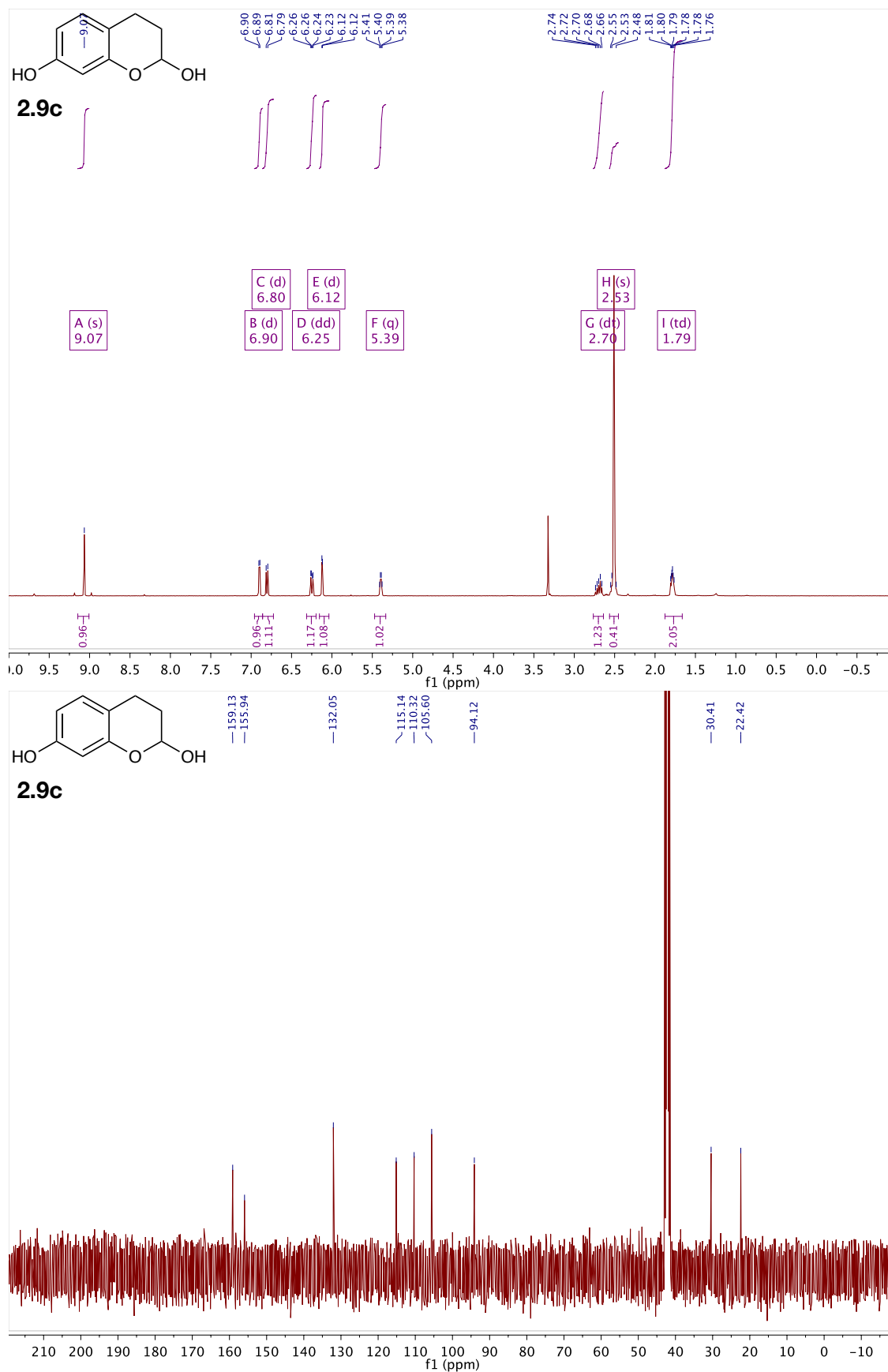


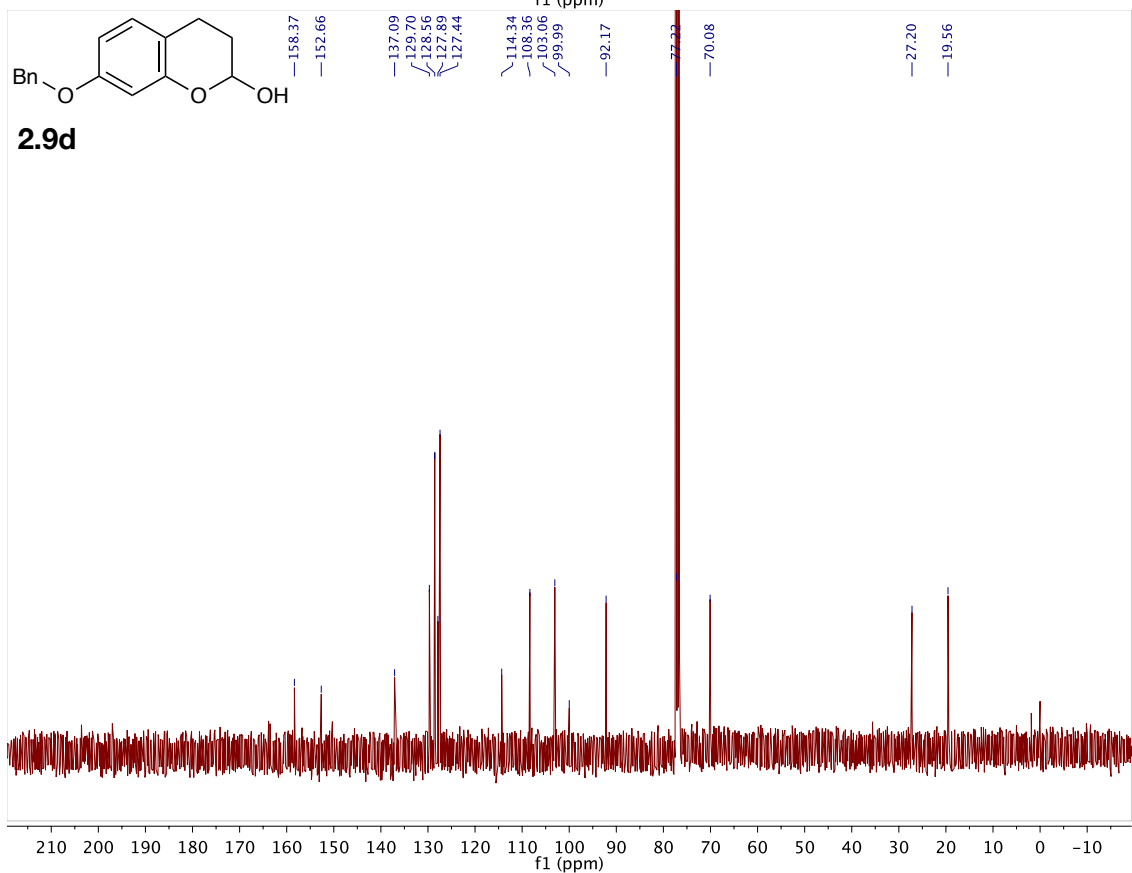
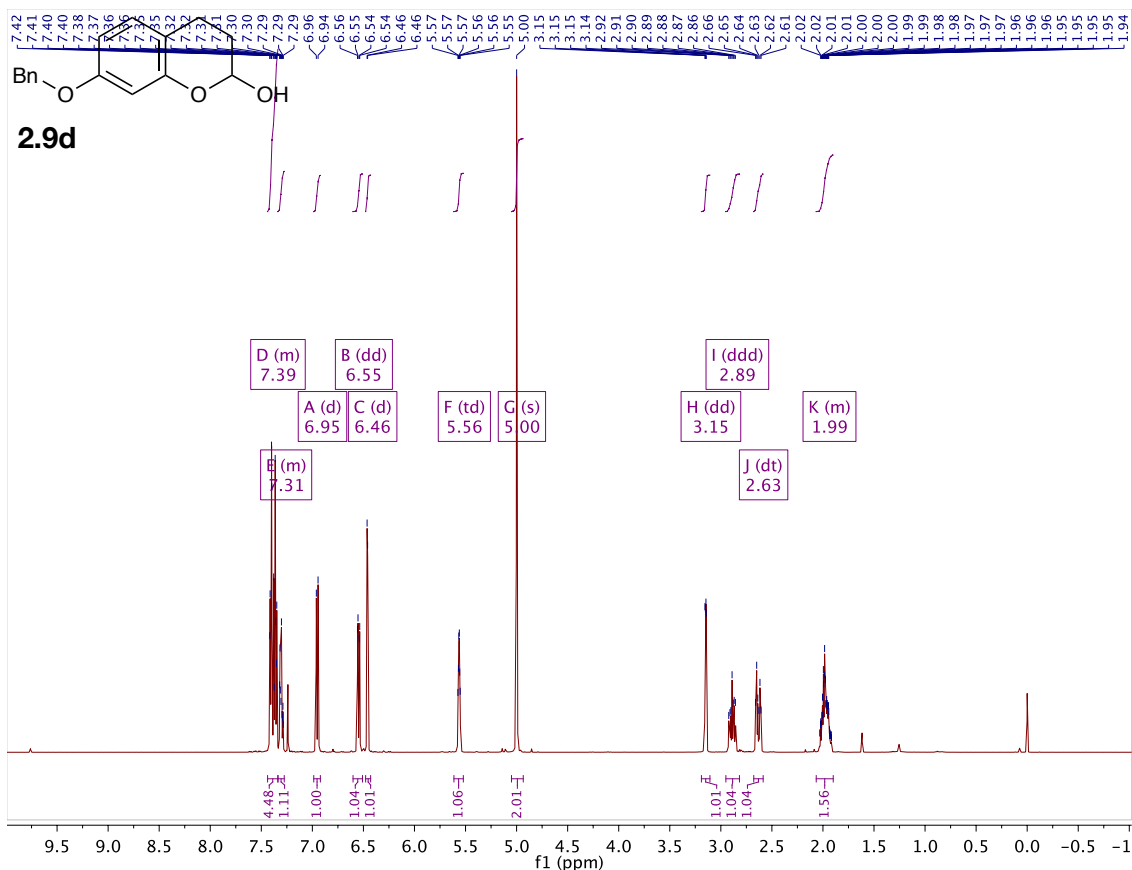


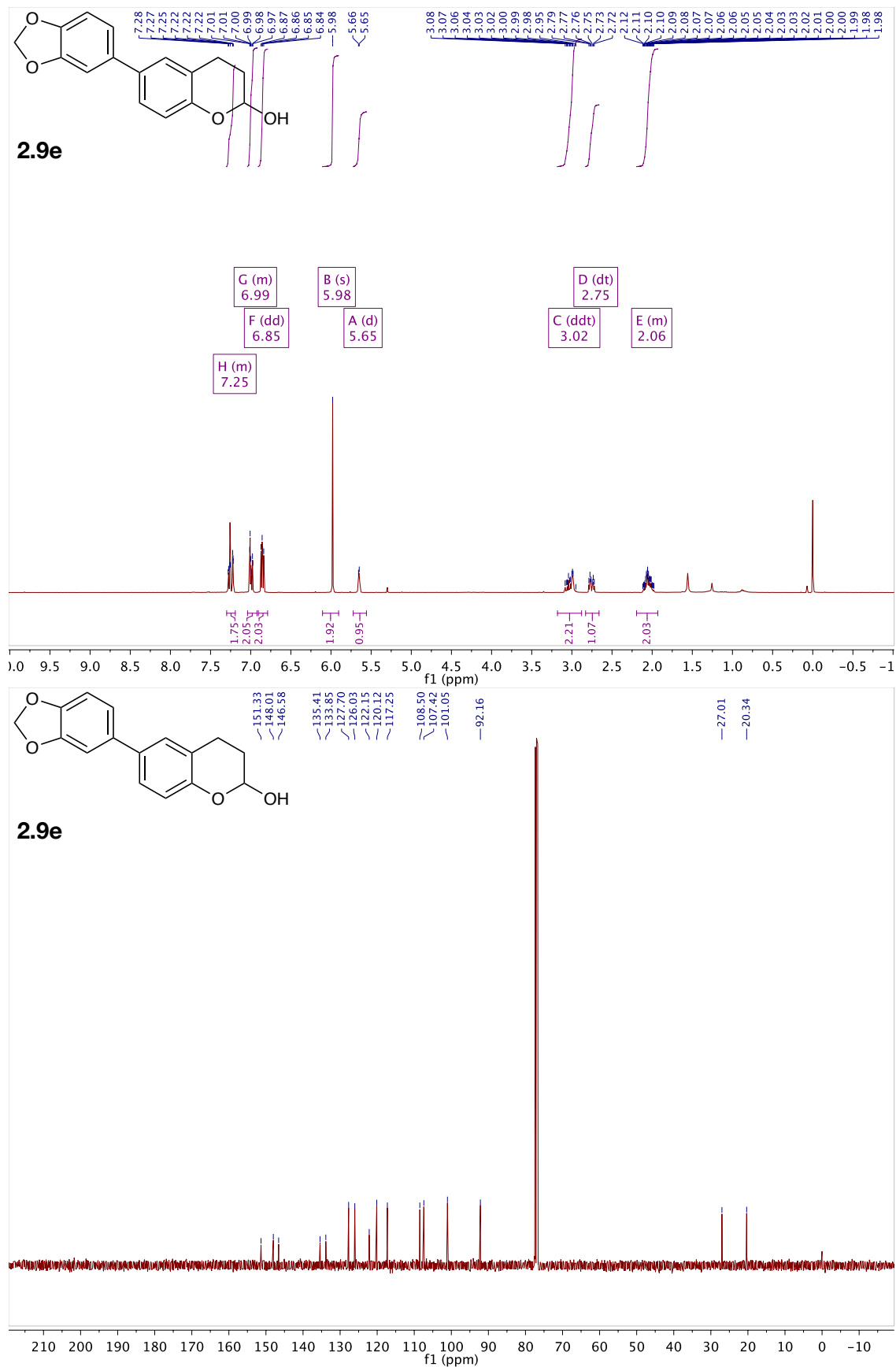


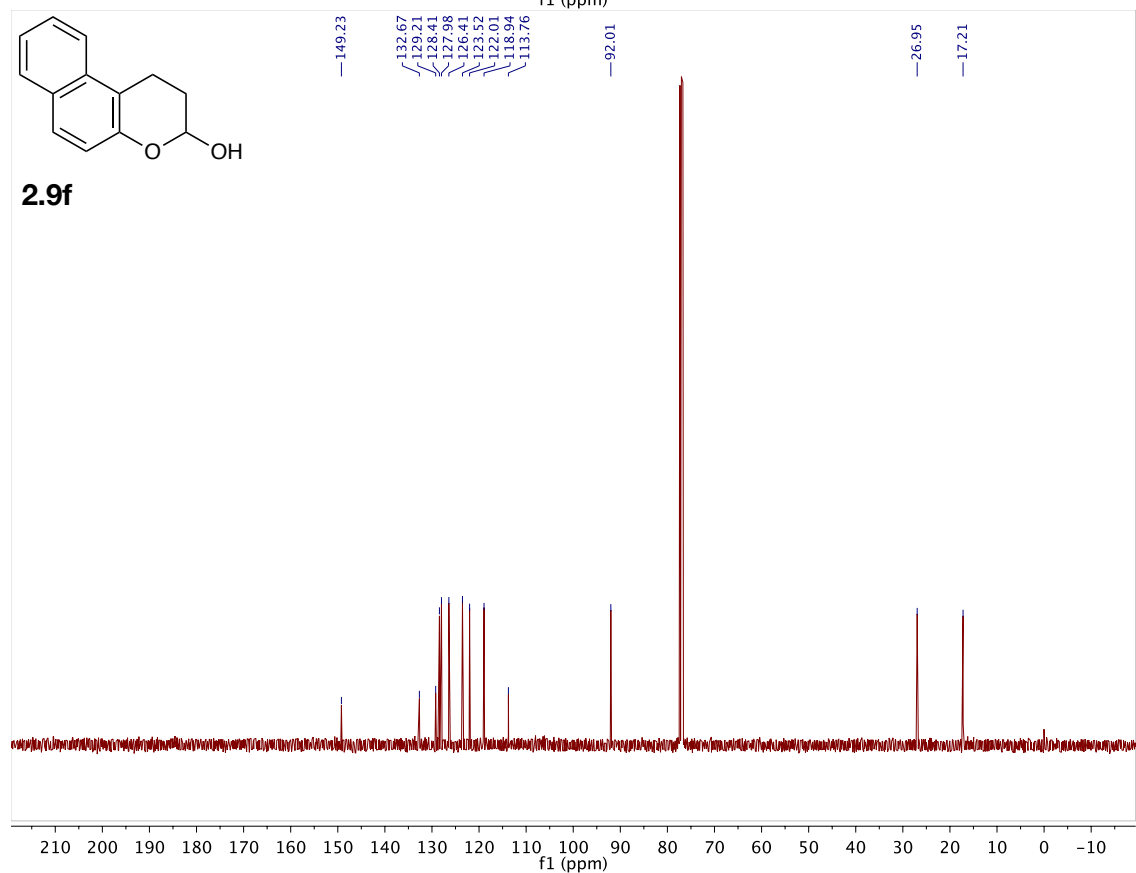
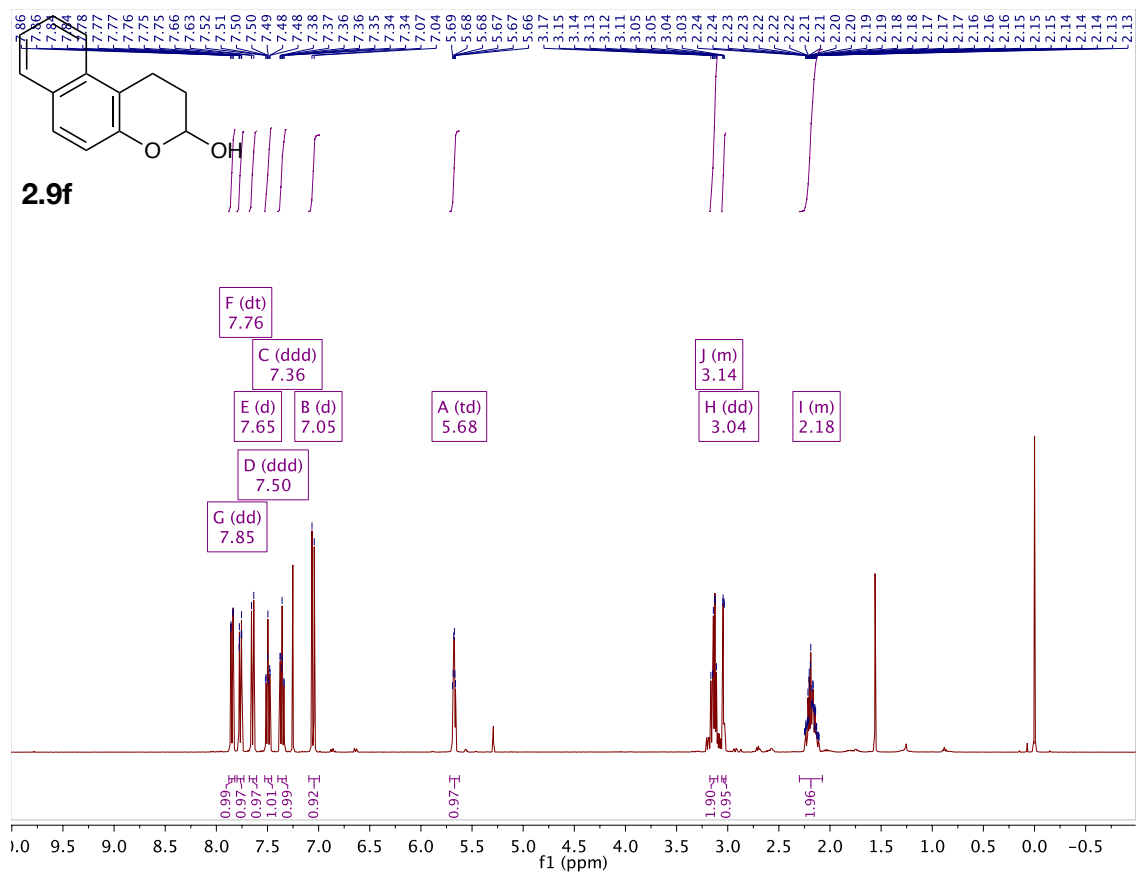


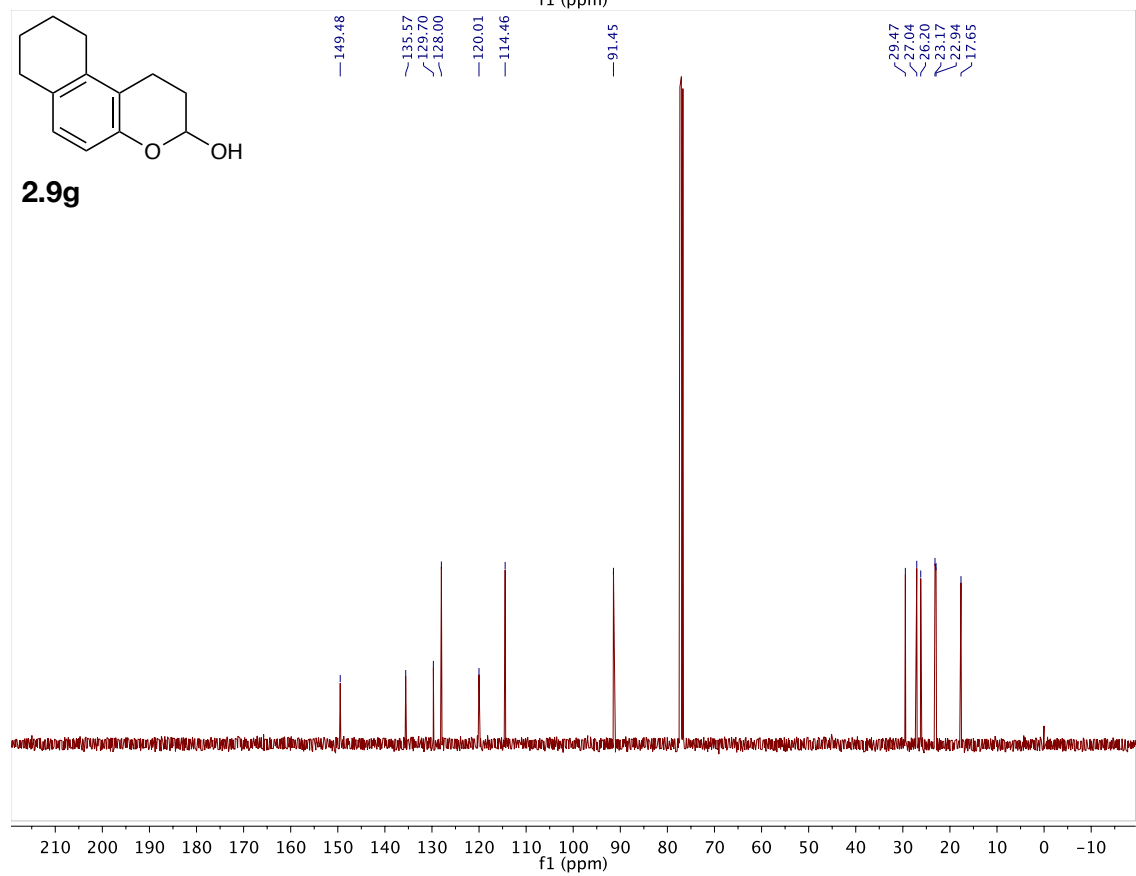
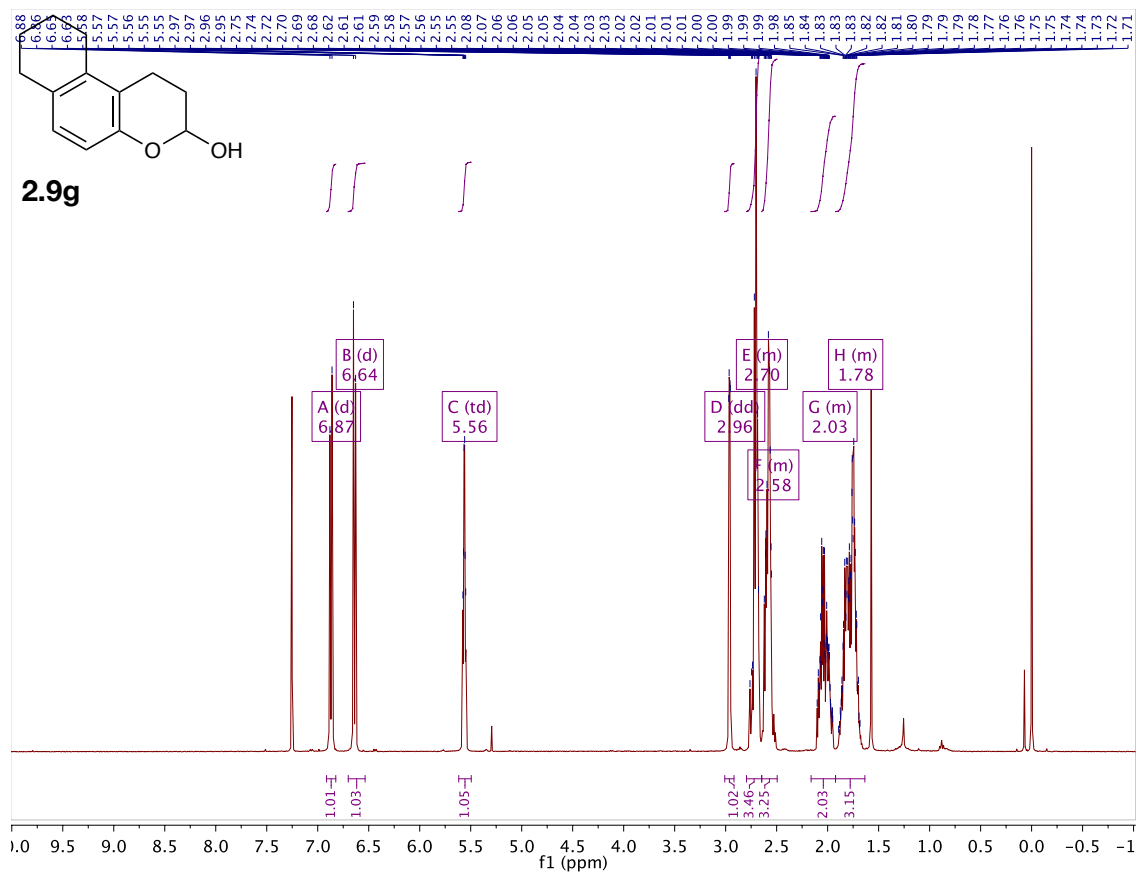


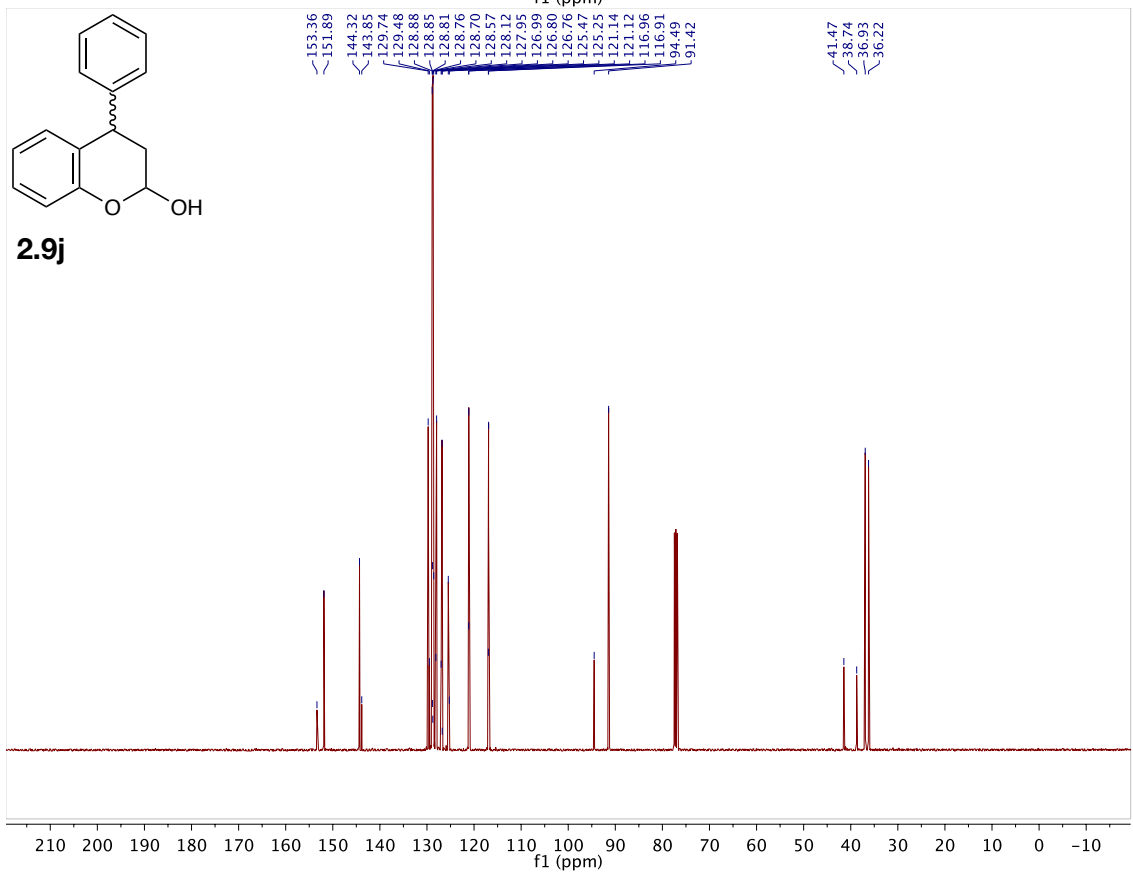
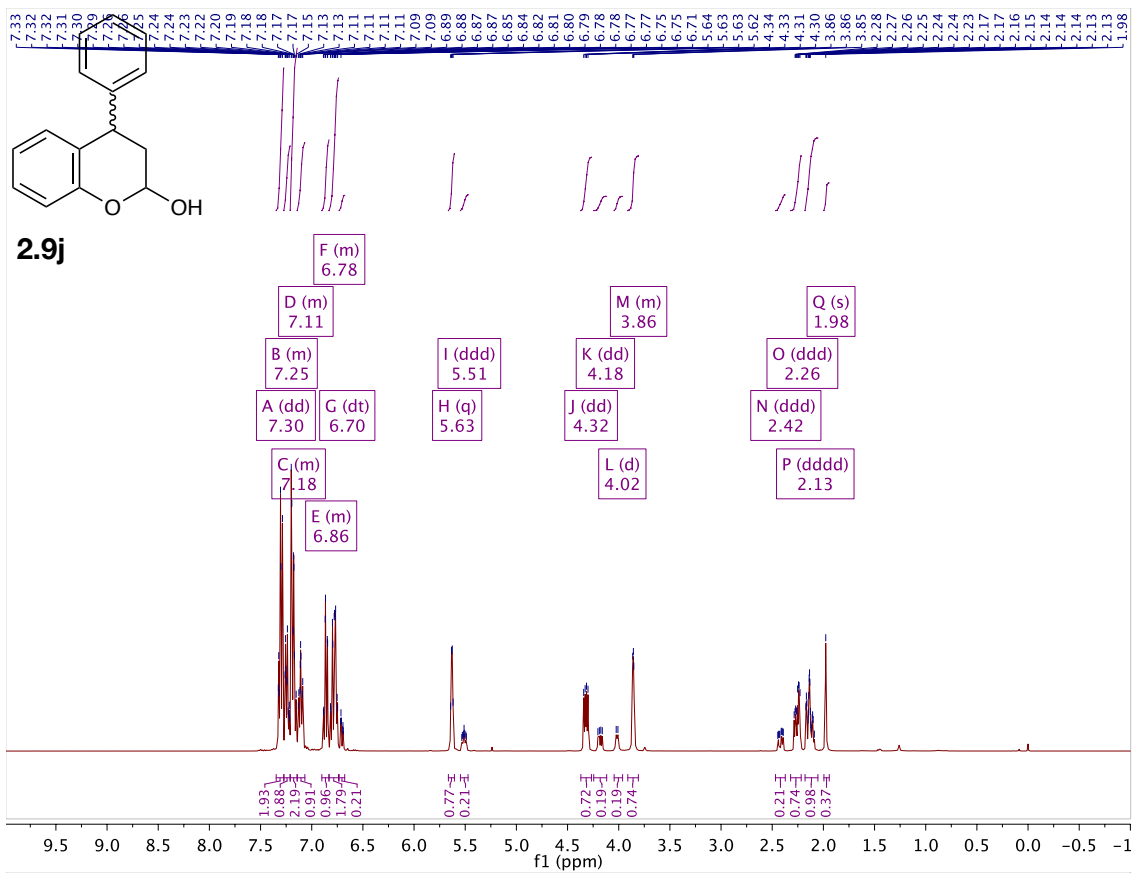


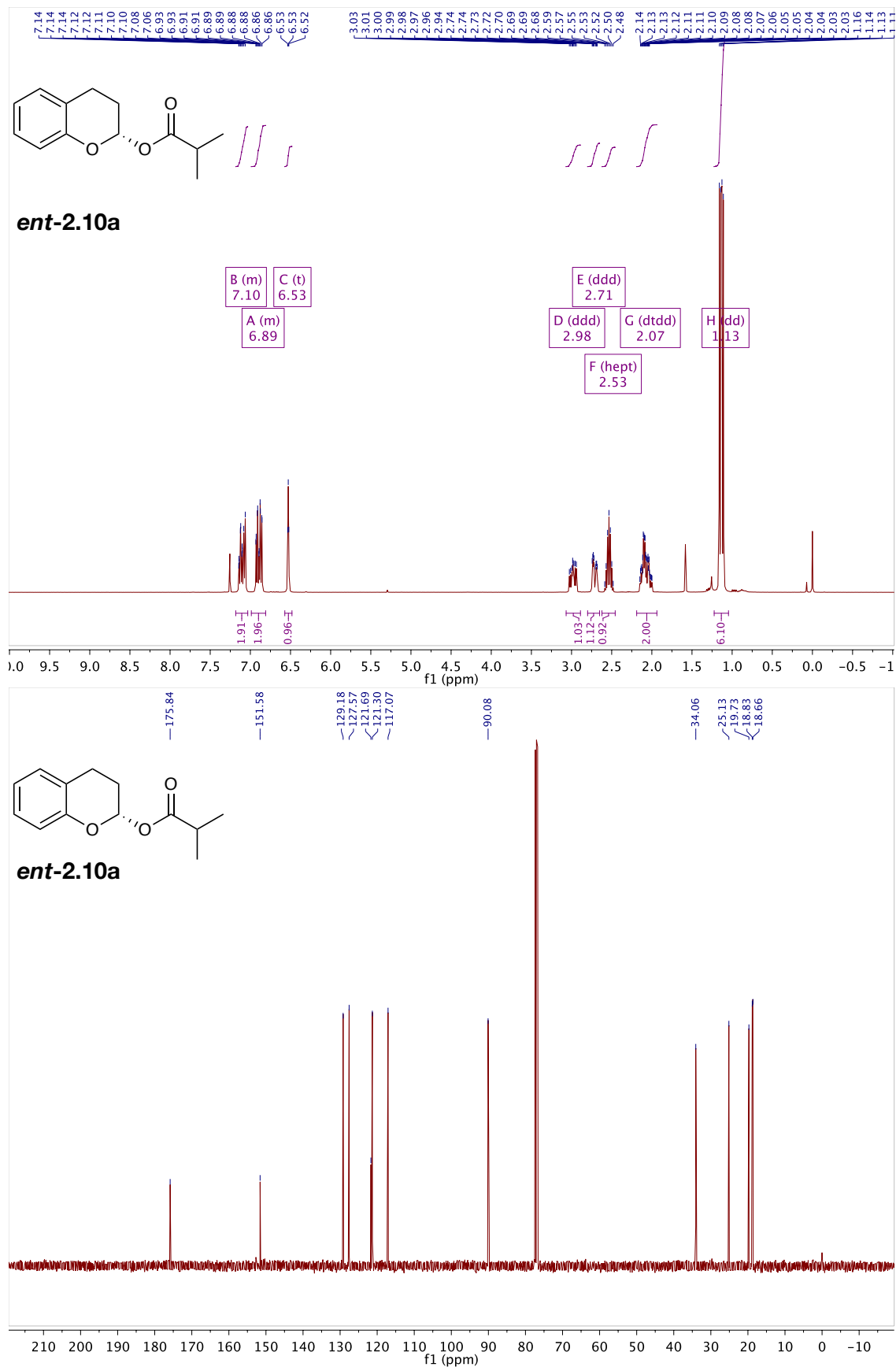


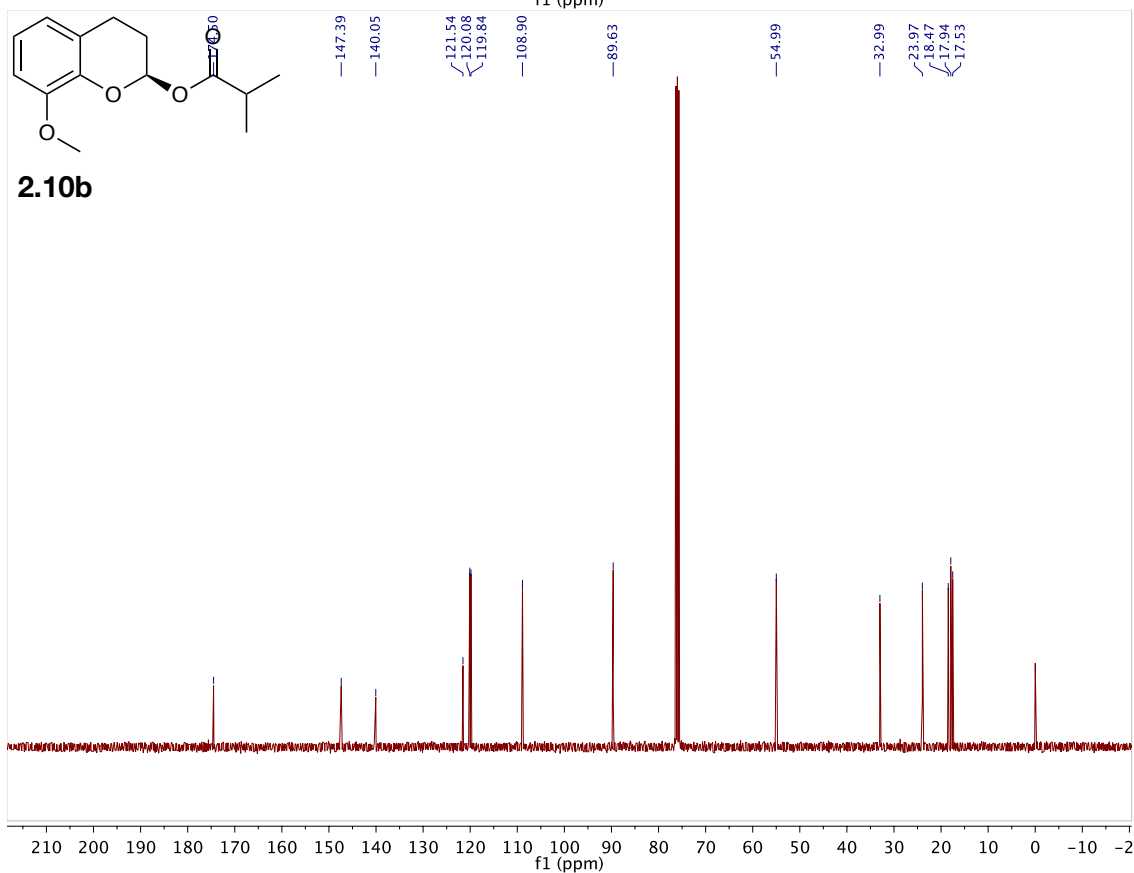
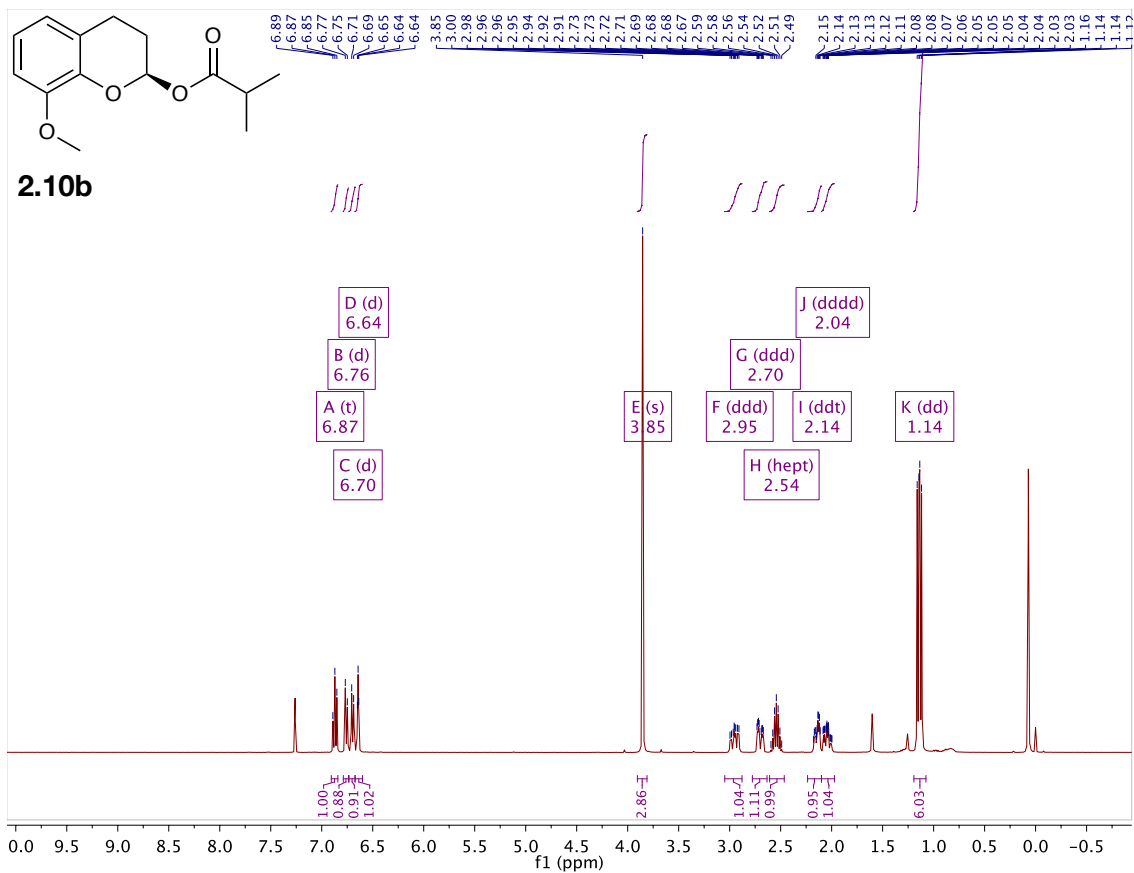


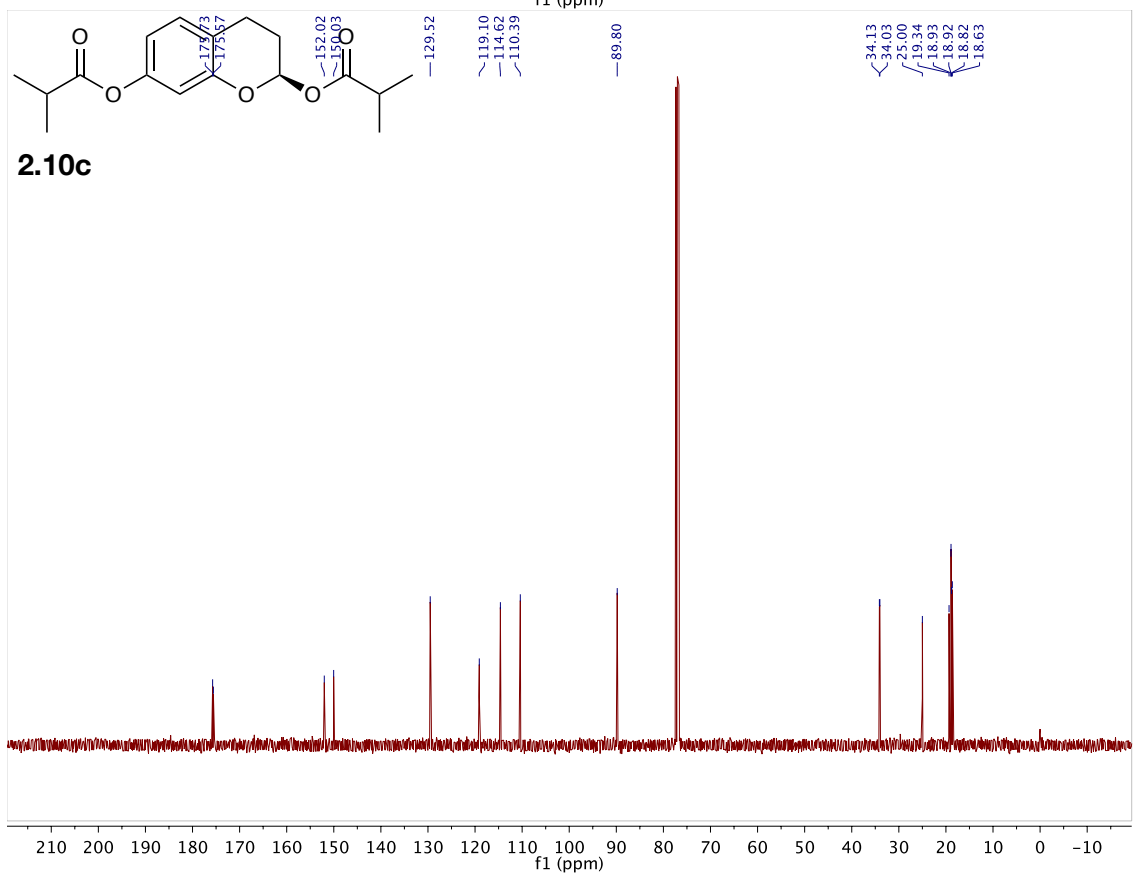
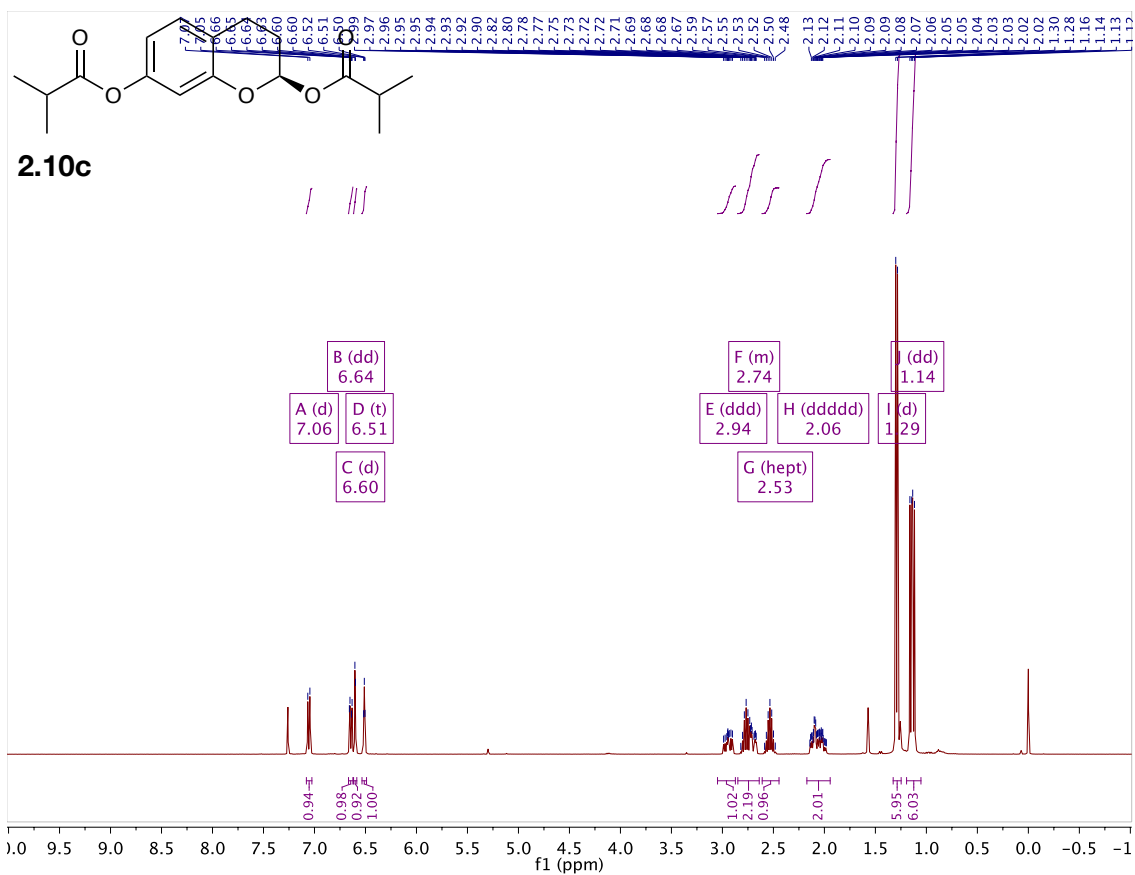


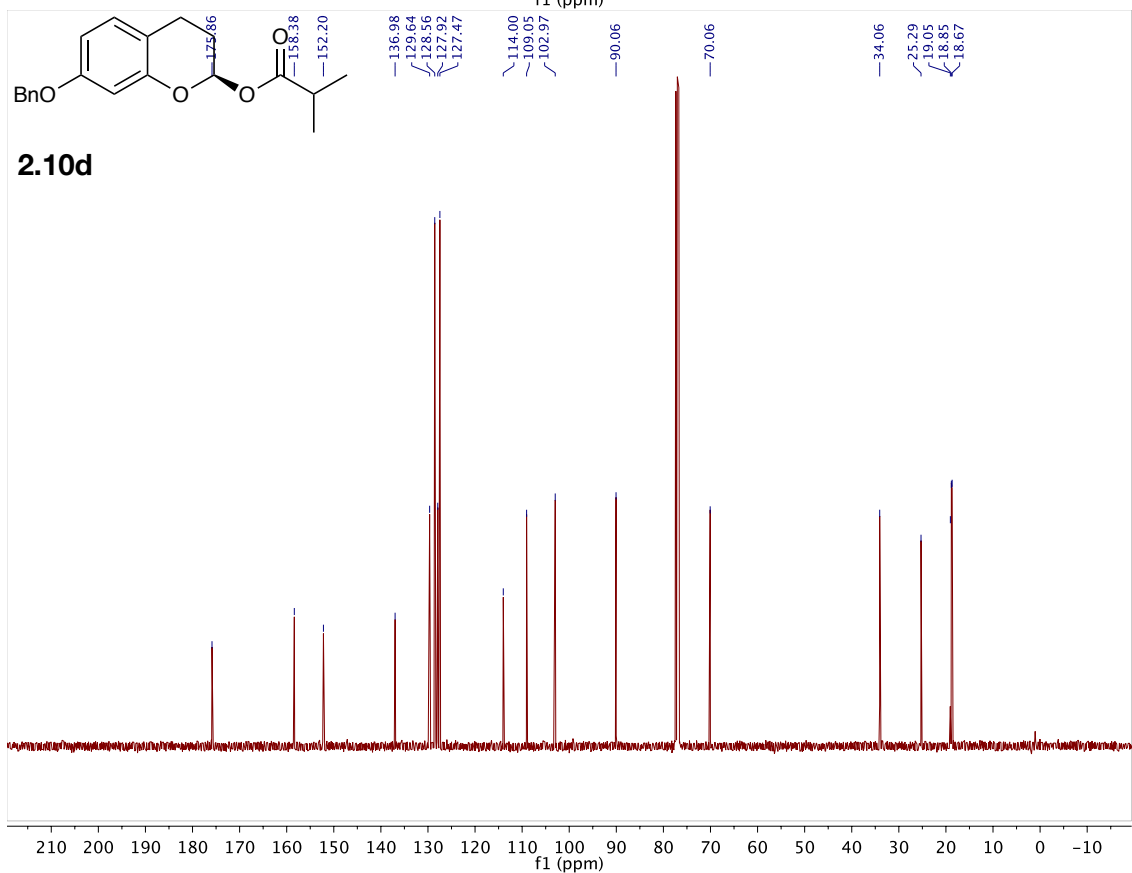
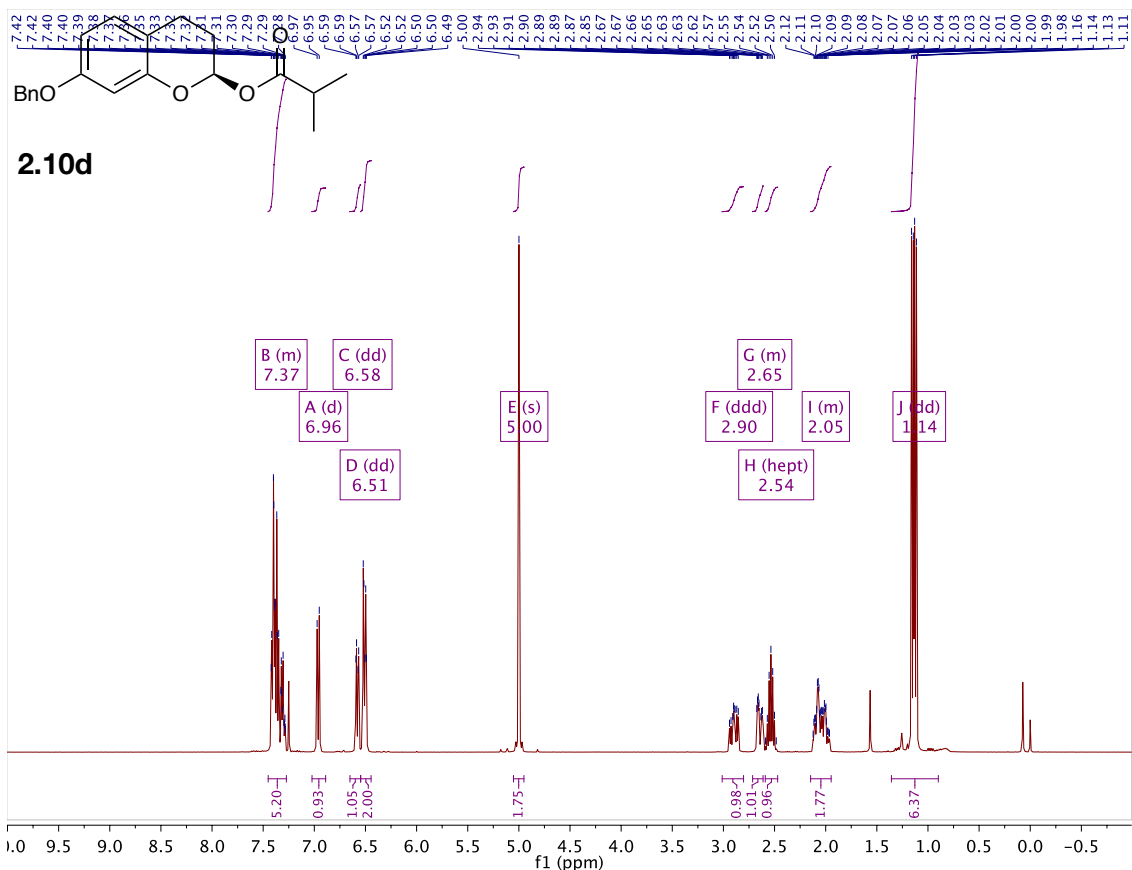


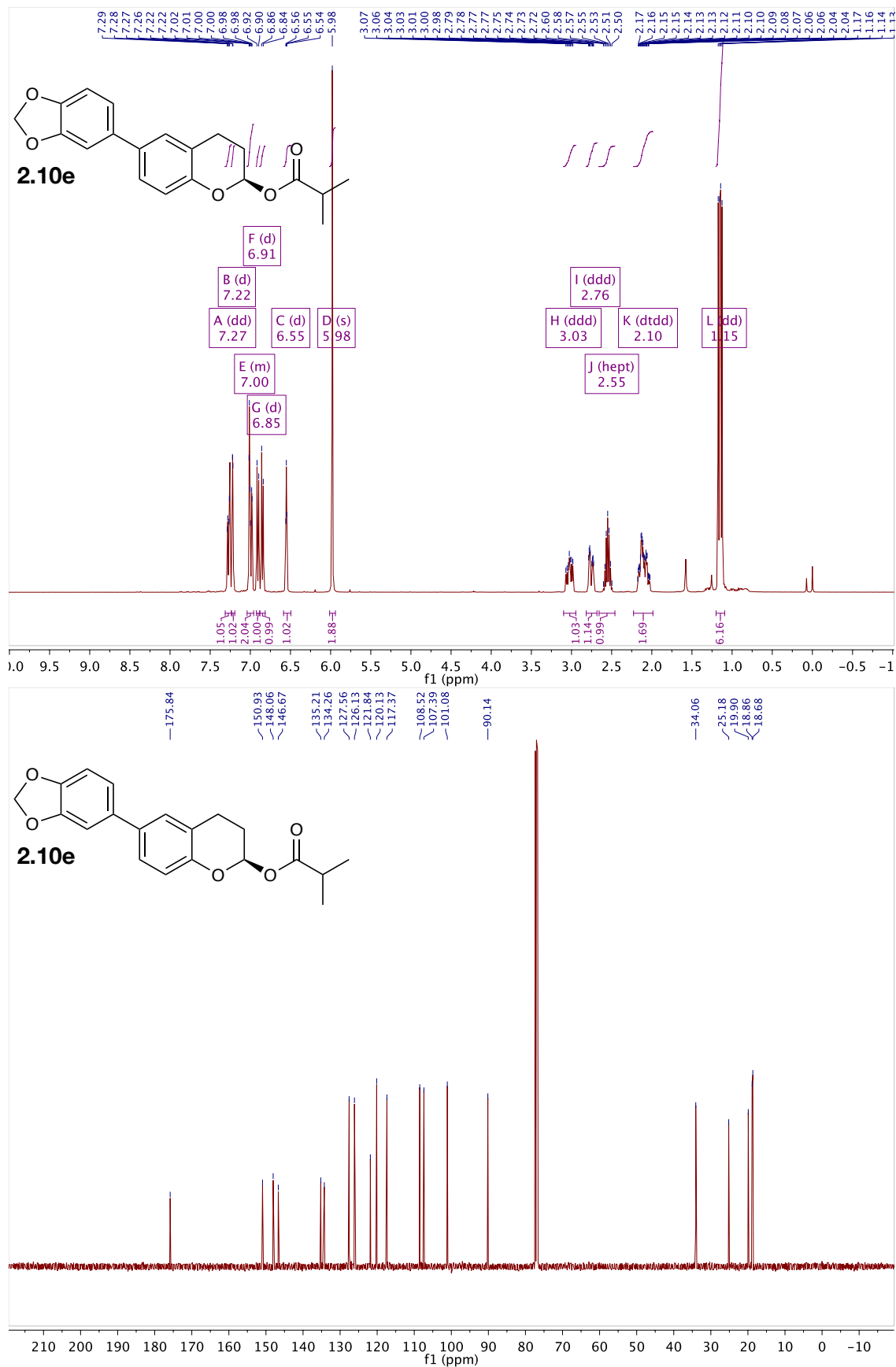


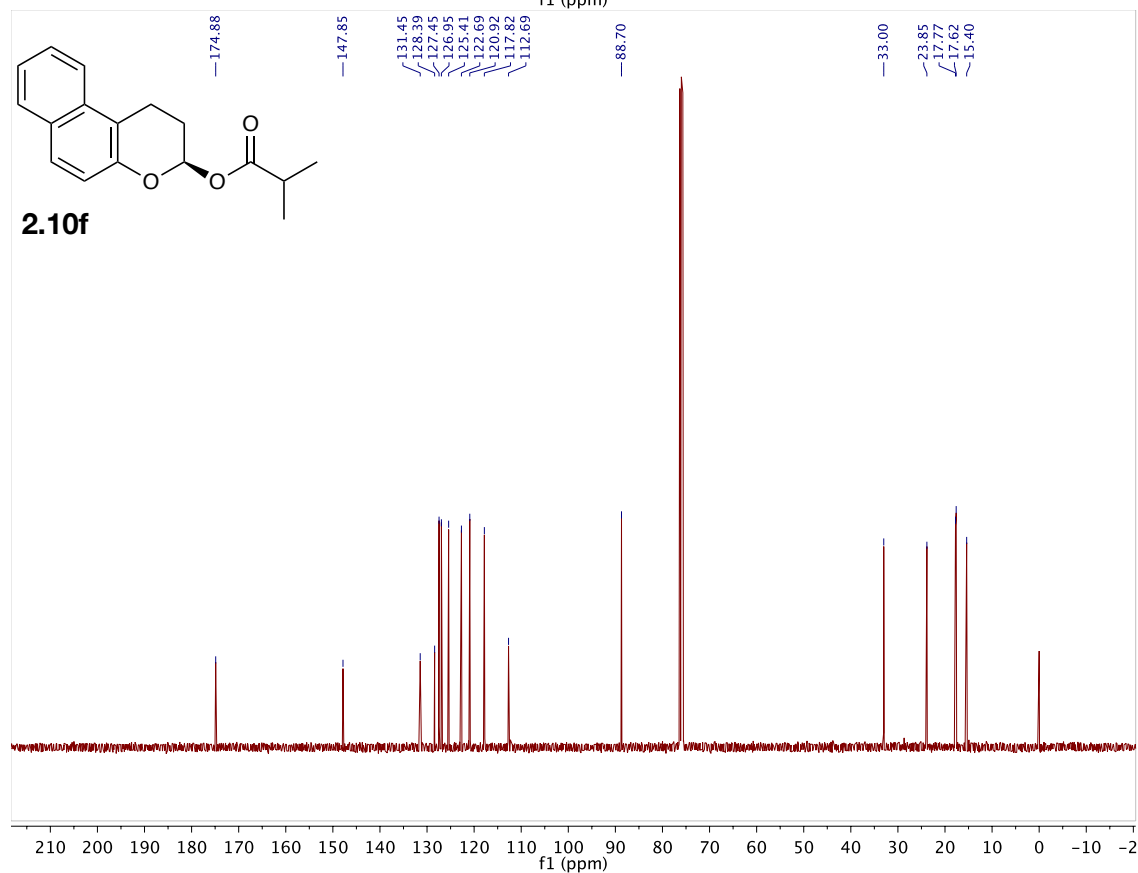
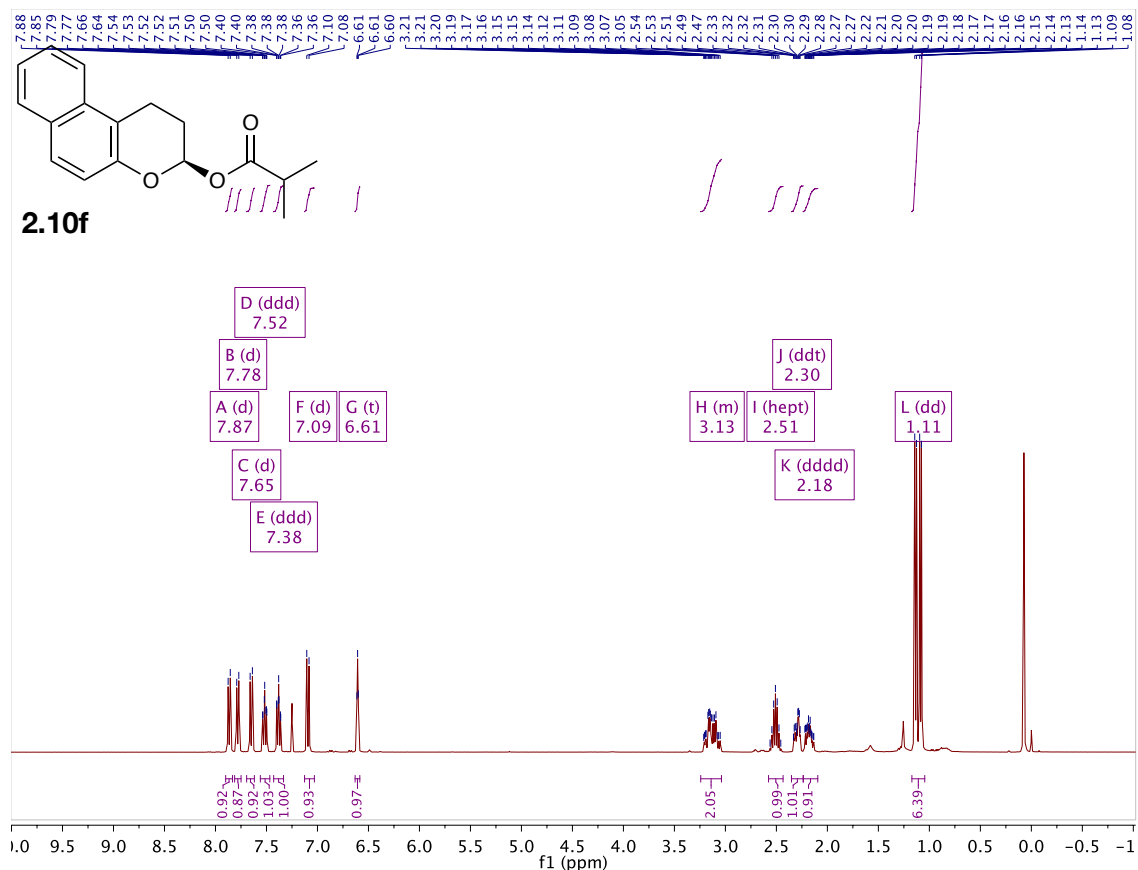


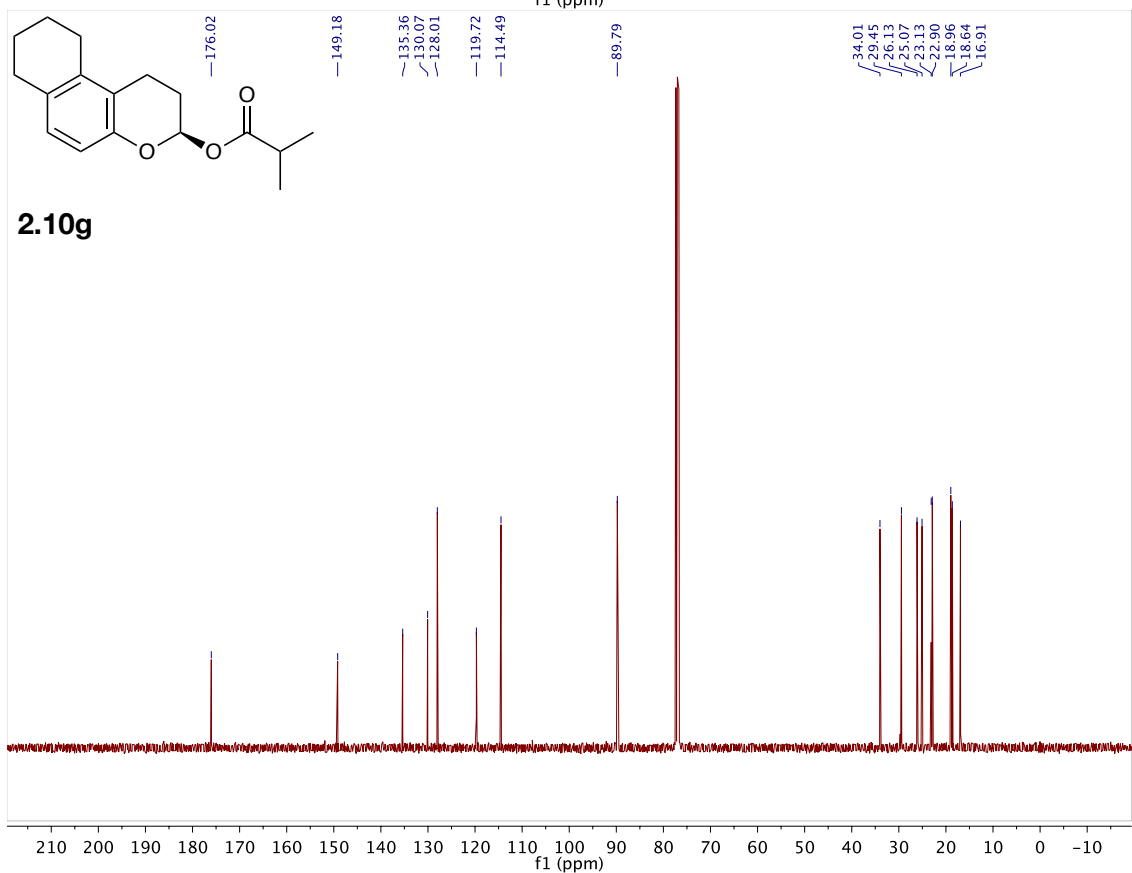
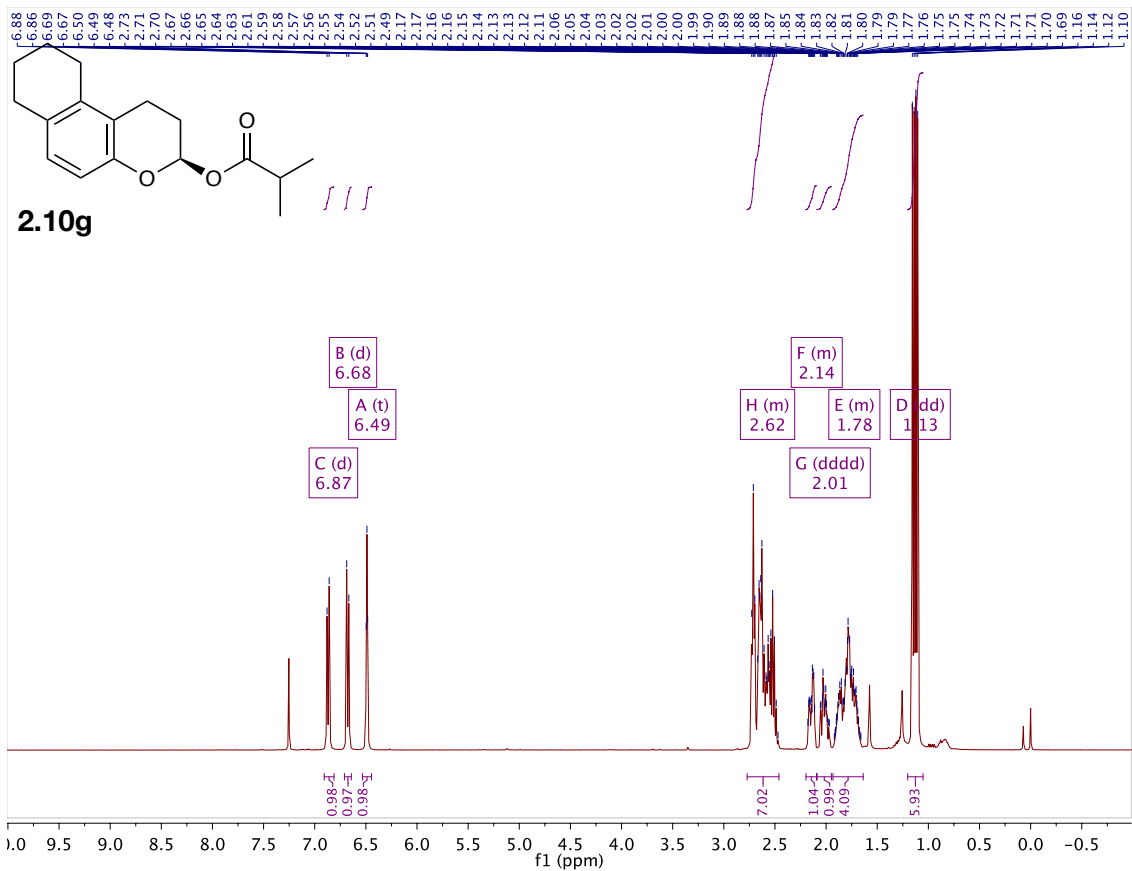


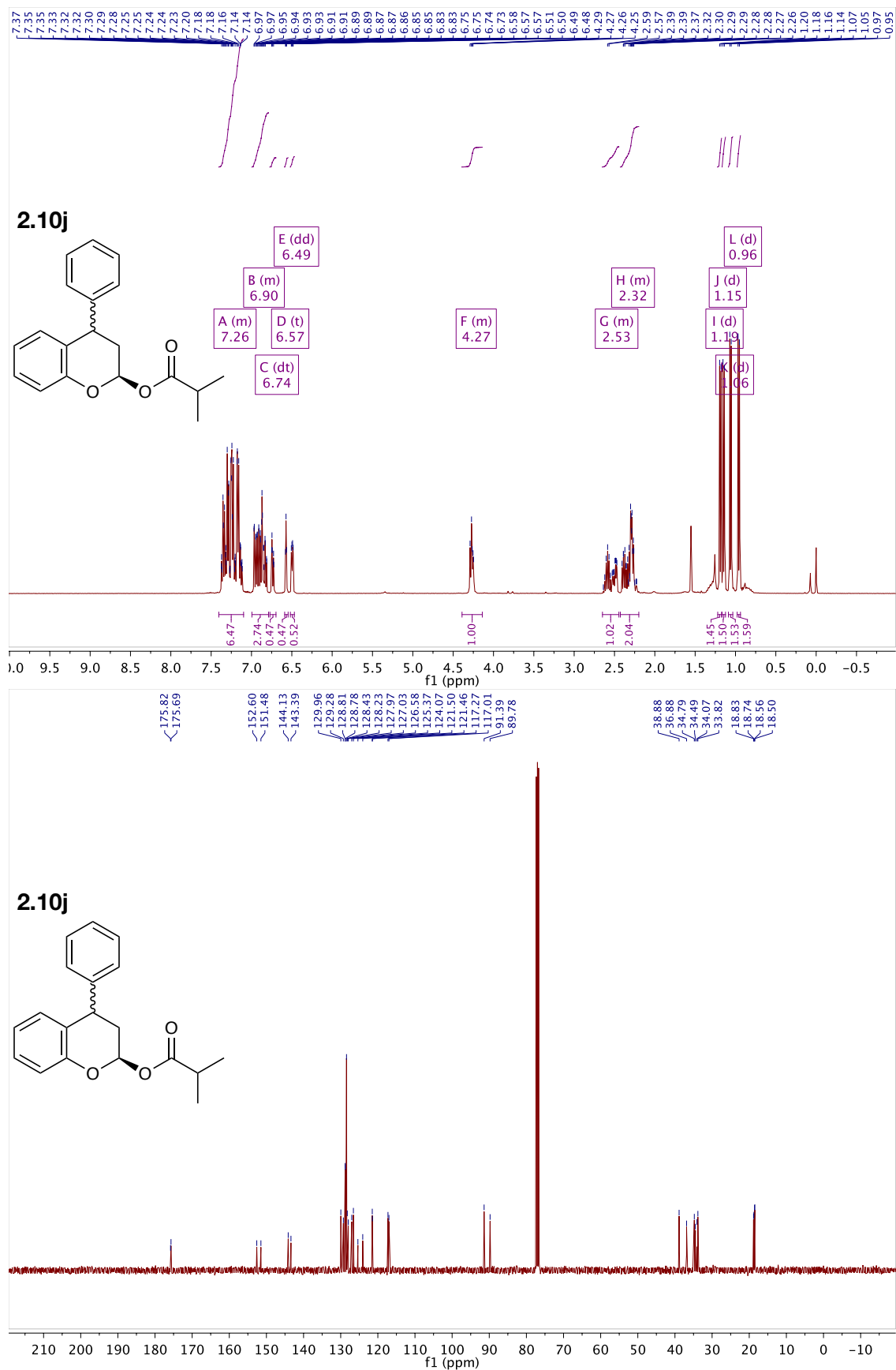


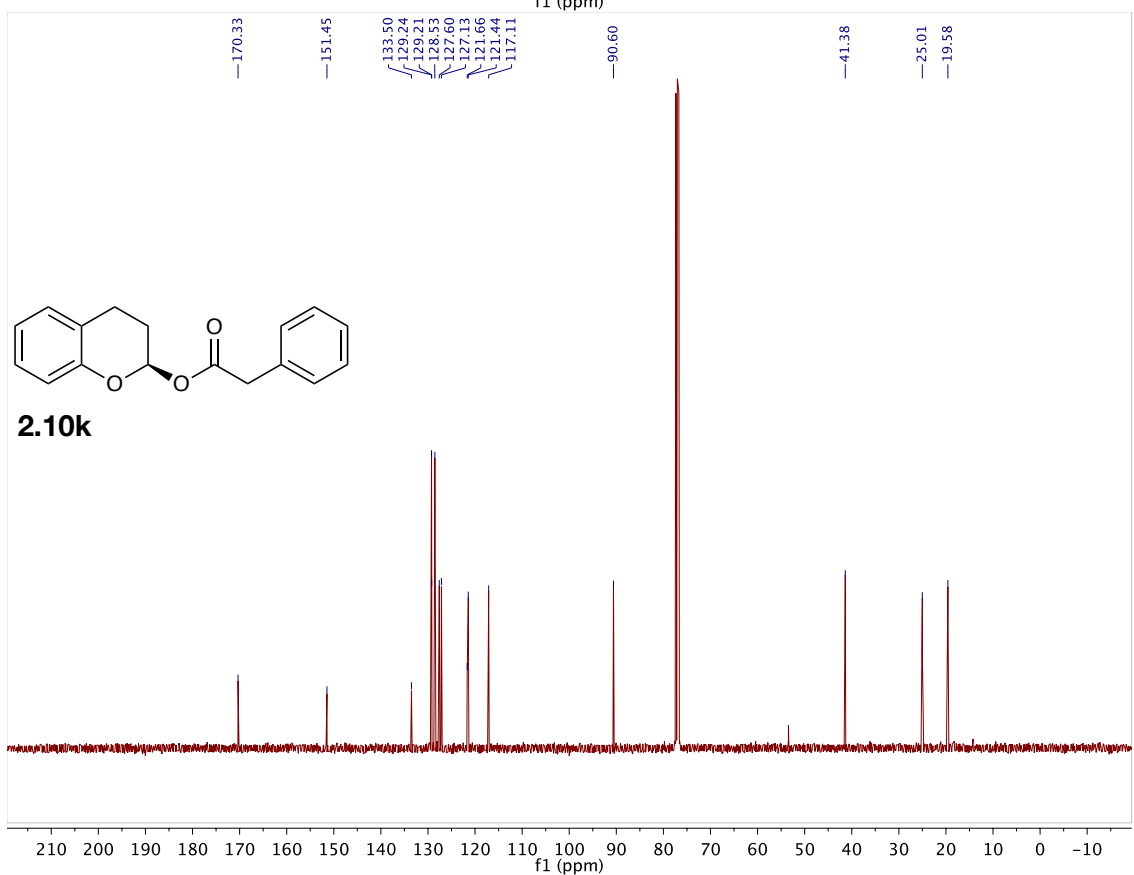
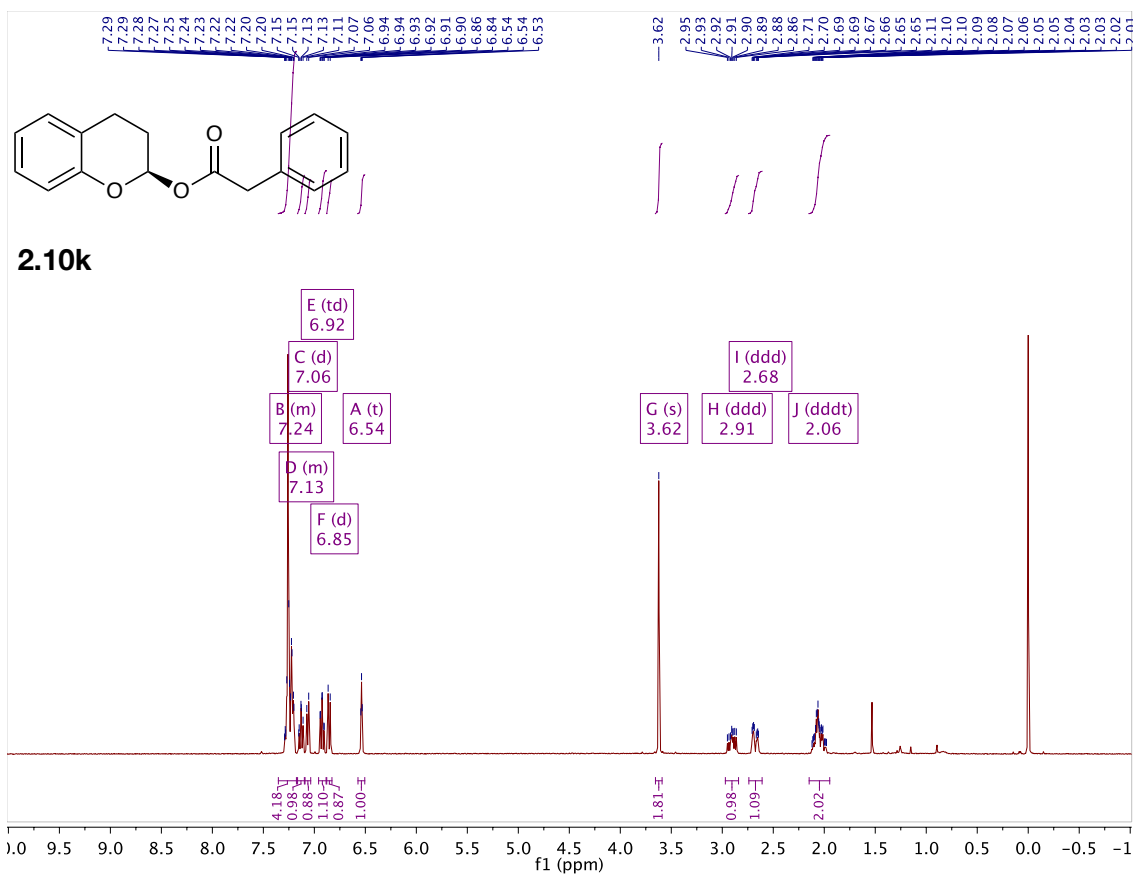


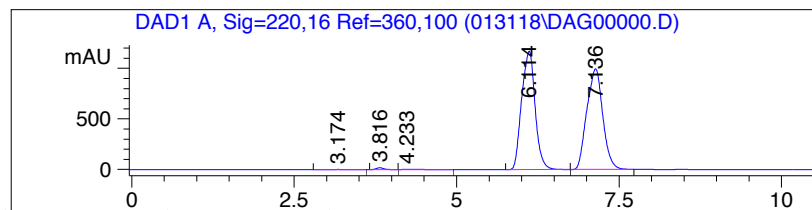






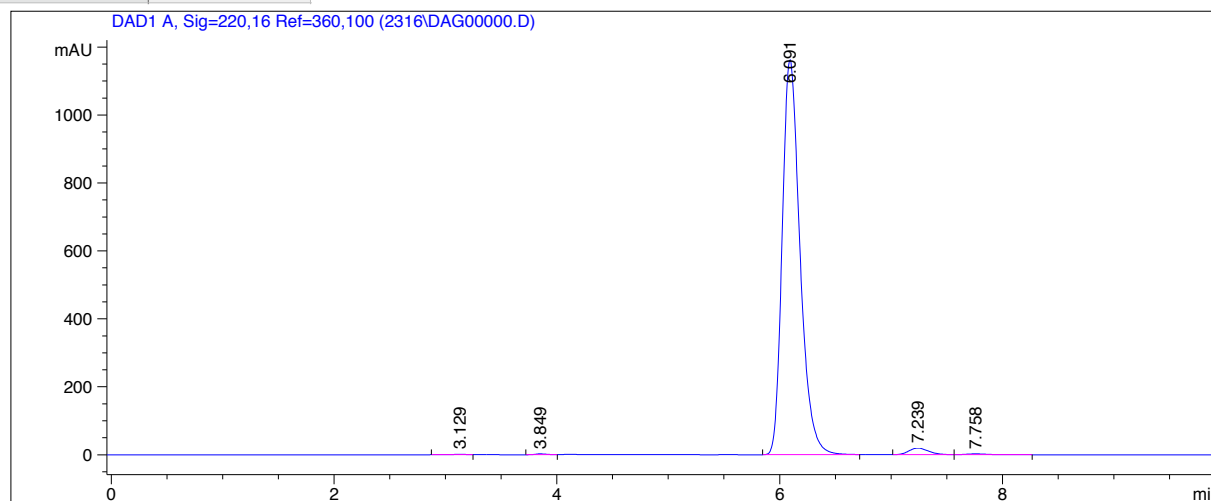
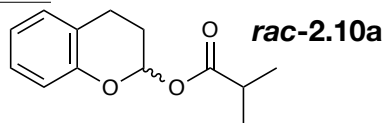






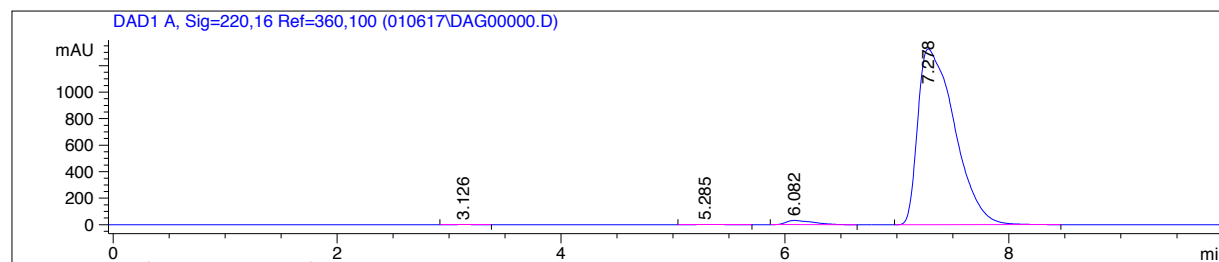
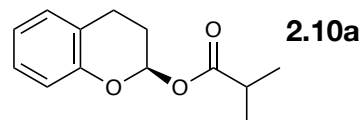
Retention Time	Area %
6.114	49.2874
7.136	49.6398

Column: Chiralcel OD-H
 Solvent: 1:99 IPA:Hex
 Flow rate: 1 mL/min
 Wavelength: 220 nm



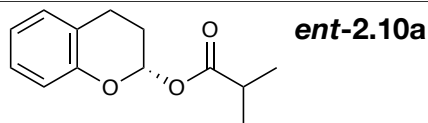
Retention Time	Area %
6.082	1.7948
7.278	98.0740

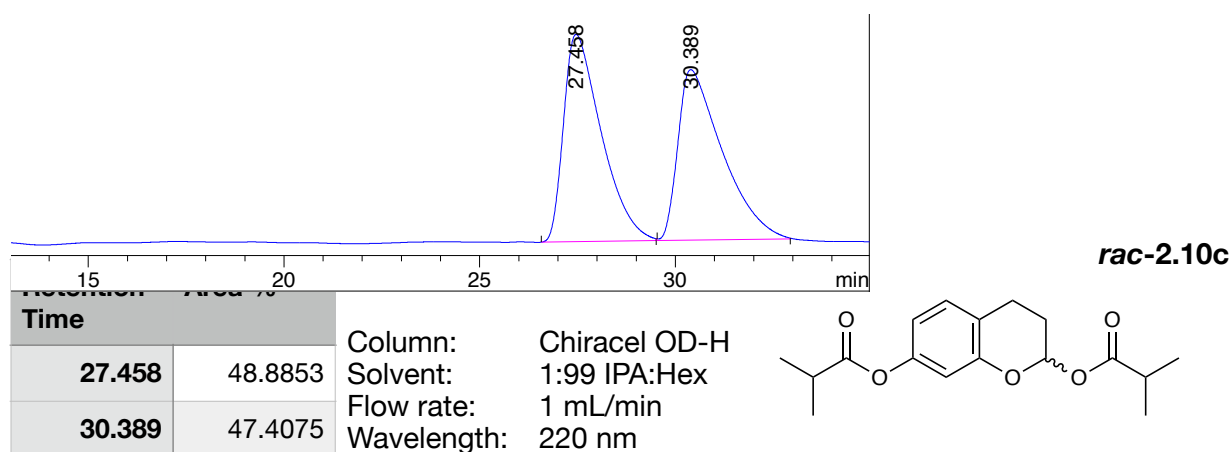
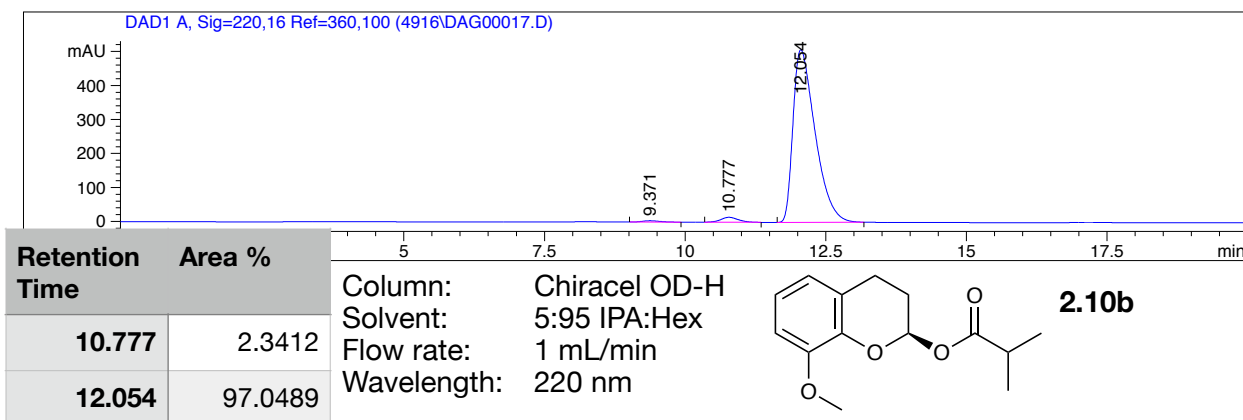
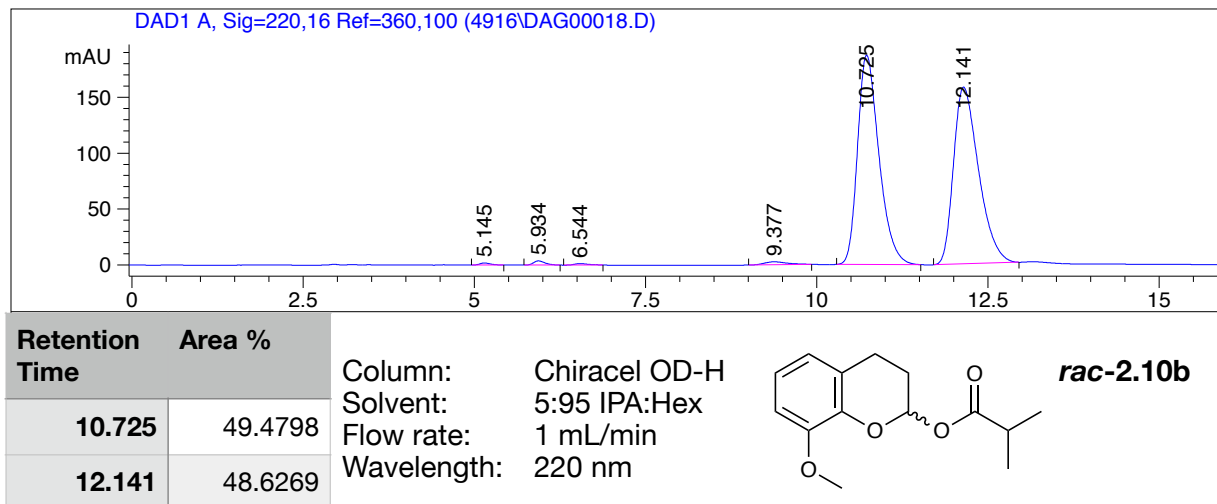
Column: Chiralcel OD-H
 Solvent: 1:99 IPA:Hex
 Flow rate: 1 mL/min
 Wavelength: 220 nm

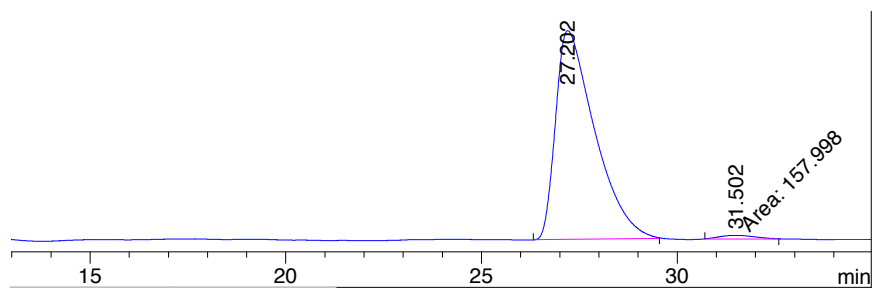


Retention Time	Area %
6.091	97.5832
7.239	1.8373

Column: Chiralcel OD-H
 Solvent: 1:99 IPA:Hex
 Flow rate: 1 mL/min
 Wavelength: 220 nm

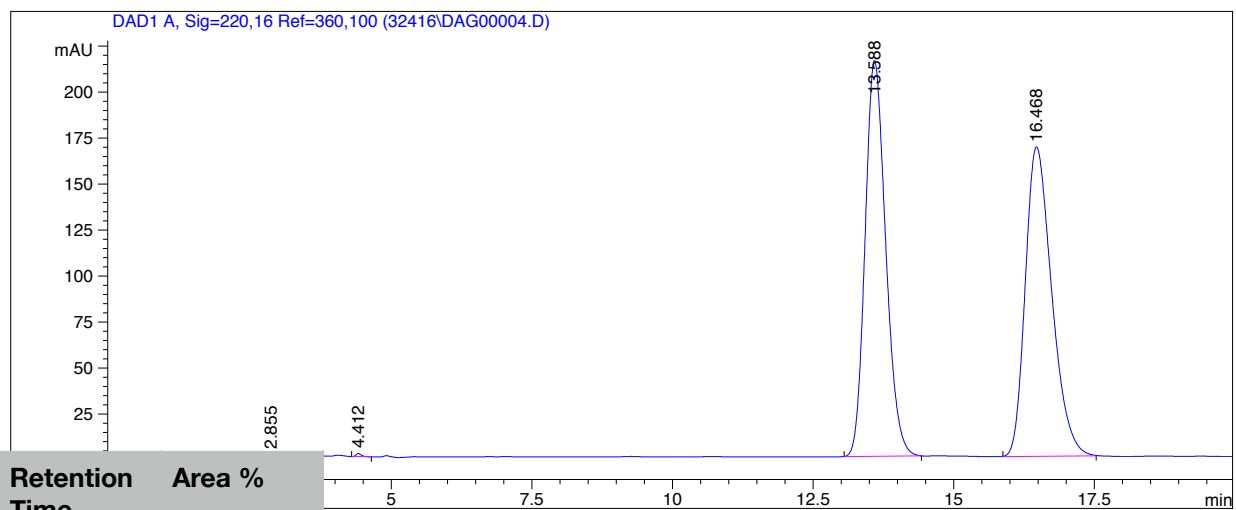
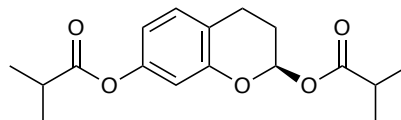






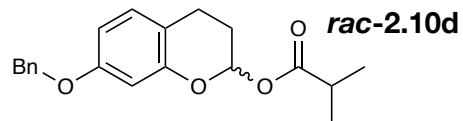
Retention Time	Area %
27.202	93.3777
32.502	1.6283

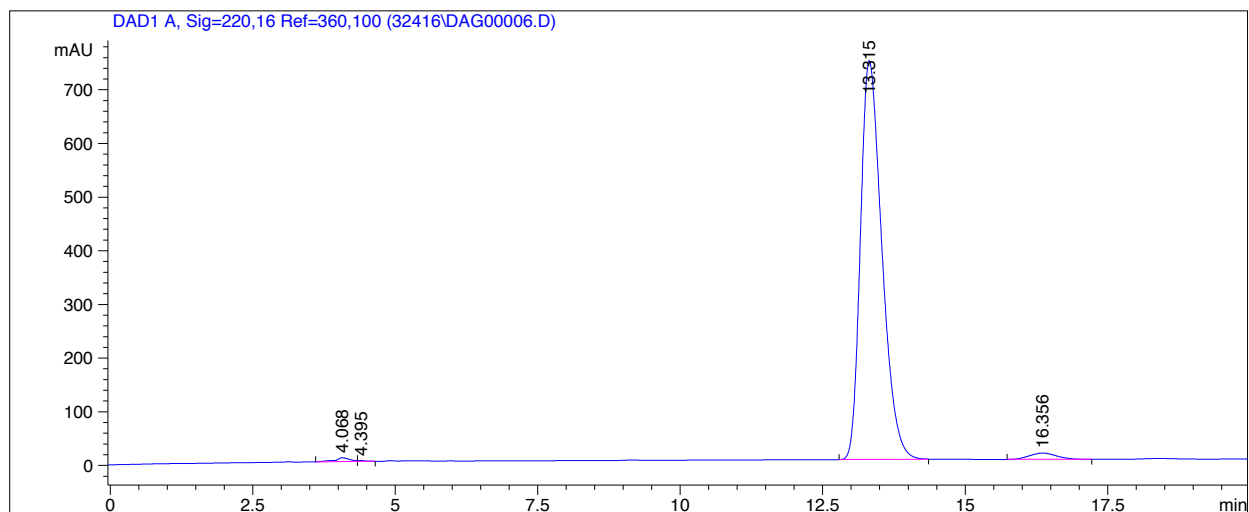
Column: Chiralcel OD-H
 Solvent: 1:99 IPA:Hex
 Flow rate: 1 mL/min
 Wavelength: 220 nm

2.10c

Retention Time	Area %
13.588	49.6218
16.468	49.7719

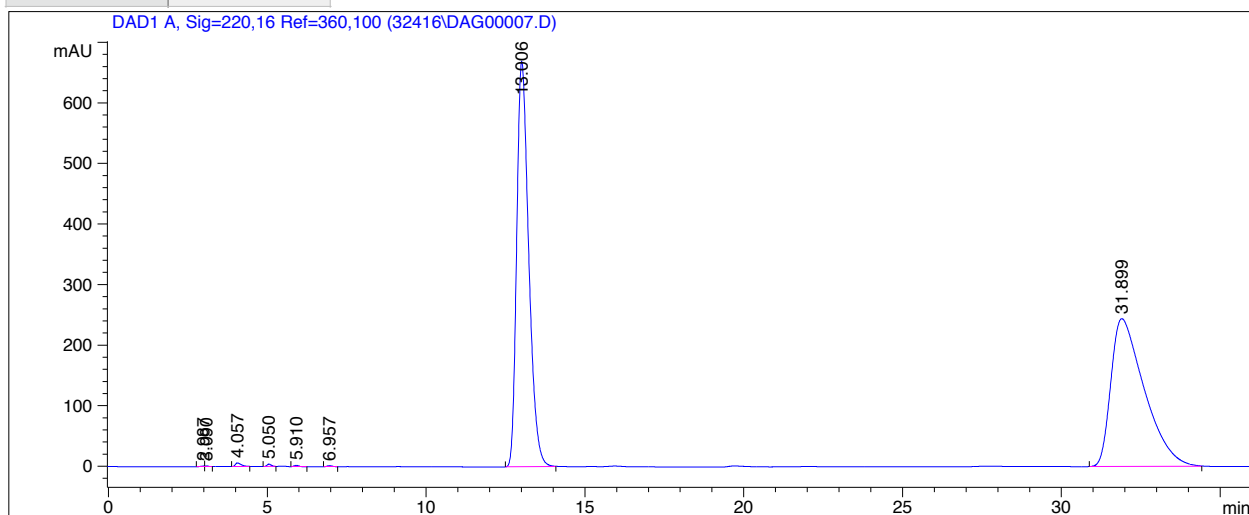
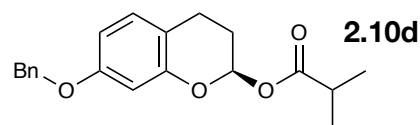
Column: Chiralcel OD-H
 Solvent: 1:99 IPA:Hex
 Flow rate: 1 mL/min
 Wavelength: 220 nm





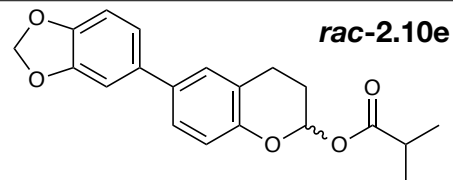
Retention Time	Area %
13.315	97.2747
16.356	1.9808

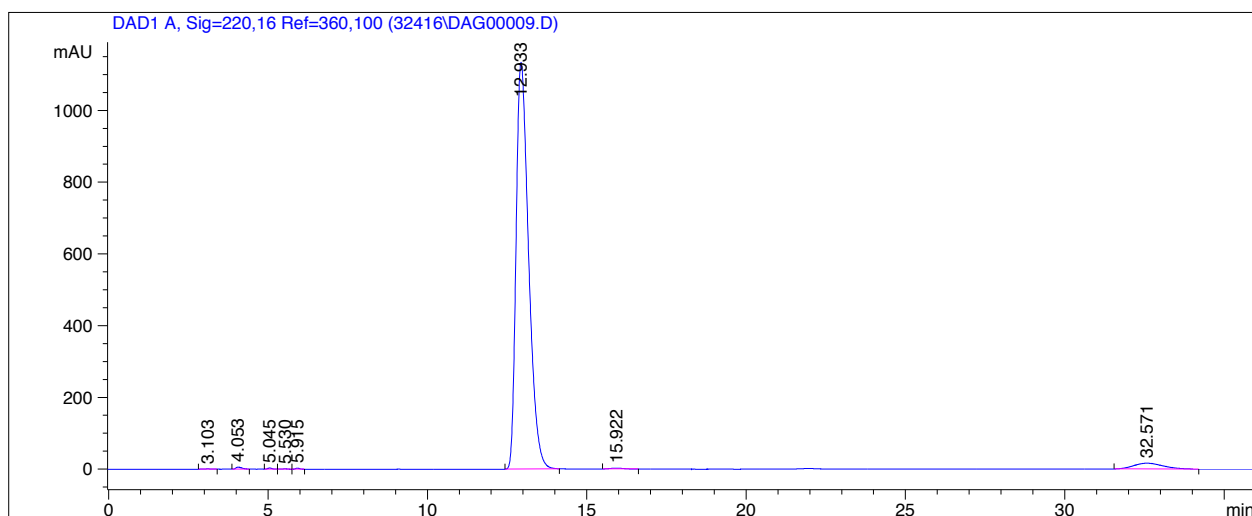
Column: Chiralcel OD-H
 Solvent: 1:99 IPA:Hex
 Flow rate: 1 mL/min
 Wavelength: 220 nm



Retention Time	Area %
13.006	49.4282
31.899	50.0984

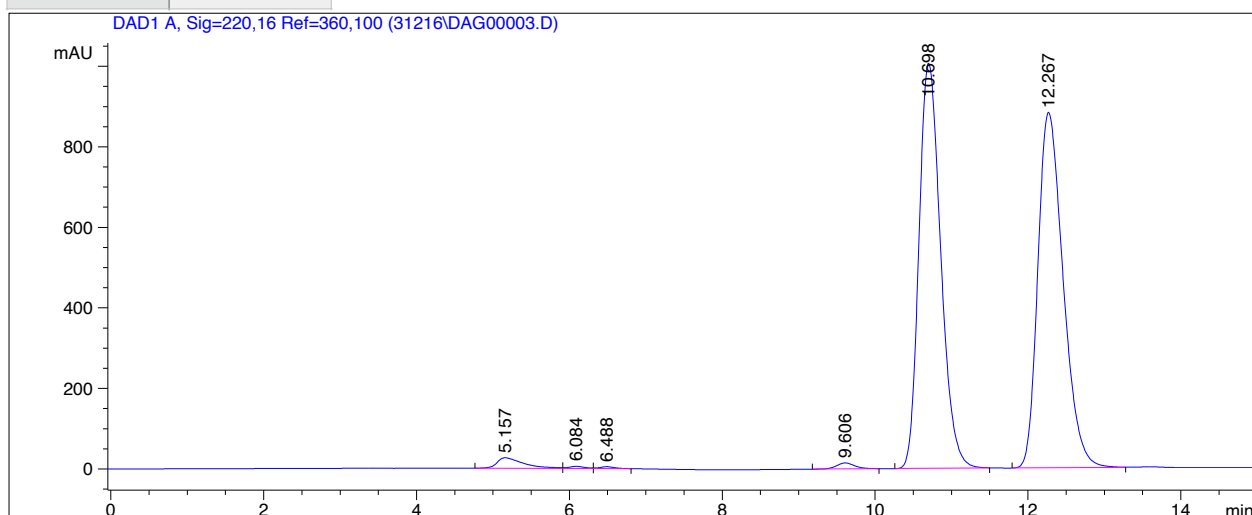
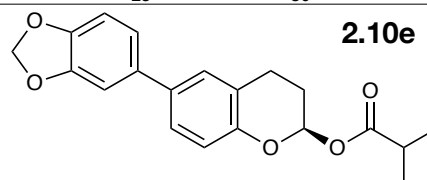
Column: Chiralcel OD-H
 Solvent: 1:99 IPA:Hex
 Flow rate: 1 mL/min
 Wavelength: 220 nm





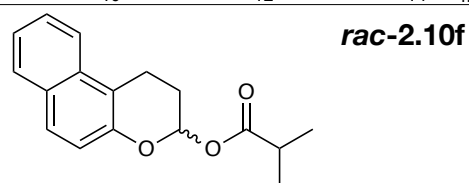
Retention Time	Area %
12.933	96.9631
32.571	3.3007

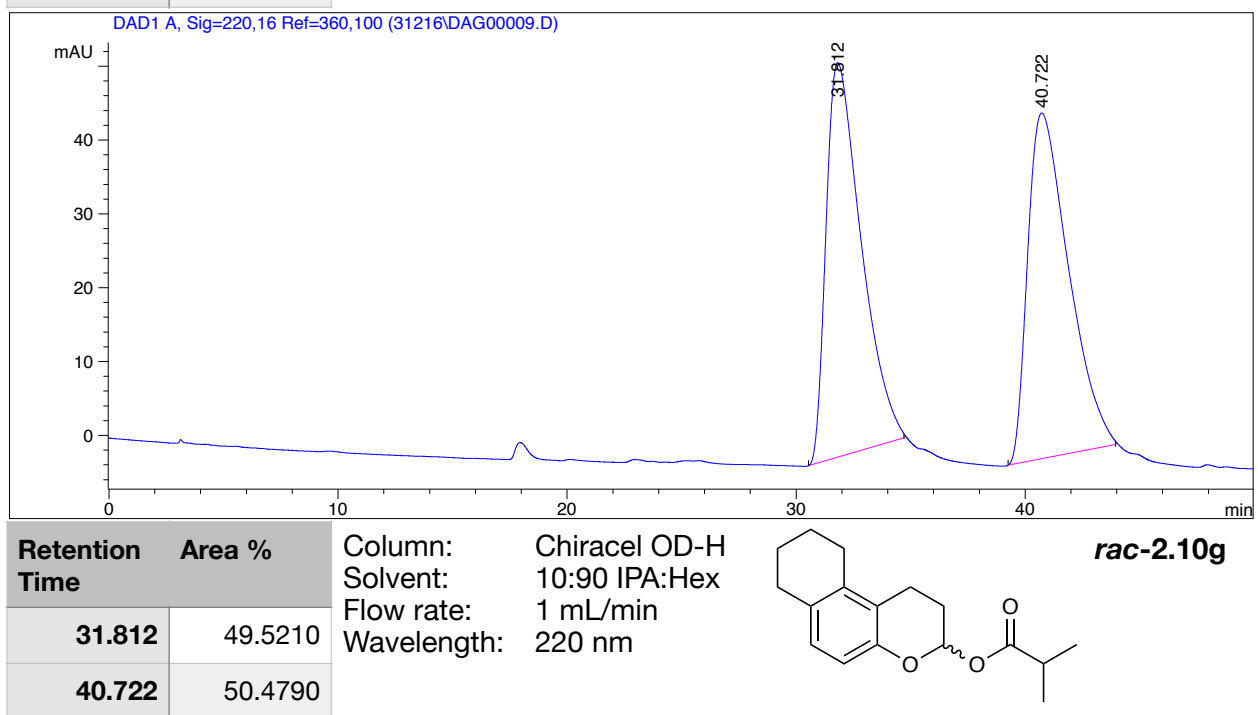
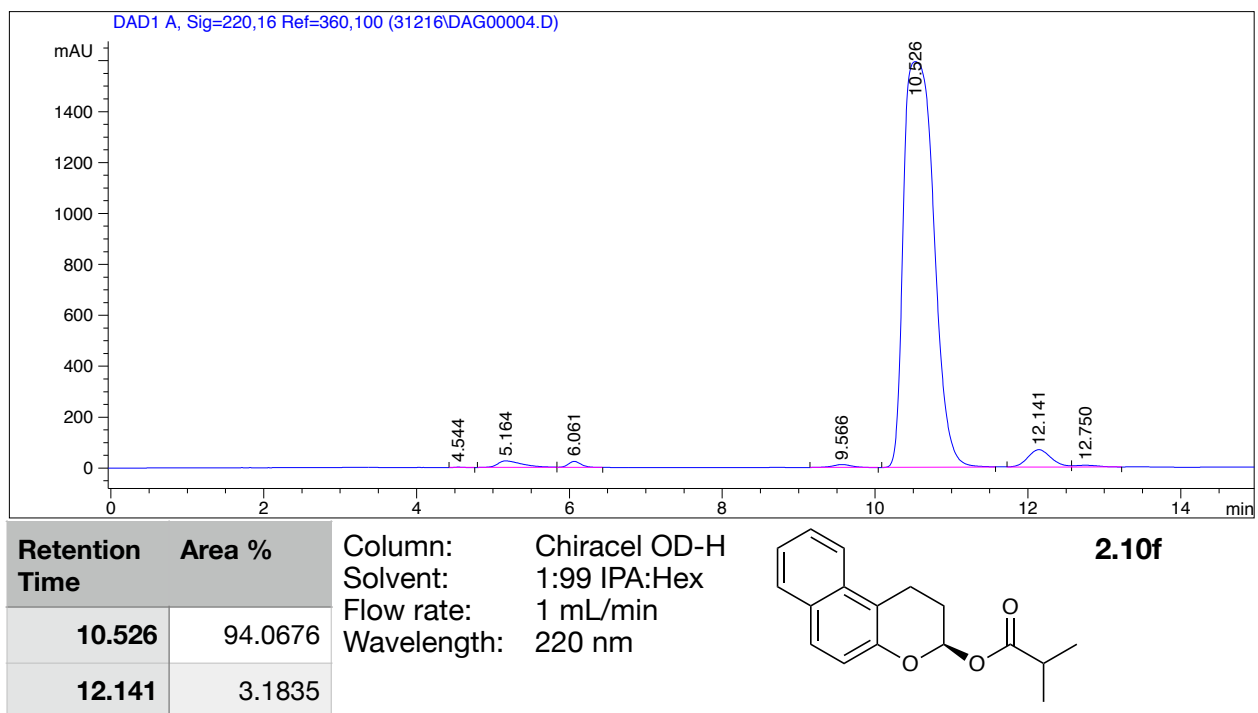
Column: Chiralcel OD-H
 Solvent: 1:99 IPA:Hex
 Flow rate: 1 mL/min
 Wavelength: 220 nm

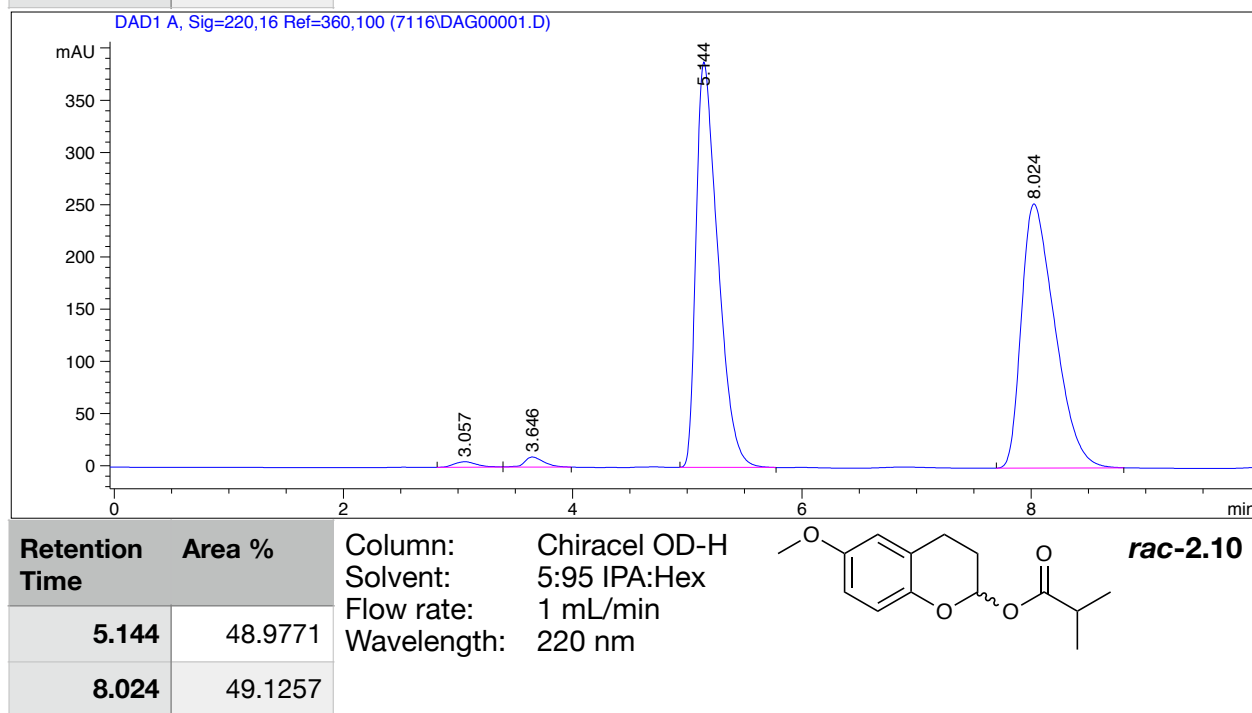
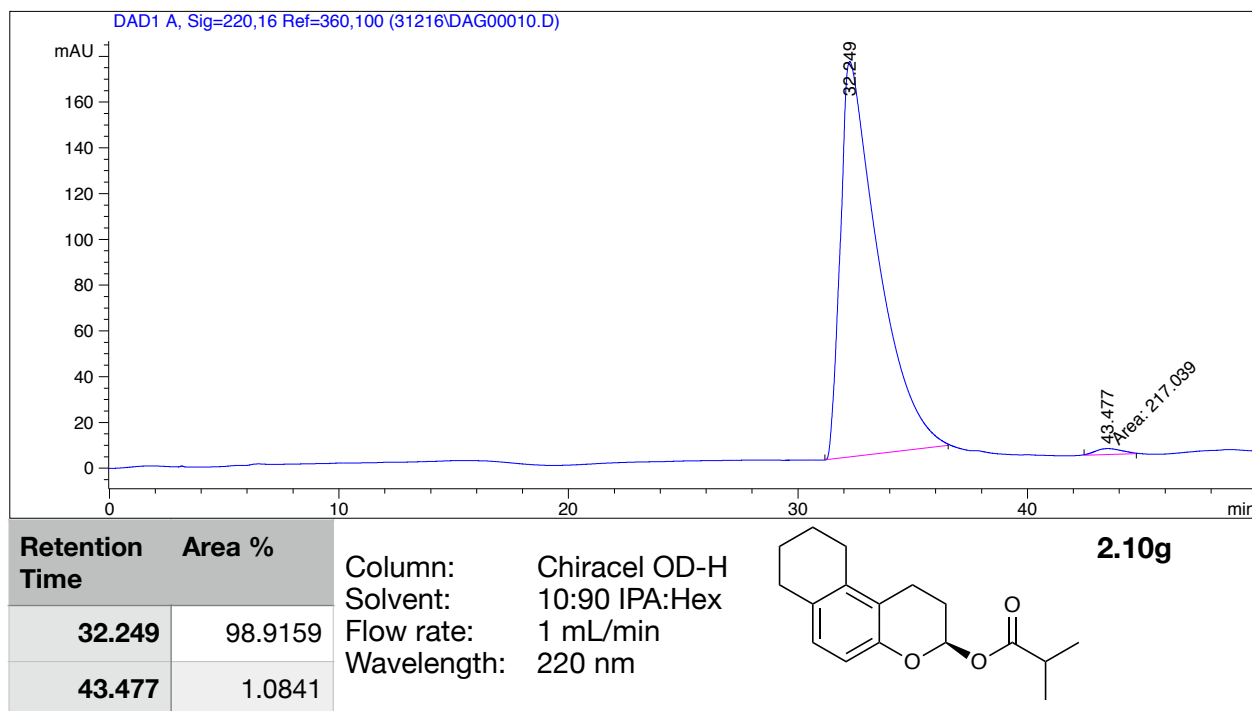


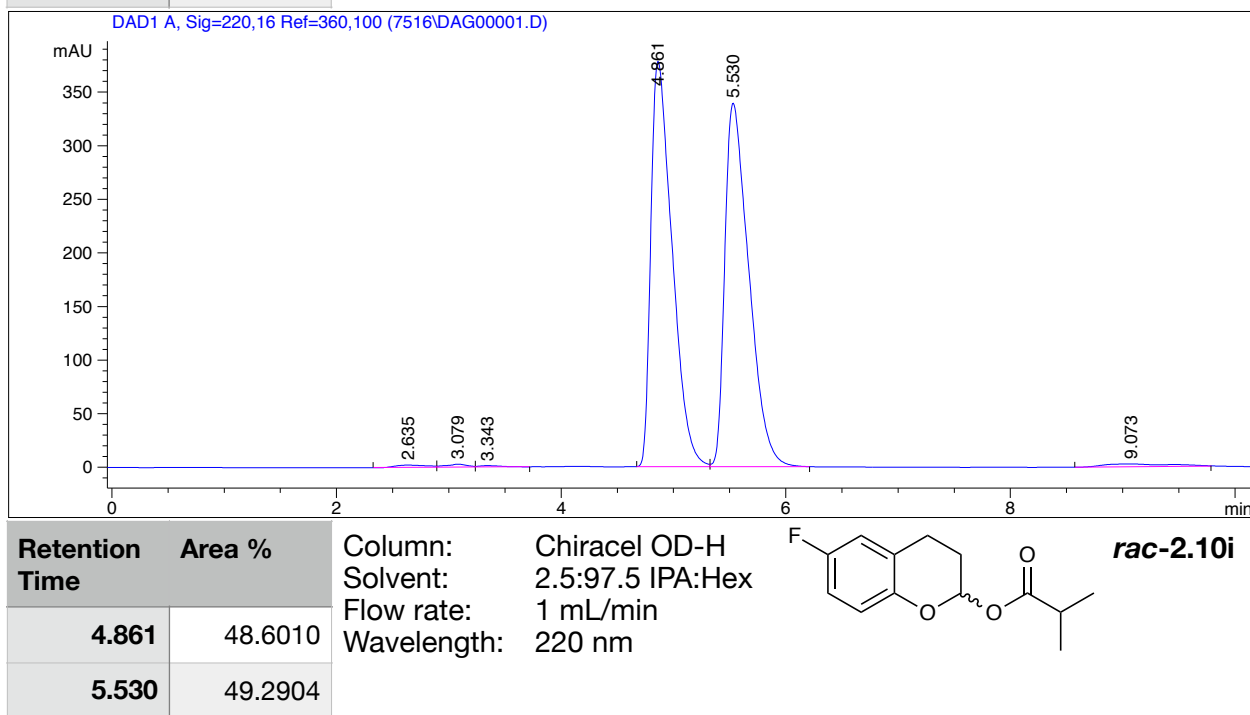
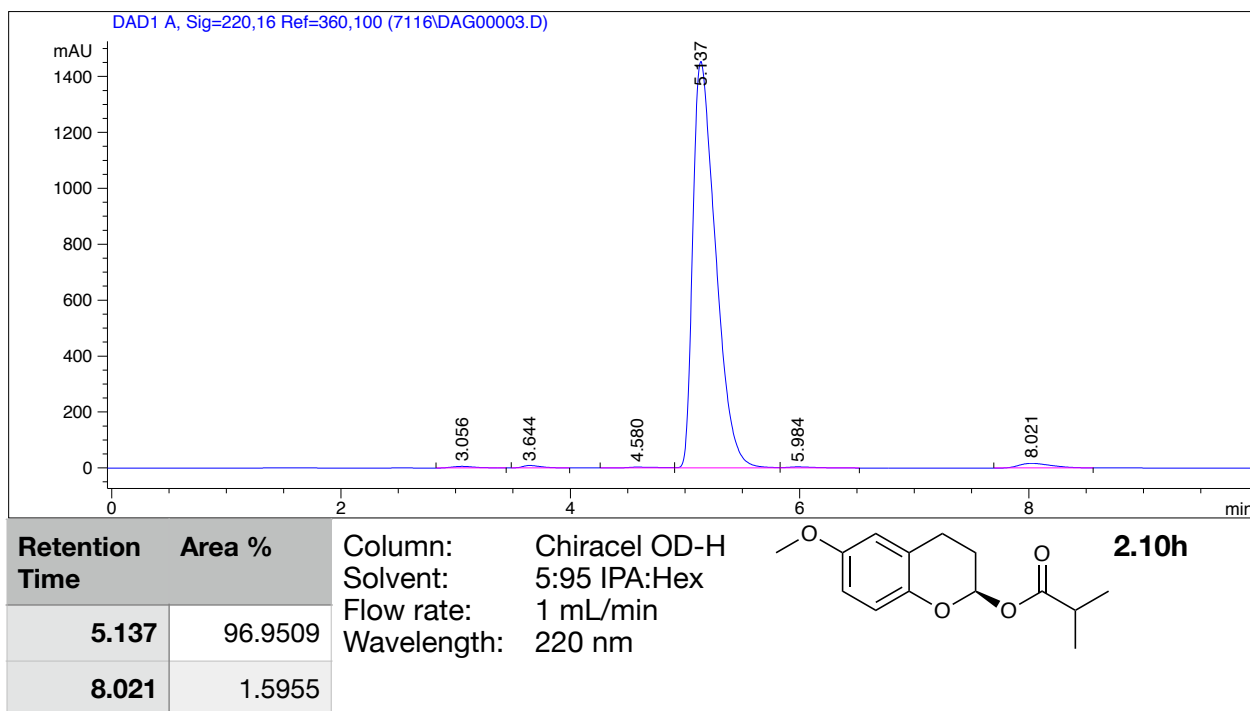
Retention Time	Area %
10.698	48.2829
12.267	49.1440

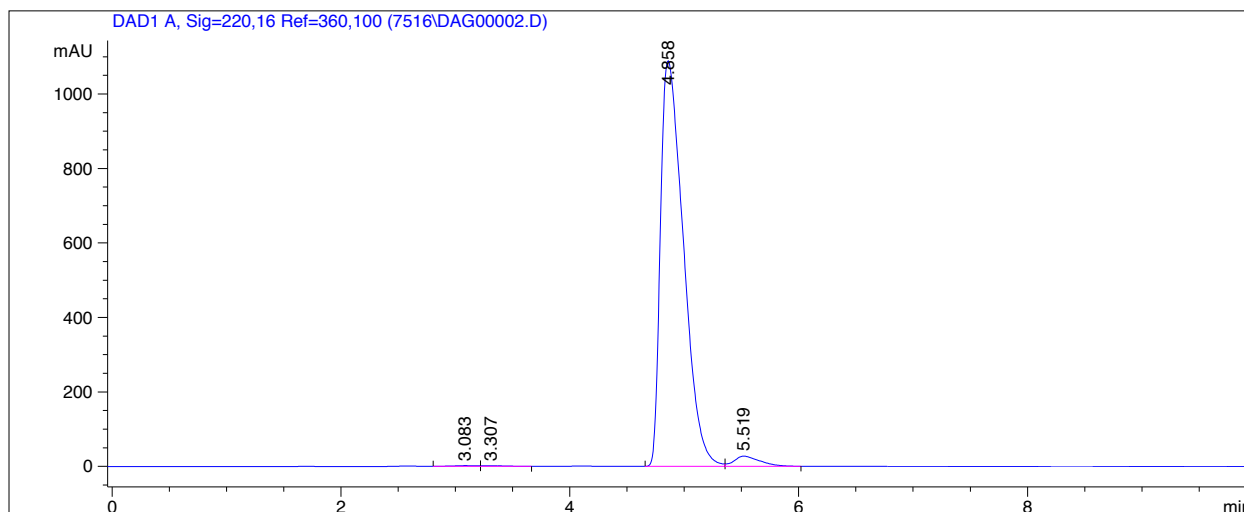
Column: Chiralcel OD-H
 Solvent: 1:99 IPA:Hex
 Flow rate: 1 mL/min
 Wavelength: 220 nm



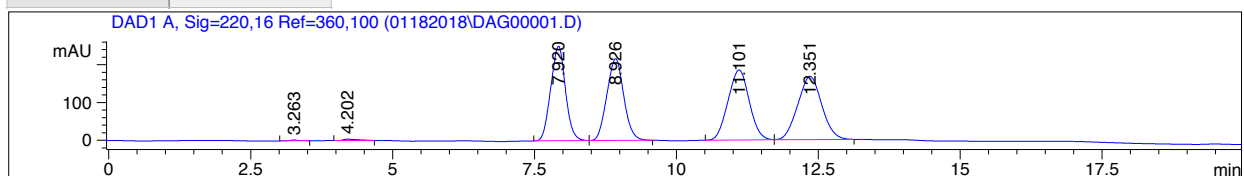




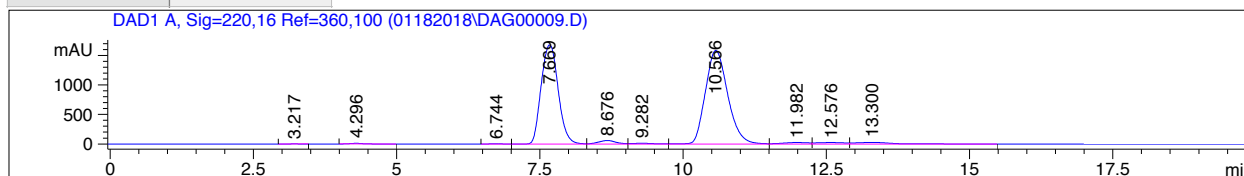




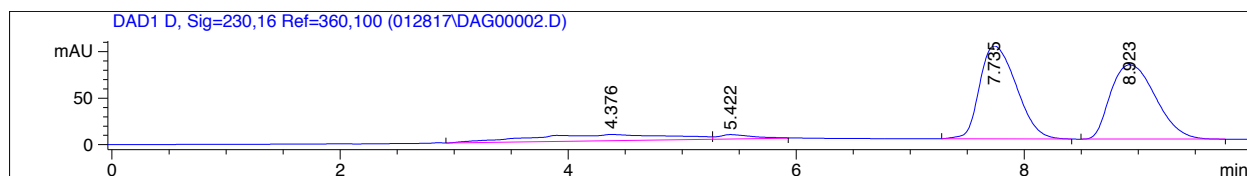
Retention Time	Area %	Column:	Chiralcel OD-H	Solvent:	2.5:97.5 IPA:Hex	Flow rate:	1 mL/min	Wavelength:	220 nm	Chemical Structure	2.10i
4.858	96.8464										
5.519	2.7713										

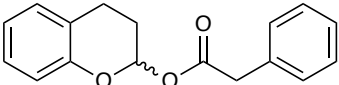


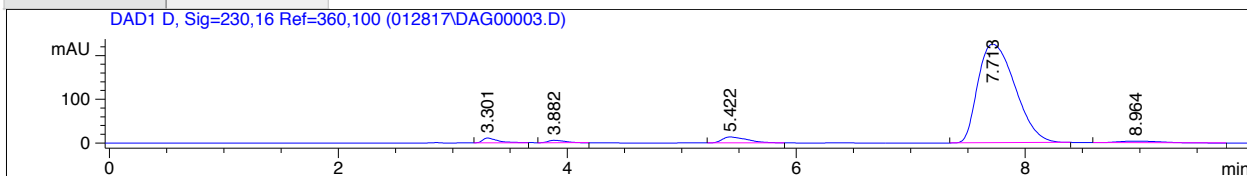
Retention Time	Area %	Column:	Chiralcel OD-H	Solvent:	1:99 IPA:Hex	Flow rate:	1 mL/min	Wavelength:	220 nm	Chemical Structure	rac-2.10j
7.920	23.961										
8.926	23.8368										
11.101	25.5178										
12.351	26.1106										

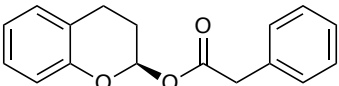


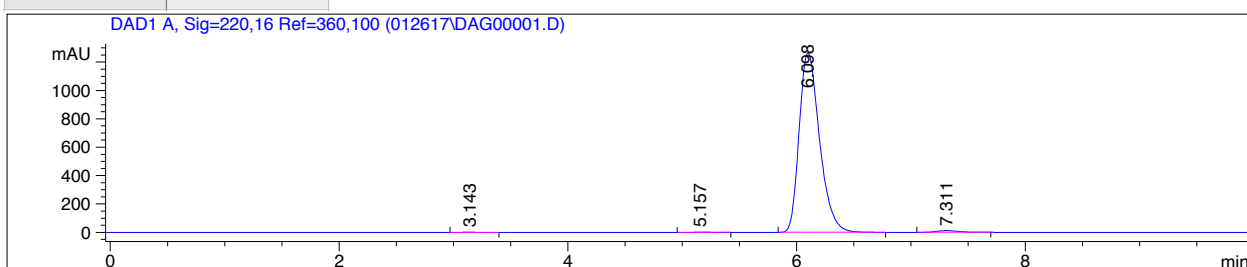
Retention Time	Area %	Column:	Chiralcel OD-H	Solvent:	1:99 IPA:Hex	Flow rate:	1 mL/min	Wavelength:	220 nm	Chemical Structure	2.10j
7.669	42.0220										
8.676	1.5803										
10.566	51.8459										
11.982	1.0313										

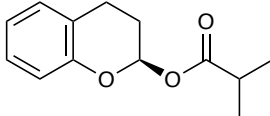


Retention Time	Area %	Column:	Chiralcel OD-H		rac-2.10j
7.735	43.7253	Solvent:	1:99 IPA:Hex		
8.923	42.7618	Flow rate:	1 mL/min		
		Wavelength:	230 nm		



Retention Time	Area %	Column:	Chiralcel OD-H		2.10j
7.713	91.5079	Solvent:	1:99 IPA:Hex		
8.964	1.6667	Flow rate:	1 mL/min		
		Wavelength:	230 nm		



Retention Time	Area %	Column:	Chiralcel OD-H		2.10a
6.096	98.6788	Solvent:	1:99 IPA:Hex		Made with mixed anhydride method
7.311	1.0941	Flow rate:	1 mL/min		
		Wavelength:	220 nm		

3. Site-Selective Functionalization of Carbohydrates

Portions of this chapter were previously published in: G. Xiao, G. A. Cintron-Rosado, D. A. Glazier, B. Xi, C. Liu, P. Liu, W. Tang, *J. Am. Chem. Soc.* **2017**, 139, 4346–4349.; D. A. Glazier, J. M. Schroeder, S. A. Blaszczyk, W. Tang, *Adv. Synth. Catal.* **2019**, 361, 3729–3732.

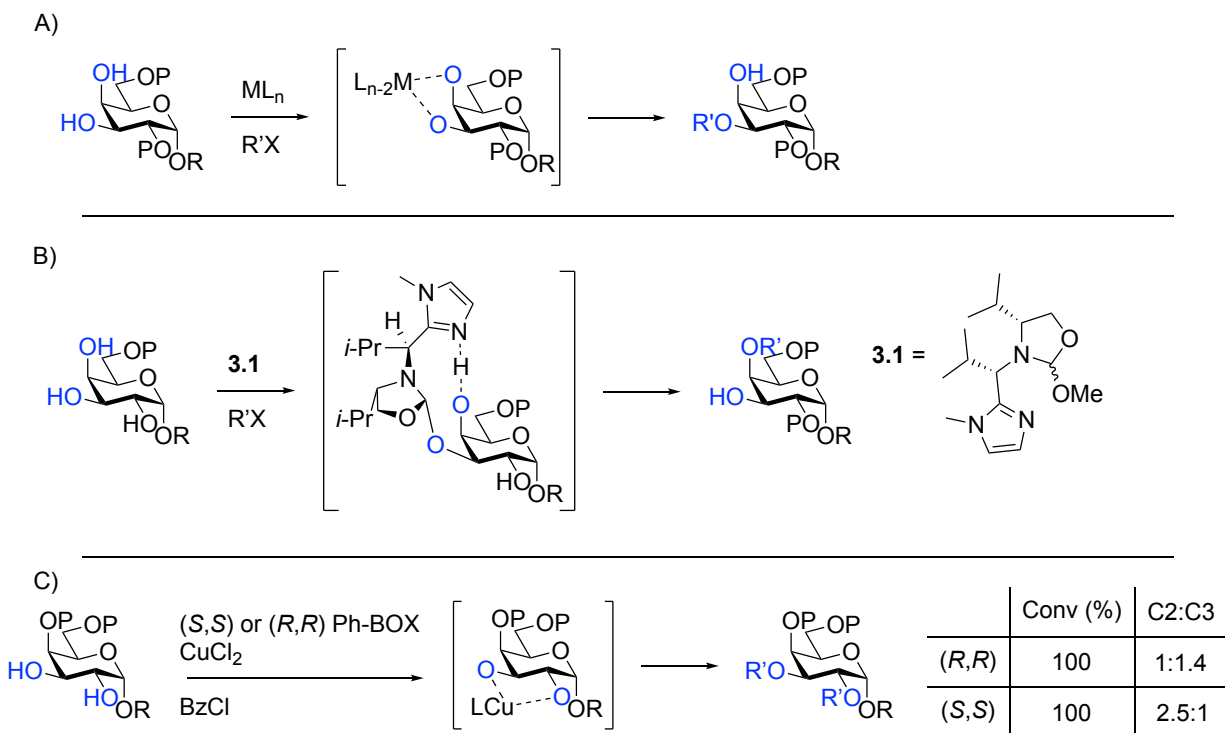
3.1. Introduction

Carbohydrates are one of the most prevalent of the four classes of bio-macromolecules and play important roles in cellular signaling, disease progression, and metabolism among other functions.^[1] Carbohydrates and their mimics and scaffolds are also prevalent in therapeutic pharmaceuticals and vaccines. In light of the importance of these compounds, significant efforts have been devoted to study their structure-function relationships and further elucidate their roles in biological processes. Unfortunately, these efforts are often limited by the synthetic difficulty of the carbohydrates of interest.

While there are less than a dozen mammalian monosaccharides, carbohydrate synthesis is complicated by the monosaccharides' different isomeric forms and the multitude of ways they can be arranged. Additionally, one of the most difficult challenges encountered in synthesizing oligosaccharides is differentiating the multiple hydroxyls in similar chemical environments on each monomer unit, making the synthesis of biologically interesting carbohydrates tedious. Other bio-macromolecules, such as proteins, nucleic acids, and lipids, have less varied, often linear, structures which are easier to access. Nevertheless, multiple methods have been developed, after significant effort, to site-selectively functionalize carbohydrates.

Numerous methods have been developed for the differentiation of *cis*-1,2-diols.^[2] Most of these methods take advantage of the intrinsic selectivity preference for the equatorial hydroxyl group which can be amplified by external reagents and catalysts. The most successful strategy for the differentiation of *cis*-1,2-diols is the use of metal acetal catalysts (**Scheme 3.1A**). The metal (Fe, Sn, or B) is chelated by the *cis*-1,2-diol, forming a cyclic species where the selectivity preference for the equatorial hydroxyl group is magnified.^[3,4,5] These catalysts can be used for the site-selective installation of multiple electrophiles such as acyl, benzyl, and tosyl groups. Site-selective glycosylations have even been reported using B.^[6] Methods that can invert this selectivity have been developed as well using chiral catalysts or other reagents.^[7,8] In one exciting example, Kian Tan's group designed a catalyst that forms a reversible covalent bond with the more reactive equatorial hydroxyl group, and then act as an internal base for the

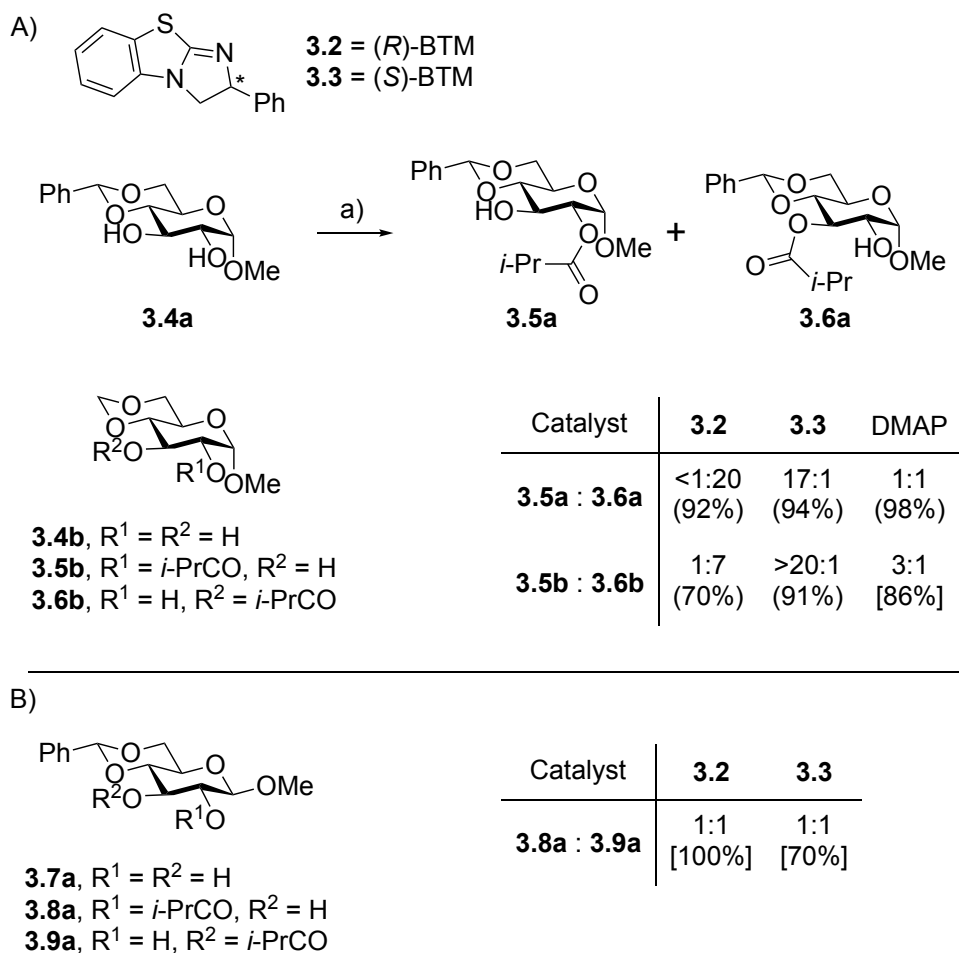
functionalization of the axial hydroxyl with acyl, mesyl, or silyl groups (**Scheme 3.1B**).^[8] A novel chiral catalyst was developed for site-selective acylation of β -glucopyranosides.^[9] These methods cannot be used for the differentiation of most *trans*-1,2-diols where both hydroxyls are either axial or equatorial. Attempts to develop general methods using chiral or achiral catalysts for the differentiation of *trans*-1,2-diols have been unsuccessful as most methods suffer from a very limited substrate scope and either poor selectivity or only enhancing the intrinsic selectivity of the substrate.^[3,10] The copper catalyzed functionalization of *trans*-1,2-diols developed by Miller is an excellent example of the field. The copper forms a cyclic intermediate, like the Sn, Fe, or B methods remarked on above, but because of the chiral Ph-BOX ligand there is some selectivity. However, the selectivity is highly dependent on the substrate and the electrophile used (**Scheme 3.1C**).^[10g]



Scheme 3.1. Representative methods for the functionalization of carbohydrate diols. A) Selective functionalization of the equatorial OH of a *cis*-1,2-diol using metal acetal catalysts. B) Selective functionalization of the axial OH of a *cis*-1,2-diol using Kian Tan's catalyst. C) Selective functionalization of *trans*-1,2-diols by Miller using a chiral Cu catalyst.

3.2 Site-Selective Acylation of Carbohydrate *Trans*-1,2-Diols

Because of the lack of general methods for the differentiation of *trans*-1,2-diols I endeavored to develop a site-selective acylation reaction for this common motif. Dr. Guozhi Xiao and I started screening acylation conditions with the amidine based catalyst (ABC) benzotetramisole (BTM). This chiral catalyst was originally developed by Birman for the kinetic resolution of allylic, propargylic, and benzylic alcohols.^[11] We and others recently applied these catalysts for dynamic kinetic stereoselective acylation of lactols.^[12] Our initial results are shown in **Scheme 3.2**. We started screening conditions and were pleasantly surprised to see that acylation of α -glucoside substrate **3.4a** with isobutyric anhydride and (*R*)-BTM (catalyst **3.2**) gave an excellent selectivity of >20:1 for acylation of the C(3)-OH (compound **3.6a**) with exceptional isolated yield. We were excited when the use (*S*)-BTM (catalyst **3.3**) under the same conditions resulted in a complete inversion of the selectivity yielding C(2)-OH acylated product **3.5a** in a ratio of 17:1 in exceptional yield. The achiral catalyst DMAP gives no site-selectivity (**Scheme 3.2A**).



Scheme 3.2. Conditions: a) catalyst (10 mol%), (*i*-PrCO)₂O (2.5 equiv), *i*-Pr₂NEt (3.0 equiv), rt. Isolated yields of the major isomer are in (). Conversions are in []. Product ratios were determined by ¹H NMR of the crude products.

The BTM catalyst selectivity model for the kinetic resolution of α -unsaturated alcohols elucidated by Birman and Houk is that the catalyst interacts with the π -system in one enantiomer of the substrate via a stabilizing cation- π interaction.^[13] We hypothesized that the selectivity we observed may have resulted from a cation- π between the BTM catalysts and the phenyl group of the 4,6-O-benzylidene protecting group. To test this hypothesis Guozhi synthesized **3.4b**, an analogue compound **3.4a** with the 4,6-O-benzylidene protecting group replaced with a 4,6-O-formyl moiety. When **3.4b** was subjected the same conditions as **3.4a** using (*R*)-BTM we obtained the C3-OH acylated product **3.5b** preferentially in a 7:1 ratio and in high yield. Using (*S*)-BTM in place of (*R*)-BTM favored the C2-OH acylated product **3.6b** in a ratio of >20:1 and excellent yield. DMAP favored the C(2)-OH acylated product **3.5b** 3:1 (**Scheme 3.2A**). These results imply that the selectivity doesn't arise from a cation- π interaction

like the selectivity for the kinetic resolution of alcohols and indicate that the observed selectivity may arise from a novel mode of catalyst-substrate interaction. When we tried to extend the method to β -glucoside **3.7a** we observed equal amount of acylation products **3.8a** and **3.9a** by using (*R*)- or (*S*)-BTM catalyst (**Scheme 3.2B**)

Because we suspected that an unrecognized mode of catalyst-substrate interaction governs the dramatically different selectivity between O-glucosides **3.4a** and **3.7a**, we performed density functional theory (DFT) calculations to explore the origin of the site-selectivity in the acylation of α -glucosides **3.4a** and **3.4b** using (*R*)- and (*S*)-BTM catalysts (**Figures 3.1-3.4**). I focused on the reaction of (*R*)-BTM with compound **3.4b**. The DFT investigations of the other reactions were performed by Prof. Liu and his student Gabrielle Cintron-Rosado.

Careful conformational searches of all transition state structures were performed by systematically altering the dihedral angle of the forming O-C bond in the acylation transition state and changing the direction of the acylated catalyst approaching the substrate. The carbonyl of the acylated (*R*)- or (*S*)-BTM catalyst may approach the catalyst either syn to the C-H bond on the carbon that is being acylated (referred to here as “C-H down”), or anti to that C-H bond (referred to as “C-H up”). The two different approaches position different O-containing groups on the substrate to interact with the positively charged acylated catalyst. For example, in the (*R*)-BTM-catalyzed acylation of the C(3)-OH group in α -O-glucoside **3.4a**, the C(4)-OR is placed above the cationic catalyst in the “C-H down” conformer **3.6a-TS1**, while the C(2)-OH is placed above the cationic catalyst in the “C-H up” TS conformer **3.6a-TS1'** (**Figure 3.1**).

The lowest energy “C-H down” and “C-H up” TS isomers for the acylation of α -O-glucosides **3.4a** and **3.4b** with (*R*)- and (*S*)-BTM catalysts are shown in **Figure 3.1-3.4**. In all low-energy TS conformers, there exists some level of cation-*n* interaction with either an OH or OR group on the substrate. The magnitude of the stabilizing cation-*n* interactions is significantly impacted by the stereochemical environment around the O lone pair. A detailed analysis of factors that control the stability of the acylation transition state is provided below.

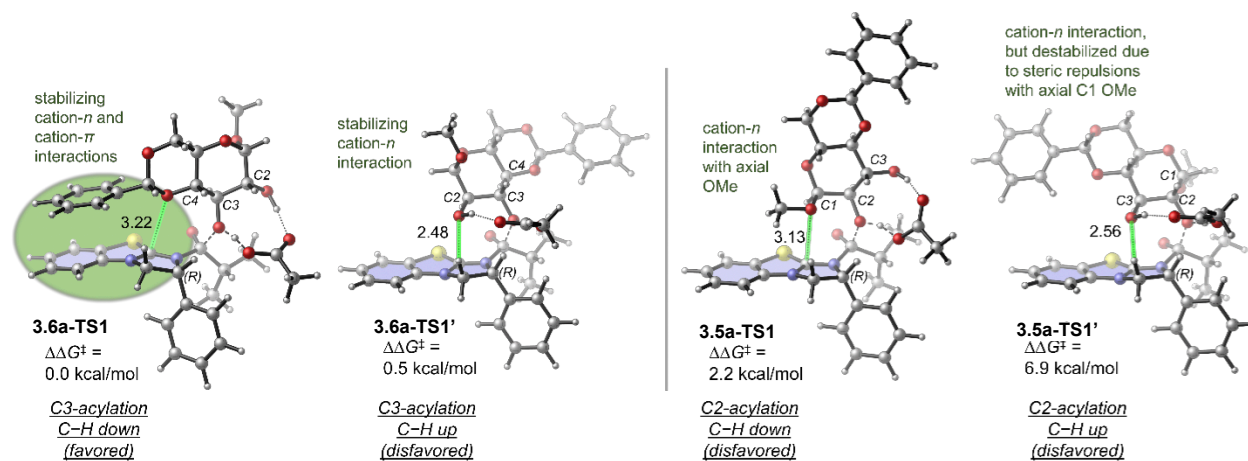


Figure 3.1. Transition state isomers of (R)-BTM-catalyzed acylation of α -O-glucoside **3.4a**.

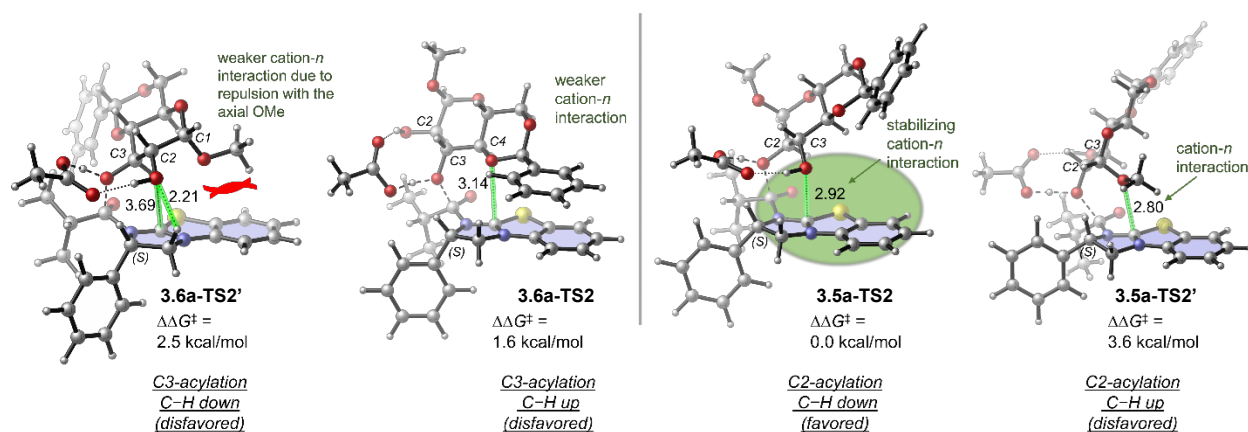


Figure 3.2. Transition state isomers of (S)-BTM-catalyzed acylation of α -O-glucoside **3.4a**.

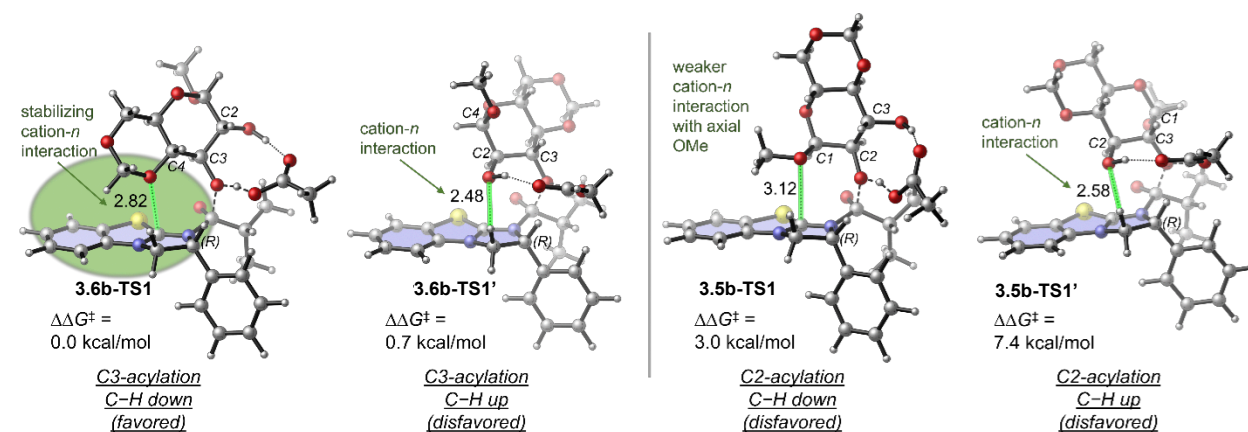


Figure 3.3. Transition state isomers of (R)-BTM-catalyzed acylation of α -O-glucoside **3.4b**.

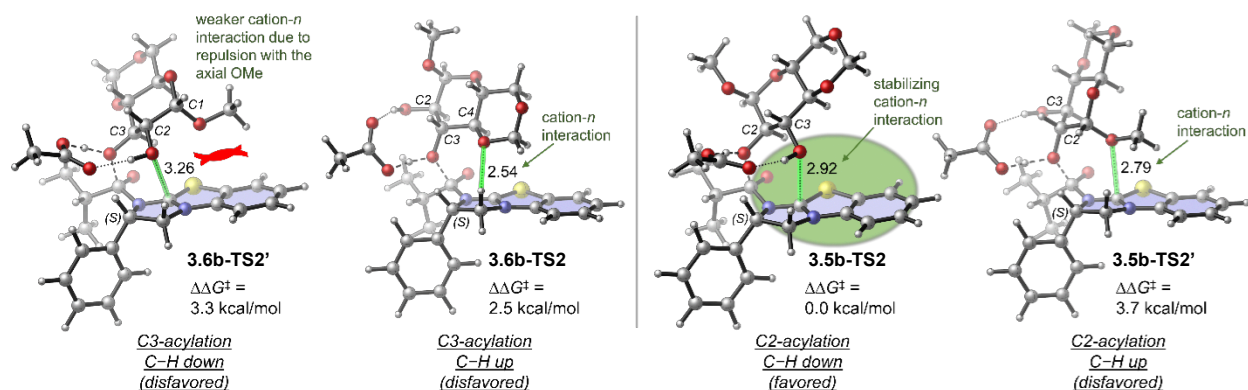


Figure 3.4. Transition state isomers of (S)-BTM-catalyzed acylation of α -O-glucoside **3.4b**.

The “C–H up” conformation leads to more significant steric repulsions between the acylated catalyst and the adjacent carbons on the substrate (i.e. C2 and C4 in C(3)-acylation TSs and C1 and C3 in C(2)-acylation TSs). Indeed, most of the lowest energy TS conformers calculated have the “C–H down” conformation to minimize the steric repulsions between the catalyst and the substrate. The only two exceptions are the (S)-BTM-catalyzed C(3)-acylation TS of α -O-glucosides **3.4a** and **3.4b**, in which the “C–H up” conformers (**3.6a-TS2** and **3.6b-TS2**) are 0.9 and 0.8 kcal/mol lower than in energy than the corresponding “C–H down” conformers (**3.6a-TS2'** and **3.6b-TS2'**, see **Figures 3.2, 3.4**). Here the “C–H down” conformers **3.6a-TS2'** and **3.6b-TS2'** are destabilized due to the unfavorable steric repulsions between the axial OMe group and the catalyst. It should be noted that although **3.6a-TS2** is stabilized by a cation- π interaction with the benzylidene protecting group on the substrate, it is still less stable than **3.5a-TS2**, due to the unfavorable steric interactions in this “C–H up” conformation.

Since the nature of the cation- n interactions is most likely a charge-dipole type electrostatic interaction,^[14] its strength is expected to be dependent upon the distance of the O atom and the cationic catalyst. In nearly all favored transition states with strong cation- n interactions (e.g., **3.6b-TS1**, **3.5a-TS2**, **3.5b-TS2**), the distance between the O atom and the amidine carbon in the catalyst is shorter than 3 Å. The only exception is **3.6a-TS1**, in which the O–C distance is 3.22 Å. This longer distance is necessary to achieve the favorable cation- π interaction with the benzylidene protecting group. In contrast, the corresponding O–C distance with the axial OMe

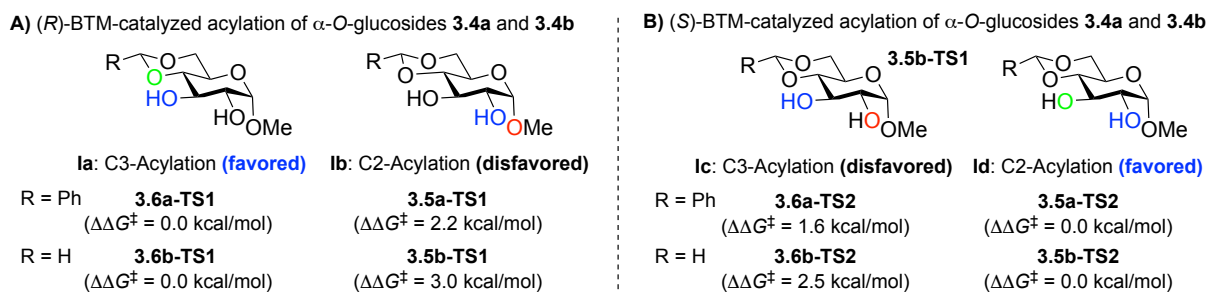
group in **3.5a-TS1** and **3.5b-TS1** and with the C(2)-OH in **3.6a-TS2'** and **3.6b-TS2'** that is blocked by the adjacent axial OMe are all significantly longer than 3 Å, indicating significantly diminished cation- n interactions in these disfavored TSs.

In summary, although there are a number of TS conformers in each acylation pathway, the most favorable acylation TS always adapts the “C–H down” conformation to avoid substrate- catalyst steric repulsions, and involves a stabilizing cation- n interaction as evidenced by a short distance between the oxygen atom and the cationic catalyst. In reactions with the benzylidene protected glucoside **3.4a**, cation- π interaction also contributes to the stability of the acylation transition state.

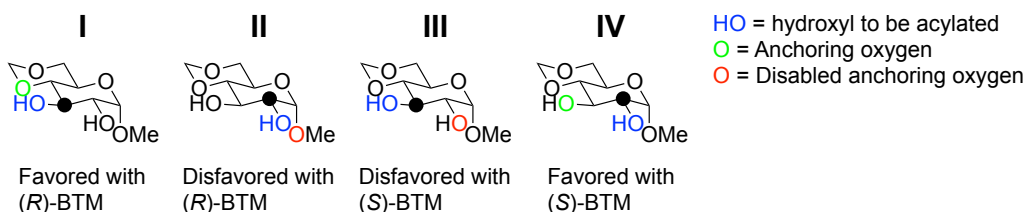
The most stable transition states of the C(3)- and C(2)-acylation of α -O-glucoside **3.4b** with the (*R*)- and (*S*)-BTM catalysts are shown in **Figures 3.3** and **3.4**. The DFT calculations predicted the same major product as in the reactions with the benzylidene-protected α -O-glucoside **3.4a**. C(3)-acylation is favored in the reaction with the (*R*)-BTM catalyst, while C(2)-acylation is favored in the reaction with (*S*)-BTM. The geometries of the C(2)-acylation TSs (**3.5b-TS1** and **3.5b-TS2**) are grossly similar to the corresponding TSs with **3.4a** (**3.5a-TS1** and **3.5a-TS2**, respectively), while the geometries of the C(3)-acylation TSs (**3.6b-TS1** and **3.6b-TS2**) are somewhat different from those in the reaction with **3.4a** (**3.6a-TS1** and **3.6a-TS2**). In the absence of the benzylidene-protecting group, the cation- π interaction is not possible. Thus, cation- n interaction becomes the only factor that stabilizes the C(3)-acylation TS. Nonetheless, the relative energies between the TS isomers are in fact similar in the reactions with **3.4a** and **3.4b**. This indicates that the cation- n interaction is the dominant factor that controls the site-selectivity.

Similar to the (*R*)-BTM-catalyzed reaction of **3.4a**, the (*R*)-BTM-catalyzed acylation of **3.4b** is C3 selective. The (*R*)-BTM-catalyzed C(3)-acylation TS (**3.6b-TS1**) is stabilized by a strong cation- n interaction with the C(4)-OR group on the substrate, as evidenced by the short O–C distance (2.82 Å). In **3.5b-TS1**, the cation- n interaction is much weaker because the axial OMe group on C1 is not perfectly oriented towards the positively charged aromatic system in the acylated

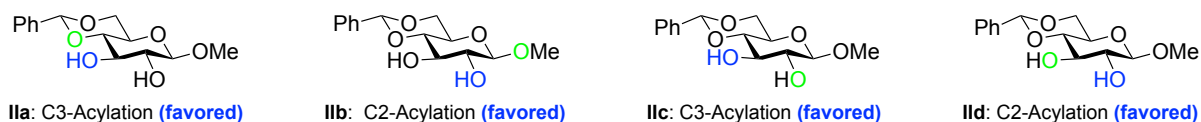
catalyst. The corresponding O–C distance between the O lone pair and the catalyst in **3.5b-TS1** is significantly longer (3.12 Å). In the reaction with the (*S*)-BTM catalyst, the site-selectivity is reversed to favor C(2)-acylation, because **3.5b-TS2** is stabilized by a strong cation-*n* interaction, while the cation-*n* interaction in the C(3)-acylation TS (**3.6b-TS2**) is much weaker due to the steric repulsions between the catalyst and the C1 axial OMe group on the substrate.



C) Predictive model for site-selectivity



D) Predictive model applied to β -O-glucoside **3.7a**



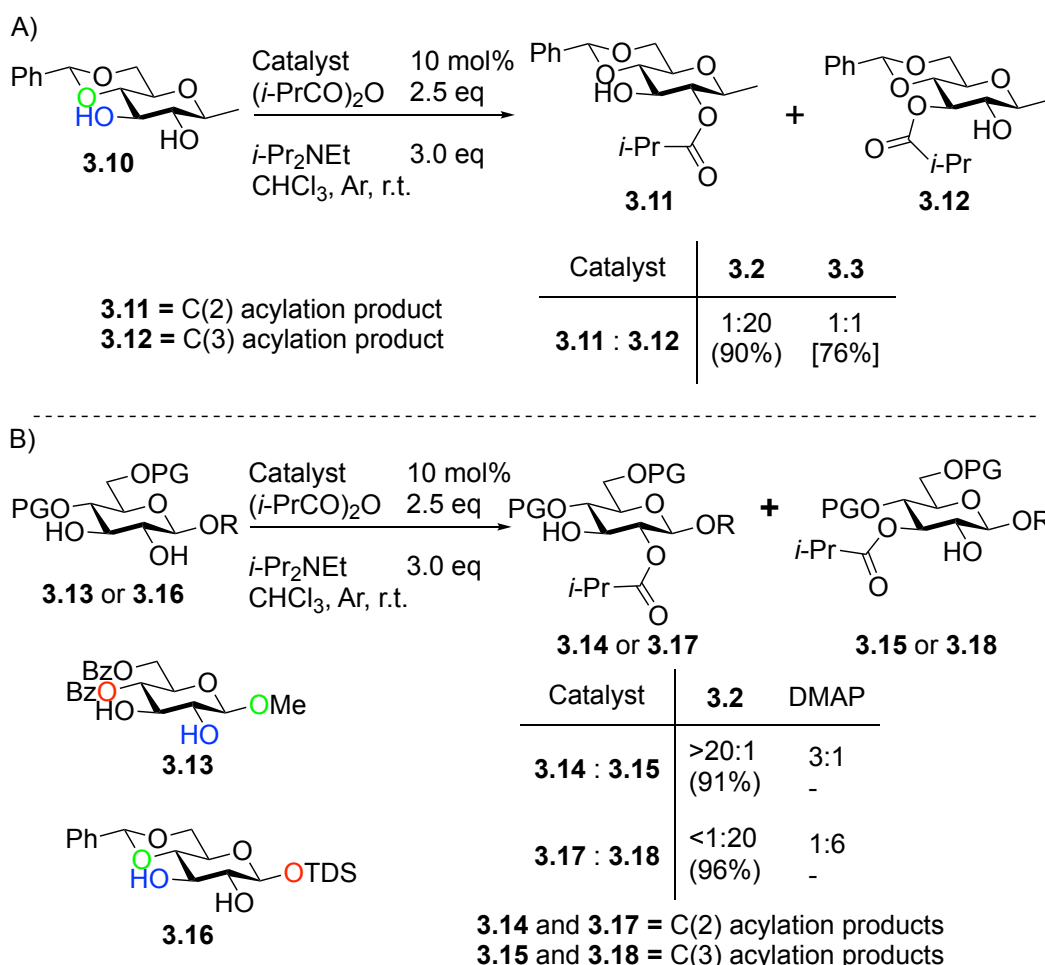
Scheme 3.3. Working model for site-selective acylation. DFT calculations were performed using the M06-2X/6-311++G(d,p)/SMD//M06-2X/6-31G(d) level of theory.

We generalized the above analysis to a predictive working model that can be easily applied to other monosaccharides (**Scheme 3.3C**). We can use our right-hand to predict the site-selectivity of (*R*)-BTM-catalyzed acylation, and our left-hand to predict the site-selectivity of (*S*)-BTM-catalyzed acylation. If the thumb aligns with the C–H bond on the dotted carbon and points to the hydrogen atom, the rest of the fingers will curve toward the adjacent anchor OH or OR that is supposed to interact with the acylated catalyst. If the anchor OH or OR is on the equatorial position and there is no adjacent axial substituent, it is a favored situation (e.g., **I** and **IV**). If the

anchor OH or OR is on the axial position (e.g., **II**) or on the equatorial position with an adjacent axial substituent (e.g., **III**), the anchor is not able to interact with the catalyst (defined as disabled anchoring O). It is therefore a disfavored situation. It is also a disfavored situation if the anchor OH or OR is replaced by a group without any lone pair, such as a C(1)-carbon atom in C-glycosides. One would also expect a disabled anchor if the oxygen is attached to an electron-withdrawing or sterically demanding group. If the C(1)-OR group in **II** and **III** is changed to β -configuration, such as β -O-glucoside **3.7a**, they should become favored. Strong cation- n interactions are predicted to be present in all four TSs as favored situations for β -O-glucoside **3.7a**. Thus, no selectivity is expected for the acylation of **3.7a** using either (*R*)- or (*S*)-BTM catalyst, which is consistent with experimental results in **Scheme 3.2B**.

Based on the above analysis for O-glucosides we wanted to make the smallest perturbation we could to substrate **3.7a** to see if we could obtain selectivity. If we replace the β -OMe anchor on the C(1)-position in **3.7a** with a methyl group in β -C-glucoside **3.10** (**Scheme 3.4A**), we will remove the cation- n interaction that anchors the (*R*)-BTM-catalyzed acylation of C(2)-OH in **3.7a**, while leaving the rest of the interactions the same as in **3.7a**. We predict that high selectivity for the acylation of C(3)-OH of **3.10** can be achieved by using (*R*)-BTM as the catalyst, whereas no selectivity is expected for the (*S*)-BTM-catalyzed acylation. Indeed, a ratio of 1:20 for products **3.11/3.12** was observed in (*R*)-BTM-catalyzed acylation of **3.10**, and a ratio of 1:1 was obtained by using (*S*)-BTM catalyst. We then decided to see what modifications to **3.7a** can be made to enable selective acylation of β -O-glucosides and to further test our selectivity model. We then tested the hypothesis that β -O-glucosides could be turned into selective substrate by tuning the electronic and steric properties of the anchoring oxygen as shown in **3.13** and **3.16** (**Scheme 3.4B**). The electron-withdrawing Bz-group on the C(4)-position of **3.13** disables the anchor oxygen on C(4) so (*R*)-BTM should only be anchored by the oxygen at C(1) for the acylation of the C(2)-OH. Indeed, we observed an over 20:1 ratio favoring product **3.14** for (*R*)-BTM-catalyzed acylation of **3.13**. The sterically demanding TDS-group in **3.16** should disable the anchoring ability of the oxygen on the anomeric position, resulting in

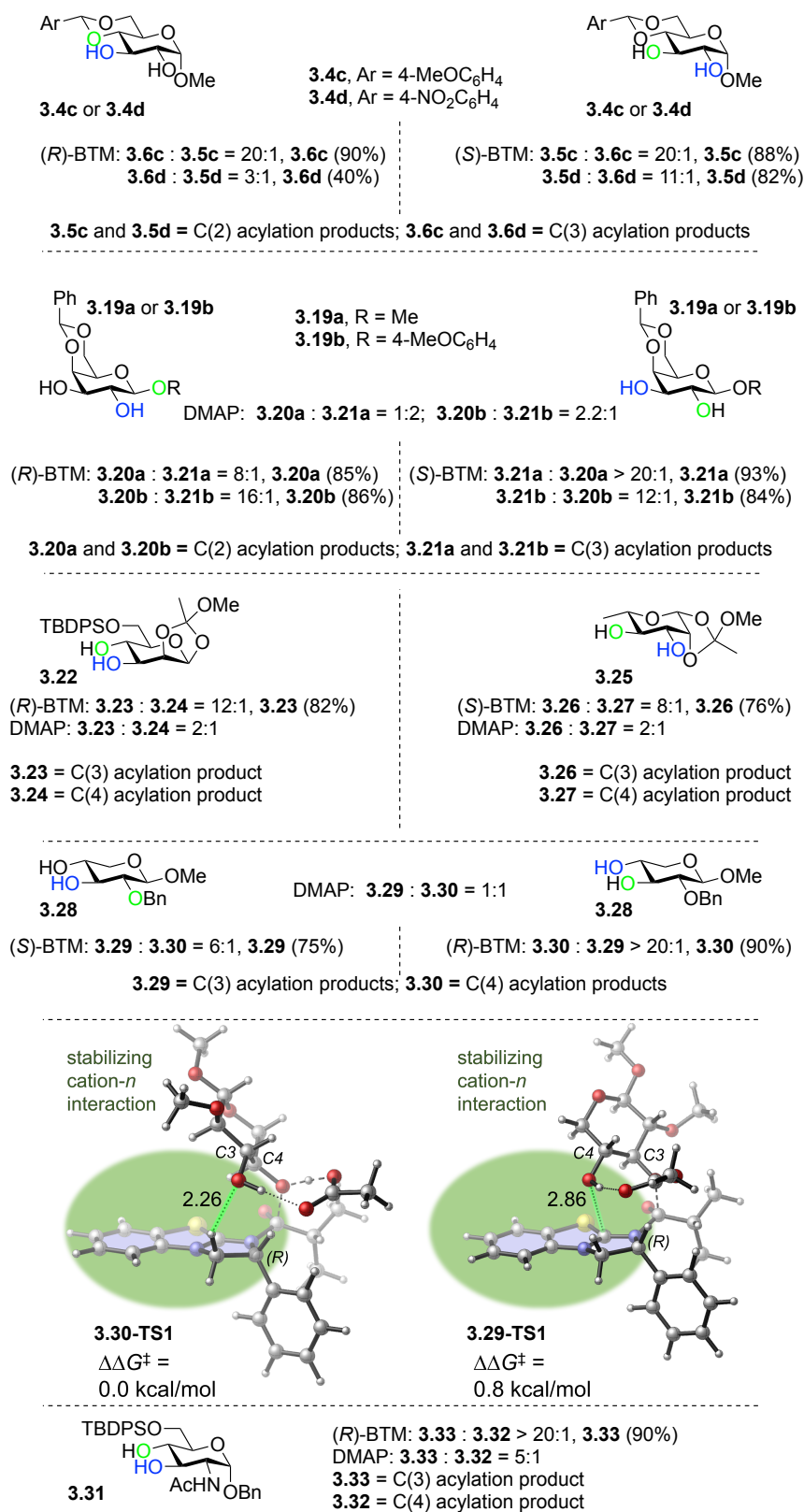
similar selectivity as C-glucoside **3.10**. We observed an over 20:1 ratio favoring product **3.18** for (*R*)-BTM-catalyzed acylation of **3.14**. These results are in sharp contrast to the 1:1 ratio for the formation of **3.8a** and **3.9a** from **3.7a** using the same catalysts (**Scheme 3.2B**) and show not only that our selectivity model can be used to predict the selectivity of a broad scope of substrates, but that previously unselective substrates can be easily modified via changes in protecting groups into selective substrates.



Scheme 3.4. Tuning unselective substrates with different protecting groups to obtain selectivity. Isolated yields of major products in (). Conditions: catalyst (10 mol%), $(i\text{-PrCO})_2\text{O}$ (2.5 equiv), $i\text{-Pr}_2\text{NEt}$ (3.0 equiv), rt. Product ratios were determined by ^1H NMR of the crude products.

Next, we explored the substrate scope of the reaction (**Scheme 3.5**). The green anchor “O” in each structure is predicted to interact with the catalyst by a cation- n interaction for the acylation of blue OH. We first examined the electronic effect of the protecting group in α -glucosides **3.4c**

and **3.4d**. Results for the acylation of substrate **3.4c** are almost the same as those for **3.4a**. When (*R*)-BTM was employed as the catalyst for the acylation of **3.4d**, the selectivity for acylation of the C(3)-OH (product **3.6d**) dropped significantly due to the decreased cation-*n* and cation- π interactions with the electron-deficient phenyl ring in **3.4d**. For β -galactosides **3.19a** and **3.19b**, the C(2)-OH acylated products **3.20a** and **3.20b** were the major products using (*R*)-BTM catalyst, whereas the C(3)-OH acylated products **3.21a** and **3.21b** were the major products using (*S*)-BTM as the catalyst. For D-mannoside **3.22** and L-rhamnoside **3.25**, the anomeric OH can be protected together with the C(2)-OH as an orthoester. Guozhi demonstrated that as expected, the C(3)-OH in **3.22** was selectively acylated using (*R*)-BTM as the catalyst, and the C(3)-OH in **3.25** was selectively acylated using (*S*)-BTM as the catalyst. When I acylated xyloside **3.28** with (*R*)-BTM, I was surprised to observe a >20:1 ratio favoring C(4)-OH acylated product **3.30** using (*R*)-BTM because our model predicts no selectivity for this catalyst and substrate. I hypothesized that because xyloside **3.28** lacks a C(5)-substituent, the C(4)-OH is much more accessible than the C(3)-OH and any OH on previously discussed monosaccharides as well. DFT calculations I performed show that even though strong cation-*n* interactions are present in both C(3)- and C(4)-OH TSs, in the C(4)-OH TS, **3.30-TS1**, the cation-*n* interaction is much shorter and therefore stronger. This is because adjacent methylene group, C(5), does not clash with the carbonyl on the catalyst, which allows the C4-H that is pointing towards carbonyl to slightly rotate away from the carbonyl to decrease steric contact with the catalyst in **3.30-TS1**. We predicted that the (*S*)-BTM catalyst would selectively acylate the more hindered C(3)-OH group in xyloside **3.28**, which was confirmed by the observed 6:1 ratio favoring the formation of C(3)-OH acylated product **3.29**. This moderate selectivity again reflects the less sterically hindered nature of C(4)-OH. N-acyl glucosamine derivative **3.31** is predicted to be an unselective substrate for (*R*)-BTM according to our selectivity model, but acylation using (*R*)-BTM gave solely the C(3)-OH acylated product **3.33**. I believe this is because the amide N-H is hydrogen bonded to the C(3)-oxygen, reducing the C(3)-oxygen's anchoring ability.



Scheme 3.5. Site-selective acylation of monosaccharides. Isolated yields of major products in (). Conditions: catalyst (10 mol%), (*i*-PrCO)₂O (2.5 equiv), *i*-Pr₂NEt (3.0 equiv), rt. Product ratios were determined by ¹H NMR of the crude products. DFT calculations were performed using the M06-2X/6-311++G(d,p)/SMD//M06-2X/6-31G(d) level of theory.

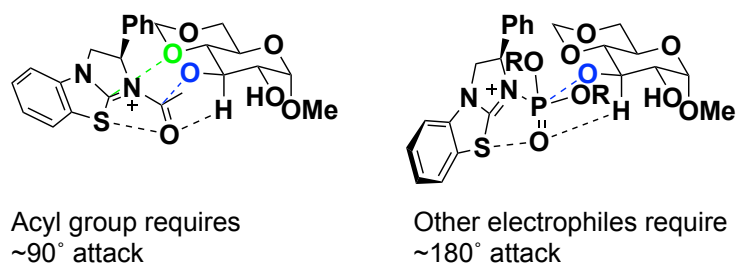
Guozhi next examined the site-selective acylation of OHs in more complex settings such as diols and found that our cation- n interaction model predicted the selectivities for those substrates as well. Additionally BTM is a competent catalyst for the site selective mixed anhydride acylation of carbohydrate diols as well.

Based solely on the cation- n interaction alone, we are able to differentiate hydroxyl groups in a variety of different pyranoses. The combination of the cation- n interaction with other factors, such as sterics, hydrogen bonding, and protecting group electronics can further expand the scope of the site-selective acylation. The recognition of cation- n interaction as one of the determining factors for selectivity will also have broad implications in other related site-selective reactions.^[15]

3.3 Attempts to use Chiral Catalysts to Site-Selectively Functionalize Carbohydrate *Trans*-1,2-Diols

I attempted to functionalize carbohydrate *trans*-1,2-diols using different electrophiles (silyl halides, tosyl chloride, mesyl chloride, methanesulfonic anhydride, chloro diphenyl phosphate, and others). In no case did I observe any catalyst controlled site-selectivity when using BTM or other chiral organocatalysts like **3.1** or bicycle imidazole catalysts (**Scheme 3.8**) with the substrates previously used in section **3.2**. I attempted to rationalize why only acylation showed any catalyst controlled selectivity and I decided that it largely comes down to the angle of attack of the nucleophile. The acyl group is unique among electrophiles in that it demands a roughly 90° angle of attack of the nucleophile. This allows the substrate and catalyst to interface which leads to favorable or unfavorable interactions for each OH group leading to selectivity (**Scheme 3.6**). Other electrophiles, like phosphate, require a 180° of attack. This means that the catalyst must try to interact with the substrate through the bulky electrophile which is often not possible. One way to get the catalyst to interact with the substrate through a bulky electrophile is to use a bigger catalyst that can reach around the electrophile, such as a peptide catalyst. These catalysts tend to be very substrate specific so I wanted to avoid this strategy. Another option would be to use a chiral electrophile so that something chiral is interfacing with the substrate. I

decided to use chloro phosphoramides as an electrophile for the site-selective functionalization of carbohydrates.



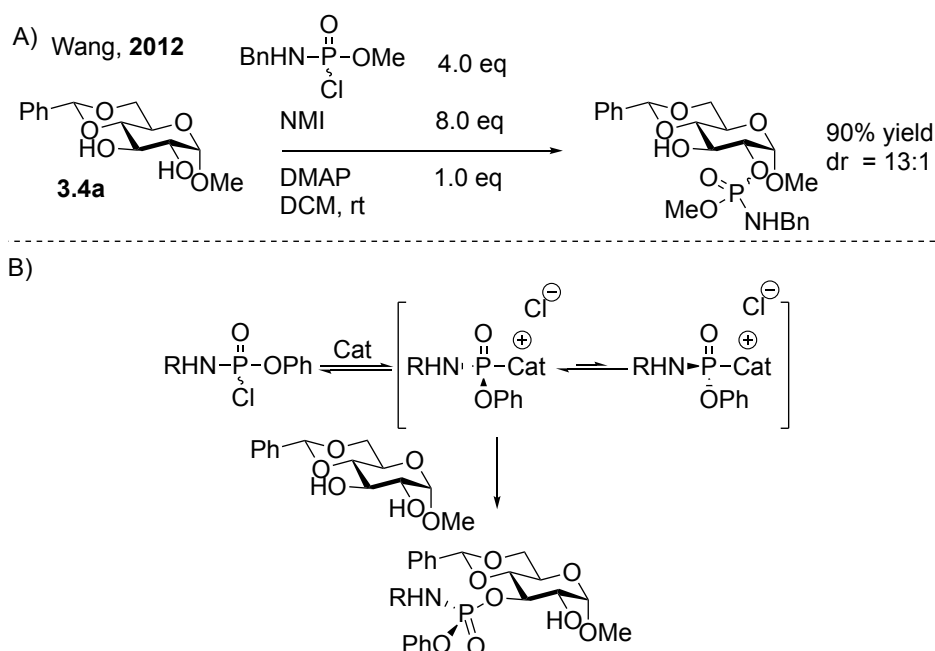
Scheme 3.6. Model TSs that demonstrate the uniqueness of the acyl group as an electrophile.

3.4 Site- and Stereo-Selective Phosphoramidation of Carbohydrate *Trans*-1,2-Diols

I choose to pursue site-selective phosphoramidation because phosphoramidated carbohydrates have been used as prodrugs,^[16] studied as anti-tumor agents,^[17] and are prevalent in *Campylobacter jejuni* (*C. Jejuni*) capsular polysaccharides (CPSs).^[18] *C. Jejuni* CPSs are proposed to be responsible for its virulence. Currently, there are no methods for the site-selective phosphoramidation of diol pairs within carbohydrates. Phosphoramidation poses a unique challenge because phosphoramidates are chiral at phosphorus, so high levels of stereoselectivity and site-selectivity must be achieved in order for any method to be broadly utilized.

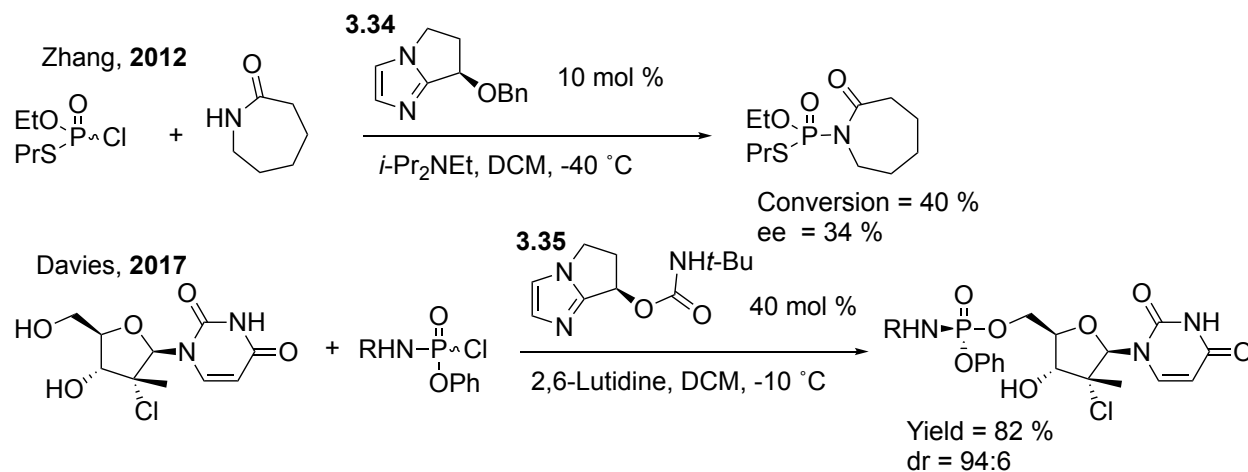
My previous work on the site-selective acylation of carbohydrates used chiral catalysts to give acylated products in high site-selectivity and yield (**Section 3.2**). I hypothesized that a similar strategy employing chiral catalysts would be compatible with phosphoramidates. When designing the site-selective protocol, I envisioned that the chiral nature of phosphoramidates might help to achieve both site- and stereoselective functionalization. Lowry and others have developed methods for the phosphoramidation of protected carbohydrates with only one free OH.^[19] This need to protect every OH except the one to be functionalized lengthens syntheses, lowers yields, and hurts atom economy. Wang and coworkers have reported that some partially protected carbohydrate diols can be site-selectively phosphoramidated on the more intrinsically reactive hydroxyl group using the achiral catalyst dimethylamino pyridine (DMAP). Interestingly

they also observed high stereoselectivity (>10:1) at phosphorus for some carbohydrate substrates (**Scheme 3.7A**).^[20] This diastereoselectivity presumably arises from matched/mismatched interactions between the enantiomeric phosphoramidate/catalyst complexes and the carbohydrate substrate; in other words, the hydroxyl on the carbohydrate has a stereo-preference for the phosphoramidate. I hypothesized that the reverse could also be true. The different enantiomeric phosphoramidate/catalyst complexes might have different site-preferences when it comes to functionalizing carbohydrate diols (**Scheme 3.7B**). Thus, to achieve site-selectivity I would need a catalyst/electrophile system that could provide high stereoselectivity via a dynamic kinetic resolution (DKR) of the phosphorus.



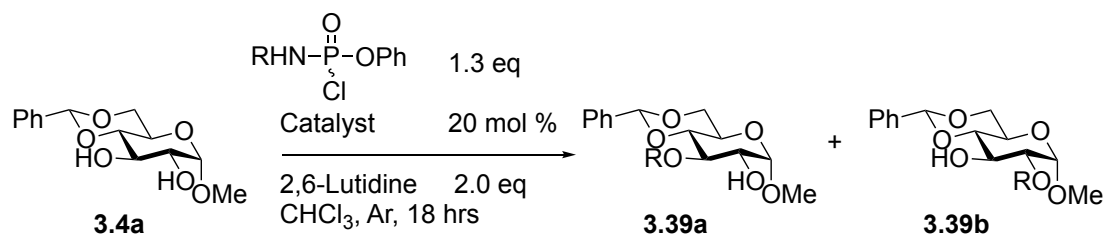
Scheme 3.7. A) Wang's 2015 report of an unusually site- and stereoselective phosphoramidation using achiral catalysts. B) Proposed site- and stereo-selective phosphoramidation of carbohydrates via a DKR of the phosphorus.

Chiral bicycloimidazole-based catalysts, such as **3**, have been used for the DKR of phosphorus centers since 2012.^[21] A group at Merck demonstrated that **3** and similar catalysts could be used to install phosphoramidates on the primary alcohol of the 5' position of a nucleotide in high yield and diastereomeric ratio (dr) (**Scheme 3.8**).^[22] Based on this precedent, my condition screening employed bicycloimidazole-based catalysts and a variety of chloro phosphoramidate electrophiles against model substrate **1**.



Scheme 3.8. Previous examples of bicycloimidazole-based catalysts used for the DKR of phosphorus centers.

I started screening with (L)-alanine derived electrophile **3.37**. Entries 1-3 (**Table 3.1**) resulted in complex mixtures and low selectivity, which indicated that electrophile **3.37** was not amenable to site-selective phosphoramidation. Switching to glycine-derived electrophile **3.38** (entries 4-6) resulted in low conversion, suggesting that the alpha-position of the phosphoramidate needs to be substituted. Using (D)-alanine derived electrophile *ent*-**3.37** and catalyst **3.36** provided C(3)-OH functionalized product **3.39a** in high yield, site-selectivity, and dr (>20:1, entry 7). This is the less reactive hydroxyl group that can't be functionalized with achiral catalysts. The high dr supports my hypothesis that a DKR of the phosphorus center is what is providing the high site-selectivity. Results from entries 2 and 7 are not unexpected, because the OH group is in a chiral environment. Catalysts *ent*-**3.35** and *ent*-**3.36** did not match with electrophile *ent*-**3.37**. Increasing the equivalents of electrophile and base loading significantly improved the isolated yield (entry 10). No site-selectivity was obtained when achiral catalyst N-methyl imidazole (NMI) was used, but interestingly, the dr of isolated product **3.39b** was still high (10:1, entry 11).



Entry	Catalyst	Phosphoramidate	Yield (%)	C3/C2
1	3.36	3.37	~a	1:1
2	<i>ent</i> - 3.36	3.37	~a	1:3
3	<i>ent</i> - 3.35	3.37	~a	1:1
4	3.36	3.38	<10	-
5	<i>ent</i> - 3.36	3.38	<10	-
6	<i>ent</i> - 3.35	3.38	<10	-
7	3.36	<i>ent</i> - 3.37	63	>10:1
8	<i>ent</i> - 3.36	<i>ent</i> - 3.37	70 ^b	1:1
9	<i>ent</i> - 3.35	<i>ent</i> - 3.37	<10	2:1
10^c	3.36	<i>ent</i> - 3.37	82^d	10:1
11 ^c	NMI	<i>ent</i> - 3.37	47 ^e	1:1

3.36

ent-**3.35**

3.37, R = Me
3.38, R = H

^a Products not isolated. ^b Conversion.

^c 2.0 eq of electrophile and 2.5 eq of base used.

^d Yield of C3 product. ^e Yield of C2 product.

Table 3.1. Site- and stereo-selective phosphoramidation condition screening. Product ratios were determined by ¹H NMR of the crude products.

With optimized conditions that promoted high degrees of both site- and stereoselectivity, I proceeded to explore the substrate scope of the reaction. β -Galactoside **3.19a** gave C2 phosphoramidate product **3.40b** in high site-selectivity, dr, and yield. Once again, This is the less reactive hydroxyl group. The stereochemistry of the phosphorous center for **3.39a** and **3.40b** was assigned based on literature precedent.^[22] β -Glucoside **3.7a** exhibited excellent conversion and dr, but no site-selectivity. This is likely due to the highly symmetric structure of **3.7a**, which renders the C(2) and C(3) hydroxyl groups too similar to differentiate by the chiral catalyst/electrophile system. α -Galactoside **3.42** shows moderate site-selectivity, but poor dr with both the chiral and achiral catalysts. Allyl glycosides **3.44** and **3.46** gave excellent site- and stereoselectivities in synthetically useful yields of products **3.45a** and **3.47b**, respectively, when

using chiral catalyst **3.36**. The achiral catalyst NMI yielded either a complex mixture or low selectivity. S- α -Glucoside **3.48** and C-glucoside **3.50** both provided C(3) phosphoramidated products, **3.49a** and **3.51a** respectively, with high site- and stereoselectivity and high yields with chiral catalyst **3.36**. Once again, a complex mixture was observed with the achiral catalyst in both cases. S- β -galactosides and O- α -mannosides gave poor conversions. C-glucoside **3.10** exhibited unexpected behavior. Substrate **3.10** was employed to investigate the reactivity of β -glucosides that exhibit a lower degree symmetry than substrate **3.7a**. As I hoped, using catalyst **3.36** I obtained high site-selectivity for the C(3) phosphoramidated product **3.42a** along with high stereoselectivity and excellent yield. However, with NMI we saw the same excellent site-selectivity, but significantly lower yield. We hypothesize that the equatorial methyl group at C(1) sterically hinders the C(2) hydroxyl group, which results in the observed C(3) selectivity. β -Glucoside **3.13** was designed by deactivating the (C3)-OH group with two electron-withdrawing benzoyl groups, but the deactivating effect led to low conversion. Clearly, the combination of chiral catalyst **3.36** and electrophile *ent*-**3.37** yields primarily C(3) phosphoramidated products for α -O-, α -S-, and α -C-glucosides. The same combination of catalyst and electrophile afforded C(2) phosphoramidated products for β -galactosides. This observation is not surprising because the diols in α -glucosides and β -galactosides are in opposite stereochemical environments. Other diol motifs I have examined so far have no strong site preference using the same chiral catalyst/electrophile pair.

Catalyst	Substrate	Results (a: C3 product; b: C2 product)	Catalyst	Substrate	Results (a: C3 product; b: C2 product)
3.36		3.39a/3.39b = 10:1, 3.39a (82 %, >20:1 dr)	3.36		3.47a/3.47b = 1:16, 3.47b (60 %, >20:1 dr)
NMI	3.4a	3.39a/3.39b = 1:1, 3.39b (47 %, dr > 20:1)	NMI	3.46	3.47a/3.47b = 5:1 3.47a (44 %, dr = 5:1)
3.36		3.40a/3.40b = 1:16, 3.40b (77 %, >20:1 dr) ^b	3.36		3.49a/3.49b > 20:1, 3.49a (67 %, >20:1 dr)
NMI	3.19a	3.40a/3.40b = 2:1, 3.40a (52 %, dr > 20:1) ^b	NMI	3.48	Complex Mixture
3.36		3.41a/3.41b = 1:1, 3.41a/3.41b (100 %, >20:1 dr) ^c	3.36		3.51a/3.51b > 20:1, 3.51a (77 %, >20:1 dr)
NMI	3.7a	3.41a/3.41b = 1:1, 3.41a/3.41b (100 %, dr > 20:1) ^c	NMI	3.50	Complex Mixture
3.36		3.43a/3.43b = 5:1, 3.43a (57 %, 5:1 dr)	3.36		3.52a/3.52b > 20:1, 3.52a (80 %, >20:1 dr) ^c
NMI	3.42	3.43a/3.43b = 5:1, 3.43a (61 %, dr > 5:1)	NMI	3.10	3.52a/3.52b > 20:1 3.52a (<30 %) ^c
3.36		3.45a/3.45b > 20:1, 3.45a (63 %, >20:1 dr)	3.36		<10 % ^c
NMI	3.44	Complex Mixture	NMI	3.13	<10 % ^c

Table 3.2. Site- and stereo-selective phosphoramidation substrate scope. Product ratios were determined by ¹H NMR of the crude products. Conditions: substrate (1 equiv.), catalyst (20 mol %) *ent*-**3.47** (2.0 eq) 2,6-lutidine (2.5 eq), amylene stabilized chloroform (1 M), unless noted otherwise. Yields in parentheses. dr is of the isolated products. [b] 1.3 equiv. of the electrophile and 2.0 eq of 2,6-lutidine used. [c] The numbers represent conversions. Reaction are performed in trichloroethylene when the substrates are not very soluble in chloroform.

In summary, I have developed an efficient and practical stereoselective and site-selective phosphoramidation reaction for carbohydrates using a chiral catalyst and a chiral electrophile. The stereoselectivity arises due to the DKR at the phosphorous center.¹⁰ The high stereoselectivity then promotes the high site-selectivity; in other words, the chirality at phosphorus controls the site-preference of the catalyst/electrophile complex. This method is amenable to a variety of β -galactosides and α -glucosides. To the best of my knowledge, this is the first site- and stereoselective phosphoramidation reaction reported in the literature. This methodology will allow for the synthesis of phosphoramidated carbohydrate *trans*-1,2-diols in

high yield and dr. Furthermore, this approach can streamline the synthesis of phosphoramidated carbohydrate-containing prodrugs and natural products.

3.5 1

I have been involved in the development of two methods for the site-selective functionalization of carbohydrate *trans*-1,2-diols. The first, a site-selective acylation using BTM catalysts, is a general method for the differentiation of *trans*-1,2-diols. In the process of developing this reaction we discovered the novel cation-*n* interaction as the major determining factor for selectivity of the reaction. This discovery will have import for the design of future selective organocatalyst controlled reactions. We have continued to pursue the development of site-selective acylation reactions of carbohydrate *trans*-1,2-diols with the recent publication of a method for the S-adamantyl directed site-selective acylation of β -S-glucosides. The selectivity of the reaction is mediated by dispersion interactions between the adamantyl C-H bonds and the π system of the cationic acylated catalyst. This may have broad implications for the development of related site-selective reactions.

The second method, the first site- and stereo-selective phosphoramidation, applies only to α -O-, α -S-, α -C-glucosides, and β -galactosides. I rationally designed this method by using a chiral catalyst and a chiral electrophile to affect a DKR at the phosphorous center which leads to high site-selectivity because the different diastereomeric phosphoramidate/catalyst complexes should have different site preferences. If the DKR of a phosphorous center can lead to site-selectivity, using another chiral electrophile might work as well. Sulfinyl and sulfurous chlorides are chiral at sulfur and if they can be site-selectively installed on a carbohydrate they can be easily oxidized into sulfonates and sulfates respectively. Additionally, stereochemically defined chiral electrophiles may be selective electrophiles. Exploring stereochemically defined chiral electrophiles like Baran's Psi reagent^[23] or chiral sulfuryl imidazolium salts^[24] may prove fruitful.

3.6 References

- (1) (a) R. A. Dwek, *Chem. Rev.* **1996**, 96, 683–720. (b) C. R. Bertozzi, and L. L. Kiessling, *Science* (80-.). **2001**, 291, 2357 LP – 2364.
- (2) For recent reviews, see: (a) Giuliano, M. W.; Miller, S. J. In *Topics in Current Chemistry*; Kawabata, T., Ed.; Springer International Publishing AG: Gewerbestrasse, 2016; Vol. 372, p 157. (b) Ueda, Y.; Kawabata, T. In *Topics in Current Chemistry*; Kawabata, T., Ed.; Springer International Publishing AG: Gewerbestrasse, 2016; Vol. 372, p 203. (c) Lawandi, J.; Rocheleau, S.; Moitessier, N. *Tetrahedron* **2016**, 72, 6283.
- (3) B. Ren, O. Ramström, Q. Zhang, J. Ge, H. Dong, *Chem. – A Eur. J.* **2016**, 22, 2481–2486.
- (4) S. David, S. Hanessian, *Tetrahedron* **1985**, 41, 643–663.
- (5) (a) K. Oshima, E. Kitazono, Y. Aoyama, *Tetrahedron Lett.* **1997**, 38, 5001–5004. (b) D. Lee, M. S. Taylor, *J. Am. Chem. Soc.* **2011**, 133, 3724–3727. (c) C. Gouliaras, D. Lee, L. Chan, M. S. Taylor, *J. Am. Chem. Soc.* **2011**, 133, 13926–13929.
- (6) (a) T. M. Beale, M. S. Taylor, *Org. Lett.* **2013**, 15, 1358–1361. (b) R. S. Mancini, C. A. McClary, S. Anthonipillai, M. S. Taylor, *J. Org. Chem.* **2015**, 80, 8501–8510.
- (7) P. Peng, M. Linseis, R. F. Winter, R. R. Schmidt, *J. Am. Chem. Soc.* **2016**, 138, 6002–6009.
- (8) X. Sun, H. Lee, S. Lee, K. L. Tan, *Nat. Chem.* **2013**, 5, 790.
- (9) T. Kawabata, W. Muramatsu, T. Nishio, T. Shibata, H. Schedel, *J. Am. Chem. Soc.* **2007**, 129, 12890–12895.
- (10) (a) Y. Zhou, M. Rahm, B. Wu, X. Zhang, B. Ren, H. Dong, *J. Org. Chem.* **2013**, 78, 11618–11622. (b) B. Ren, M. Rahm, X. Zhang, Y. Zhou, H. Dong, *J. Org. Chem.* **2014**, 79, 8134–8142. (c) T. Kurahashi, T. Mizutani, J. Yoshida, *Tetrahedron* **2002**, 58, 8669–8677. (d) K. S. Griswold, S. J. Miller, *Tetrahedron* **2003**, 59, 8869–8875. (e) M. Sánchez-Roselló, A. L. A. Puchlopek, A. J. Morgan, S. J. Miller, *J. Org. Chem.* **2008**, 73, 1774–1782. (f) C. L. Allen, S. J. Miller, *Org. Lett.* **2013**, 15, 6178–6181. (g) C. L. Allen, S. J. Miller, *Org. Lett.* **2013**, 15, 6178–6181. (h) I.-H. Chen, K. G. M. Kou, D. N. Le, C. M. Rathbun, V. M. Dong, *Chem. – A Eur. J.* **2014**, 20, 5013–5018. (i) F. Huber, S. F. Kirsch, *Chem. – A Eur. J.* **2016**, 22, 5914–5918. (j) D. L. Cramer, S. Bera, A. Studer, *Chem. – A Eur. J.* **2016**, 22, 7403–7407.
- (11) (a) V. B. Birman, X. Li, *Org. Lett.* **2006**, 8, 1351–1354. (b) V. B. Birman, E. W. Uffman, H. Jiang, X. Li, C. J. Kilbane, *J. Am. Chem. Soc.* **2004**, 126, 12226–12227.
- (12) (a) A. Ortiz, T. Benkovics, G. L. Beutner, Z. Shi, M. Bultman, J. Nye, C. Sfougataki, D. R. Kronenthal, *Angew. Chemie Int. Ed.* **2015**, 54, 7185–7188. (b) H.-Y. Wang, K. Yang, D. Yin, C. Liu, D. A. Glazier, W. Tang, *Org. Lett.* 2015, 17, 5272–5275. (c) H.-Y. Wang, C. J. Simmons, Y. Zhang, A. M. Smits, P. G. Balzer, S. Wang, W. Tang, *Org. Lett.* 2017, 19, 508–511.
- (13) (a) X. Yang, P. Liu, K. N. Houk, V. B. Birman, *Angew. Chemie Int. Ed.* 2012, 51, 9638–9642. (b) X. Li, P. Liu, K. N. Houk, V. B. Birman, *J. Am. Chem. Soc.* 2008, 130, 13836–13837. (c) P. Liu, X. Yang, V. B. Birman, K. N. Houk, *Org. Lett.* 2012, 14, 3288–3291.
- (14) (a) S. E. Wheeler, J. W. G. Bloom, *J. Phys. Chem. A* 2014, 118, 6133–6147. (b) S. E. Wheeler, K. N. Houk, *J. Phys. Chem. A* 2010, 114, 8658–8664. (c) I. Pavlakos, T. Arif, A. E. Aliev, W. B. Motherwell, G. J. Tizzard, S. J. Coles, *Angew. Chemie Int. Ed.* 2015, 54, 8169–8174.
- (15) (a) B. S. Fowler, K. M. Laemmerhold, S. J. Miller, *J. Am. Chem. Soc.* **2012**, 134, 9755–9761. (b) S. Han, S. J. Miller, *J. Am. Chem. Soc.* **2013**, 135, 12414–12421. (c) S. Han, B. V. Le, H. S. Hajare, R. H. G. Baxter, S. J. Miller, *J. Org. Chem.* **2014**, 79, 8550–8556.
- (16) A. S. Alanazi, E. James, Y. Mehellou, *ACS Med. Chem. Lett.* **2019**, 10, 2–5.

- (17) R.-Y. Chen, X.-R. Chen, *Heteroat. Chem.* **1993**, 4, 587–592.
- (18) P. Guerry, F. Poly, M. Riddle, A. Maue, Y.-H. Chen, M. Monteiro, *Front. Cell. Infect. Microbiol.* **2012**, 2, 7.
- (19) (b) V. N. Thota, M. J. Ferguson, R. P. Sweeney, T. L. Lowary, *Angew. Chemie Int. Ed.* **2018**, 57, 15592–15596. (b) R. A. Ashmus, T. L. Lowary, *Org. Lett.* **2014**, 16, 2518–2521. (c) Y. Jiao, Z. Ma, C. P. Ewing, P. Guerry, M. A. Monteiro, *Carbohydr. Res.* **2015**, 418, 9–12.
- (20) V. M. Dhurandhare, G. P. Mishra, S. Lam, C.-C. Wang, *Org. Biomol. Chem.* **2015**, 13, 9457–9461.
- (21) S. Liu, Z. Zhang, F. Xie, N. A. Butt, L. Sun, W. Zhang, *Tetrahedron: Asymmetry* **2012**, 23, 329–332.
- (22) D. A. DiRocco, Y. Ji, E. C. Sherer, A. Klapars, M. Reibarkh, J. Dropinski, R. Mathew, P. Maligres, A. M. Hyde, J. Limanto, et al., *Science* (80-.). **2017**, 356, 426 LP – 430.
- (23) K. W. Knouse, J. N. deGruyter, M. A. Schmidt, B. Zheng, J. C. Vantourout, C. Kingston, S. E. Mercer, I. M. McDonald, R. E. Olson, Y. Zhu, et al., *Science* (80-.). **2018**, 361, 1234 LP – 1238.
- (24) L. J. Ingram, S. D. Taylor, *Angew. Chemie Int. Ed.* **2006**, 45, 3503–3506.

Supporting Information

Chapter 3: Site-Selective Functionalization of Carbohydrates

Table of Contents

General remarks.....	126
Procedures for site-selective acylation of carbohydrates	126
Characterization acylation data	127
Procedures for site- and stereo-selective phosphoramidation of carbohydrates.....	131
Characterization of phosphoramidation data	132
Computational Details.....	143
References	154
Copy of NMR spectra	155

General remarks:

All reactions in non-aqueous media were conducted under a positive pressure of dry argon in glassware that had been oven dried prior to use unless noted otherwise. Anhydrous solutions of reaction mixtures were transferred via an oven dried syringe or cannula. All solvents were dried prior to use unless noted otherwise. Thin layer chromatography was performed using precoated silica gel plates. Flash column chromatography was performed with silica gel (40-63 μm). Infrared spectra (IR) were obtained on a Bruker Equinox 55 Spectrophotometer. ^1H and ^{13}C nuclear magnetic resonance spectra (NMR) were obtained on a Bruker Ascend 400 MHz recorded in ppm (δ) downfield of TMS ($\delta = 0$) in CDCl_3 unless noted otherwise. Signal splitting patterns were described as singlet (s), doublet (d), triplet (t), quartet (q), quintet (quint), or multiplet (m), with coupling constants (J) in hertz. High resolution mass spectra (HRMS) were performed by Analytical Instrument Center at the School of Pharmacy or Department of Chemistry on an Electron Spray Injection (ESI) mass spectrometer. (RT = room temperature.)

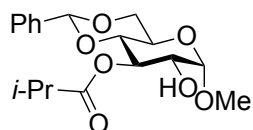
Benzylidene protected Me-O-glucoside substrates were prepared following a procedure from Miller.^[1] Compound **3.10** was prepared following a procedure from Jurczak.^[2] Compound **3.31** was prepared following a procedure from Timmer.^[3] Compound **3.58** was prepared following a procedure from Kitamura.^[4] Compound **3.60** was prepared following a procedure from Magnusson.^[5]

Procedure A for (*R*)-BTM or (*S*)-BTM catalyzed site selective acylation using anhydride:

To a solution of substrate (0.12 mmol, 1.0 equiv) and (*R*)-BTM or (*S*)-BTM (0.012 mmol, 10 mol%) in anhydrous CHCl_3 (0.6 mL, commercially available CHCl_3 containing either ~0.75% ethanol or amylene as the preservative was dried over sodium sulfate prior to use.) was added diisopropylethyl amine (DIPEA) (0.37 mmol, 3.0 equiv), followed by dropwise addition of isobutyric anhydride (0.31 mmol, 2.5 equiv.) at room temperature. The reaction mixture was stirred at room temperature for 12 h and monitored by TLC. After the reaction was completed, the reac-

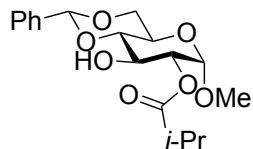
tion mixture was quenched with MeOH (1 mL) and the mixture was stirred for an additional 10 minutes. A solution of saturated aqueous NH₄Cl (3 mL) was added. The reaction mixture was extracted with CH₂Cl₂ (3 × 3 mL). The organic layers were combined, dried with anhydrous Na₂SO₄, filtrated and concentrated under vacuum to give the crude product. Ratios of site selective acylation are determined by ¹H NMR of the crude product. Purification of the crude product by column chromatography on silica gel using the indicated solvent system afforded the desired product.

Methyl 4,6-O-benzylidene-3-O-isobutyryl- α -D-glucopyranoside (3.6a)



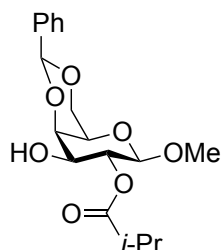
3.4a and (*R*)-BTM were used according to procedure A. The product was isolated by column chromatography on silica gel (Hexane/Ethyl acetate = 3/1) as a white solid (40 mg, 92%). mp = 206-207 °C. $[\alpha]_{22} = +88.8^\circ$ (c = 0.25, CH₂Cl₂) ¹H NMR (400 MHz, CDCl₃): δ 7.43-7.40 (m, 2H), 7.36-7.31 (m, 3H), 5.49 (s, 1H), 5.30 (t, J = 10.0 Hz, 1H), 4.78 (d, J = 4.0 Hz, 1H), 4.31 (dd, J = 4.8, 10.0 Hz, 1H), 3.87-3.81 (m, 1H), 3.74 (t, J = 10.4 Hz, 1H), 3.67-3.62 (m, 1H), 3.58 (t, J = 9.6 Hz, 1H), 3.45 (s, 3H), 2.65-2.55 (m, 1H), 2.24-2.22 (m, 1H), 1.18 (d, J = 6.8 Hz, 3H), 1.16 (d, J = 6.8 Hz, 3H). ¹³C NMR (101 MHz, CDCl₃) δ 177.4, 137.2, 129.1, 128.3, 126.2, 101.4, 100.4, 78.9, 72.2, 72.1, 69.1, 62.9, 55.7, 34.3, 19.3, 19.0. IR (neat) ν 2927, 2855, 1732, 1344, 1211, 1036, 970, 742. HRMS (ESI) m/z calcd for C₁₈H₂₄O₇ + Na = 375.1414, found 375.1415.

Methyl 4,6-O-benzylidene-2-O-isobutyryl- α -D-glucopyranoside (3.5a)



3.4a and (*s*)-BTM were used according to procedure A. The product was isolated by column chromatography on silica gel (Hexane/Ethyl acetate = 3/1) as a colorless oil (41 mg, 94%). $[\alpha]_{22} = +53.6^\circ$ ($c = 0.25$, CH_2Cl_2) $^1\text{H NMR}$ (400 MHz, CDCl_3): δ 7.50-7.48 (m, 2H), 7.38-7.36 (m, 3H), 5.55 (s, 1H), 4.94 (d, $J = 3.6$ Hz, 1H), 4.78 (dd, $J = 9.6, 4.0$ Hz, 1H), 4.29 (dd, $J = 10.0, 4.8$ Hz, 1H), 4.18 (t, $J = 9.6$ Hz, 1H), 3.85-3.73 (m, 2H), 3.56 (t, $J = 9.6$ Hz, 1H), 3.39 (s, 3H), 2.68-2.64 (m, 1H), 1.21 (d, $J = 2.4$ Hz, 3H), 1.19 (d, $J = 2.4$ Hz, 3H). $^{13}\text{C NMR}$ (101 MHz, CDCl_3): δ 177.1, 137.2, 129.4, 128.5, 126.5, 102.2, 97.8, 81.5, 73.5, 69.0, 68.9, 62.2, 55.7, 34.0, 19.2, 19.0. IR (neat) ν 2923, 2851, 2360, 1734, 1456, 1193, 1040, 895, 766. HRMS (ESI) m/z calcd for $\text{C}_{18}\text{H}_{24}\text{O}_7 + \text{Na} = 375.1414$, found 375.1415.

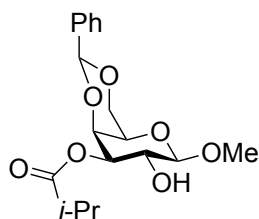
Methyl 4,6-O-benzylidene-2-O-isobutyryl- β -D-galactopyranoside (3.20a)



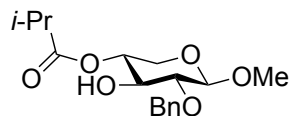
3.9a and (*R*)-BTM were used according to procedure A. According to the procedure A, **3.19a** (35 mg, 0.12 mmol), The product was isolated by column chromatography on silica gel (Hexane/Ethyl acetate = 1.3/1) as a colorless oil (37 mg, 85%). $[\alpha]_{22} = +5.0^\circ$ ($c = 1.2$, CHCl_3). $^1\text{H NMR}$ (400 MHz, CDCl_3): δ 7.50 (m, 2H), 7.35 (m, 3H), 5.53 (s, 1H), 5.11 (dd, $J = 8.0, 10.0$ Hz, 1H), 4.36 (d, $J = 8.0$ Hz, 1H), 4.31 (dd, $J = 1.6, 12.4$ Hz, 1H), 4.18 (dd, $J = 0.8, 3.6$ Hz, 1H), 4.08 (dd, $J = 1.6, 12.4$ Hz, 1H), 3.74 (dd, $J = 3.6, 9.6$ Hz, 1H), 3.49 (s, 3H), 3.46 (m, 1H), 2.62 (m, 1H), 1.18 (d, $J = 6.8$ Hz, 6H). $^{13}\text{C NMR}$ (101 MHz, CDCl_3) δ 176.9, 137.5, 129.4, 128.4, 126.6,

101.9, 101.6, 75.7, 71.9, 69.1, 66.7, 56.7, 34.2, 19.2, 19.0. IR (neat) ν 3016, 2971, 2939, 2918, 2877, 2360, 2341, 1736, 1539, 1456, 1387, 1216, 1085, 1057, 1027, 1000. HRMS (ESI) m/z calcd for $C_{18}H_{24}O_7 + K = 391.1159$, found 391.1149.

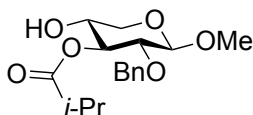
Methyl 4,6-O-benzylidene-3-O-isobutyryl- β -D-galactopyranoside (3.20b)



3.19a and (S)-BTM were used according to procedure A. The product was isolated by column chromatography on silica gel (Hexane/Ethyl acetate = 1.3/1) as a white solid (40 mg, 93%). mp = 160-164 °C. $[\alpha]_{22} = +69.2^\circ$ (c = 2.0, $CHCl_3$). 1H NMR (500 MHz, $CDCl_3$): δ 7.47 (m, 2H), 7.32 (m, 3H), 5.48 (s, 1H), 4.82 (dd, J = 4.0, 10.5 Hz, 1H), 4.37 (d, J = 3.5 Hz, 1H), 4.32 (dd, J = 1.0, 12.5 Hz, 1H), 4.26 (d, J = 8.0 Hz, 1H), 4.05 (dd, J = 2.0, 12.5 Hz, 1H), 4.00 (dd, J = 8.0, 10.5 Hz, 1H), 3.55 (s, 3H), 3.48 (s, 1 H), 2.62 (m, 1H), 2.52 (br, 1 H), 1.16 (d, J = 7.0 Hz, 6H). ^{13}C NMR (126 MHz, $CDCl_3$) δ 177.3, 137.8, 129.0, 128.2, 126.2, 104.1, 100.9, 73.7, 73.4, 69.2, 68.7, 66.6, 57.3, 34.1, 19.3, 18.8. IR (neat) ν 3649, 3524, 2980, 2930, 2889, 2361, 2342, 1720, 1454, 1386, 1369, 1203, 1171. HRMS (ESI) m/z calcd for $C_{18}H_{24}O_7 + Na = 375.1420$, found 375.1409.

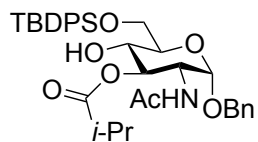
Methyl 2-O-benzyl-4-O-isobutyryl-β-D-xylopyranoside (3.30)

3.28 and (*R*)-BTM were used according to procedure A. The product was isolated by column chromatography on silica gel (Hexane/Ethyl acetate = 3.6/1) as a white solid (29 mg, 90%). mp = 48-50 °C. $[\alpha]_{22} = -19.8^\circ$ ($c = 0.67$, CHCl_3). $^1\text{H NMR}$ (400 MHz, CDCl_3): δ 7.35-7.26 (m, 5 H), 4.86 (d, $J = 11.6$ Hz, 1H), 4.78 (m, 1H), 4.65 (d, $J = 11.6$ Hz, 1H), 4.35 (d, $J = 6.4$ Hz, 1H), 4.05 (dd, $J = 5.2, 12.0$ Hz, 1H), 3.73 (m, 1H), 3.50 (s, 3H), 3.30-3.25 (m, 2H), 2.55 (m, 2H), 1.15 (d, $J = 6.8$ Hz, 3H), 1.14 (d, $J = 6.8$ Hz, 3H). $^{13}\text{C NMR}$ (101 MHz, CDCl_3) δ 176.9, 138.3, 128.7, 128.2, 128.1, 104.1, 80.2, 74.2, 72.5, 71.2, 62.2, 56.8, 34.1, 19.12, 19.10. IR (neat) ν 3374, 2971, 2932, 2878, 2348, 1737, 1468, 1387, 1279, 1194, 1157, 1126, 1094, 1024, 951, 753. HRMS (ESI) m/z calcd for $\text{C}_{17}\text{H}_{24}\text{O}_6 + \text{Na} = 347.1471$, found 347.1463.

Methyl 2-O-benzyl-3-O-isobutyryl-β-D-xylopyranoside (3.29)

3.28 and (*S*)-BTM were used according to procedure A. The product was isolated by column chromatography on silica gel (Hexane/Ethyl acetate = 1.5/1) as a white solid (24 mg, 75%). mp = 70-74 °C. $[\alpha]_{22} = -21.5^\circ$ ($c = 0.8$, CHCl_3). $^1\text{H NMR}$ (400 MHz, CDCl_3): δ 7.38-7.27 (m, 5H), 4.90 (t, $J = 7.2$ Hz, 1H), 4.80 (d, $J = 11.6$ Hz, 1H), 4.68 (d, $J = 11.6$ Hz, 1H), 4.43 (d, $J = 5.6$ Hz, 1H), 4.04 (dd, $J = 4.4, 12.0$ Hz, 1H), 3.68 (m, 1H), 3.48 (s, 3H), 3.44-3.36 (m, 2H), 2.55 (m, 1H), 1.17 (d, $J = 6.8$ Hz, 3H), 1.16 (d, $J = 6.8$ Hz, 3H). $^{13}\text{C NMR}$ (101 MHz, CDCl_3) δ 178.0, 138.0, 128.5, 127.99, 127.96, 103.3, 76.9, 74.6, 74.0, 68.8, 64.1, 56.6, 34.2, 19.0. IR (neat) ν 3450, 2972, 2938, 2906, 2876, 2842, 2357, 2343, 1736, 1469, 1388, 1260, 1199, 1160, 1070, 1028, 800, 755, 698. HRMS (ESI) m/z calcd for $\text{C}_{17}\text{H}_{24}\text{O}_6 + \text{Na} = 347.1471$, found 347.1460.

Benzyl 2-N-acyl-3-O-isobutyryl-6-O-*t*-butyldiphenylsilyl- α -D-glucopyranoside (3.33)

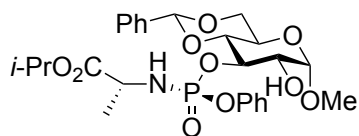


3.31a and (*R*)-BTM were used according to procedure A. The product was isolated by column chromatography on silica gel (Hexane/Ethyl acetate = 2/1) as an amorphous solid (57.7 mg, 90%). ¹H NMR (400 MHz, Chloroform-*d*) δ 7.69 (dt, *J* = 7.8, 1.4 Hz, 4H), 7.52 – 7.21 (m, 12H), 5.73 (d, *J* = 9.6 Hz, 1H), 5.14 (dd, *J* = 10.8, 8.3 Hz, 1H), 4.85 (d, *J* = 3.6 Hz, 1H), 4.67 (d, *J* = 11.9 Hz, 1H), 4.42 (d, *J* = 11.9 Hz, 1H), 4.26 (ddd, *J* = 10.7, 9.6, 3.7 Hz, 1H), 3.89 (d, *J* = 4.0 Hz, 2H), 3.85 – 3.70 (m, 2H), 2.76 – 2.66 (m, 1H), 2.60 (hept, *J* = 7.0 Hz, 1H), 1.88 (s, 3H), 1.15 (dd, *J* = 7.0, 5.4 Hz, 6H), 1.07 (s, 9H). ¹³C NMR (101 MHz, CDCl₃) δ 178.44, 169.86, 136.90, 135.68, 135.63, 133.00, 132.87, 129.92, 128.58, 128.14, 128.03, 127.83, 127.81, 96.50, 73.59, 71.41, 70.54, 69.43, 64.42, 51.60, 34.12, 26.88, 23.18, 19.25, 19.11, 18.80. HRMS (ESI) *m/z* calcd for C₃₅H₄₅NO₇Si + Na = 642.2858, found 642.2855.

Procedure B for the site- and stereo-selective phosphoramidation:

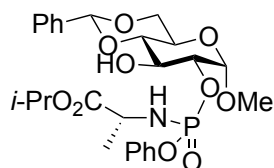
To a solution of catalyst (0.02 mmol) and substrate (0.1 mmol) in dry chloroform (stabilized by amylene) was added 2,6-Lutidine (0.029 mL, 0.25 mmol) and *ent*-**3.37** (61.1 mg, 0.2 mmol). The vial was capped with argon and the reaction mixture was stirred overnight (18 hrs). The reaction was quenched with MeOH (0.5 mL) and the resulting solution was stirred for 15 min. The solvent was removed under vacuum and the products was isolated via flash column chromatography. The stereochemistry of phosphoramidates synthesized using the chiral catalyst **3.45** were assigned based on the previously reported dynamic kinetic resolution of phosphoramidates using this catalyst.^[6]

Methyl 4,6-O-benzylidene-3-O-(*R*)-(phenyl-N-(isopropoxy-(*D*)-alaninyl)-phosphoramidyl)- α -D-glucopyranoside (3.39a)



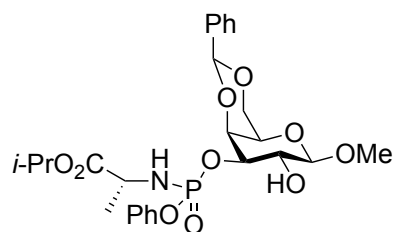
3.4a and **3.36** were used according to procedure B. The product was isolated by column chromatography on silica gel (2:1 hexanes/EtOAc to 1:2 hexanes/EtOAc) as an amorphous solid (45.5 mg, 82 % yield). $^1\text{H NMR}$ (400 MHz, CDCl_3) δ 7.47 (dd, $J = 6.7, 3.0$ Hz, 2H), 7.36 (q, $J = 3.1, 2.7$ Hz, 3H), 7.25 – 7.17 (m, 4H), 7.14 – 7.06 (m, 1H), 5.54 (s, 1H), 4.95 (hept, $J = 6.3$ Hz, 1H), 4.84 (d, $J = 3.8$ Hz, 1H), 4.63 (td, $J = 9.2, 7.8$ Hz, 1H), 4.31 (dd, $J = 10.1, 4.6$ Hz, 1H), 4.08 – 3.95 (m, 2H), 3.90 – 3.79 (m, 3H), 3.75 (t, $J = 10.2$ Hz, 1H), 3.65 (t, $J = 9.4$ Hz, 1H), 3.45 (s, 3H), 1.26 (d, $J = 7.0$ Hz, 3H), 1.18 (d, $J = 4.4$ Hz, 3H), 1.16 (d, $J = 4.6$ Hz, 3H). $^{13}\text{C NMR}$ (101 MHz, CDCl_3) δ 172.83 (d, $J = 8.7$ Hz), 150.85 (d, $J = 7.0$ Hz), 136.87, 129.53, 129.17, 128.28, 126.23, 124.80, 120.30 (d, $J = 5.0$ Hz), 101.84, 100.06, 79.41 (d, $J = 5.5$ Hz), 77.87 (d, $J = 5.6$ Hz), 71.93 (d, $J = 1.9$ Hz), 69.11, 68.94, 62.23, 55.58, 50.18 (d, $J = 2.2$ Hz), 21.64, 21.59, 20.59 (d, $J = 4.4$ Hz). $^{31}\text{P NMR}$ (162 MHz, CDCl_3) δ 3.63. IR: 3384, 2982, 2936, 1732, 1637, 1592, 1491, 1456, 1376, 1257, 1211, 1150, 1072, 1043, 989, 938, 905, 816, 761, 735, 699 cm^{-1} . HRMS (ESI): calcd. for $\text{C}_{26}\text{H}_{34}\text{NO}_{10}\text{P} + \text{Na} = 574.1813$, found 574.1785. $[\alpha]_{\text{D}}^{25} = 15.4^\circ$ (c 0.0052, CHCl_3).

Methyl 4,6-O-benzylidene-2-O-(phenyl-N-(isopropoxy)-(D)-alaninyl)-phosphoramidyl- α -D-glucopyranoside (3.39b)



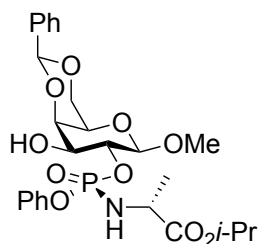
3.4a and NMI were used according to procedure B. The product was isolated by column chromatography on silica gel (2:1 hexanes/EtOAc to 1:2 hexanes/EtOAc) as an amorphous solid (26.1 mg, 47 % yield). ^1H NMR (400 MHz, CDCl_3) δ 7.52 – 7.46 (m, 2H), 7.41 – 7.27 (m, 5H), 7.28 – 7.21 (m, 3H), 7.20 – 7.12 (m, 1H), 5.54 (s, 1H), 5.03 (hept, $J = 6.2$ Hz, 1H), 4.81 (d, $J = 3.8$ Hz, 1H), 4.42 (td, $J = 9.4, 3.9$ Hz, 1H), 4.28 (dd, $J = 10.1, 4.7$ Hz, 1H), 4.19 (td, $J = 9.4, 3.6$ Hz, 1H), 4.07 (dp, $J = 9.2, 7.1$ Hz, 1H), 3.86 (td, $J = 9.8, 4.6$ Hz, 1H), 3.81 – 3.70 (m, 2H), 3.53 (t, $J = 9.4$ Hz, 1H), 3.48 – 3.39 (m, 1H), 3.36 (s, 2H), 1.36 (d, $J = 7.1$ Hz, 3H), 1.25 (d, $J = 6.2$ Hz, 3H), 1.22 (d, $J = 6.2$ Hz, 3H). ^{13}C NMR (101 MHz, CDCl_3) δ 173.59 (d, $J = 7.2$ Hz), 137.01, 129.60, 129.23, 128.31, 126.33, 125.01, 120.46 (d, $J = 4.8$ Hz), 102.02, 98.83 (d, $J = 3.7$ Hz), 81.31, 76.94, 69.62 (d, $J = 4.5$ Hz), 69.36, 68.93, 62.09, 55.56, 50.61 (d, $J = 2.0$ Hz), 21.73, 21.65, 20.74 (d, $J = 5.6$ Hz). The phenol carbon is not observed. ^{31}P NMR (162 MHz, CDCl_3) δ 3.79. IR: 3371, 2925, 2853, 1732, 1592, 1491, 1456, 1376, 1265, 1211, 1151, 1065, 1041, 994, 937, 903, 737, 699, 676 cm^{-1} . HRMS (ESI): calcd. for $\text{C}_{26}\text{H}_{34}\text{NO}_{10}\text{P} + \text{Na} = 574.1813$, found 574.1806. $[\alpha]_{\text{D}25} = 33.9^\circ$ (c 0.0021, CHCl_3).

Methyl 4,6-O-benzylidene-3-O-(phenyl-N-(isopropoxy)-(D)-alaninyl)-phosphoramidyl)- β -D-galactopyranoside (3.40a)



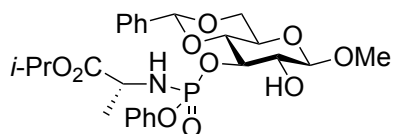
3.19a and NMI were used according to a modified procedure B. 2,6-Lutidine (0.029 mL, 0.2 mmol) and *ent*-**3.37** (61.1 mg, 0.13 mmol) were used. The product was isolated by column chromatography on silica gel (2:1 hexanes/EtOAc to 1:2 hexanes/EtOAc) as an amorphous solid (28.8 mg, 52 % yield). ^1H NMR (400 MHz, CDCl_3) δ 7.44 (dd, $J = 6.8, 2.9$ Hz, 2H), 7.30 – 7.21 (m, 5H), 7.18 (d, $J = 8.4$ Hz, 2H), 7.08 (t, $J = 7.3$ Hz, 1H), 5.48 (s, 1H), 4.94 (hept, $J = 6.3$ Hz, 1H), 4.34 (q, $J = 8.6$ Hz, 1H), 4.29 – 4.21 (m, 2H), 4.17 (d, $J = 3.7$ Hz, 1H), 4.01 (qd, $J = 6.4, 3.0$ Hz, 2H), 3.89 (dd, $J = 12.4, 9.4$ Hz, 1H), 3.78 (dd, $J = 9.3, 3.7$ Hz, 1H), 3.44 (s, 3H), 3.38 (s, 1H), 1.34 (d, $J = 7.0$ Hz, 3H), 1.15 (d, $J = 6.3$ Hz, 3H), 1.15 (d, $J = 6.3$ Hz, 3H). ^{13}C NMR (101 MHz, CDCl_3) δ 171.72 (d, $J = 9.0$ Hz), 149.86 (d, $J = 6.9$ Hz), 136.45, 128.55, 127.98, 127.05, 125.39, 123.81, 119.20 (d, $J = 5.1$ Hz), 100.87 (d, $J = 7.5$ Hz), 100.26, 76.11 (d, $J = 5.3$ Hz), 74.43, 70.84 (d, $J = 1.7$ Hz), 68.20, 67.86, 65.61, 55.92, 49.26 (d, $J = 2.1$ Hz), 20.68, 20.62, 20.11 (d, $J = 3.6$ Hz). ^{31}P NMR (162 MHz, CDCl_3) δ 4.15. IR: 3373, 3065, 2983, 2936, 1732, 1592, 1491, 1454, 1399, 1376, 1266, 1211, 1158, 1104, 1071, 1026, 1001, 940, 908, 858, 821, 759, 734, 699 cm^{-1} . HRMS (ESI): calcd. for $\text{C}_{26}\text{H}_{34}\text{NO}_{10}\text{P} + \text{Na} = 574.1813$, found 574.1802. $[\alpha]_{\text{D}25} = -31.2^\circ$ (c 0.0010, CHCl_3).

Methyl 4,6-O-benzylidene-2-O-(*R*)-(phenyl-N-(isopropoxy-(*D*)-alaninyl)-phosphoramidyl)- β -D-galactopyranoside (3.40b)



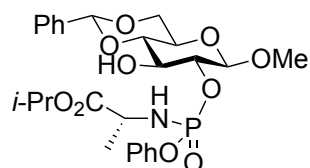
3.19a and **3.36** were used according to a modified procedure B. 2,6-Lutidine (0.029 mL, 0.2 mmol) and *ent*-**3.37** (61.1 mg, 0.13 mmol) were used. The product was isolated by column chromatography on silica gel (2:1 hexanes/EtOAc to 1:2 hexanes/EtOAc) as an amorphous solid (42.7 mg, 77 % yield). ¹H NMR (400 MHz, CDCl₃) δ 7.53 – 7.48 (m, 2H), 7.37 – 7.29 (m, 5H), 7.27 – 7.23 (m, 3H), 7.19 – 7.11 (m, 1H), 5.56 (s, 1H), 5.02 (hept, J = 6.3 Hz, 1H), 4.45 – 4.37 (m, 1H), 4.36 – 4.30 (m, 2H), 4.25 (dd, J = 3.8, 1.0 Hz, 1H), 4.19 (d, J = 5.3 Hz, 1H), 4.13 – 4.02 (m, 2H), 3.93 (dd, J = 12.4, 9.4 Hz, 1H), 3.89 – 3.82 (m, 1H), 3.52 (s, 3H), 3.46 (q, J = 1.5 Hz, 1H), 1.41 (d, J = 7.1 Hz, 3H), 1.23 (d, J = 6.3 Hz, 3H), 1.23 (d, J = 6.0 Hz, 3H). ¹³C NMR (101 MHz, CDCl₃) δ 172.74 (d, J = 9.1 Hz), 150.89 (d, J = 7.0 Hz), 137.45, 129.58, 129.02, 128.09, 126.42, 124.84, 120.22 (d, J = 5.1 Hz), 101.95, 101.91 (d, J = 7.6 Hz), 77.12 (d, J = 5.3 Hz), 75.45, 71.91 (d, J = 1.8 Hz), 69.25, 68.90, 66.66, 56.96, 50.29 (d, J = 2.1 Hz), 21.71, 21.65, 21.16 (d, J = 3.4 Hz). ³¹P NMR (162 MHz, CDCl₃) δ 4.20. IR: 3392, 2983, 1731, 1592, 1491, 1454, 1376, 1266, 1210, 1157, 1104, 1071, 1025, 1000, 938, 821, 759, 734, 698 cm⁻¹. HRMS (ESI): calcd. for C₂₆H₃₄NO₁₀P + Na = 574.1813, found 574.1785. [α]_D²⁵ = 83.3° (c 0.0018, CHCl₃).

Methyl 4,6-O-benzylidene-3-O-(phenyl-N-(isopropoxy-(D)-alaninyl)-phosphoramidyl)- β -D-glucopyranoside (3.41a)



3.7a and NMI were used according to a modified procedure B. 1,2,2-trichloroethylene (1.0 mL) was used in place of CHCl_3 . ^1H NMR (400 MHz, CDCl_3) δ 7.50 – 7.43 (m, 2H), 7.37 (q, $J = 2.8$ Hz, 3H), 7.31 – 7.23 (m, 2H), 7.23 – 7.17 (m, 2H), 7.17 – 7.09 (m, 1H), 5.55 (s, 1H), 4.94 (hept, $J = 6.3$ Hz, 1H), 4.61 (s, 1H), 4.49 – 4.32 (m, 3H), 4.04 (h, $J = 7.3$ Hz, 1H), 3.81 (dt, $J = 15.9, 10.8$ Hz, 2H), 3.67 (dt, $J = 11.7, 8.7$ Hz, 2H), 3.59 (s, 3H), 3.46 (tt, $J = 9.8, 4.7$ Hz, 1H), 1.30 (d, $J = 7.0$ Hz, 3H), 1.17 (d, $J = 6.2$ Hz, 3H), 1.14 (d, $J = 6.3$ Hz, 3H). ^{13}C NMR (101 MHz, CDCl_3) δ 172.67 (d, $J = 9.6$ Hz), 150.69 (d, $J = 7.0$ Hz), 136.99, 129.69, 129.10, 128.26, 126.10, 125.05 (d, $J = 1.4$ Hz), 120.21 (d, $J = 5.0$ Hz), 101.59, 81.51 (d, $J = 5.0$ Hz), 79.28 (d, $J = 6.9$ Hz), 76.87, 75.28, 70.19, 69.38, 68.87, 50.14 (d, $J = 2.1$ Hz), 21.61, 21.58, 20.57 (d, $J = 3.5$ Hz), 18.03. ^{31}P NMR (162 MHz, CDCl_3) δ 4.39. IR: 3372, 2983, 1732, 1592, 1491, 1455, 1377, 1266, 1212, 1151, 1095, 1069, 1025, 993, 940, 893, 734, 699 cm^{-1} . HRMS (ESI): calcd. for $\text{C}_{26}\text{H}_{34}\text{NO}_{10}\text{P} + \text{H} = 552.1993$, found 552.1975. $[\alpha]_{\text{D}}^{25} = -52.9^\circ$ (c 0.0132, CHCl_3).

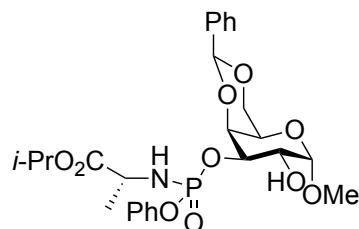
Methyl 4,6-O-benzylidene-2-O-(phenyl-N-(isopropoxy-(D)-alaninyl)-phosphoramidyl)- β -D-glucopyranoside (3.41b)



3.7a and NMI were used according to procedure B. 1,2,2-trichloroethylene (1.0 mL) was used in place of CHCl_3 . ^1H NMR (400 MHz, CDCl_3) δ 7.49 (dd, $J = 6.8, 2.8$ Hz, 2H), 7.38 – 7.29 (m, 5H), 7.23 (d, $J = 8.1$ Hz, 2H), 7.17 (t, $J = 7.4$ Hz, 1H), 5.55 (s, 1H), 5.05 (hept, $J = 6.3$ Hz, 1H), 4.40 (d, $J = 7.5$ Hz, 1H), 4.35 (dd, $J = 10.5, 5.0$ Hz, 1H), 4.07 (tdd, $J = 8.8, 5.7, 2.9$ Hz, 2H), 3.96

(t, J = 8.8 Hz, 1H), 3.90 (dd, J = 12.8, 9.4 Hz, 1H), 3.77 (t, J = 10.3 Hz, 1H), 3.60 (t, J = 9.3 Hz, 1H), 3.52 (s, 3H), 3.45 (td, J = 9.8, 5.0 Hz, 1H), 1.43 (d, J = 7.0 Hz, 3H), 1.27 (d, J = 6.3 Hz, 3H), 1.26 (d, J = 6.3 Hz, 3H). ¹³C NMR (101 MHz, CDCl₃) δ 172.71 (d, J = 9.5 Hz), 150.69 (d, J = 6.9 Hz), 136.90, 129.72, 129.13, 128.23, 126.33, 125.11, 120.10 (d, J = 5.0 Hz), 102.27 (d, J = 9.0 Hz), 101.88, 80.24, 80.18, 72.55, 69.38, 68.52, 66.09, 57.44, 50.24 (d, J = 2.0 Hz), 21.74, 21.68, 21.17 (d, J = 3.3 Hz). ³¹P NMR (162 MHz, CDCl₃) δ 4.62. IR: 3372, 2983, 1732, 1592, 1491, 1455, 1377, 1266, 1212, 1151, 1095, 1069, 1025, 993, 940, 893, 734, 699 cm⁻¹. HRMS (ESI): calcd. for C₂₆H₃₄NO₁₀P + H = 552.1993, found 552.1981. [α]_D²⁵ = -66.8° (c 0.0125, CHCl₃).

Methyl 4,6-O-benzylidene-3-O-(phenyl-N-(isopropoxy-(D)-alaninyl)-phosphoramidyl)-α-D-galactopyranoside (3.43a)

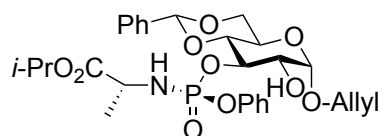


3.42 and **3.36** were used according to a modified procedure B. The product was isolated by column chromatography on silica gel (2:1 hexanes/EtOAc to 1:2 hexanes/EtOAc) as a foam (31.6 mg, 57 % yield). ¹H NMR (400 MHz, CDCl₃) δ 7.54 – 7.49 (m, 2H), 7.36 (dd, J = 5.2, 2.0 Hz, 3H), 7.32 – 7.24 (m, 3H), 7.18 – 7.11 (m, 1H), 5.56 (s, 1H), 5.01 – 4.87 (m, 3H), 4.79 – 4.70 (m, 1H), 4.48 (dd, J = 3.6, 1.1 Hz, 1H), 4.28 (dd, J = 12.4, 1.7 Hz, 1H), 4.18 (ddt, J = 11.4, 7.2, 3.6 Hz, 1H), 4.07 (dd, J = 12.5, 1.8 Hz, 1H), 4.04 – 3.94 (m, 1H), 3.73 – 3.64 (m, 2H), 3.45 (s, 3H), 2.75 (d, J = 7.9 Hz, 1H), 1.36 (d, J = 7.0 Hz, 3H), 1.18 (d, J = 6.2 Hz, 3H), 1.15 (d, J = 6.3 Hz, 3H). ¹³C NMR (101 MHz, CDCl₃) δ 172.9 (d, J = 8.7 Hz), 137.61, 129.62, 128.94, 128.12, 126.17, 120.31 (d, J = 4.8 Hz), 100.75, 100.31, 75.95 (d, J = 6.2 Hz), 75.11 (d, J = 2.7 Hz), 69.33, 69.12, 67.43 (d, J = 5.6 Hz), 62.51, 55.70, 50.44 (d, J = 1.4 Hz), 21.63, 21.57, 20.87 (d, J = 4.4 Hz). ³¹P NMR (162 MHz, CDCl₃) δ 4.38, 2.39. IR: 3394, 2986, 2923, 1731, 1638, 1592,

1491, 1456, 1405, 1376, 1345, 1211, 1149, 1104, 1045, 935, 901, 835, 767, 736, 699 cm⁻¹.

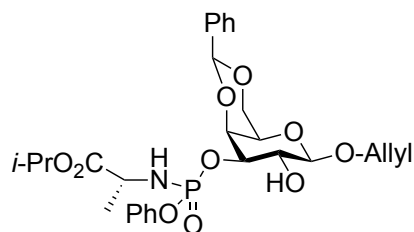
HRMS (ESI): calcd. for C₂₆H₃₄NO₁₀P + Na = 574.1813, found 574.1819. [α]_D²⁵ = -36.2° (c 0.0080, CHCl₃).

Allyl 4,6-O-benzylidene-3-O-(*R*)-(phenyl-N-(isopropoxy-(*D*)-alaninyl)-phosphoramidyl)-α-*D*-glucopyranoside (3.45a)



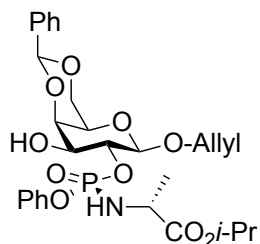
3.44 and **3.36** were used according to a modified procedure B. The product was isolated by column chromatography on silica gel (9:1 hexanes/EtOAc to 1:1 hexanes/EtOAc) as a foam (36.2 mg, 83 % yield). ¹H NMR (400 MHz, CDCl₃) δ 7.52 – 7.43 (m, 2H), 7.36 (dp, J = 4.8, 1.7 Hz, 3H), 7.25 – 7.18 (m, 4H), 7.13 – 7.07 (m, 1H), 5.93 (dddd, J = 16.8, 10.3, 6.2, 5.4 Hz, 1H), 5.54 (s, 1H), 5.34 (dd, J = 17.2, 1.6 Hz, 1H), 5.24 (dd, J = 10.4, 1.4 Hz, 1H), 4.99 (d, J = 3.8 Hz, 1H), 4.94 (h, J = 6.3 Hz, 1H), 4.66 (q, J = 8.9 Hz, 1H), 4.30 (dd, J = 10.3, 4.8 Hz, 1H), 4.23 (ddt, J = 12.8, 5.4, 1.4 Hz, 1H), 4.12 – 3.96 (m, 2H), 3.91 (td, J = 9.9, 4.8 Hz, 1H), 3.81 (ddd, J = 11.5, 9.3, 3.4 Hz, 2H), 3.75 (t, J = 10.3 Hz, 1H), 3.65 (t, J = 9.4 Hz, 1H), 1.25 (d, J = 7.0 Hz, 3H), 1.18 (d, J = 6.25 Hz, 3H), 1.17 (d, J = 6.3 Hz, 3H). ¹³C NMR (101 MHz, CDCl₃) δ 172.89 (d, J = 8.3 Hz), 150.89 (d, J = 7.2 Hz), 136.84, 133.28, 129.51, 129.18, 128.29, 126.24, 124.76, 120.31 (d, J = 5.1 Hz), 118.34, 101.84, 98.18, 79.48 (d, J = 5.1 Hz), 77.81 (d, J = 5.6 Hz), 71.91 (d, J = 2.1 Hz), 69.08, 69.03, 68.89, 62.52, 50.20 (d, J = 2.2 Hz), 21.66, 21.60, 20.61 (d, J = 4.5 Hz). ³¹P NMR (162 MHz, CDCl₃) δ 3.45. IR: 3395, 2984, 2921, 2852, 1732, 1634, 1592, 1492, 1455, 1376, 1262, 1212, 1155, 1105, 1073, 1038, 1027, 1000, 939, 820, 760, 736, 699, 669 cm⁻¹. HRMS (ESI): calcd. for C₂₈H₃₆NO₁₀P + Na = 600.1969, found 600.1968. [α]_D²⁵ = 20.0° (c 0.0008, CHCl₃).

Allyl 4,6-O-benzylidene-3-O-(phenyl-N-(isopropoxy)-(D)-alaninyl)-phosphoramidyl)- β -D-galactopyranoside (3.47a)



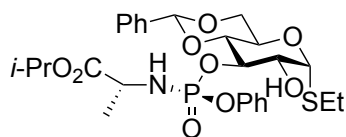
3.46 and NMI were used according to a modified procedure B. The product was isolated by column chromatography on silica gel (9:1 hexanes/EtOAc to 1:1 hexanes/EtOAc) as an amorphous solid (25.1 mg, 44 % yield). ^1H NMR (400 MHz, CDCl_3) δ 7.46 (dd, $J = 6.7, 2.9$ Hz, 2H), 7.38 – 7.32 (m, 3H), 7.20 (dt, $J = 8.1, 1.3$ Hz, 2H), 7.13 (t, $J = 7.8$ Hz, 2H), 7.08 – 7.03 (m, 1H), 5.95 (dddd, $J = 17.0, 10.4, 6.4, 5.3$ Hz, 1H), 5.45 (s, 1H), 5.32 (dd, $J = 17.2, 1.6$ Hz, 1H), 5.25 – 5.20 (m, 1H), 5.02 (hept, $J = 6.3$ Hz, 1H), 4.51 (td, $J = 9.6, 3.7$ Hz, 1H), 4.44 (ddt, $J = 12.7, 5.3, 1.4$ Hz, 1H), 4.39 (d, $J = 7.8$ Hz, 1H), 4.33 – 4.25 (m, 2H), 4.17 – 3.98 (m, 4H), 3.80 (t, $J = 10.1$ Hz, 1H), 3.44 (d, $J = 1.5$ Hz, 1H), 2.82 (s, 1H), 1.38 (d, $J = 7.1$ Hz, 3H), 1.24 (d, $J = 6.4$ Hz, 3H), 1.22 (d, $J = 6.4$ Hz, 3H). ^{13}C NMR (101 MHz, CDCl_3) δ 173.50 (d, $J = 7.0$ Hz), 150.76 (d, $J = 7.6$ Hz), 137.59, 133.76, 129.46, 128.90, 128.06, 126.28, 124.83, 120.47 (d, $J = 4.8$ Hz), 118.00, 101.76, 100.85, 77.15 (d, $J = 5.4$ Hz), 74.84 (d, $J = 1.7$ Hz), 70.16, 69.58 (d, $J = 5.3$ Hz), 69.14, 68.93, 66.30, 50.45, 21.74, 21.67, 20.77 (d, $J = 6.0$ Hz). ^{31}P NMR (162 MHz, CDCl_3) δ 3.75. IR: 3334, 2981, 2926, 2869, 1736, 1590, 1489, 1456, 1405, 1369, 1266, 1246, 1211, 1180, 1157, 1095, 1079, 1042, 998, 945, 922, 841, 818, 769, 740, 702, 693 cm^{-1} . HRMS (ESI): calcd. for $\text{C}_{28}\text{H}_{36}\text{NO}_{10}\text{P} + \text{Na} = 600.1969$, found 600.1955. $[\alpha]_{\text{D}}^{25} = 32.5^\circ$ (c 0.0008, CHCl_3).

Allyl 4,6-O-benzylidene-2-O-(*R*)-(phenyl-N-(isopropoxy-(*D*)-alaninyl)-phosphoramidyl)- β -D-galactopyranoside (3.47b)



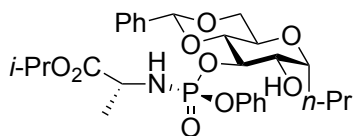
3.46 and **3.36** were used according to a modified procedure B. The product was isolated by column chromatography on silica gel (9:1 hexanes/EtOAc to 1:1 hexanes/EtOAc) as an amorphous solid (34.3 mg, 60 % yield). $^1\text{H NMR}$ (400 MHz, CDCl_3) δ 7.55 – 7.47 (m, 2H), 7.37 – 7.27 (m, 5H), 7.28 – 7.20 (m, 2H), 7.18 – 7.12 (m, 1H), 5.89 (dddd, $J = 17.0, 10.4, 6.5, 5.2$ Hz, 1H), 5.56 (s, 1H), 5.34 – 5.26 (m, 1H), 5.21 (dq, $J = 10.4, 1.3$ Hz, 1H), 5.01 (hept, $J = 6.3$ Hz, 1H), 4.50 – 4.42 (m, 2H), 4.39 (ddt, $J = 12.7, 5.2, 1.5$ Hz, 1H), 4.32 (dd, $J = 12.4, 1.6$ Hz, 1H), 4.28 – 4.20 (m, 2H), 4.15 – 4.05 (m, 3H), 3.92 (dd, $J = 12.1, 9.3$ Hz, 1H), 3.86 (dt, $J = 8.7, 4.5$ Hz, 1H), 3.45 (q, $J = 1.5$ Hz, 1H), 1.41 (d, $J = 7.0$ Hz, 3H), 1.22 (d, $J = 6.4$ Hz, 3H), 1.22 (d, $J = 6.3$ Hz, 3H). $^{13}\text{C NMR}$ (101 MHz, CDCl_3) δ 172.76 (d, $J = 8.8$ Hz), 150.89 (d, $J = 7.2$ Hz), 137.45, 133.69, 129.58, 129.02, 128.09, 126.40, 124.86, 120.32 (d, $J = 5.1$ Hz), 118.12, 101.29, 99.62 (d, $J = 7.9$ Hz), 77.19 (d, $J = 5.7$ Hz), 75.46, 71.96 (d, $J = 1.5$ Hz), 70.07, 69.22, 68.91, 66.69, 50.29 (d, $J = 2.3$ Hz), 21.70, 21.65, 21.06 (d, $J = 3.7$ Hz). $^{31}\text{P NMR}$ (162 MHz, CDCl_3) δ 4.17. IR: 3375, 3065, 2984, 2923, 1732, 1648, 1592, 1491, 1455, 1405, 1375, 1266, 1211, 1157, 1103, 1070, 1025, 998, 936, 911, 859, 821, 759, 734, 698 cm^{-1} . HRMS (ESI): calcd. for $\text{C}_{28}\text{H}_{36}\text{NO}_{10}\text{P} + \text{Na} = 600.1969$, found 600.1953. $[\alpha]_{\text{D}25} = -33.8$ (c 0.0079, CHCl_3).

S-Ethyl 4,6-O-benzylidene-3-O-(*R*)-(phenyl-N-(isopropoxy-(*D*)-alaninyl)-phosphoramidyl)- α -D-glucopyranoside (3.49a)



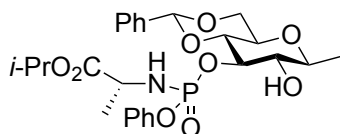
3.48 and **3.36** were used according to a modified procedure B. The product was isolated by column chromatography on silica gel (9:1 hexanes/EtOAc to 1:1 hexanes/EtOAc) as a crystalline solid (38.9 mg, 67 % yield). ¹H NMR (400 MHz, CDCl₃) δ 7.48 (dd, *J* = 6.7, 3.0 Hz, 2H), 7.37 (q, *J* = 2.8 Hz, 3H), 7.29 – 7.23 (m, 2H), 7.20 (dt, *J* = 8.6, 1.3 Hz, 2H), 7.13 (td, *J* = 7.4, 1.2 Hz, 1H), 5.55 (s, 1H), 5.50 (d, *J* = 5.7 Hz, 1H), 4.96 (hept, *J* = 6.3 Hz, 1H), 4.67 (s, 1H), 4.50 (td, *J* = 9.1, 7.2 Hz, 1H), 4.35 – 4.25 (m, 2H), 4.12 (dd, *J* = 9.1, 5.7 Hz, 1H), 4.04 (dt, *J* = 8.6, 7.3 Hz, 1H), 3.83 – 3.73 (m, 2H), 3.66 (t, *J* = 9.3 Hz, 1H), 2.71 – 2.53 (m, 2H), 1.33 – 1.27 (m, 6H), 1.18 (d, *J* = 6.3 Hz, 3H), 1.17 (d, *J* = 6.3 Hz, 3H). ¹³C NMR (101 MHz, CDCl₃) δ 172.70 (d, *J* = 9.1 Hz), 150.69 (d, *J* = 7.1 Hz), 136.86, 129.62, 129.18, 128.28, 126.20, 124.98, 120.25 (d, *J* = 5.0 Hz), 101.86, 85.85, 79.36 (d, *J* = 6.2 Hz), 78.53 (d, *J* = 5.4 Hz), 71.66 (d, *J* = 1.6 Hz), 69.29, 68.81, 62.89, 50.27 (d, *J* = 2.1 Hz), 24.57, 21.65, 21.60, 20.64 (d, *J* = 3.9 Hz), 14.82. ³¹P NMR (162 MHz, CDCl₃) δ 4.25. IR: 3346, 2983, 2934, 1732, 1593, 1491, 1455, 1376, 1266, 1210, 1151, 1107, 1071, 1049, 1028, 996, 938, 897, 816, 734, 699 cm⁻¹. HRMS (ESI): calcd. for C₂₇H₃₆NO₉SP + Na = 604.1741, found 604.1730. [α]_D²⁵ = 86.6° (c 0.0090, CHCl₃). Melting point: Decomposes into a brown syrup at 140 °C.

C-Propyl 4,6-O-benzylidene-3-O-(*R*)-(phenyl-N-(isopropoxy-(*D*)-alaninyl)-phosphoramidyl)- α -D-glucopyranoside (3.51a)



3.50 and **3.36** were used according to a modified procedure B. The product was isolated by column chromatography on silica gel (9:1 hexanes/EtOAc to 1:1 hexanes/EtOAc) as a crystalline solid (43.2 mg, 77 % yield). $^1\text{H NMR}$ (400 MHz, CDCl_3) δ 7.50 – 7.44 (m, 2H), 7.37 (dt, $J = 4.6$, 2.9 Hz, 3H), 7.31 – 7.25 (m, 3H), 7.21 (dt, $J = 8.7$, 1.3 Hz, 2H), 7.15 (td, $J = 7.3$, 1.1 Hz, 1H), 5.54 (s, 1H), 4.95 (hept, $J = 6.3$ Hz, 1H), 4.60 (s, 1H), 4.47 (td, $J = 8.7$, 6.7 Hz, 1H), 4.28 (dd, $J = 10.2$, 3.8 Hz, 1H), 3.80 (dd, $J = 11.9$, 8.5 Hz, 1H), 3.73 – 3.66 (m, 1H), 3.63 – 3.54 (m, 2H), 1.80 (dtd, $J = 14.2$, 6.5, 3.3 Hz, 1H), 1.66 (dddd, $J = 14.6$, 11.5, 9.5, 4.8 Hz, 1H), 1.54 – 1.41 (m, 1H), 1.31 (d, $J = 7.1$ Hz, 4H), 1.17 (d, $J = 6.3$ Hz, 3H), 1.14 (d, $J = 6.3$ Hz, 3H), 0.96 (t, $J = 7.4$ Hz, 3H). $^{13}\text{C NMR}$ (101 MHz, CDCl_3) δ 172.72 (d, $J = 9.3$ Hz), 150.70 (d, $J = 7.0$ Hz), 136.98, 129.67, 129.09, 128.27, 126.11, 125.04 (d, $J = 1.3$ Hz), 120.25 (d, $J = 5.0$ Hz), 101.72, 80.09 (d, $J = 6.3$ Hz), 78.91 (d, $J = 5.4$ Hz), 76.80, 71.60 (d, $J = 1.4$ Hz), 69.43, 69.35, 63.20, 50.20 (d, $J = 2.0$ Hz), 26.63, 21.61, 21.58, 20.54 (d, $J = 3.8$ Hz), 18.50, 13.82. $^{31}\text{P NMR}$ (162 MHz, CDCl_3) δ 4.56. IR: 3358, 2929, 2873, 1732, 1593, 1491, 1456, 1377, 1265, 1210, 1151, 1107, 1076, 1055, 1024, 994, 940, 901, 816, 735, 699 cm^{-1} . HRMS (ESI): calcd. for $\text{C}_{28}\text{H}_{38}\text{NO}_9\text{P} + \text{Na} = 586.2176$, found 586.2161. $[\alpha]_{\text{D}25} = -15.2^\circ$ (c 0.0129, CHCl_3). Melting point: 107-119 $^\circ\text{C}$.

C-Methyl 4,6-O-benzylidene-3-O-(phenyl-N-(isopropoxy)-(D)-alaninyl)-phosphoramidyl)- β -D-glucopyranoside (3.52a)



3.10 and **3.36** were used according to a modified procedure B. The product was isolated by column chromatography on silica gel (4:1 hexanes/EtOAc to 1:1 hexanes/EtOAc) as an amorphous solid (42.8 mg, 80 % yield). ^1H NMR (400 MHz, CDCl_3) δ 7.47 (dd, $J = 6.6, 3.1$ Hz, 2H), 7.37 (dd, $J = 5.0, 2.0$ Hz, 3H), 7.30 (dd, $J = 8.5, 7.2$ Hz, 2H), 7.25 – 7.20 (m, 2H), 7.19 – 7.13 (m, 1H), 5.54 (s, 1H), 4.95 (hept, $J = 6.3$ Hz, 1H), 4.83 (s, 1H), 4.40 – 4.26 (m, 2H), 4.07 (h, $J = 7.3$ Hz, 1H), 3.77 (dd, $J = 11.8, 8.4$ Hz, 1H), 3.68 (dt, $J = 19.0, 9.8$ Hz, 2H), 3.57 – 3.40 (m, 3H), 1.35 (d, $J = 5.7$ Hz, 3H), 1.32 (d, $J = 7.1$ Hz, 3H), 1.16 (d, $J = 6.2$ Hz, 3H), 1.14 (d, $J = 6.3$ Hz, 3H). ^{13}C NMR (101 MHz, CDCl_3) δ 172.67 (d, $J = 9.6$ Hz), 150.69 (d, $J = 7.0$ Hz), 136.99, 129.69, 129.10, 128.26, 126.10, 125.05 (d, $J = 1.4$ Hz), 120.21 (d, $J = 5.0$ Hz), 101.59, 81.51 (d, $J = 5.0$ Hz), 79.28 (d, $J = 6.9$ Hz), 76.87, 75.28, 70.19, 69.38, 68.87, 50.14 (d, $J = 2.1$ Hz), 21.61, 21.58, 20.57 (d, $J = 3.5$ Hz), 18.03. ^{31}P NMR (162 MHz, CDCl_3) δ 5.03. IR: 3370, 2982, 2935, 2876, 1732, 1638, 1592, 1491, 1454, 1377, 1298, 1253, 1211, 1149, 1104, 1071, 1020, 940, 895, 841, 759, 737, 699 cm^{-1} . HRMS (ESI): calcd. for $\text{C}_{26}\text{H}_{34}\text{NO}_9\text{P} + \text{Na} = 558.1863$, found 558.1851. $[\alpha]_{\text{D}25} = -701.5^\circ$ (c 0.0012, CHCl_3).

Supporting Information for DFT Calculations

All DFT calculations were performed with Gaussian 09.^[7] The transition state geometries were optimized using the M06-2X^[8,9] density functional and the 6-31G(d) basis set in the gas phase. The “ultrafine” integration grid in Gaussian was used. Single-point energies were calculated using M06-2X with the 6-311++G(d,p) basis set and include solvation energy corrections calculated using the SMD^[10] model. Chloroform was used as the solvent in the solvation energy calculations. The Gibbs free energies reported include zero-point vibrational energies and thermal cor-

rections computed at 298K. The entropic contributions to the Gibbs free energies were calculated from partition functions using Cramer and Truhlar's quasiharmonic approximation,^[11] which raises vibrational frequencies lower than 100 cm⁻¹ to 100 cm⁻¹ as a way to correct the harmonic oscillator model for low-frequency vibrational modes.

3.5b-TS1

M06-2X/6-31G(d) SCF energy:	-2310.64887892 a.u.
M06-2X/6-31G(d) enthalpy:	-2309.973842 a.u.
M06-2X/6-31G(d) free energy:	-2310.083135 a.u.
M06-2X/6-311++G(d,p) SCF energy in solution:	-2311.28469257 a.u.
M06-2X/6-311++G(d,p) enthalpy in solution:	-2310.609656 a.u.
M06-2X/6-311++G(d,p) free energy in solution:	-2310.718949 a.u.
Three lowest frequencies (cm ⁻¹):	-593.5833 21.6919 30.6410
Imaginary frequency:	-593.5833 cm ⁻¹

Cartesian coordinates

ATOM	X	Y	Z
C	0.701866	-0.754675	1.680167
C	0.994593	-2.217803	1.958533
H	1.049948	-2.756887	1.008194
O	0.421495	0.056375	2.555987
N	1.537990	-0.169617	0.573450
C	1.775912	1.118126	0.537516
N	2.170622	1.554624	-0.668607
C	1.990924	0.500539	-1.668753
C	1.785025	-0.759368	-0.774689
H	0.884867	-1.299622	-1.070455
H	1.104791	0.723179	-2.270249
H	2.875281	0.408886	-2.302580
H	-3.206632	-2.817037	0.092079
O	-2.586754	-3.729712	-1.223840
C	-1.362742	-3.775481	-1.334555
C	-0.716845	-4.822629	-2.224840
O	-0.514590	-2.993379	-0.747529
S	1.708636	2.358673	1.738596
C	2.457949	2.911242	-0.735017
C	2.289830	3.514664	0.519560
C	2.516237	4.875134	0.679366
H	2.380568	5.350624	1.645257
C	2.855363	3.642629	-1.847890
H	2.978476	3.162778	-2.813364
C	3.083574	5.004819	-1.677040
H	3.393429	5.600706	-2.528742
C	2.919490	5.614098	-0.430755
H	3.104251	6.677247	-0.323465
H	-0.087657	-4.333614	-2.974229
H	-1.479648	-5.426588	-2.714759
H	-0.070180	-5.463719	-1.617997
O	-3.359958	-2.119210	0.769050

C	-3.095156	-0.893029	0.152309
C	-4.278630	0.047422	0.259041
C	-1.884325	-0.254159	0.850026
H	-2.858911	-1.027162	-0.915066
C	-3.887706	1.435971	-0.234802
H	-4.581479	0.120245	1.318929
O	-5.363678	-0.419655	-0.519084
C	-1.664044	1.230107	0.509459
H	-2.072389	-0.297100	1.933732
O	-0.741419	-0.994863	0.533087
C	-5.107509	2.341426	-0.157407
H	-3.561569	1.357484	-1.282247
O	-2.857298	1.971780	0.576002
H	-1.011577	1.694220	1.259310
O	-1.057617	1.326021	-0.762186
H	-0.836276	-2.006509	-0.039124
H	-5.388282	2.476197	0.899926
H	-4.916026	3.322305	-0.598909
O	-6.162417	1.744276	-0.887647
C	-0.884931	2.669218	-1.163373
H	-0.239561	2.665591	-2.046563
H	-1.839036	3.143439	-1.416983
H	-0.407046	3.263565	-0.369809
C	2.980029	-1.685890	-0.754992
C	2.803047	-3.045703	-1.004830
C	4.257440	-1.193372	-0.472348
C	3.898208	-3.907551	-0.969910
H	1.799031	-3.417570	-1.198929
C	5.348057	-2.054389	-0.436287
H	4.399314	-0.133104	-0.266286
C	5.168014	-3.414856	-0.685997
H	3.755415	-4.966648	-1.160358
H	6.336940	-1.667743	-0.210732
H	6.018938	-4.088167	-0.655634
C	2.342043	-2.305350	2.682323
H	2.297111	-1.752312	3.625954
H	2.577117	-3.350416	2.903871
H	3.159203	-1.898249	2.076841
C	-0.138510	-2.801711	2.800243
H	-1.088769	-2.772682	2.259458
H	0.087376	-3.841135	3.055849
H	-0.247608	-2.231192	3.727509
C	-6.449158	0.453841	-0.411737
H	-7.248483	0.056900	-1.036542
H	-6.769755	0.517598	0.644020

3.5b-TS2

M06-2X/6-31G(d) SCF energy:	-2310.65850567 a.u.
M06-2X/6-31G(d) enthalpy:	-2309.982878 a.u.
M06-2X/6-31G(d) free energy:	-2310.094211 a.u.
M06-2X/6-311++G(d,p) SCF energy in solution:	-2311.29169398 a.u.
M06-2X/6-311++G(d,p) enthalpy in solution:	-2310.616066 a.u.
M06-2X/6-311++G(d,p) free energy in solution:	-2310.727399 a.u.
Three lowest frequencies (cm ⁻¹):	-415.5581 14.0899 20.5836

Imaginary frequency:

-415.5581 cm-1

Cartesian coordinates

ATOM	X	Y	Z
O	-0.011266	-1.507433	0.432804
C	1.296550	-1.093676	0.627995
C	2.179826	-2.221972	1.161527
C	1.888539	-0.470149	-0.643048
H	1.307522	-0.320757	1.412567
H	1.822538	-2.553621	2.146648
O	3.504088	-1.765292	1.383950
O	2.136249	-3.270714	0.243064
H	1.933585	-1.229956	-1.436651
C	3.301373	-0.036116	-0.321410
O	1.088301	0.615908	-1.059173
C	4.090893	-1.236447	0.211288
C	2.791229	-4.434448	0.698961
H	3.266175	0.745280	0.460920
O	3.971398	0.468168	-1.461634
C	5.507830	-0.777371	0.518319
H	4.128211	-1.994600	-0.583502
H	2.643562	-5.202534	-0.061366
H	3.863728	-4.259347	0.843160
H	2.359185	-4.776602	1.649686
H	6.150579	-1.612594	0.804184
H	5.483396	-0.047868	1.344273
O	6.060720	-0.195785	-0.649918
C	-1.204122	-0.690057	1.714072
C	-2.159442	-1.868458	1.773654
H	-2.452265	-2.137083	0.753399
O	-0.544535	-0.309074	2.672222
N	-1.612172	0.405062	0.794049
C	-0.943504	1.546282	0.823571
N	-1.112563	2.291422	-0.269821
C	-1.847938	1.556956	-1.294693
C	-2.209021	0.230139	-0.558178
H	-2.740567	2.112028	-1.594184
H	-1.213007	1.373741	-2.165476
S	0.106686	2.252123	1.993899
C	-0.362211	3.458431	-0.302099
C	0.354271	3.618139	0.890225
C	1.159881	4.732854	1.081307
H	1.720762	4.861844	2.001237
C	-0.292044	4.393990	-1.326825
H	-0.846552	4.252190	-2.248493
C	0.521094	5.504809	-1.129603
H	0.601708	6.248687	-1.914907
C	1.235219	5.675698	0.059481
H	1.861341	6.551764	0.188837
C	-1.457863	-3.060094	2.421945
H	-1.051395	-2.766805	3.394621
H	-2.171929	-3.875179	2.573808
H	-0.641419	-3.411822	1.788316
C	-3.393287	-1.453478	2.583440

H	-3.898070	-0.582501	2.155638
H	-4.112142	-2.277522	2.615764
H	-3.095914	-1.211671	3.608902
H	-1.680849	-0.598017	-1.027376
C	-3.693855	-0.037804	-0.521323
C	-4.574325	0.899966	0.023558
C	-4.194167	-1.230970	-1.037894
C	-5.939570	0.641800	0.060819
H	-4.184451	1.827997	0.439118
C	-5.563039	-1.490300	-1.003888
H	-3.501982	-1.962512	-1.450664
C	-6.435215	-0.556244	-0.453633
H	-6.617535	1.370509	0.493889
H	-5.945409	-2.424073	-1.403677
H	-7.501003	-0.759523	-0.422887
C	-0.631618	-2.077229	-2.693458
O	-0.673445	-2.700925	-1.561625
C	-0.958592	-2.947055	-3.887710
H	-1.870896	-3.517003	-3.696296
H	-1.066343	-2.336646	-4.783397
H	-0.148796	-3.668479	-4.029080
O	-0.363869	-0.878716	-2.844998
H	-0.294462	-2.122064	-0.641540
H	0.525485	0.230976	-1.762013
C	5.270292	0.861131	-1.122565
H	5.224382	1.655472	-0.354347
H	5.744738	1.229879	-2.031623

3.6b-TS1

M06-2X/6-31G(d) SCF energy:	-2310.65307200 a.u.
M06-2X/6-31G(d) enthalpy:	-2309.977854 a.u.
M06-2X/6-31G(d) free energy:	-2310.088899 a.u.
M06-2X/6-311++G(d,p) SCF energy in solution:	-2311.28889055 a.u.
M06-2X/6-311++G(d,p) enthalpy in solution:	-2310.613673 a.u.
M06-2X/6-311++G(d,p) free energy in solution:	-2310.724718 a.u.
Three lowest frequencies (cm-1):	-487.1530 18.1379 20.8720
Imaginary frequency:	-487.1530 cm-1

Cartesian coordinates

ATOM	X	Y	Z
C	-1.025247	0.235367	1.549500
C	-2.359589	0.938629	1.689920
H	-2.769973	1.114246	0.690482
O	-0.190155	0.181402	2.435330
N	-1.019963	-0.951001	0.647829
C	-0.055369	-1.837563	0.764671
N	0.015129	-2.684568	-0.271032
C	-0.836372	-2.228211	-1.365477
C	-1.641885	-1.063976	-0.703216
H	-1.443428	-0.119225	-1.212587
H	-0.211355	-1.875455	-2.190892
H	-1.491936	-3.030837	-1.710608
S	1.143658	-2.103819	1.972914
C	1.050075	-3.607513	-0.196179

C	1.766404	-3.450656	0.997610
C	2.845450	-4.278631	1.278267
H	3.409682	-4.161150	2.197639
C	1.386053	-4.582455	-1.128733
H	0.819922	-4.691752	-2.048346
C	2.472145	-5.403266	-0.840387
H	2.761707	-6.169125	-1.551798
C	3.191622	-5.255879	0.348177
H	4.034309	-5.907874	0.550162
C	-3.126901	-1.335257	-0.648589
C	-4.020357	-0.387608	-1.144361
C	-3.610710	-2.527222	-0.102817
C	-5.392220	-0.628928	-1.084795
H	-3.630937	0.543187	-1.553744
C	-4.978567	-2.765932	-0.043103
H	-2.913624	-3.262796	0.296877
C	-5.871555	-1.813668	-0.534713
H	-6.086152	0.113472	-1.466639
H	-5.349874	-3.689530	0.389651
H	-6.940233	-1.997702	-0.486048
C	-3.309712	0.042904	2.494811
H	-2.885072	-0.152189	3.485037
H	-4.267722	0.554116	2.628847
H	-3.504953	-0.914659	2.003867
C	-2.139391	2.271975	2.400358
H	-1.367891	2.854534	1.897006
H	-3.071523	2.844215	2.416609
H	-1.816095	2.095930	3.430419
C	2.691399	3.566943	0.007588
C	0.972136	1.724348	0.153494
C	1.197705	3.241353	-0.019667
H	2.857811	4.626072	-0.230287
H	1.365801	1.417896	1.136537
H	0.839528	3.513611	-1.027057
C	4.030787	0.755753	-1.951380
H	5.106289	0.910890	-1.847406
H	3.706648	1.140069	-2.931560
C	1.774791	1.051129	-0.954330
H	1.385850	1.397304	-1.930015
C	3.247263	1.450992	-0.851020
H	3.626623	1.120061	0.125823
O	3.386147	2.848616	-1.003805
O	3.182882	3.263767	1.272538
C	4.512855	3.691155	1.466970
H	4.772736	3.460353	2.500862
H	5.203992	3.175317	0.789390
H	4.602507	4.773873	1.304009
O	3.793702	-0.641740	-1.860341
O	1.670106	-0.373156	-0.916221
O	0.548347	4.002547	0.952576
H	-0.350505	4.171404	0.602384
C	-2.377219	3.511318	-1.204291
O	-1.979338	2.293219	-1.434605
O	-1.836507	4.296255	-0.431272

O	-0.374487	1.400561	0.095508
H	-1.129673	1.963013	-0.696299
C	-3.617598	3.908291	-1.979112
H	-4.470412	3.331145	-1.606873
H	-3.816894	4.971887	-1.854189
H	-3.490584	3.663827	-3.036428
C	2.434531	-0.933283	-1.955761
H	2.042805	-0.568029	-2.924442
H	2.339194	-2.018417	-1.882848

3.6b-TS2

M06-2X/6-31G(d) SCF energy:	-2310.65745944 a.u.
M06-2X/6-31G(d) enthalpy:	-2309.980375 a.u.
M06-2X/6-31G(d) free energy:	-2310.091426 a.u.
M06-2X/6-311++G(d,p) SCF energy in solution:	-2311.28780440 a.u.
M06-2X/6-311++G(d,p) enthalpy in solution:	-2310.610720 a.u.
M06-2X/6-311++G(d,p) free energy in solution:	-2310.721771 a.u.
Three lowest frequencies (cm-1):	-190.7629 13.8942 20.4757
Imaginary frequency:	-190.7629 cm-1

Cartesian coordinates

ATOM	X	Y	Z
O	-0.422039	0.111534	2.074086
C	-1.397492	-0.787749	1.609114
C	-2.776984	-0.154897	1.755327
C	-1.169828	-1.196212	0.144170
H	-1.397062	-1.696745	2.231557
H	-2.997446	0.074190	2.806741
O	-3.786086	-1.059016	1.353912
O	-2.778822	1.021202	0.997277
H	-1.368439	-0.326326	-0.494983
C	-2.260706	-2.206307	-0.178195
O	0.126012	-1.622075	-0.078431
C	-3.618635	-1.522837	0.023221
C	-3.953424	1.785855	1.169094
H	-2.185016	-3.070930	0.509076
O	-2.187141	-2.662897	-1.512045
C	-4.713032	-2.525599	-0.306398
H	-3.676875	-0.687182	-0.688689
H	-3.810962	2.715657	0.615191
H	-4.833662	1.255892	0.787809
H	-4.114114	2.019284	2.230655
H	-5.704973	-2.068984	-0.282210
H	-4.683290	-3.351485	0.422987
O	-4.498451	-3.005719	-1.621458
C	0.863846	-0.718176	-1.556682
C	2.015925	-1.685248	-1.764319
H	2.543990	-1.817704	-0.812064
O	0.001019	-0.510653	-2.399164
N	1.209110	0.519291	-0.770140
C	0.345137	1.518402	-0.766103
N	0.507586	2.362743	0.255215
C	1.577975	1.918449	1.142888
C	2.061337	0.603474	0.446684

H	2.371835	2.670316	1.172739
H	1.177768	1.739469	2.140875
S	-0.930959	1.966711	-1.842854
C	-0.394608	3.414226	0.296064
C	-1.253042	3.371681	-0.811086
C	-2.228761	4.346032	-0.978161
H	-2.896469	4.320350	-1.833610
C	-0.492739	4.412632	1.257378
H	0.173394	4.425917	2.113574
C	-1.477472	5.380318	1.085299
H	-1.579727	6.169478	1.822538
C	-2.332044	5.352747	-0.020103
H	-3.087531	6.122514	-0.135305
C	1.457958	-3.027794	-2.235435
H	0.868847	-2.878512	-3.144766
H	2.280151	-3.716024	-2.454494
H	0.806361	-3.469070	-1.480897
C	2.964389	-1.100782	-2.816002
H	3.364044	-0.126528	-2.522245
H	3.808880	-1.777925	-2.975479
H	2.429525	-0.983770	-3.763865
H	1.826354	-0.268112	1.058688
C	3.538519	0.634832	0.134465
C	4.073857	1.608569	-0.712426
C	4.383521	-0.301593	0.725617
C	5.437757	1.633879	-0.978493
H	3.413275	2.335553	-1.182667
C	5.751967	-0.275931	0.461663
H	3.959930	-1.044139	1.398334
C	6.278842	0.688003	-0.391935
H	5.846103	2.386504	-1.645684
H	6.404639	-1.010560	0.922684
H	7.343779	0.705698	-0.601422
C	1.647532	-2.847449	2.422328
O	1.624997	-1.657488	2.753120
C	2.372167	-3.875479	3.259699
H	1.689419	-4.692148	3.506062
H	3.191012	-4.302927	2.674352
H	2.760102	-3.417092	4.168232
O	1.090791	-3.337663	1.359364
H	0.325509	-0.452070	2.364405
H	0.634368	-2.562766	0.733836
C	-3.220607	-3.569925	-1.766379
H	-3.128994	-3.880987	-2.806426
H	-3.126623	-4.436980	-1.086450

3.30-TS1

M06-2X/6-31G(d) SCF energy:	-2197.35797291 a.u.
M06-2X/6-31G(d) enthalpy:	-2196.696348 a.u.
M06-2X/6-31G(d) free energy:	-2196.807295 a.u.
M06-2X/6-311++G(d,p) SCF energy in solution:	-2197.95640081 a.u.
M06-2X/6-311++G(d,p) enthalpy in solution:	-2197.294776 a.u.
M06-2X/6-311++G(d,p) free energy in solution:	-2197.405723 a.u.
Three lowest frequencies (cm ⁻¹):	-365.4585 14.8002 22.3573

Imaginary frequency:

-365.4585 cm-1

Cartesian coordinates

ATOM	X	Y	Z
C	-0.716776	3.656974	-0.905491
C	-1.549366	3.285510	0.157603
C	-2.047203	4.220498	1.056221
C	-1.688746	5.551412	0.866918
C	-0.863991	5.932687	-0.194163
C	-0.369340	4.988249	-1.090631
C	-1.122992	1.246927	-0.808086
H	-2.686667	3.916059	1.878221
H	-2.057258	6.303042	1.556782
H	-0.600347	6.976987	-0.321626
H	0.277386	5.284062	-1.910315
C	-2.355966	0.999224	1.121098
H	-1.856115	1.111208	2.087288
H	-3.428275	1.175755	1.235534
C	-2.066095	-0.392934	0.476530
H	-1.406542	-0.967225	1.125971
N	-1.290851	-0.058396	-0.745976
N	-1.786194	1.918001	0.140114
S	-0.201322	2.253405	-1.862174
C	-0.313223	-0.949284	-1.466656
O	0.293701	-0.362765	-2.354672
C	-0.771159	-2.393249	-1.585170
H	-1.157384	-2.721669	-0.613354
C	-3.323520	-1.174187	0.177762
C	-3.485987	-2.456597	0.696083
C	-4.329680	-0.620896	-0.618043
C	-4.639656	-3.186410	0.415306
H	-2.696233	-2.886453	1.309089
C	-5.480112	-1.347534	-0.900770
H	-4.199754	0.376795	-1.034876
C	-5.635268	-2.633854	-0.384037
H	-4.756577	-4.187438	0.818090
H	-6.253848	-0.915360	-1.527460
H	-6.532016	-3.203250	-0.607127
C	0.410994	-3.275817	-1.979249
H	0.059212	-4.287377	-2.205690
H	0.903346	-2.861139	-2.863754
H	1.145089	-3.312844	-1.174548
C	-1.879471	-2.463470	-2.641037
H	-2.256838	-3.487466	-2.719655
H	-2.724214	-1.809896	-2.404614
H	-1.475033	-2.165577	-3.613531
O	0.802003	-1.191665	0.009534
C	1.901771	-0.337953	-0.016354
H	0.550984	-1.794537	1.114261
C	3.227990	-1.086668	-0.165883
C	1.948441	0.554926	1.222967
H	1.804210	0.306723	-0.905794
O	0.311660	-2.411917	2.042523
C	4.377275	-0.073538	-0.131418

H	3.357350	-1.789098	0.674187
O	3.213032	-1.763656	-1.396881
C	3.139067	1.496308	1.115709
H	2.108076	-0.076450	2.110805
O	0.748624	1.287185	1.366868
C	-0.091353	-1.750852	3.080610
H	4.300980	0.572295	-1.030191
O	4.330354	0.739362	1.024239
O	5.581158	-0.756314	-0.129514
C	3.927016	-2.979074	-1.409996
H	3.015728	2.150711	0.235920
H	3.222993	2.122418	2.006188
H	0.220847	0.741536	1.985339
O	-0.343402	-0.540846	3.104685
C	-0.253374	-2.598357	4.322570
C	6.702916	0.092360	-0.269357
H	3.543291	-3.667707	-0.643017
H	4.998046	-2.824056	-1.245443
H	3.764707	-3.425017	-2.394120
H	-0.868102	-3.472937	4.096116
H	0.729041	-2.964670	4.633166
H	-0.700444	-2.012849	5.124751
H	6.803475	0.759022	0.591995
H	7.579778	-0.552666	-0.341068
H	6.621416	0.695851	-1.184165

3.29-TS1

M06-2X/6-31G(d) SCF energy:	-2197.35786905 a.u.
M06-2X/6-31G(d) enthalpy:	-2196.696294 a.u.
M06-2X/6-31G(d) free energy:	-2196.808871 a.u.
M06-2X/6-311++G(d,p) SCF energy in solution:	-2197.95685912 a.u.
M06-2X/6-311++G(d,p) enthalpy in solution:	-2197.295284 a.u.
M06-2X/6-311++G(d,p) free energy in solution:	-2197.407861 a.u.
Three lowest frequencies (cm ⁻¹):	-352.1592 13.9589 17.1391
Imaginary frequency:	-352.1592 cm ⁻¹

Cartesian coordinates

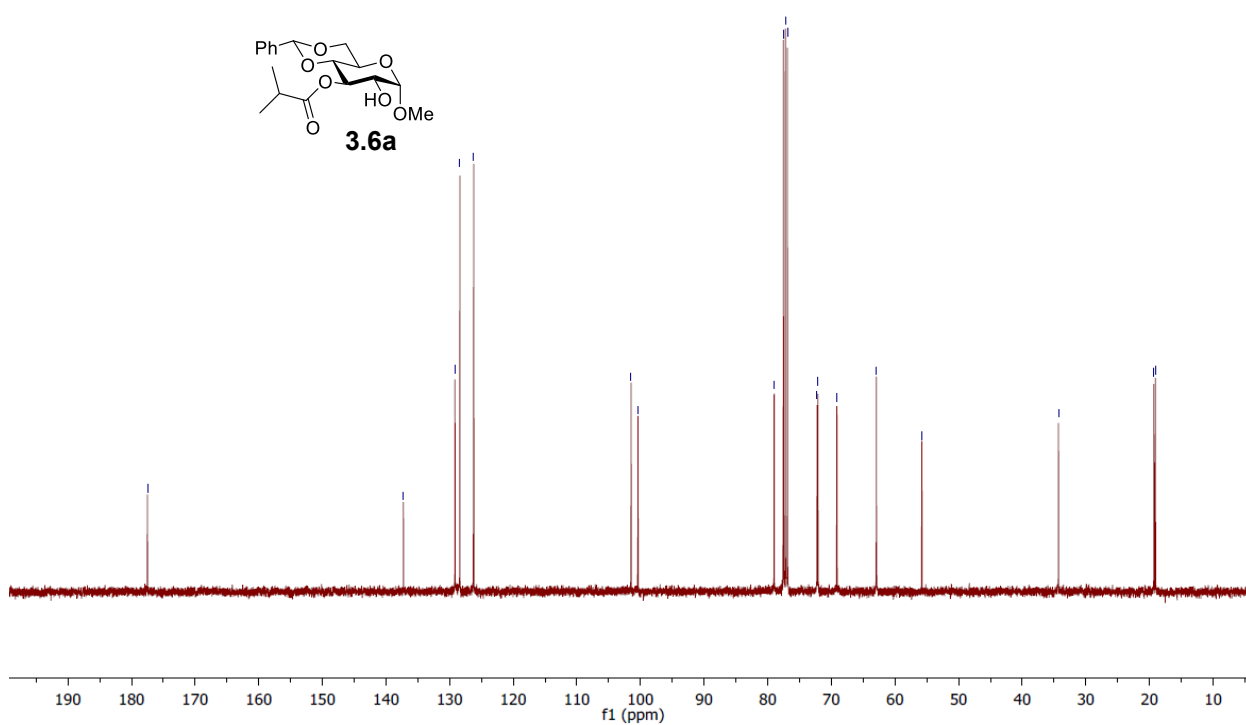
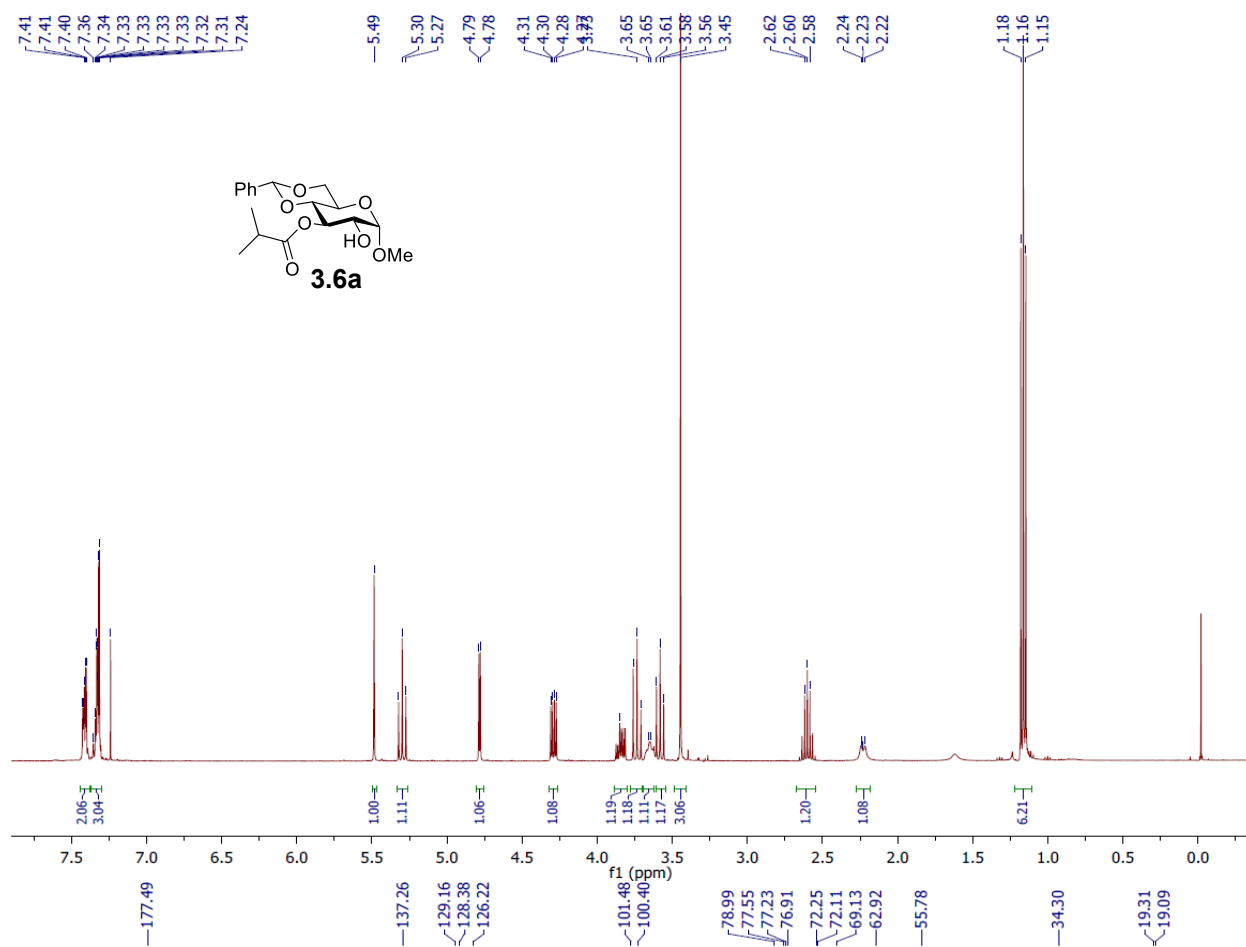
ATOM	X	Y	Z
C	-0.781801	3.759199	0.591295
C	-0.320547	3.381626	-0.677061
C	-0.641336	4.108784	-1.817458
C	-1.440594	5.235648	-1.658223
C	-1.901939	5.622364	-0.396778
C	-1.579777	4.886202	0.740253
C	0.575680	1.724284	0.634789
H	-0.282399	3.798527	-2.793110
H	-1.710549	5.821152	-2.530454
H	-2.523840	6.505523	-0.299918
H	-1.946005	5.181861	1.717886
C	1.028368	1.325558	-1.593981
H	0.216292	0.868607	-2.164821
H	1.727352	1.860108	-2.240816
C	1.755929	0.270908	-0.701195
H	1.375163	-0.730775	-0.909724

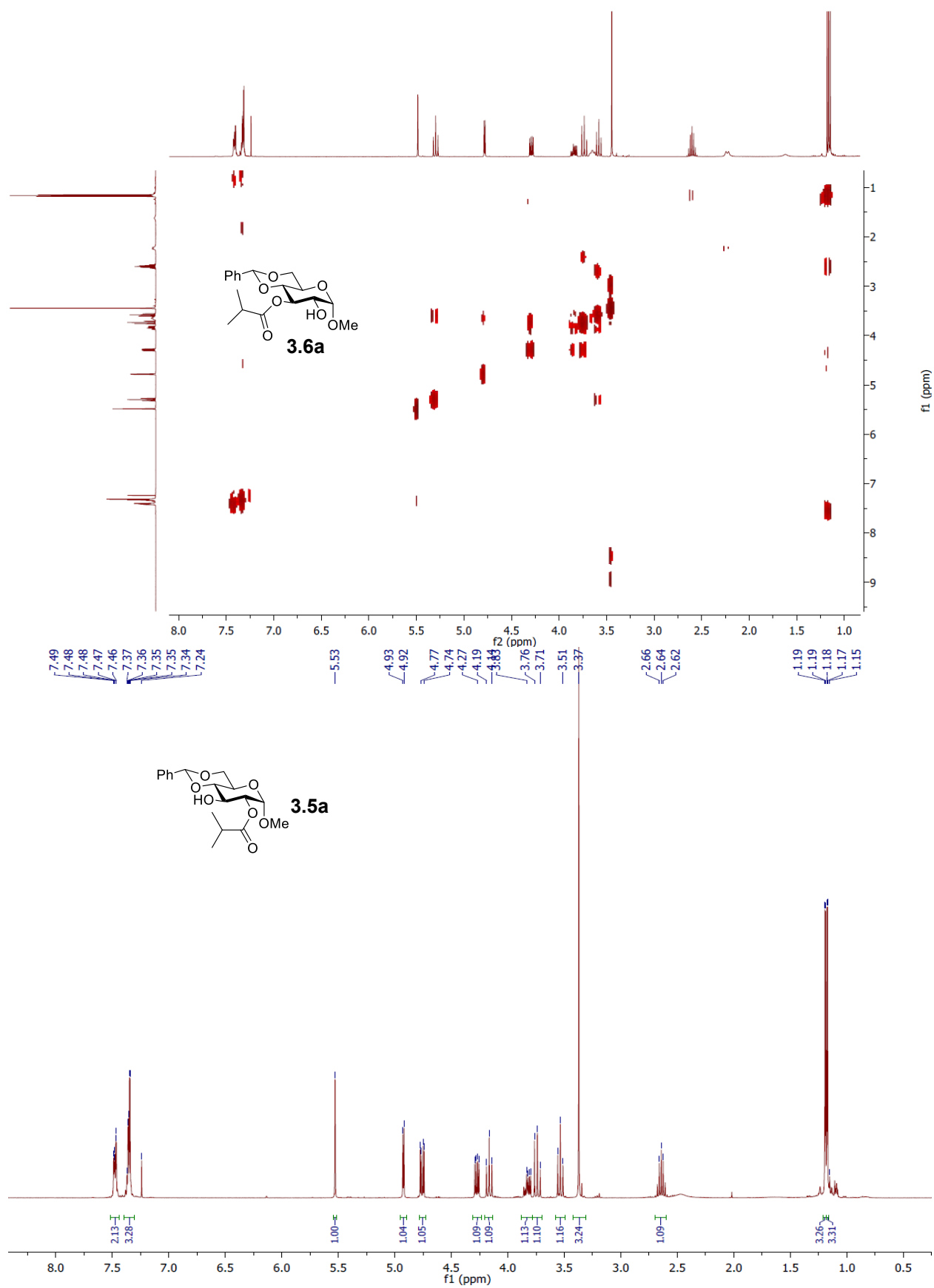
N	1.310047	0.628241	0.677789
N	0.460035	2.235714	-0.594122
S	-0.262800	2.619130	1.850002
C	1.210073	-0.266242	1.851390
O	0.590316	0.211018	2.788694
C	2.344186	-1.261782	2.002287
H	2.554599	-1.706656	1.022815
C	3.258585	0.317644	-0.842124
C	3.942702	-0.809536	-1.292350
C	3.966863	1.484707	-0.542362
C	5.330309	-0.774099	-1.425524
H	3.377445	-1.704628	-1.543570
C	5.349980	1.518515	-0.673707
H	3.433728	2.365246	-0.185814
C	6.033937	0.384686	-1.113167
H	5.860457	-1.655196	-1.773248
H	5.896198	2.424619	-0.430759
H	7.114611	0.408797	-1.212956
C	1.935674	-2.353916	2.988121
H	2.774198	-3.037122	3.151947
H	1.660078	-1.901924	3.945364
H	1.085259	-2.923768	2.612484
C	3.580475	-0.509302	2.511113
H	4.415937	-1.206222	2.624452
H	3.895080	0.285430	1.828890
H	3.366200	-0.065492	3.488750
O	0.053692	-1.534800	0.872116
C	-1.240044	-1.080759	0.661294
H	0.347125	-2.684027	0.454370
C	-1.768648	-1.535353	-0.701976
C	-2.188758	-1.525340	1.771499
H	-1.255387	0.026103	0.652598
O	0.698412	-3.728337	0.121459
C	-3.222672	-1.122263	-0.884634
H	-1.730671	-2.636803	-0.738015
O	-0.999412	-0.989873	-1.752960
H	-2.201306	-2.627351	1.826094
H	-1.849921	-1.129658	2.730932
O	-3.489788	-1.016202	1.533814
C	1.179288	-3.720166	-1.075663
C	-4.046041	-1.521963	0.342023
H	-3.272243	-0.026480	-0.986533
O	-3.727050	-1.765437	-2.030018
H	-0.253118	-1.606585	-1.902074
O	1.179911	-2.741069	-1.835980
C	1.787452	-5.035123	-1.511598
H	-4.082641	-2.629403	0.398680
O	-5.323173	-1.005966	0.197194
C	-4.595583	-0.971433	-2.804420
H	2.650923	-5.258341	-0.878478
H	1.061758	-5.838595	-1.365207
H	2.092810	-4.984803	-2.556003
C	-6.218419	-1.456848	1.194029
H	-4.072588	-0.085226	-3.191168

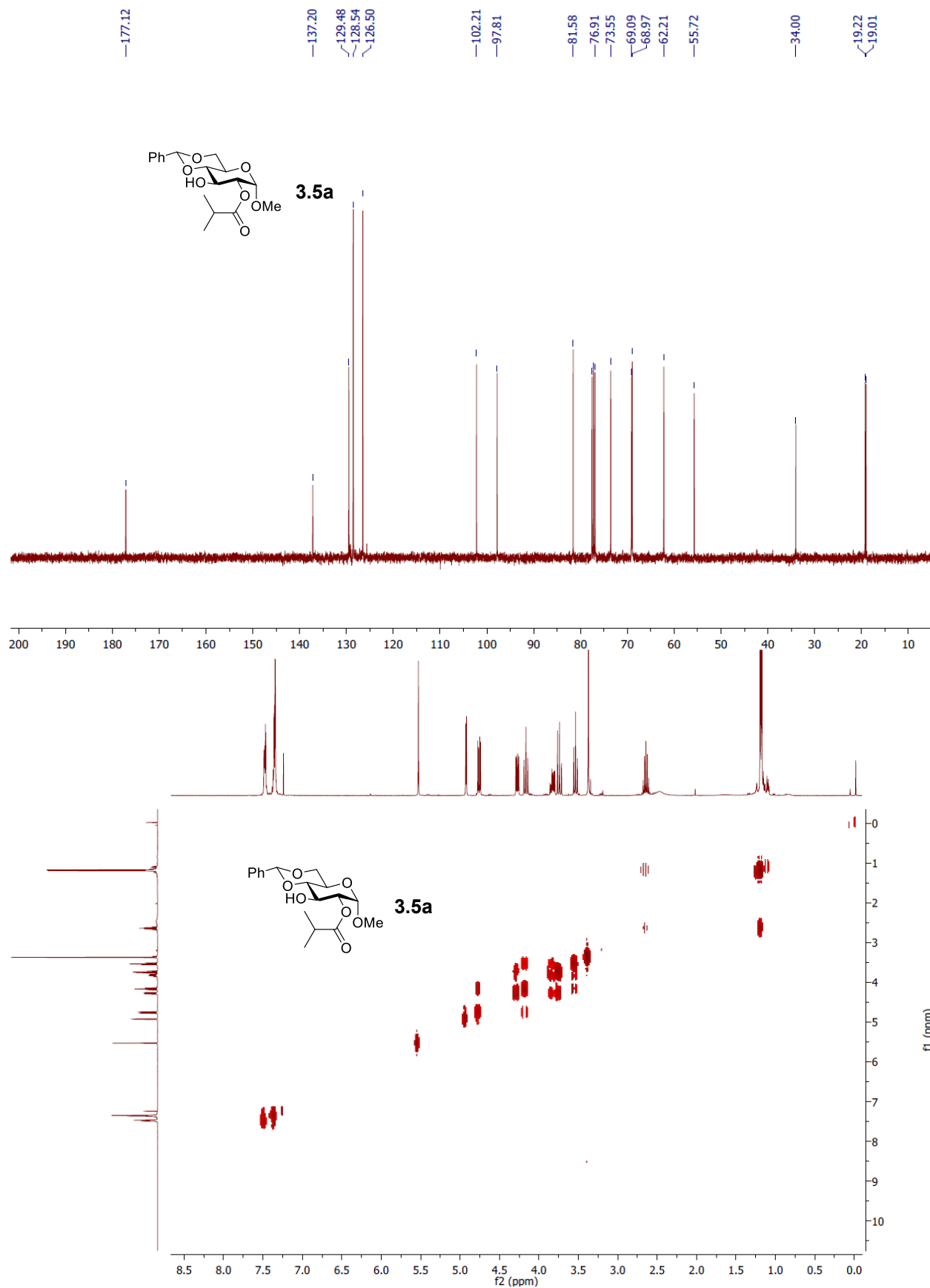
H -5.471362 -0.651607 -2.229853
 H -4.916999 -1.586761 -3.647603
 H -5.915010 -1.105980 2.184629
 H -7.200167 -1.052560 0.943207
 H -6.270093 -2.554462 1.201563

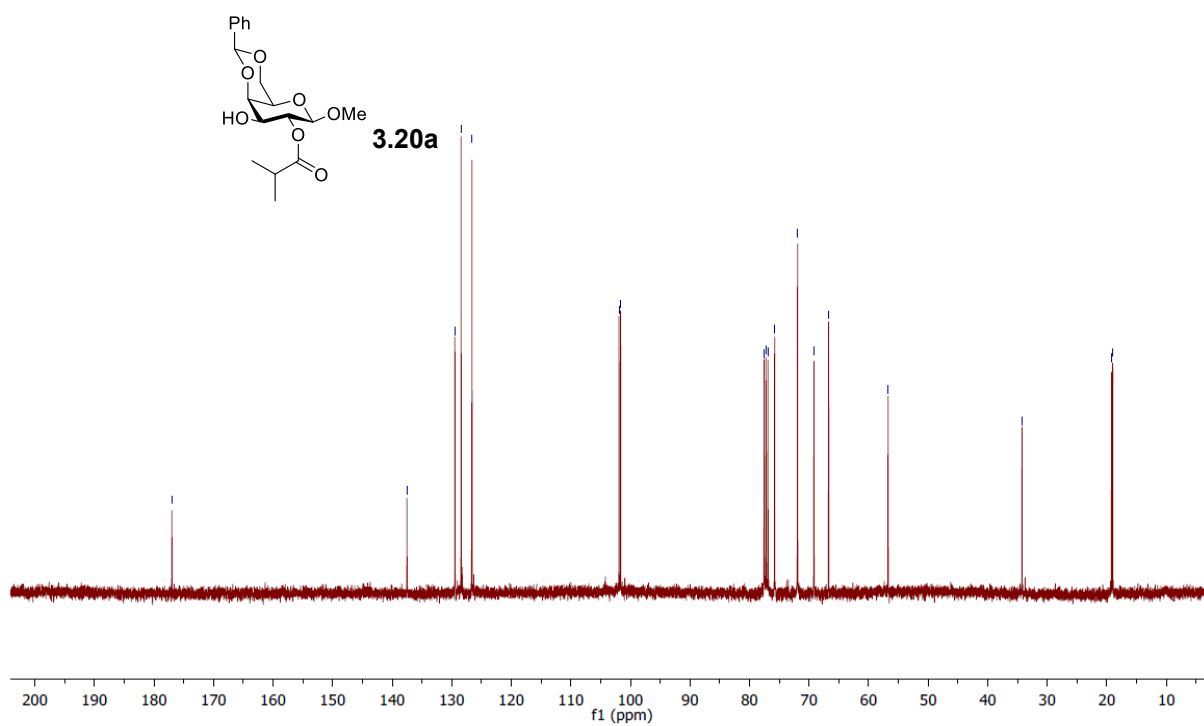
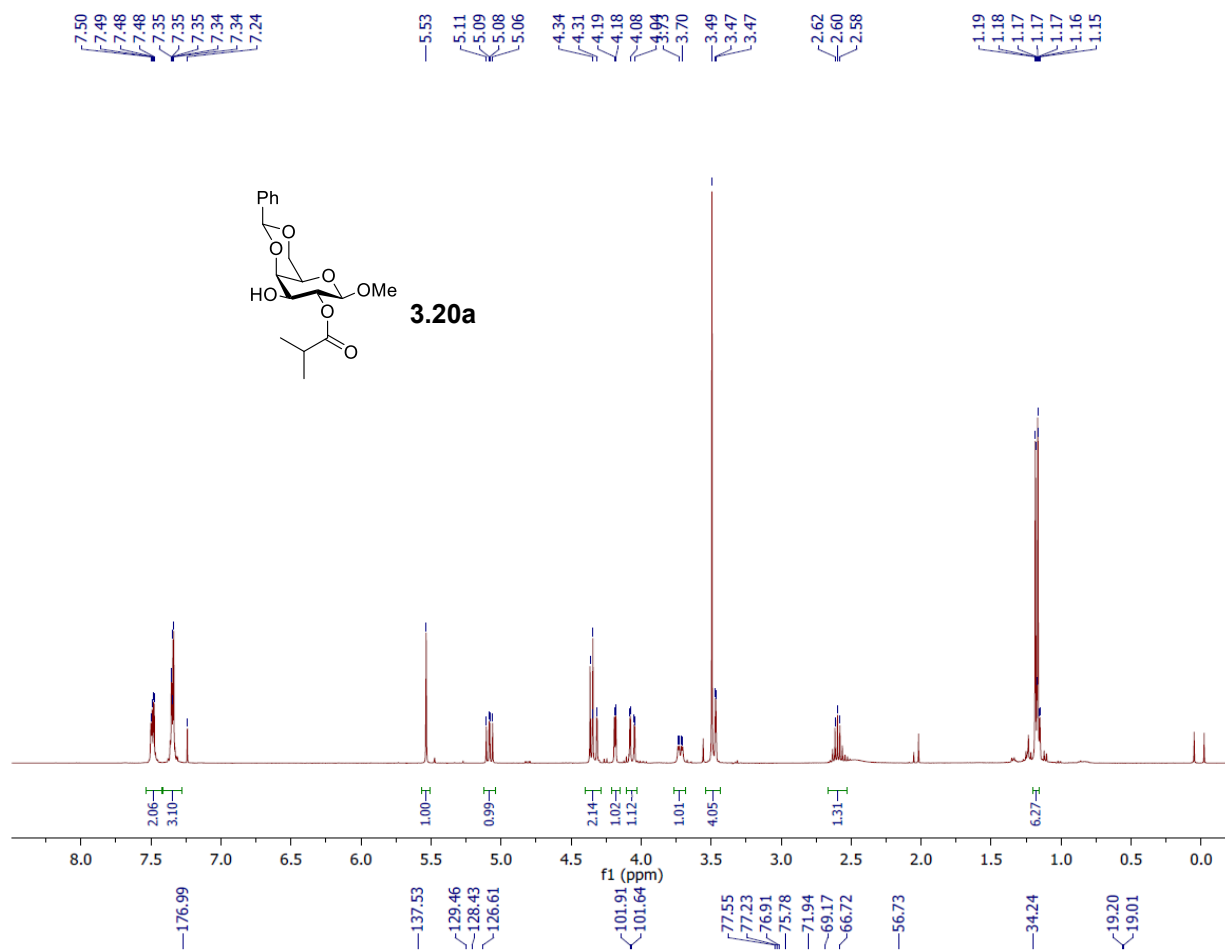
References:

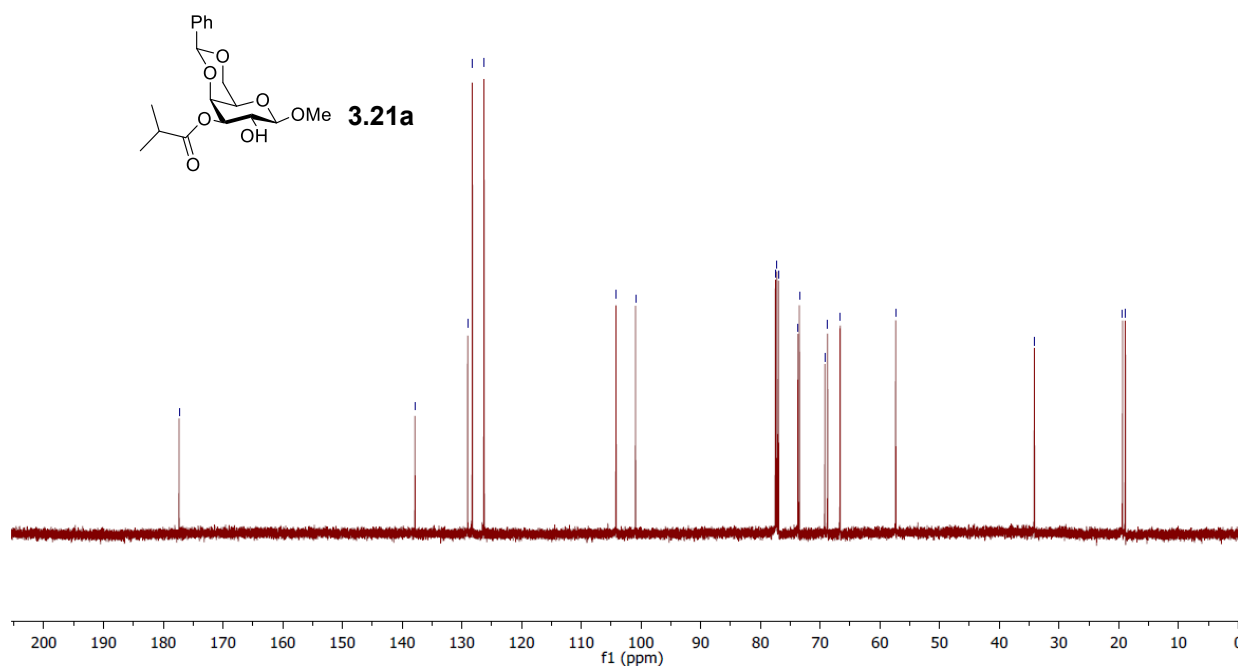
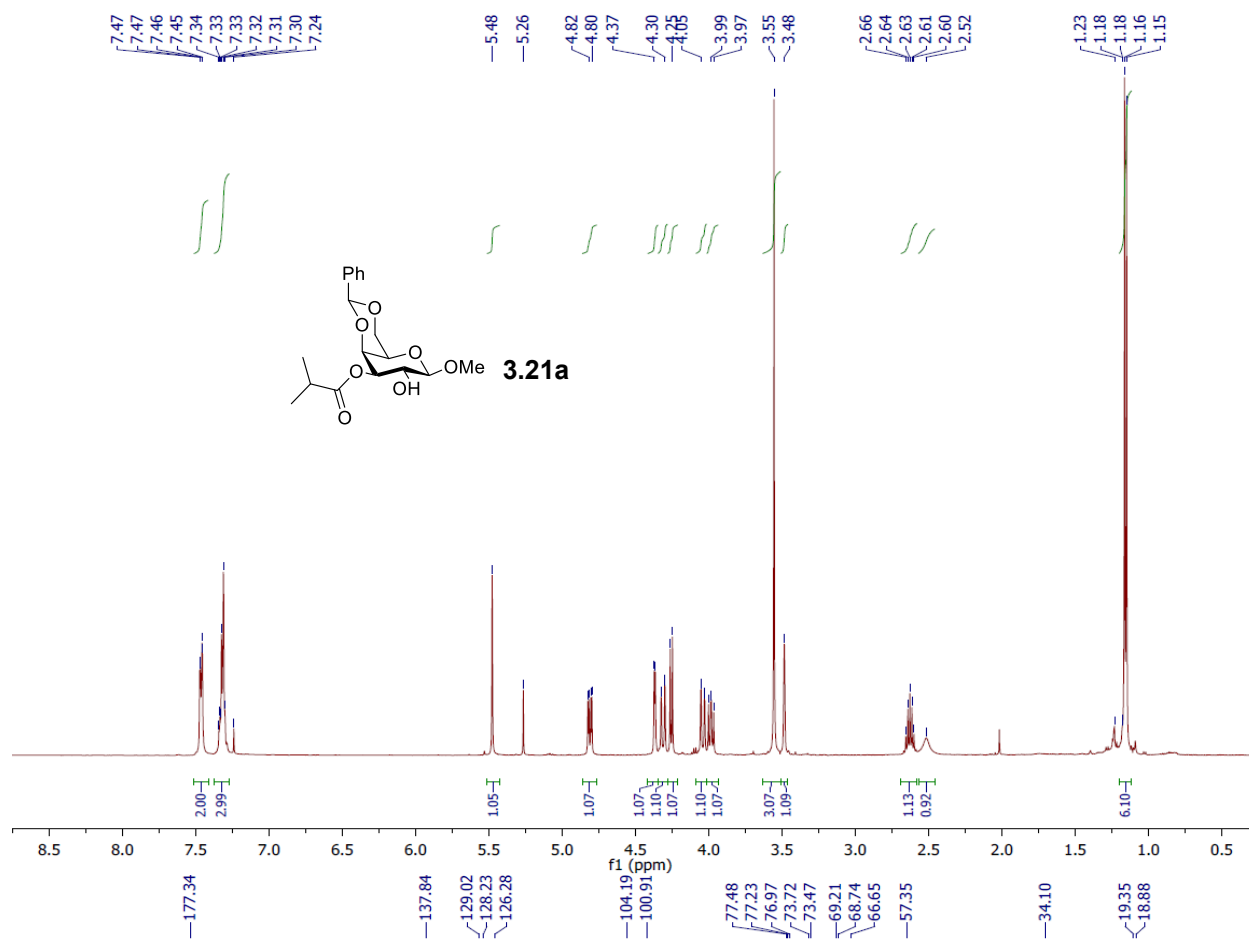
- (1) C. L. Allen, S. J. Miller, *Org. Lett.* **2013**, 15, 6178–6181.
- (2) K. Dąbrowa, P. Niedbała, J. Jurczak, *J. Org. Chem.* **2016**, 81, 3576–3584.
- (3) S. Munneke, G. F. Painter, G. J. Gainsford, B. L. Stocker, M. S. M. Timmer, *Carbohydr. Res.* **2015**, 414, 1–7.
- (4) K. Takeo, K. Maki, Y. Wada, S. Kitamura, *Carbohydr. Res.* **1993**, 245, 81–96.
- (5) F. Pontén, G. Magnusson, *J. Org. Chem.* **1997**, 62, 7972–7977.
- (6) D. A. DiRocco, Y. Ji, E. C. Sherer, A. Klapars, M. Reibarkh, J. Dropinski, R. Mathew, P. Malignes, A. M. Hyde, J. Limanto, et al., *Science* (80-.). **2017**, 356, 426 LP – 430.
- (7) Frisch, M. J., Trucks, G. W., Schlegel, H. B., Scuseria, G. E., Robb, M. A., Cheeseman, J. R., Scalmani, G., Barone, V., Mennucci, B., Petersson, G. A., Nakatsuji, H., Caricato, M., Li, X., Hratchian, H. P., Izmaylov, A. F., Bloino, J., Zheng, G., Sonnenberg, J. L., Hada, M., Ehara, M., Toyota, K., Fukuda, R., Hasegawa, J., Ishida, M., Nakajima, T., Honda, Y., Kitao, O., Nakai, H., Vreven, T., Montgomery, J. A. Jr., Peralta, J. E., Ogliaro, F., Bearpark, M., Heyd, J. J., Brothers, E., Kudin, K. N., Staroverov, V. N., Kobayashi, R., Normand, J., Raghavachari, K., Rendell, A., Burant, J. C., Iyengar, S. S., Tomasi, J., Cossi, M., Rega, N., Millam, N. J., Klene, M., Knox, J. E., Cross, J. B., Bakken, V., Adamo, C., Jaramillo, J., Gomperts, R., Stratmann, R. E., Yazyev, O., Austin, A. J., Cammi, R., Pomelli, C., Ochterski, J. W., Martin, R. L., Morokuma, K., Zakrzewski, V. G., Voth, G. A., Salvador, P., Dannenberg, J. J., Dapprich, S., Daniels, A. D., Farkas, Ö., Foresman, J. B., Ortiz, J. V., Cioslowski, J., Fox, D. J. *Gaussian 09, Revision D.01*; Gaussian, Inc.: Wallingford, CT, 2009.
- (8) S. Grimme, J. Antony, S. Ehrlich, H. Krieg, *J. Chem. Phys.* **2010**, 132, 154104.
- (9) S. Grimme, *J. Comput. Chem.* **2006**, 27, 1787–1799.
- (10) A. V Marenich, C. J. Cramer, D. G. Truhlar, *J. Phys. Chem. B* **2009**, 113, 6378–6396.
- (11) R. F. Ribeiro, A. V Marenich, C. J. Cramer, D. G. Truhlar, *J. Phys. Chem. B* **2011**, 115, 14556–14562.

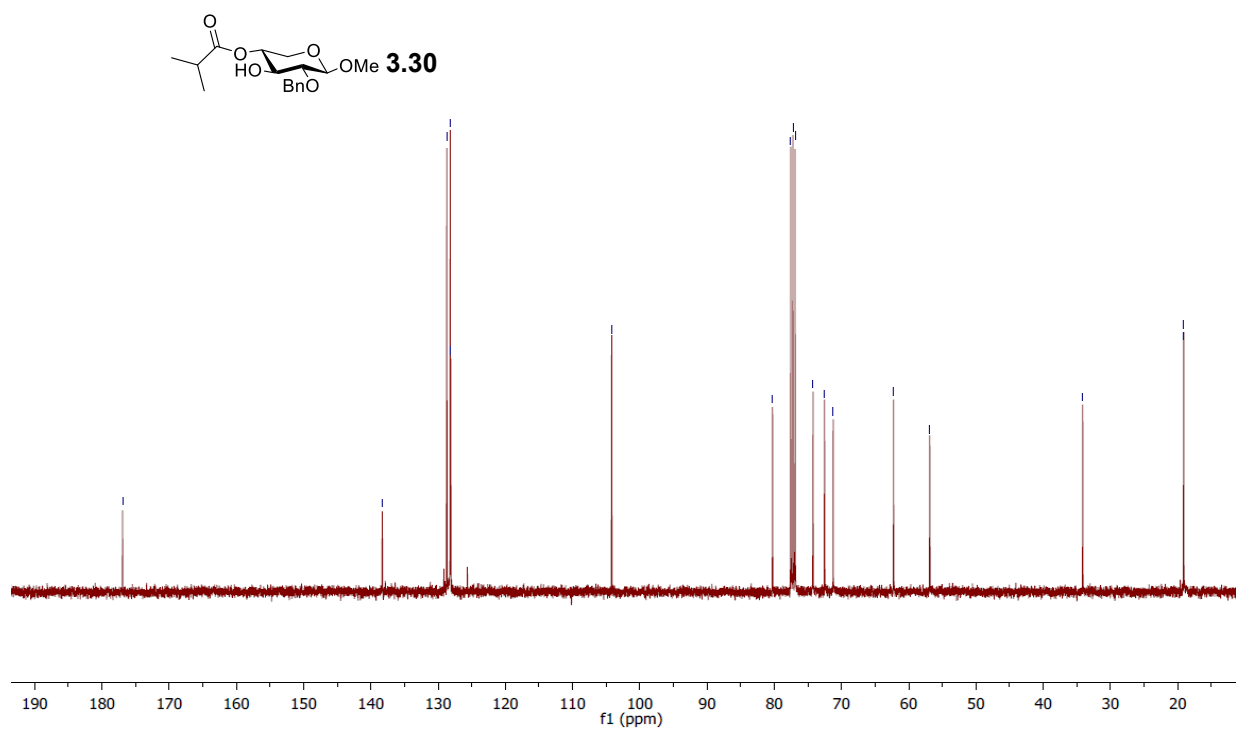
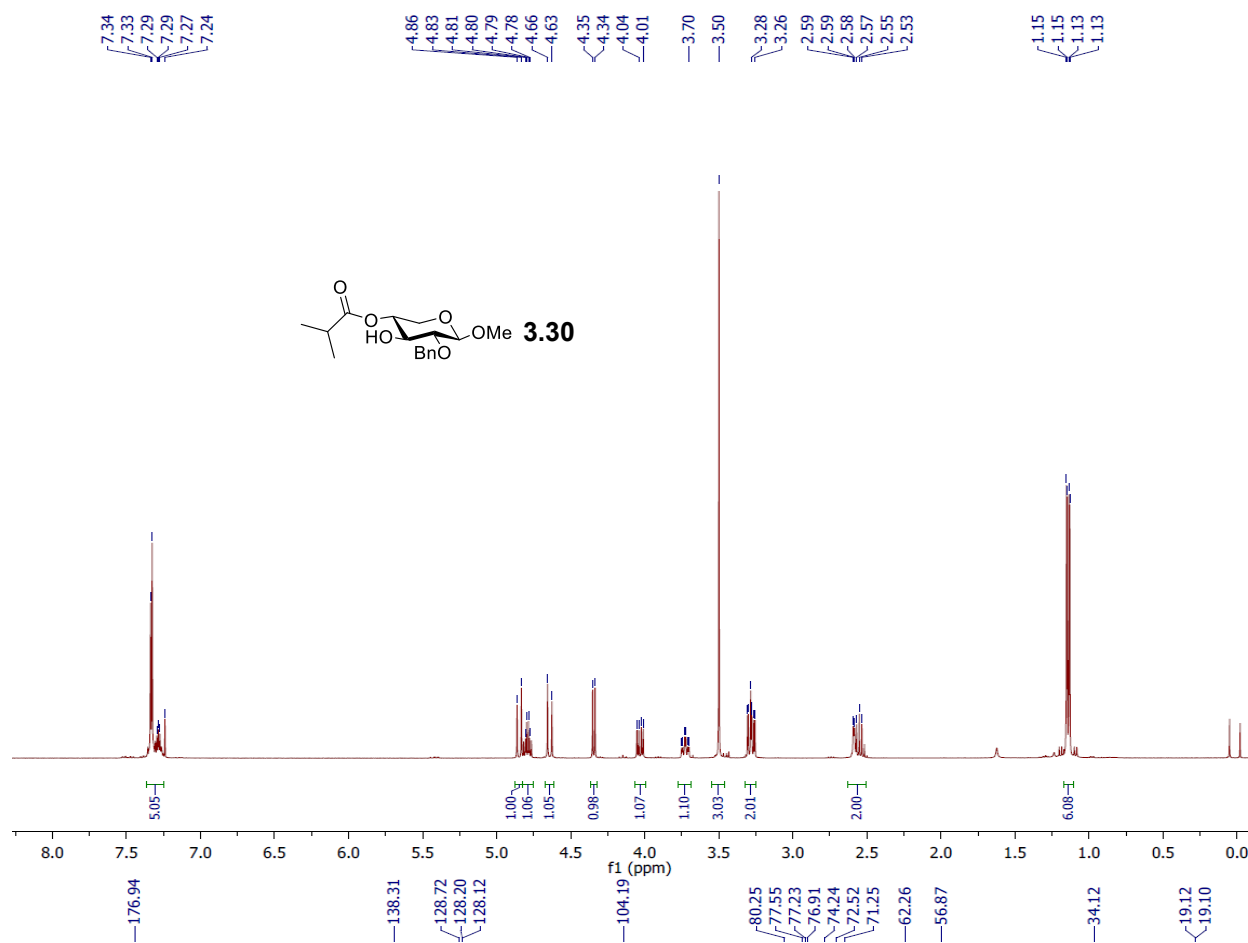


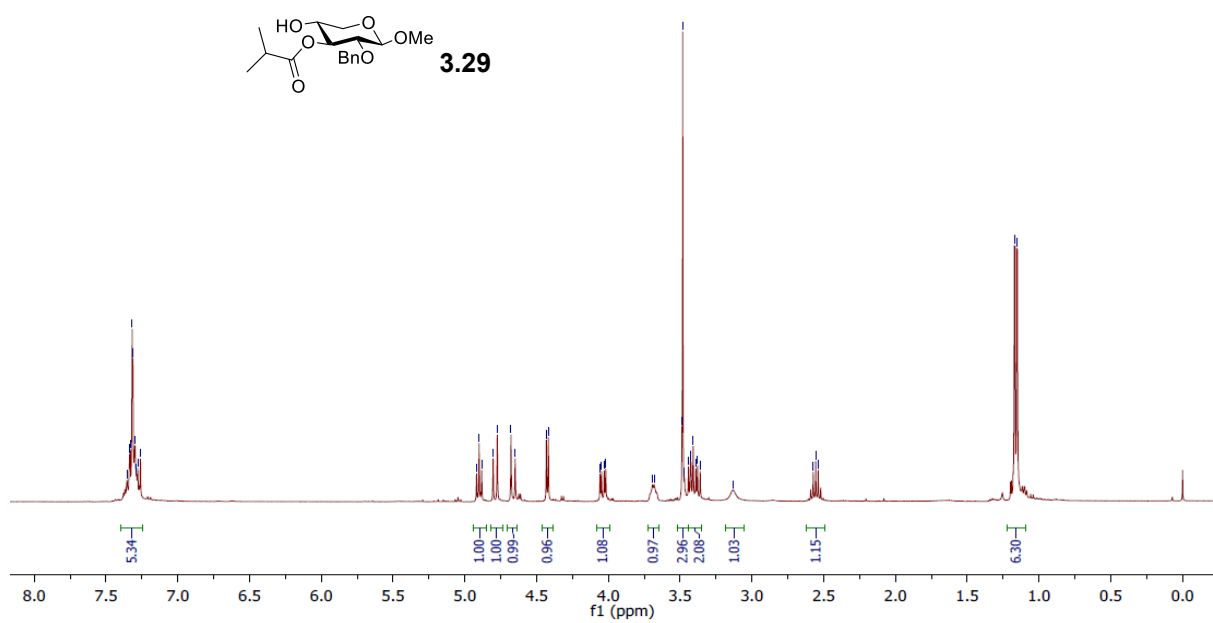
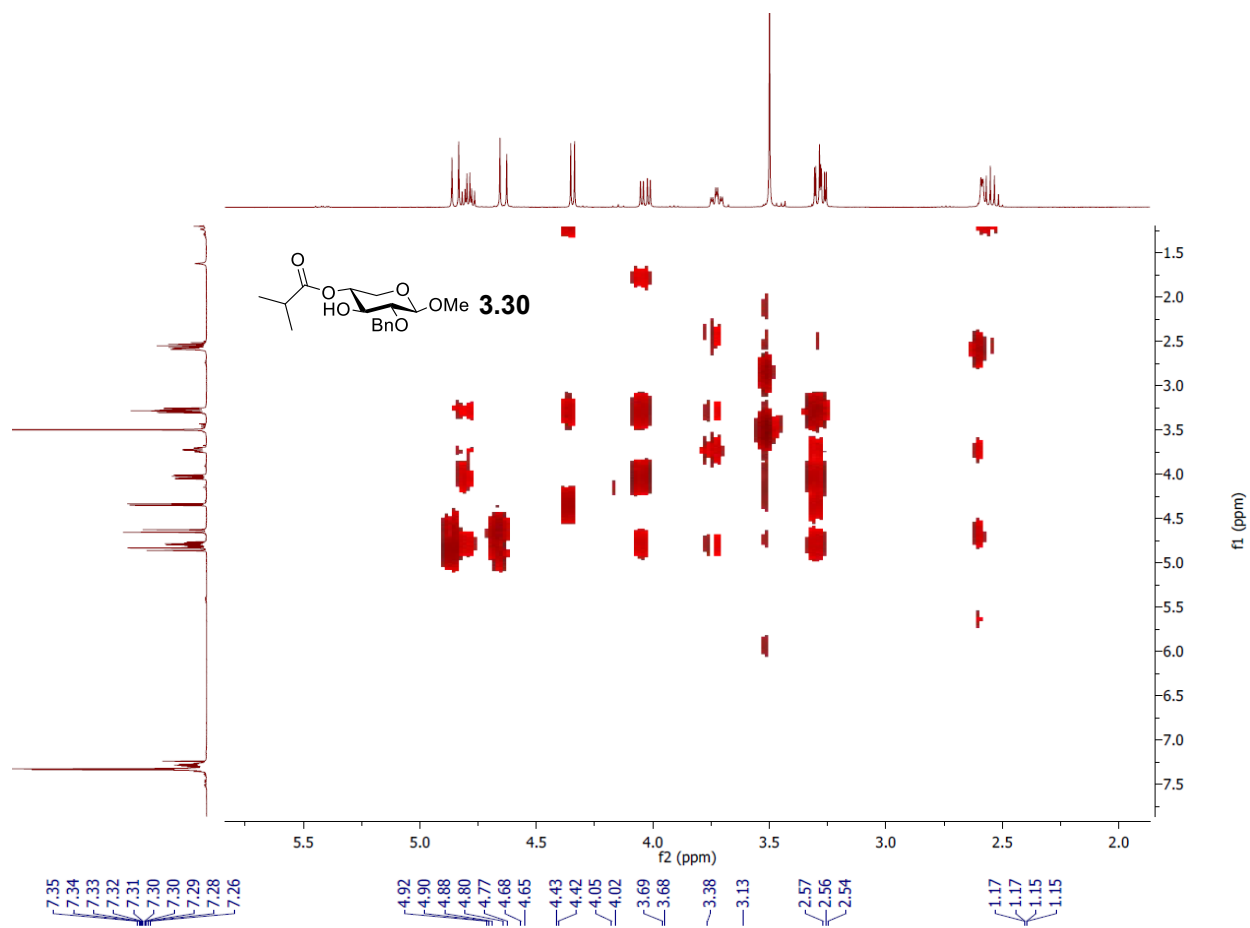


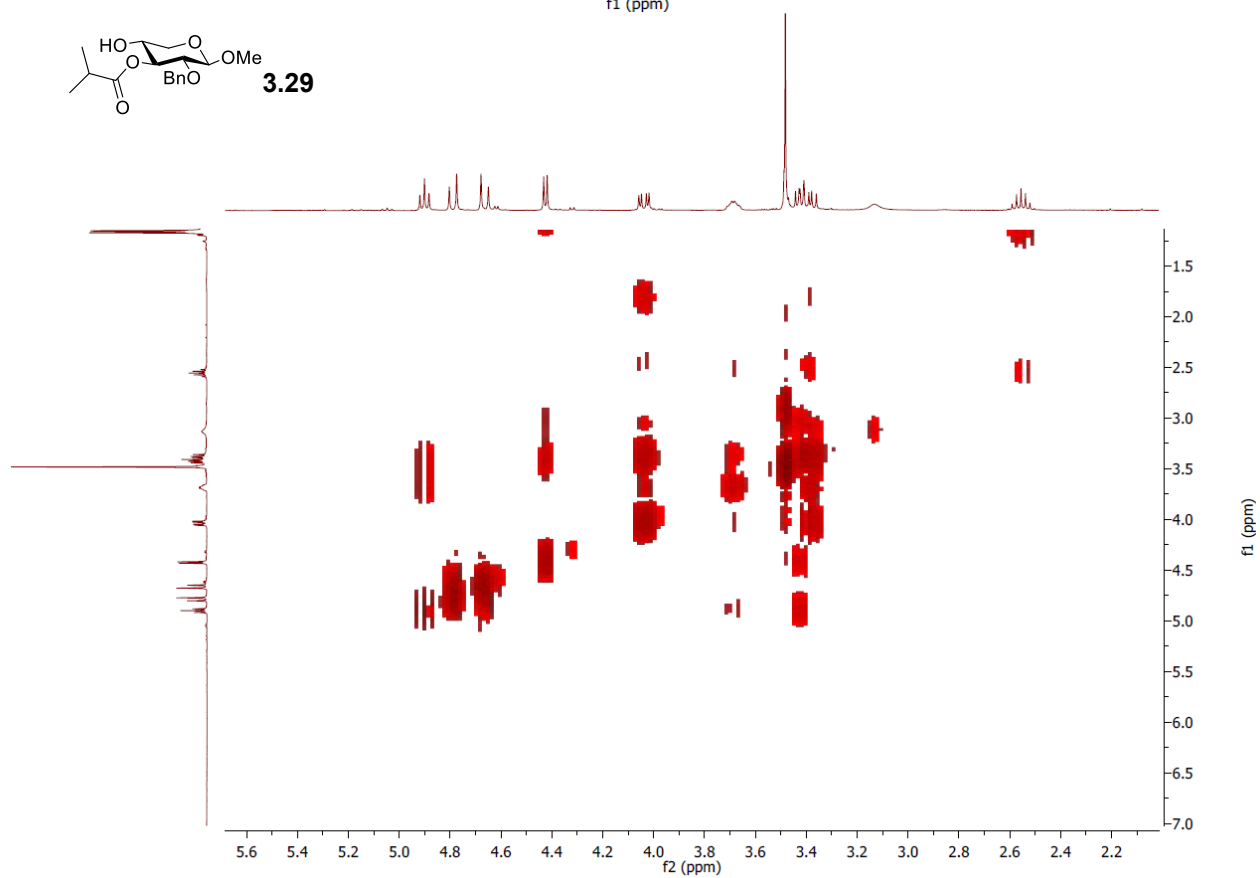
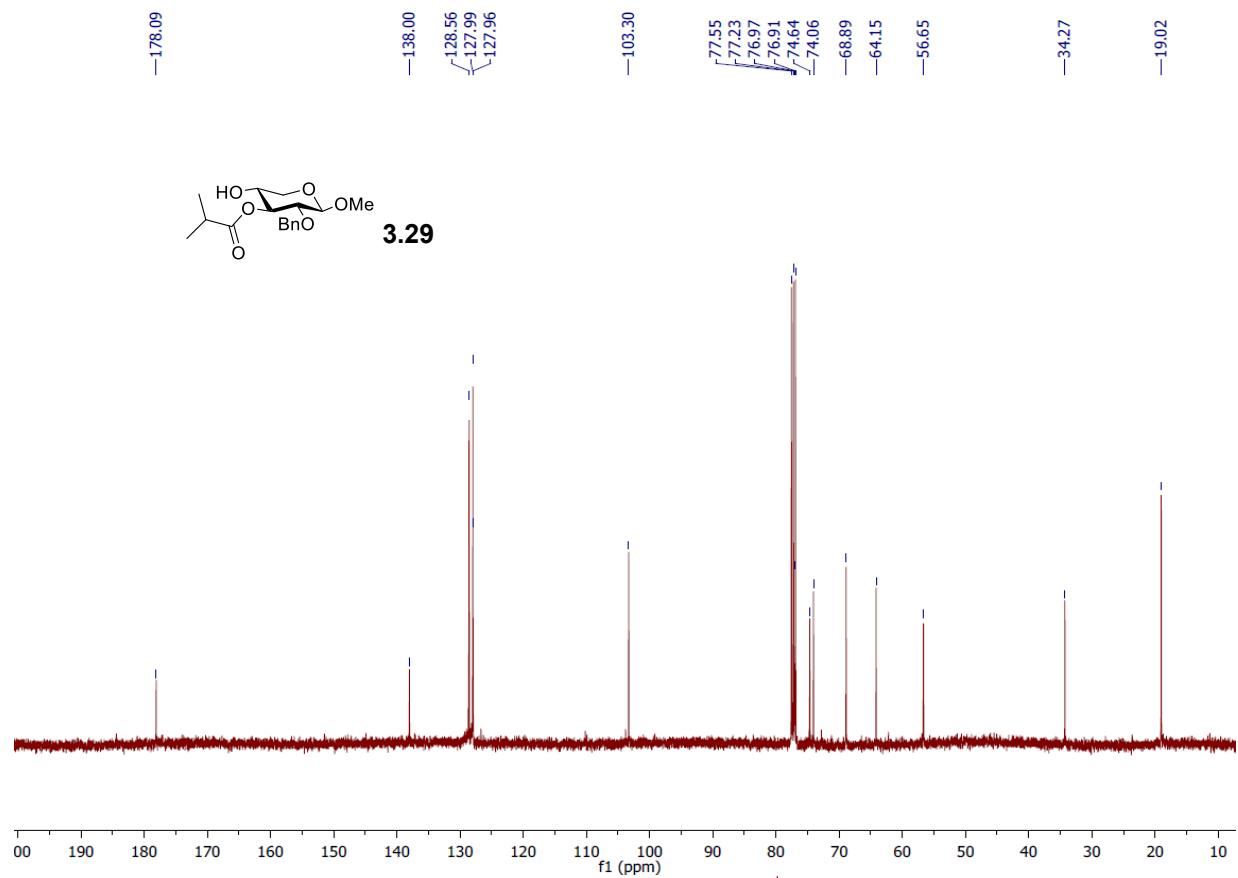


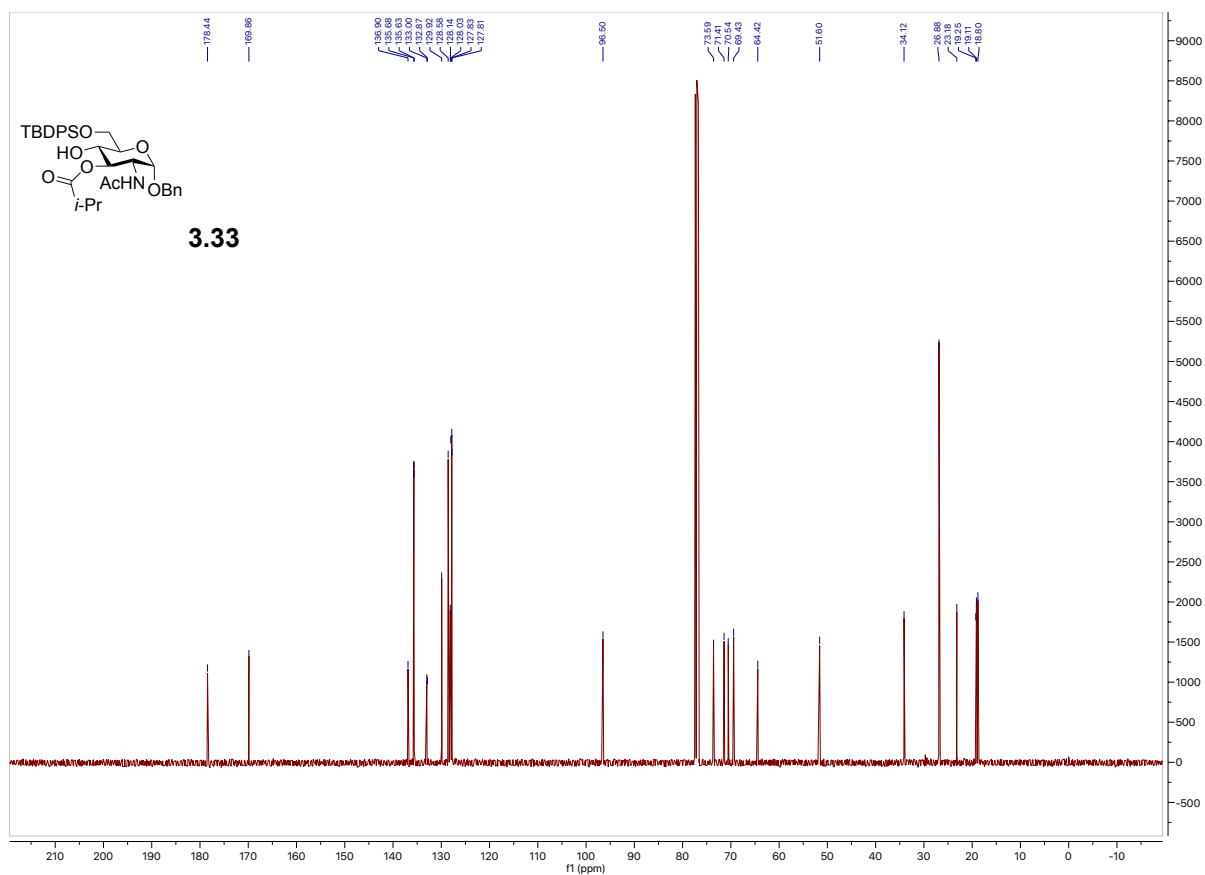
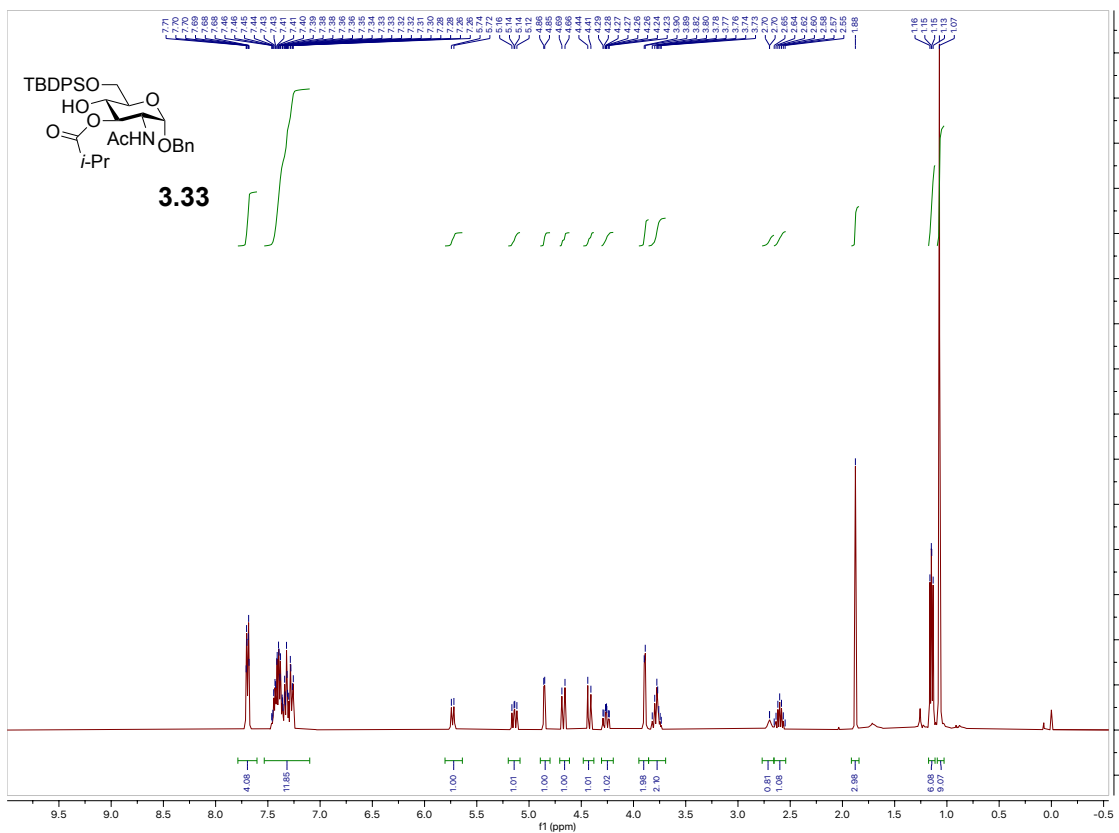


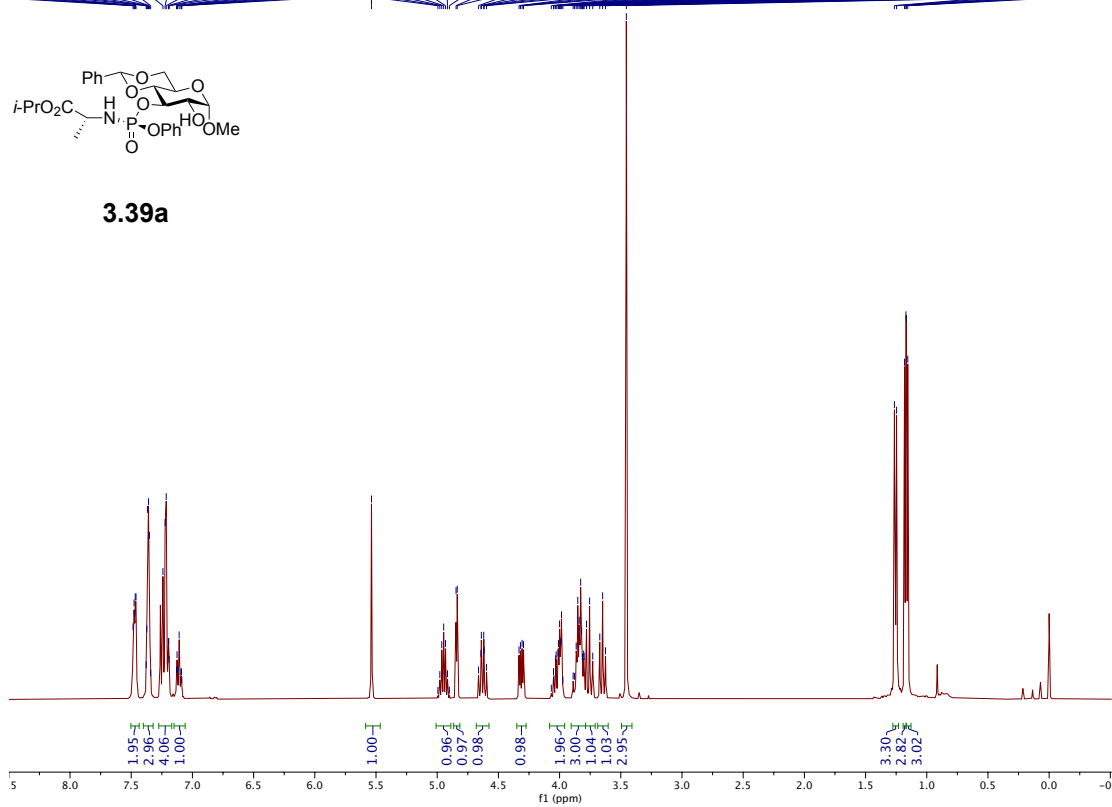
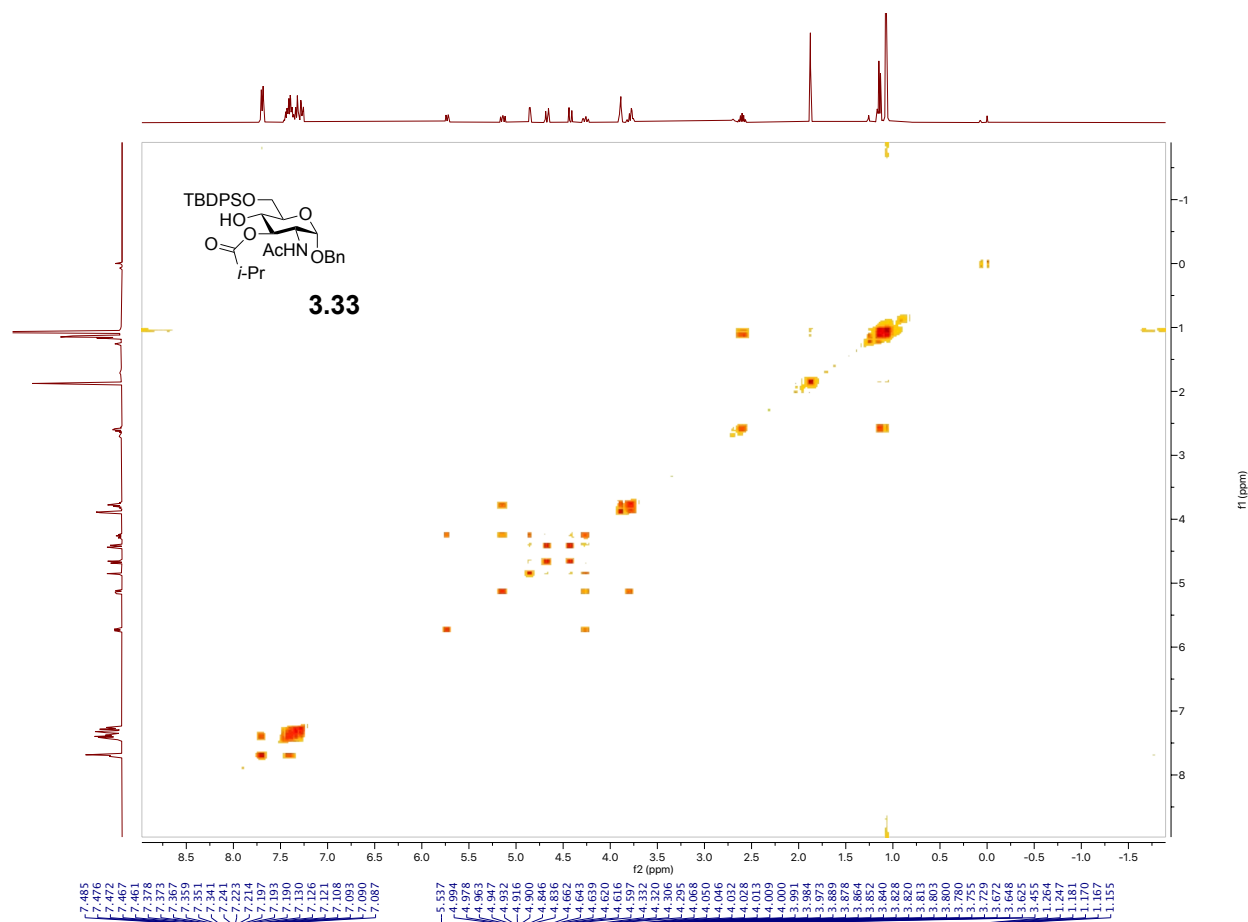


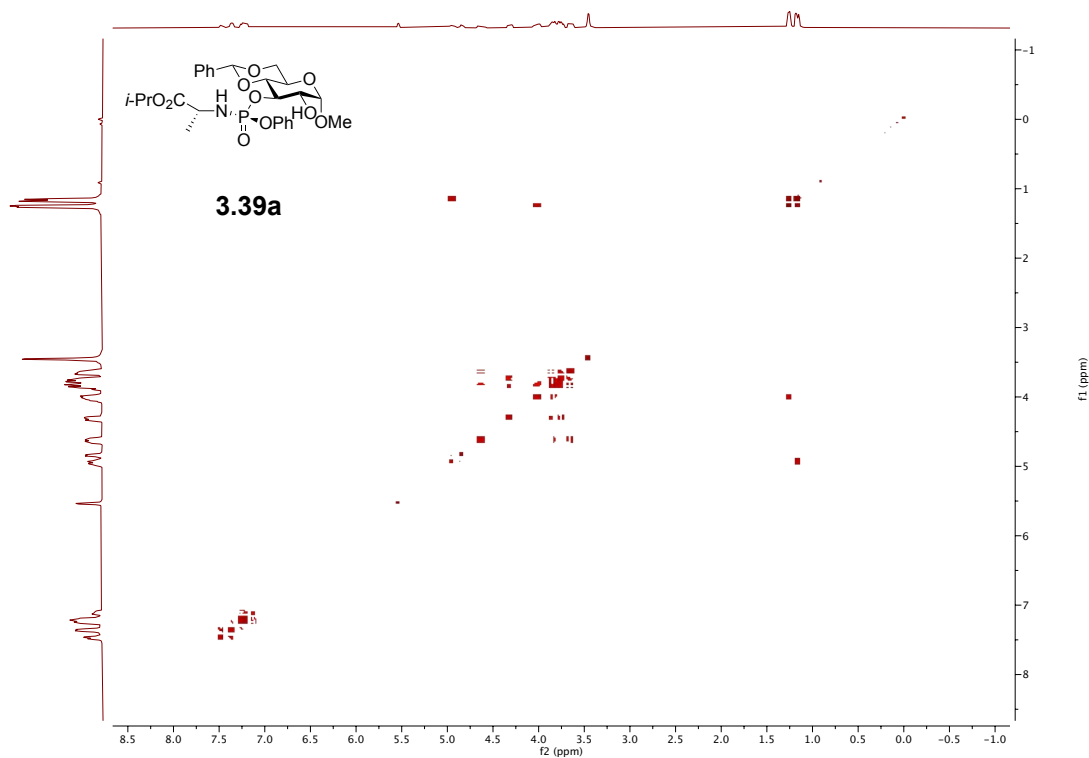
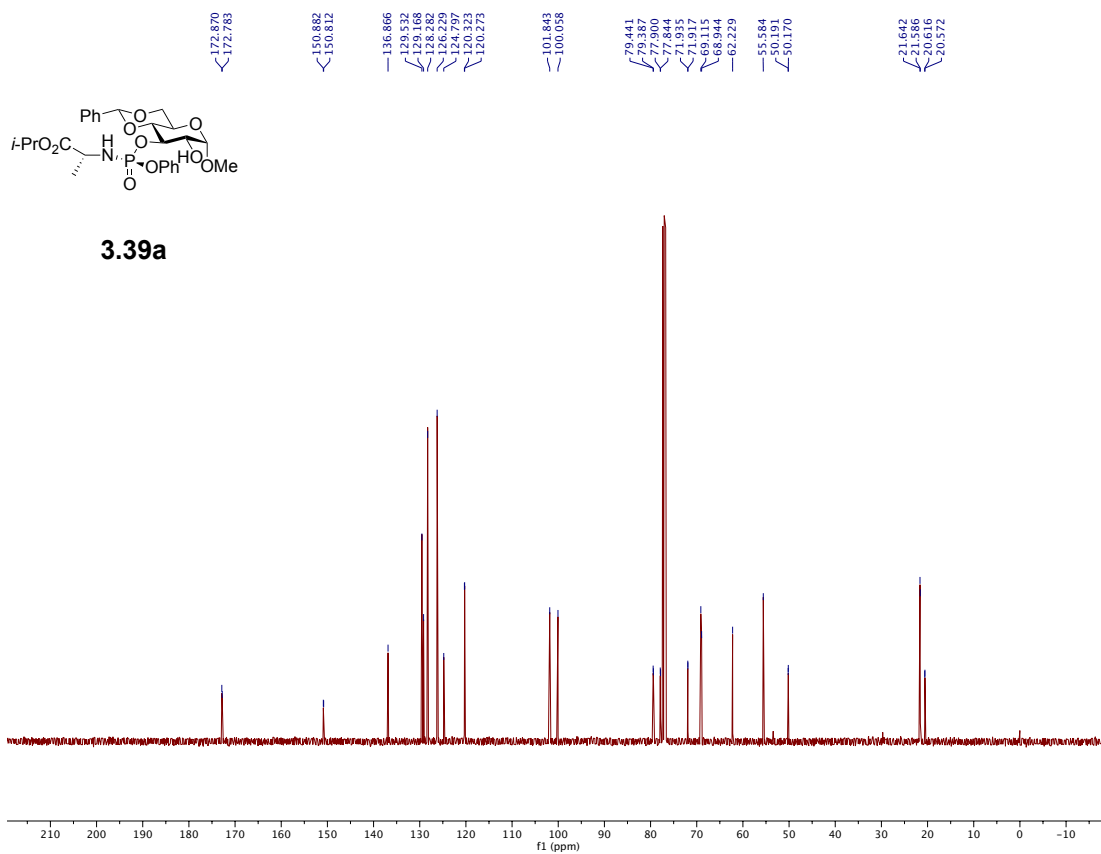


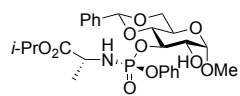




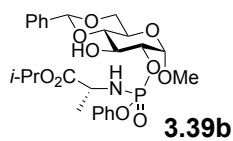
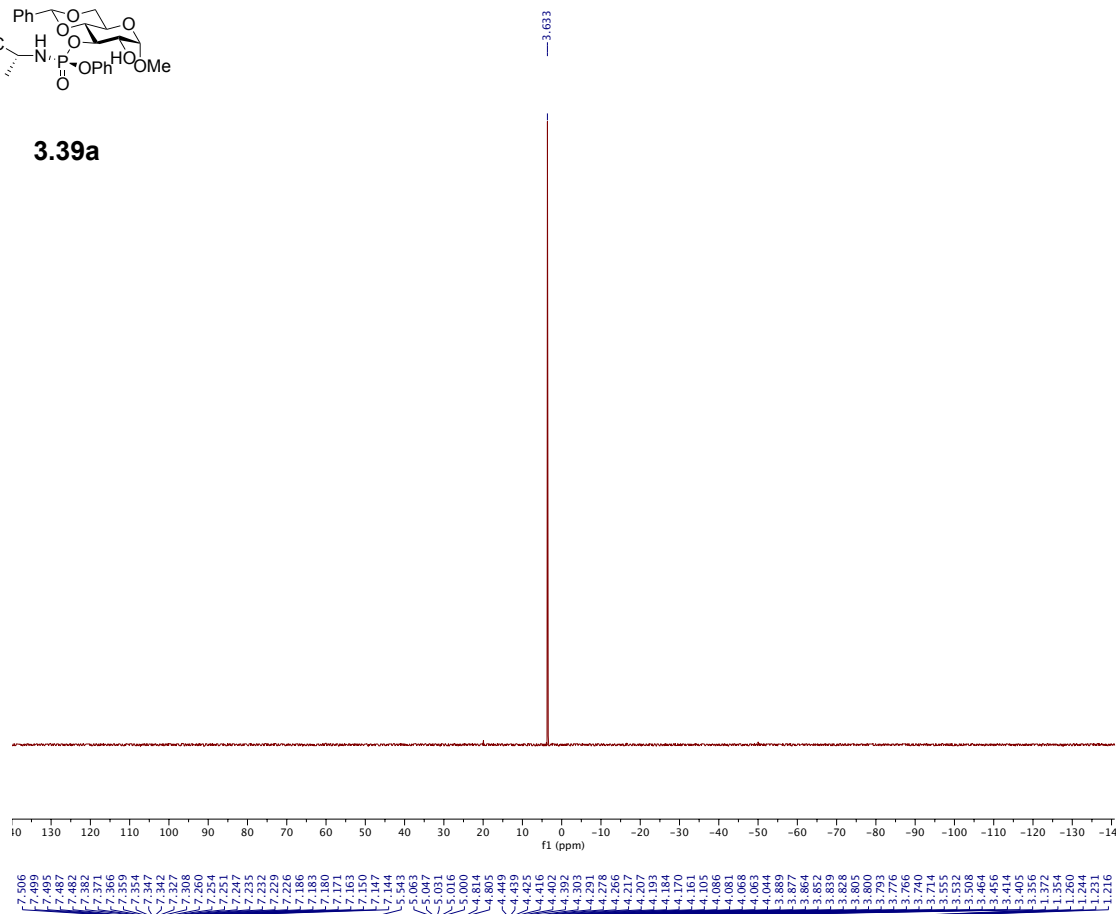




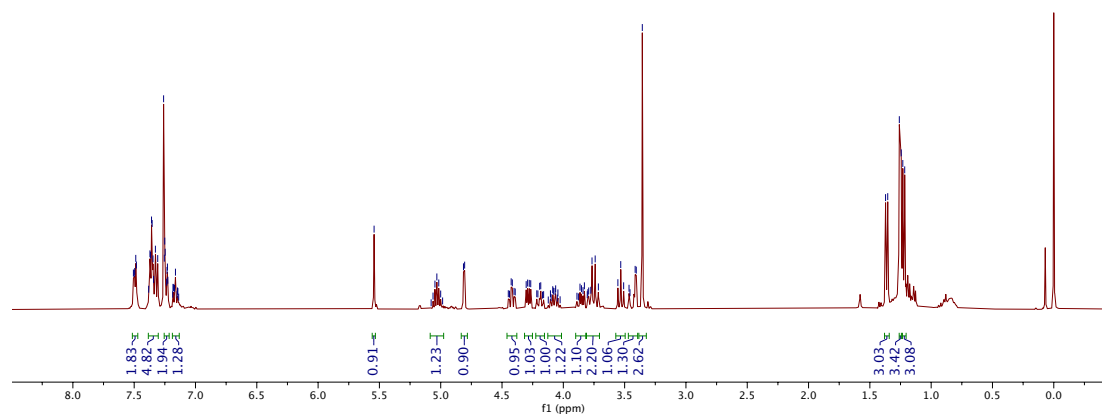


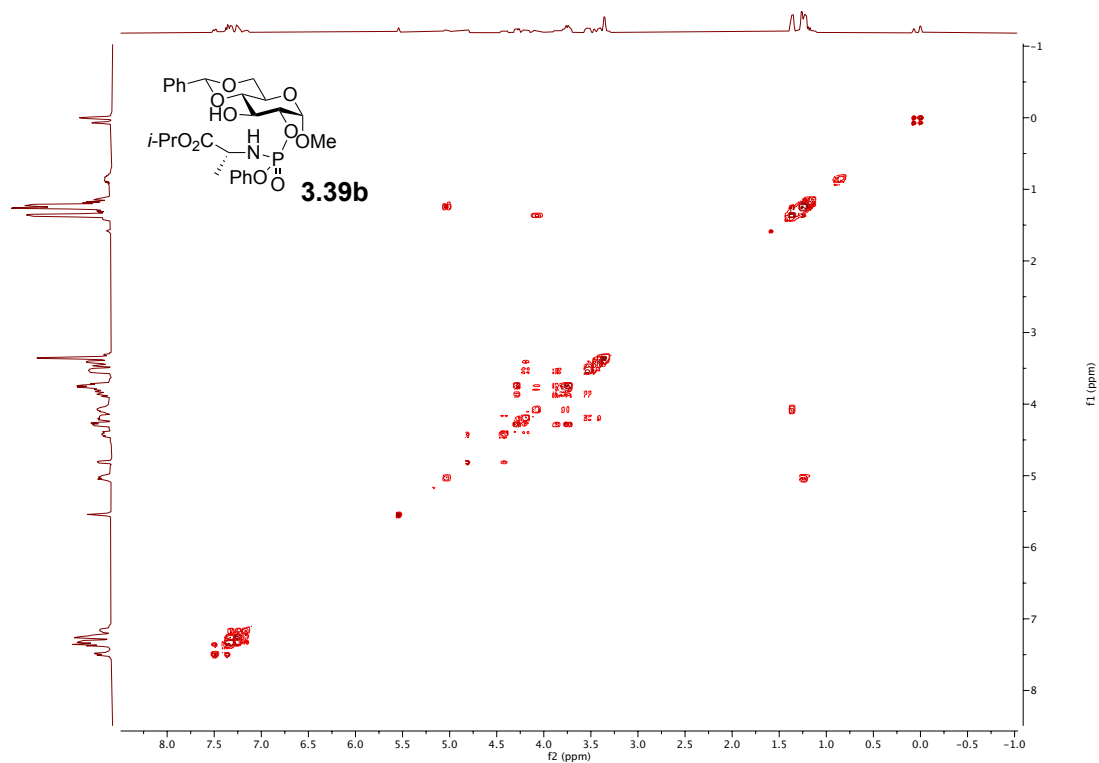
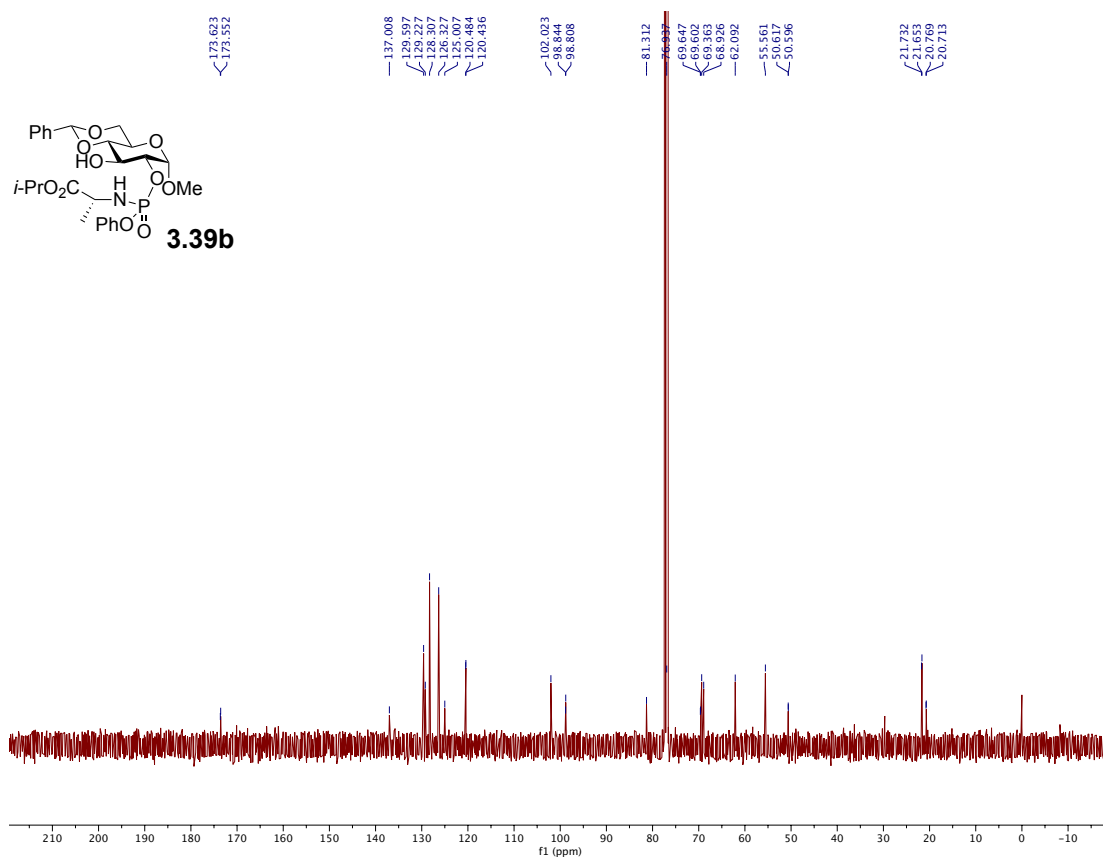


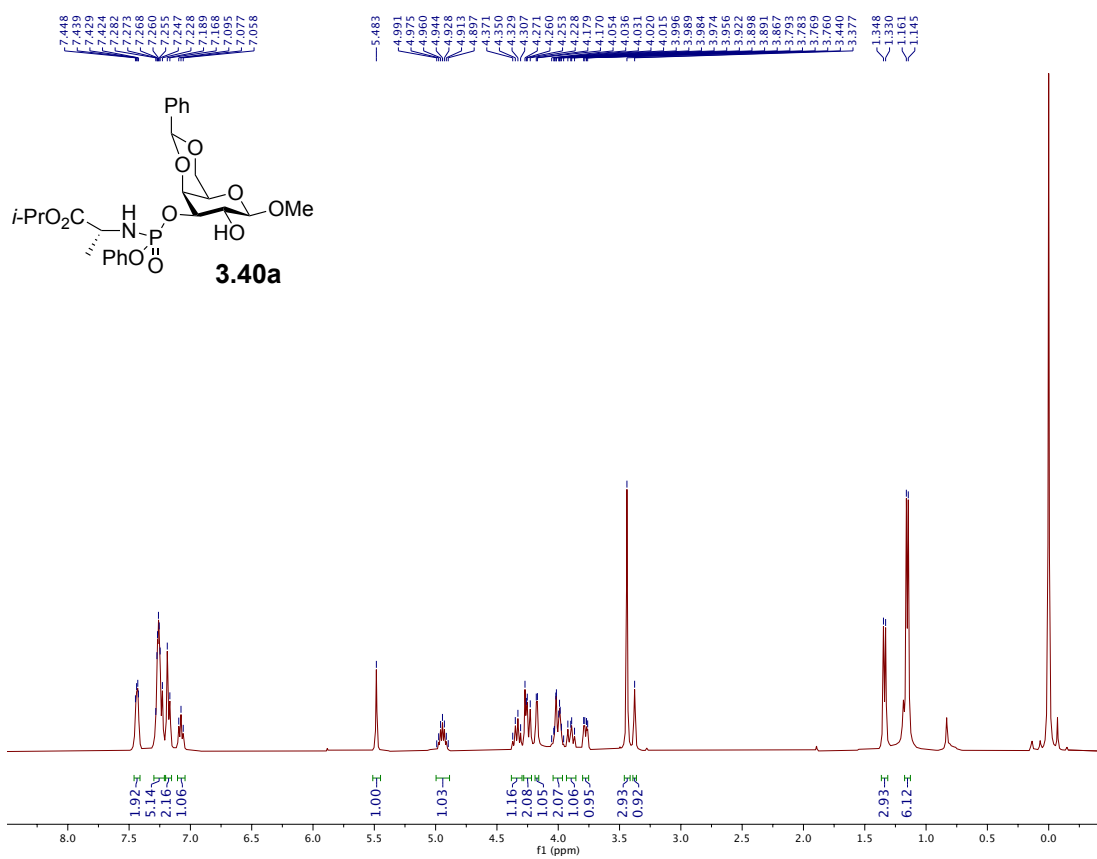
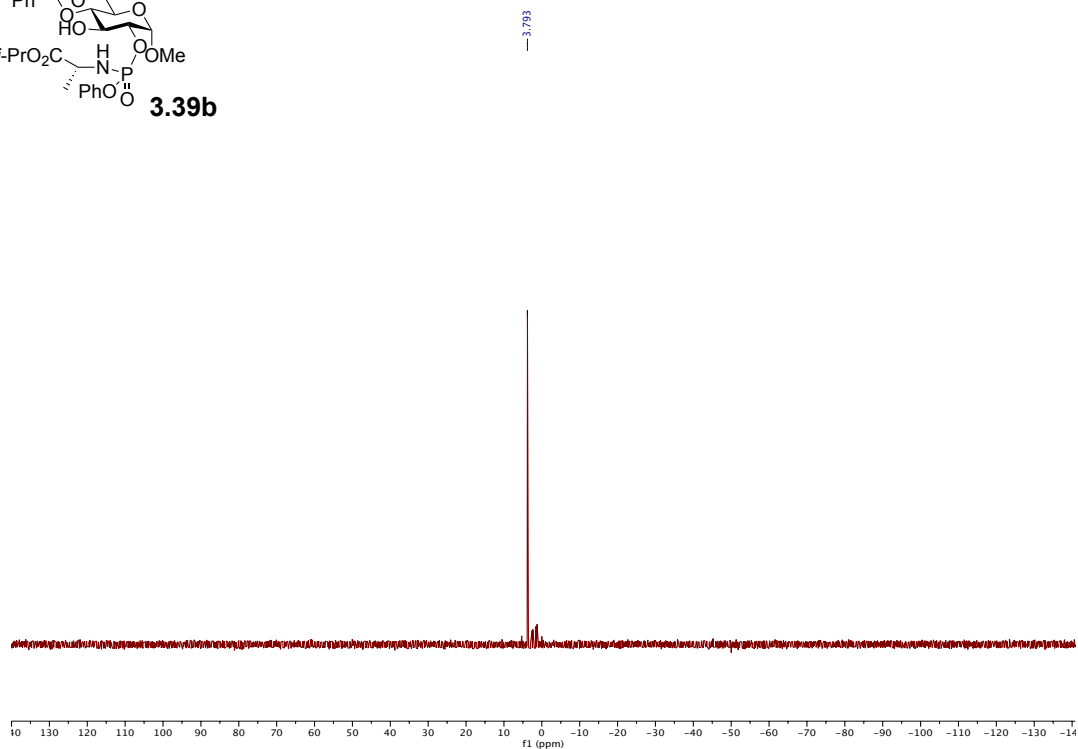
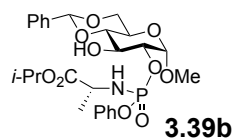
3.39a

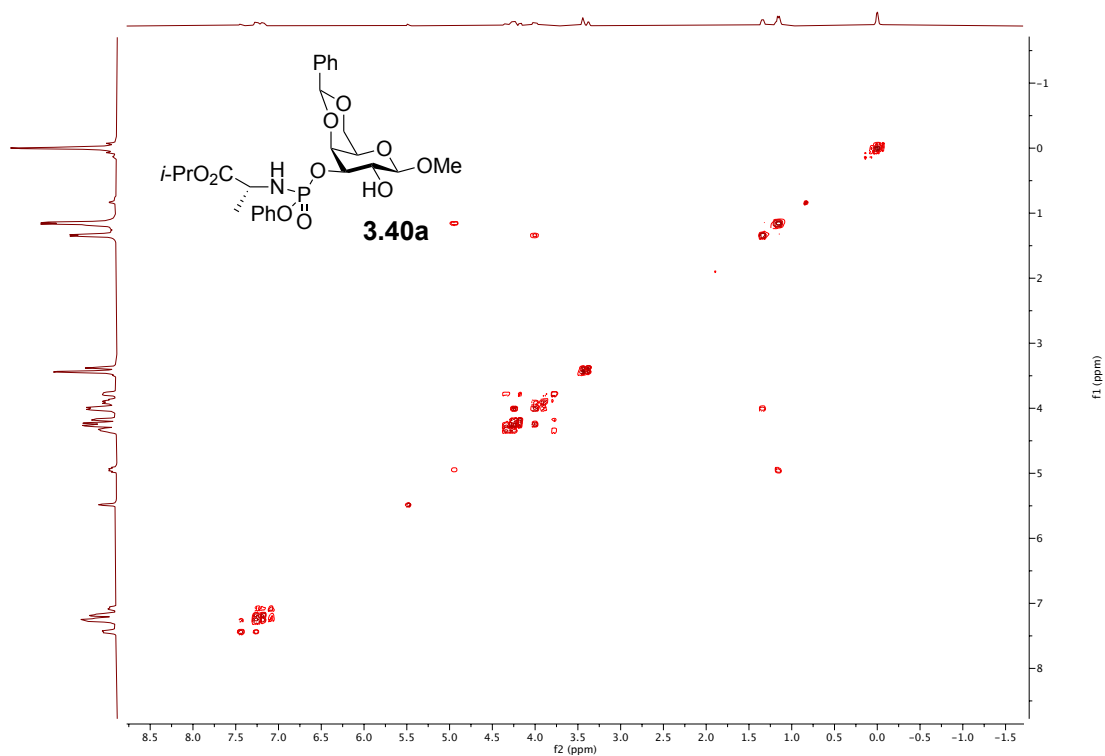
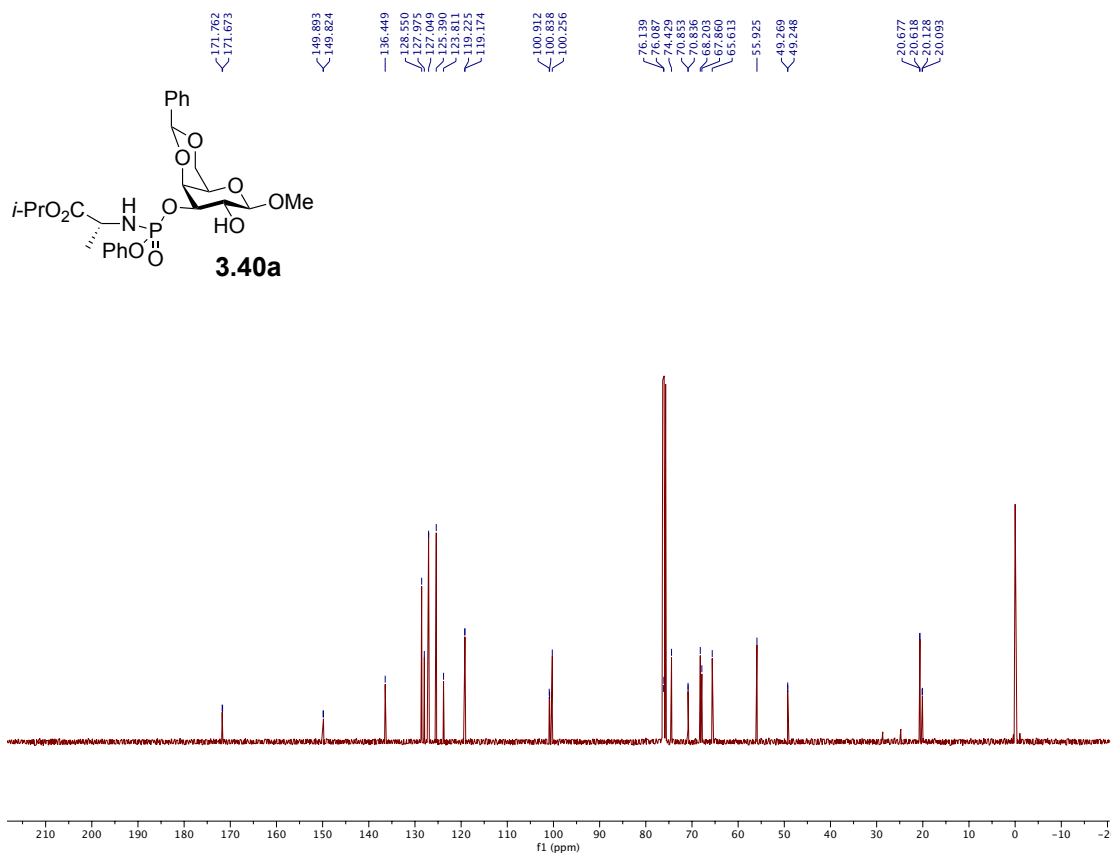


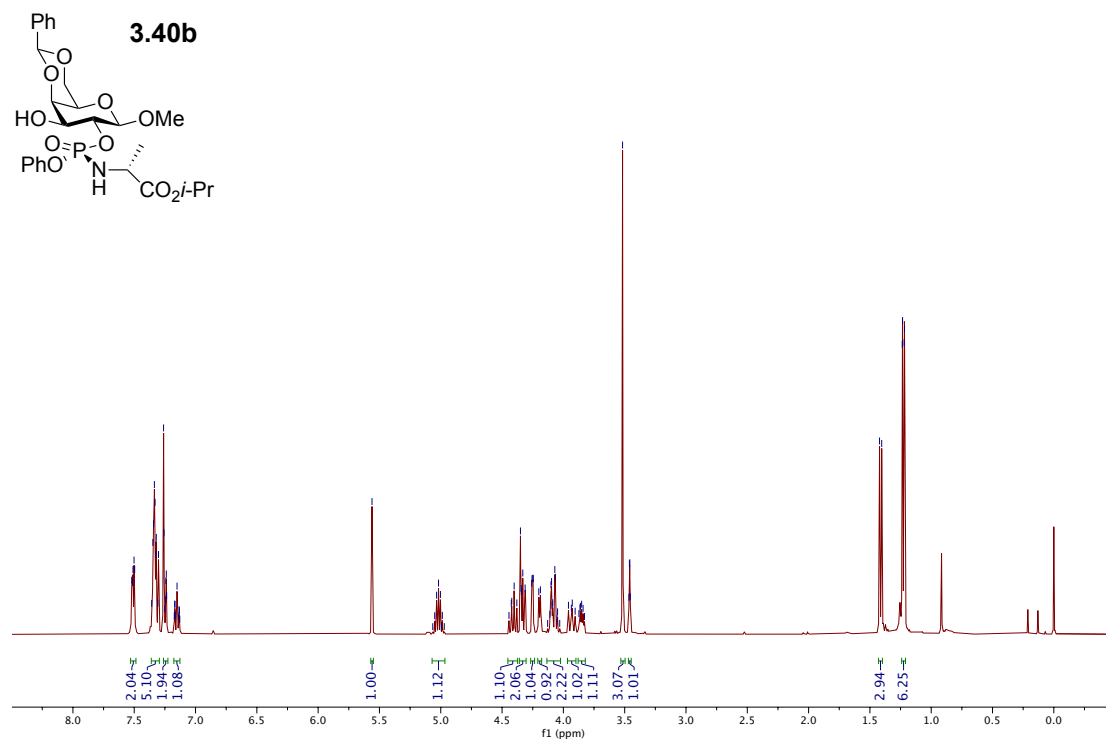
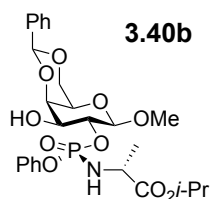
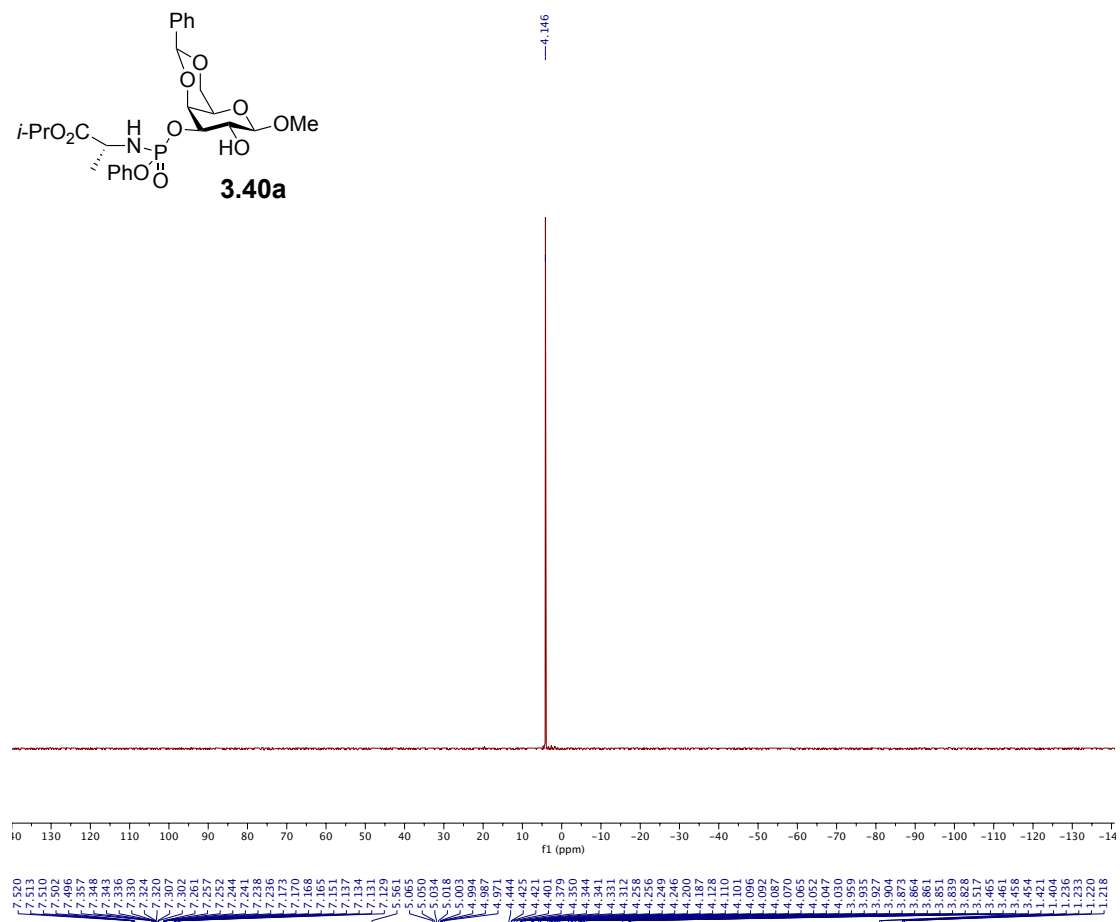
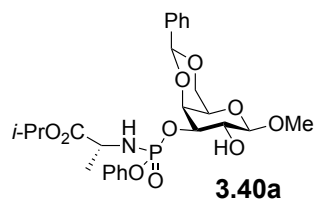
3.39b

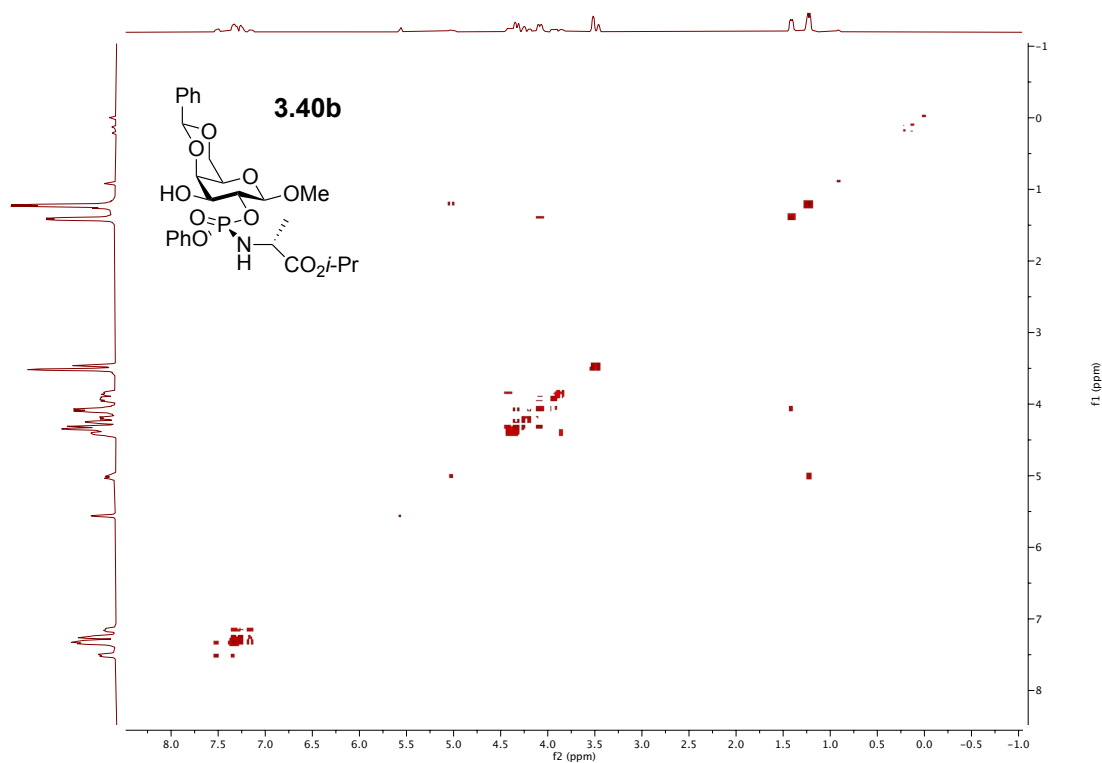
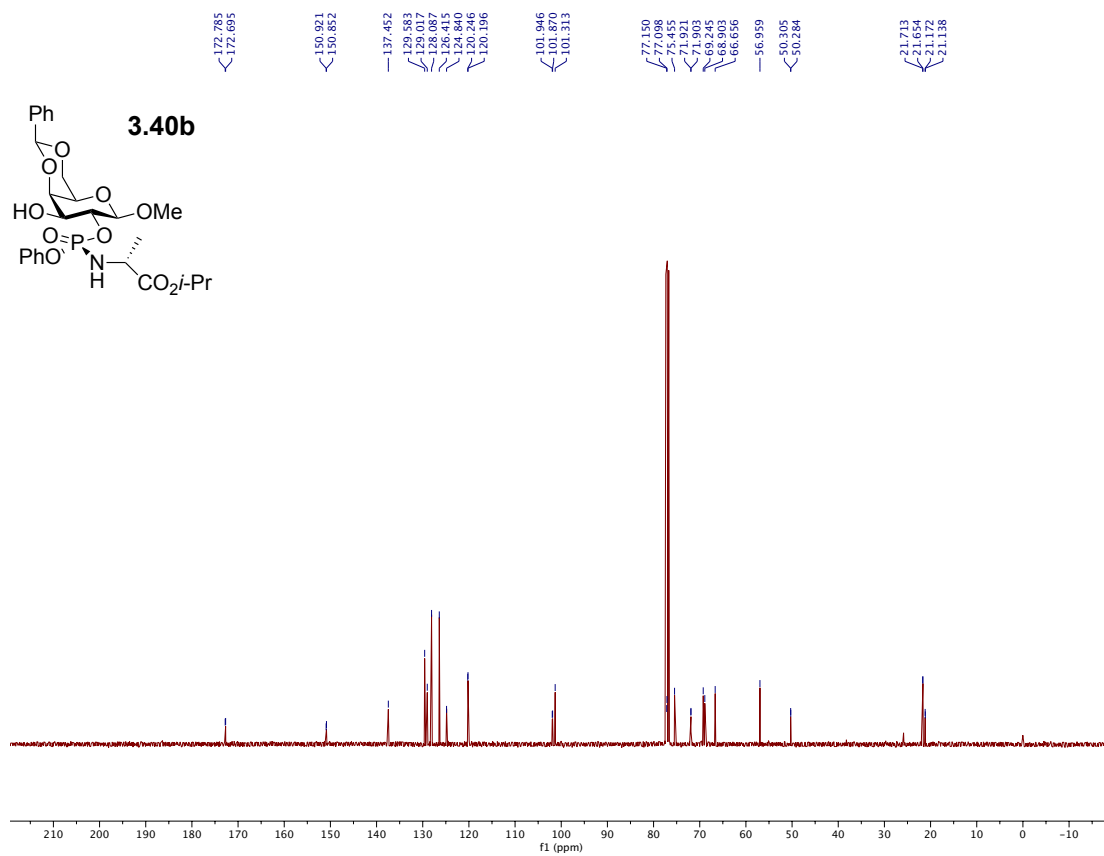


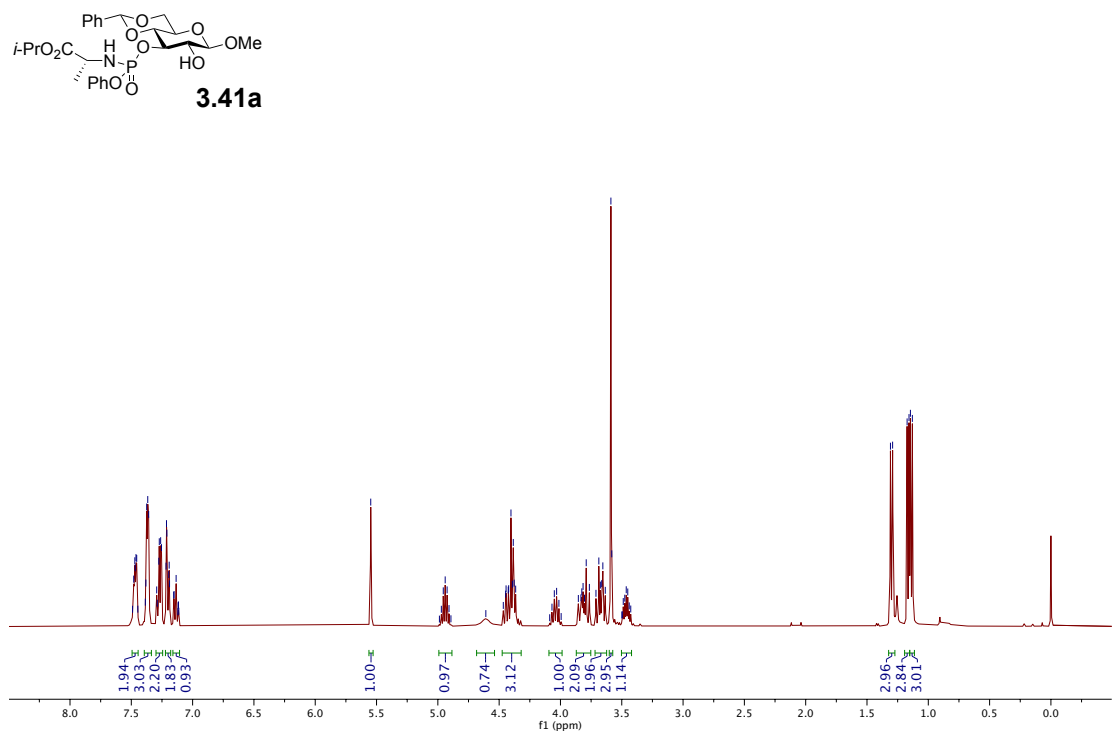
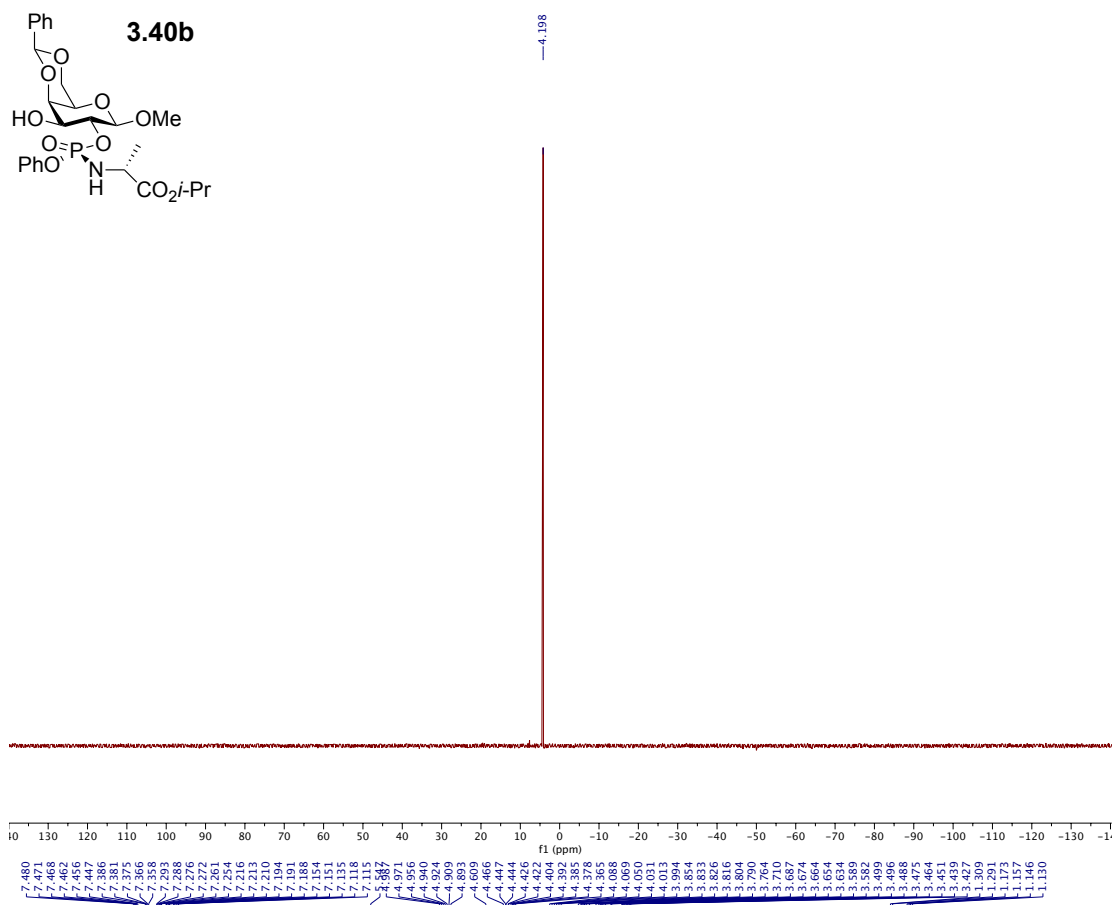


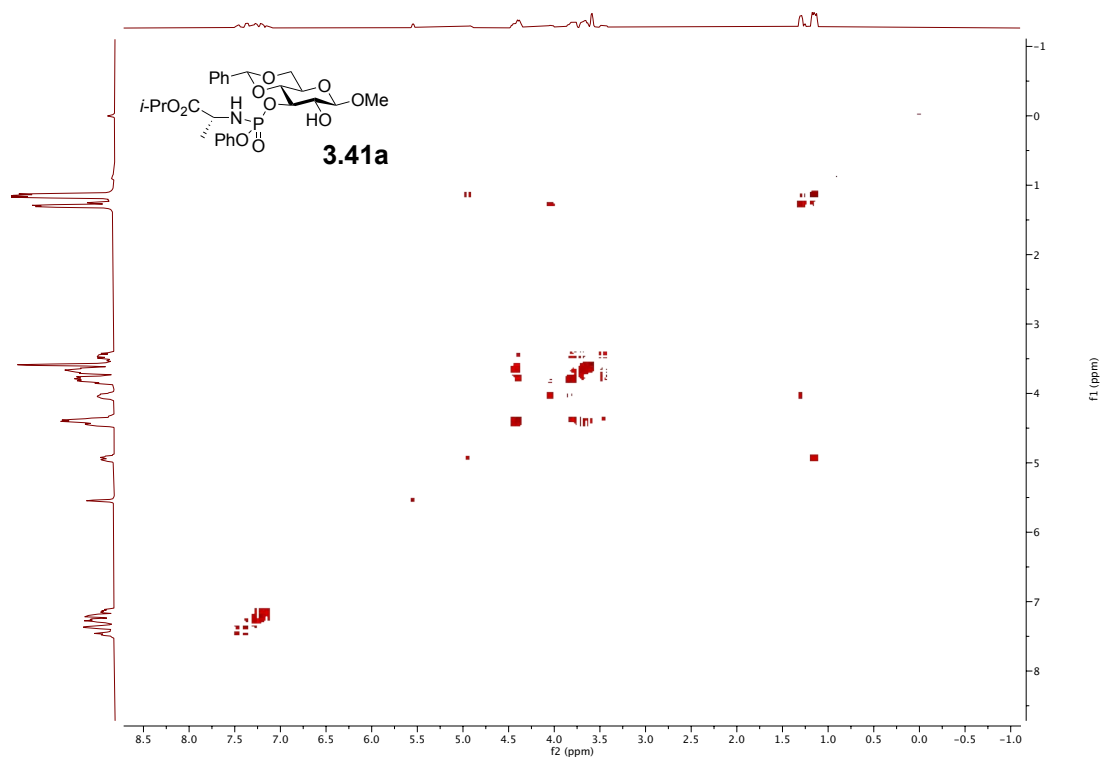
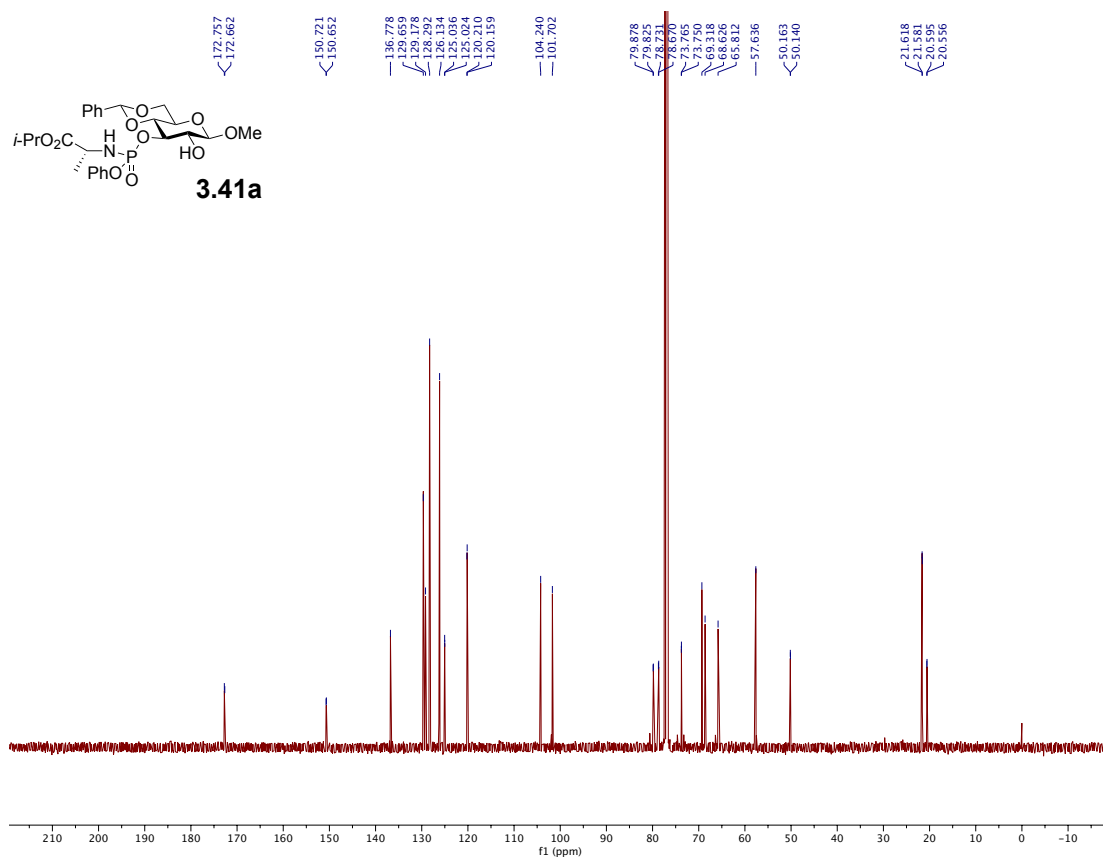


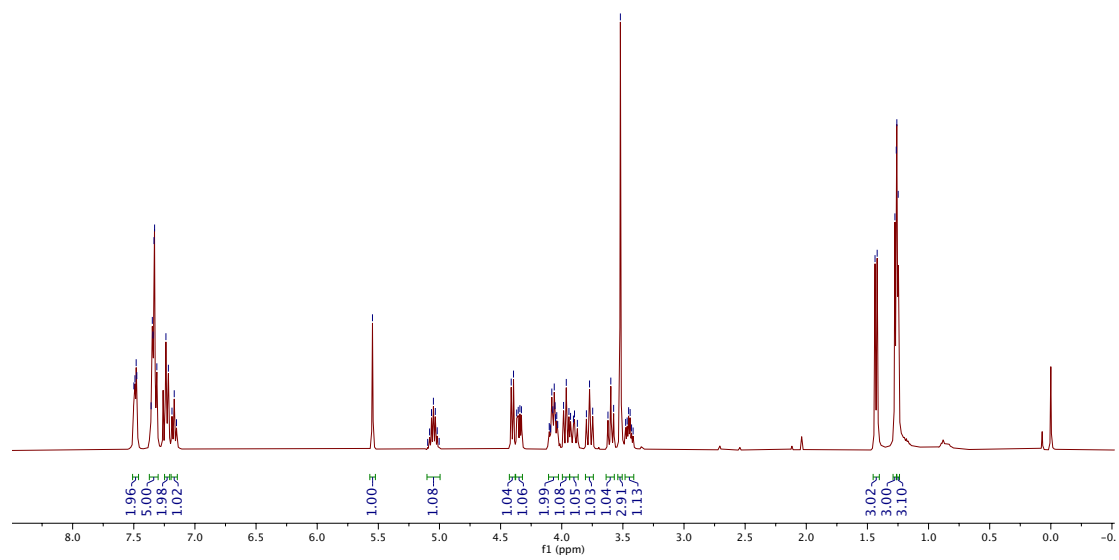
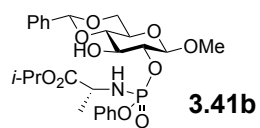
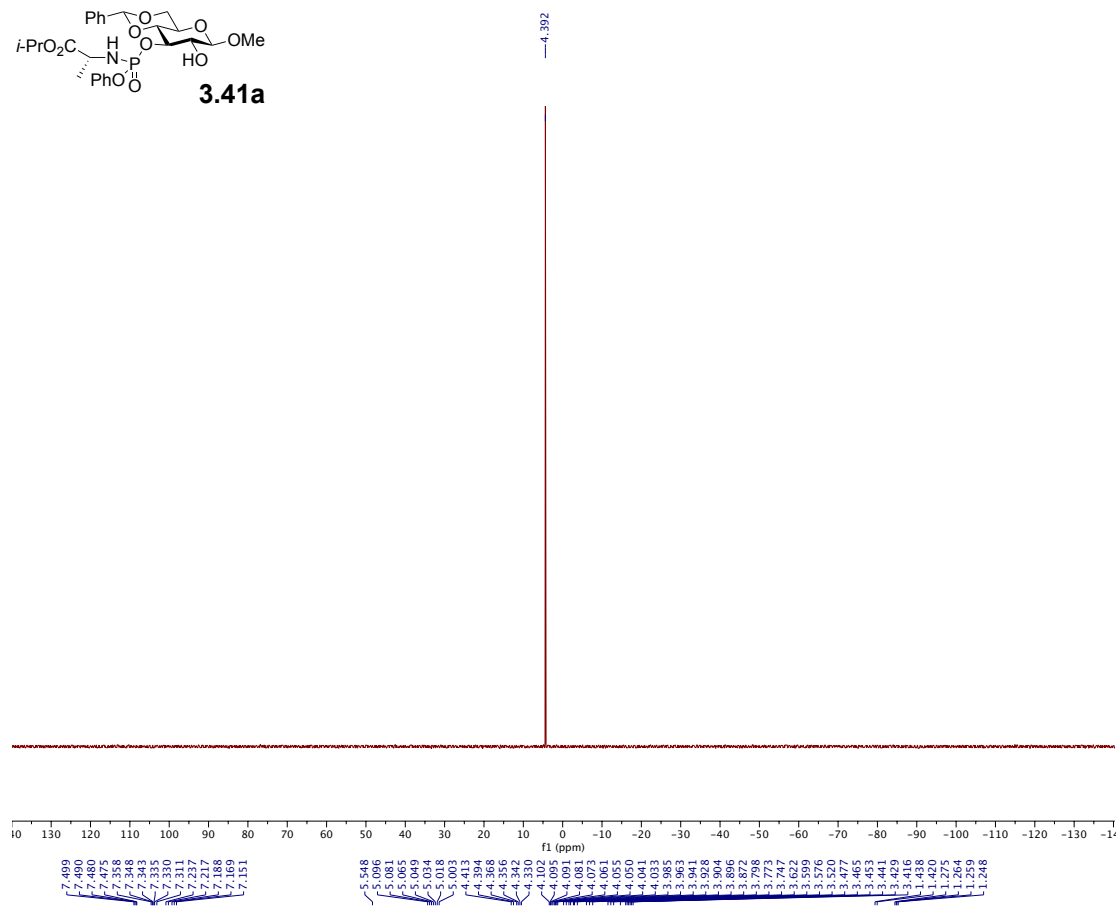
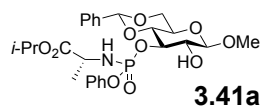


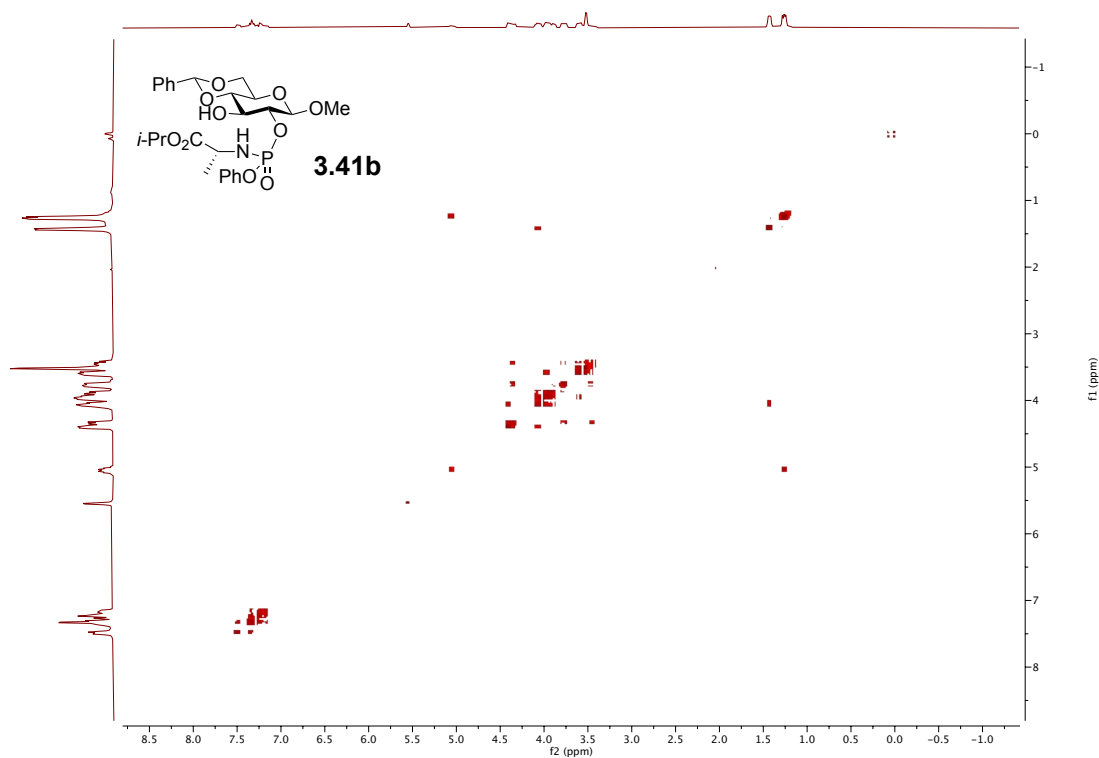
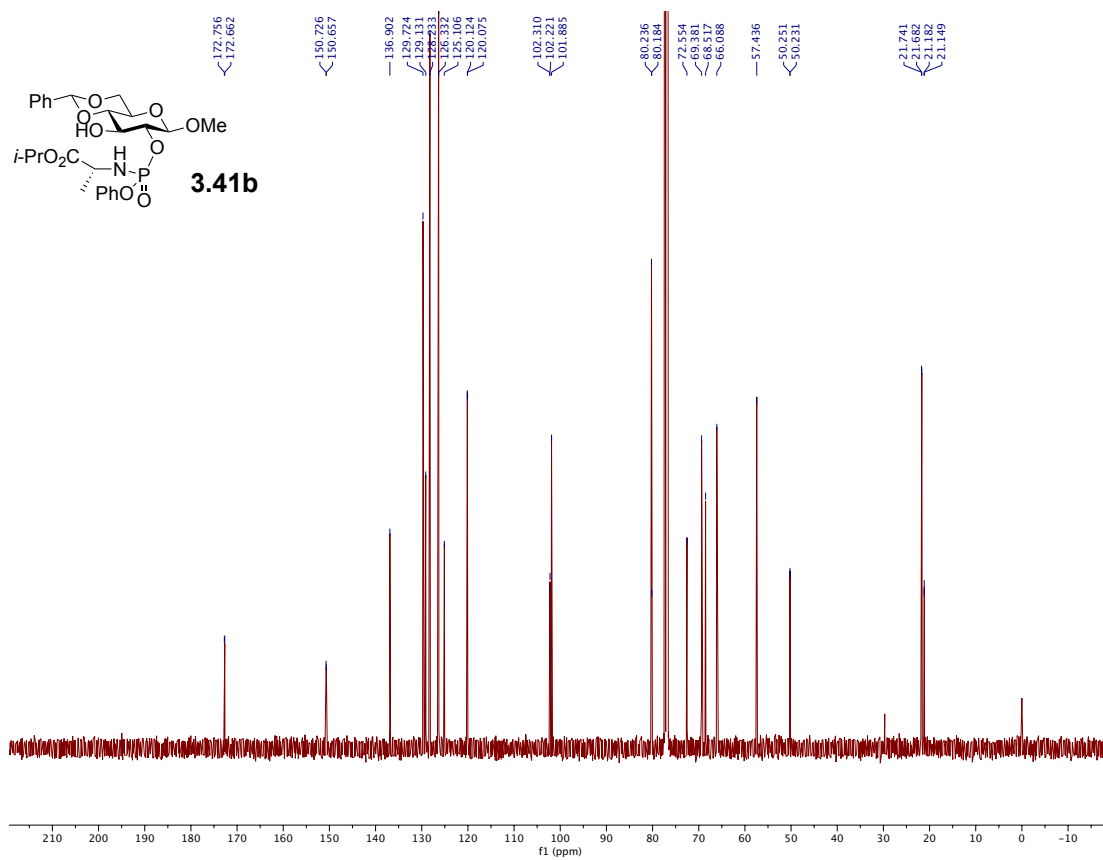


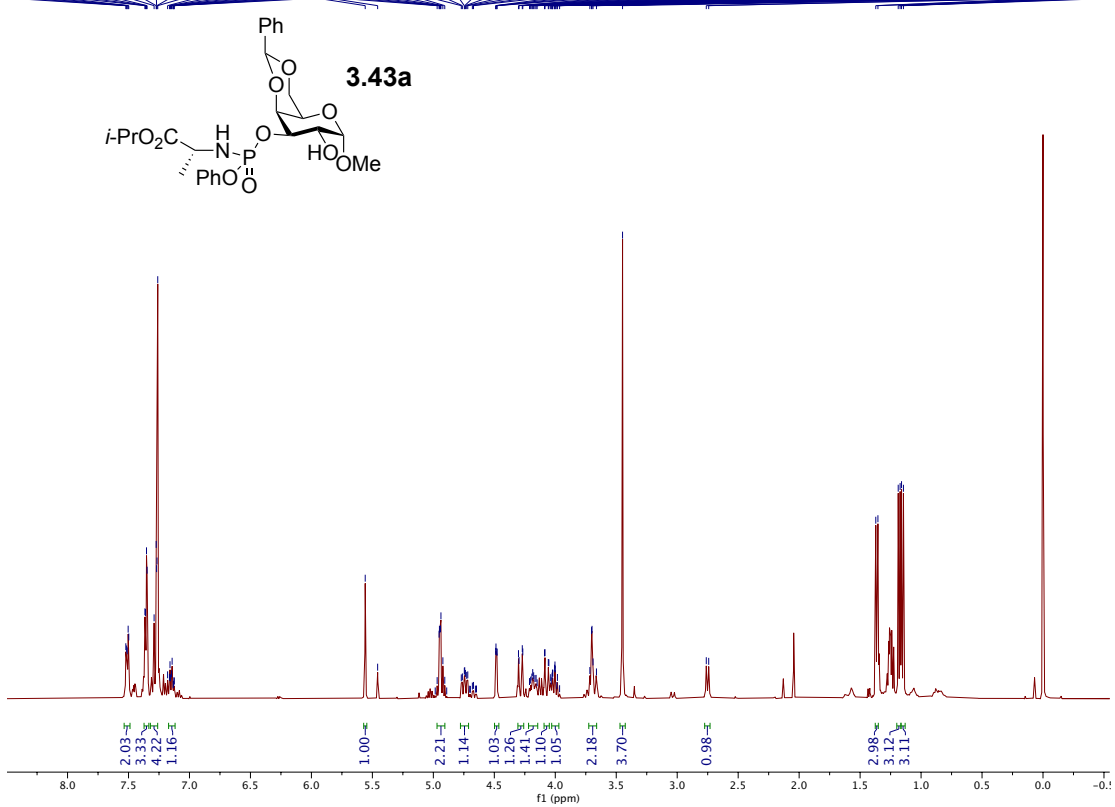
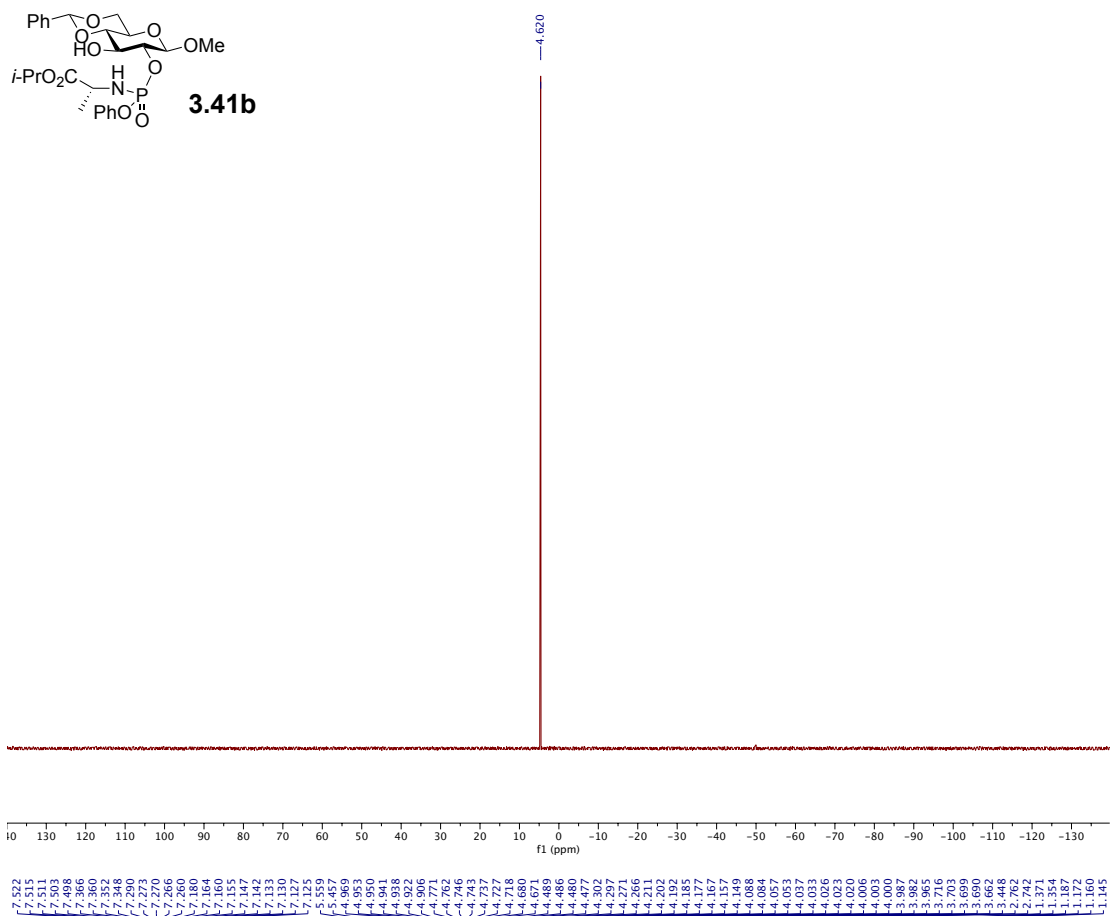


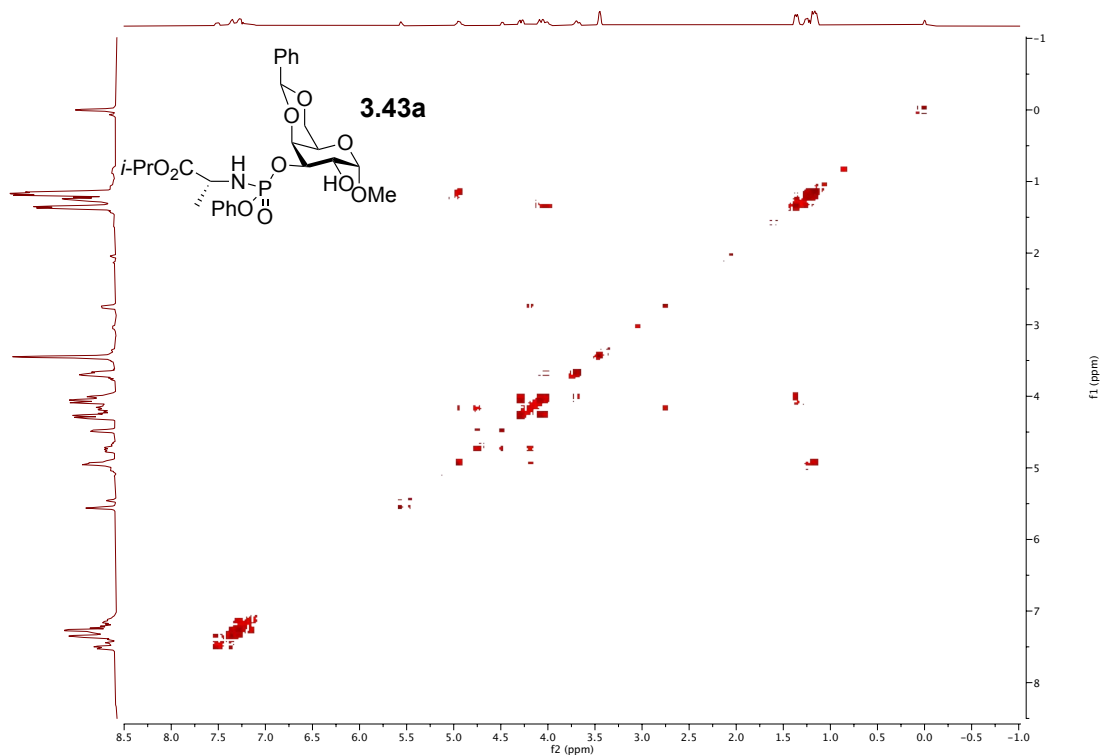
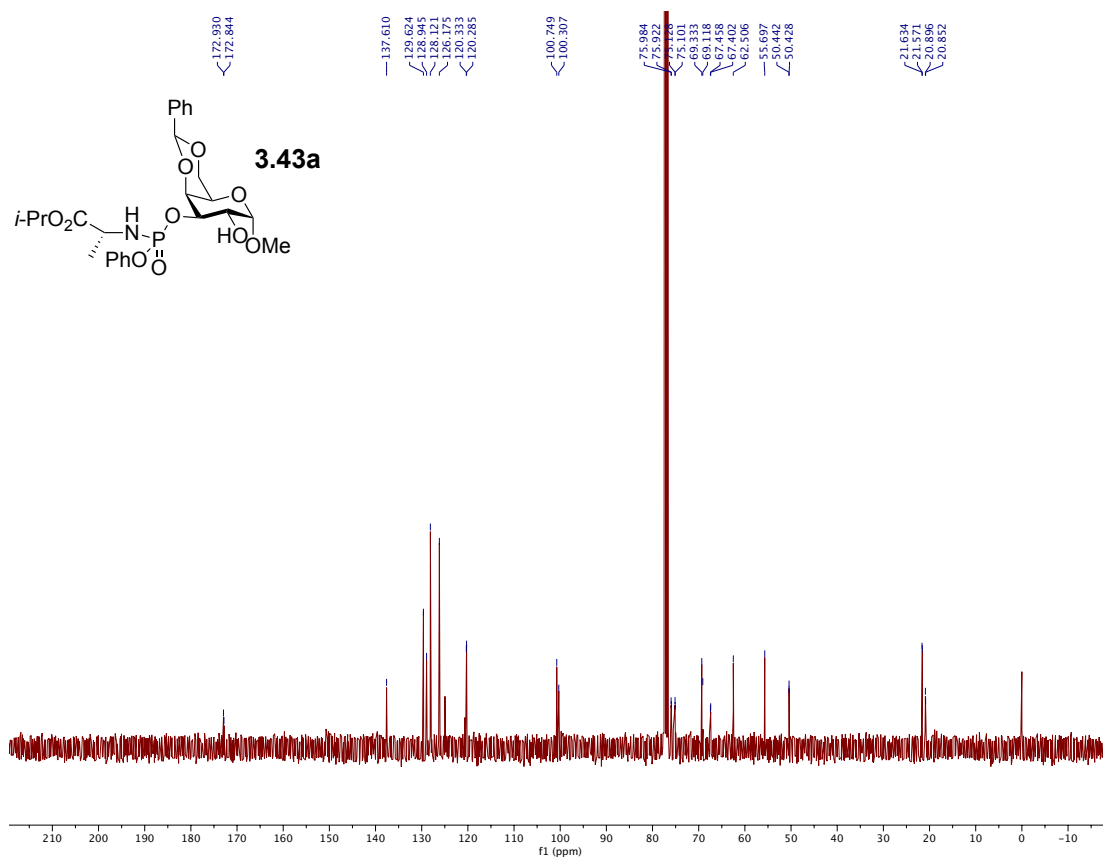


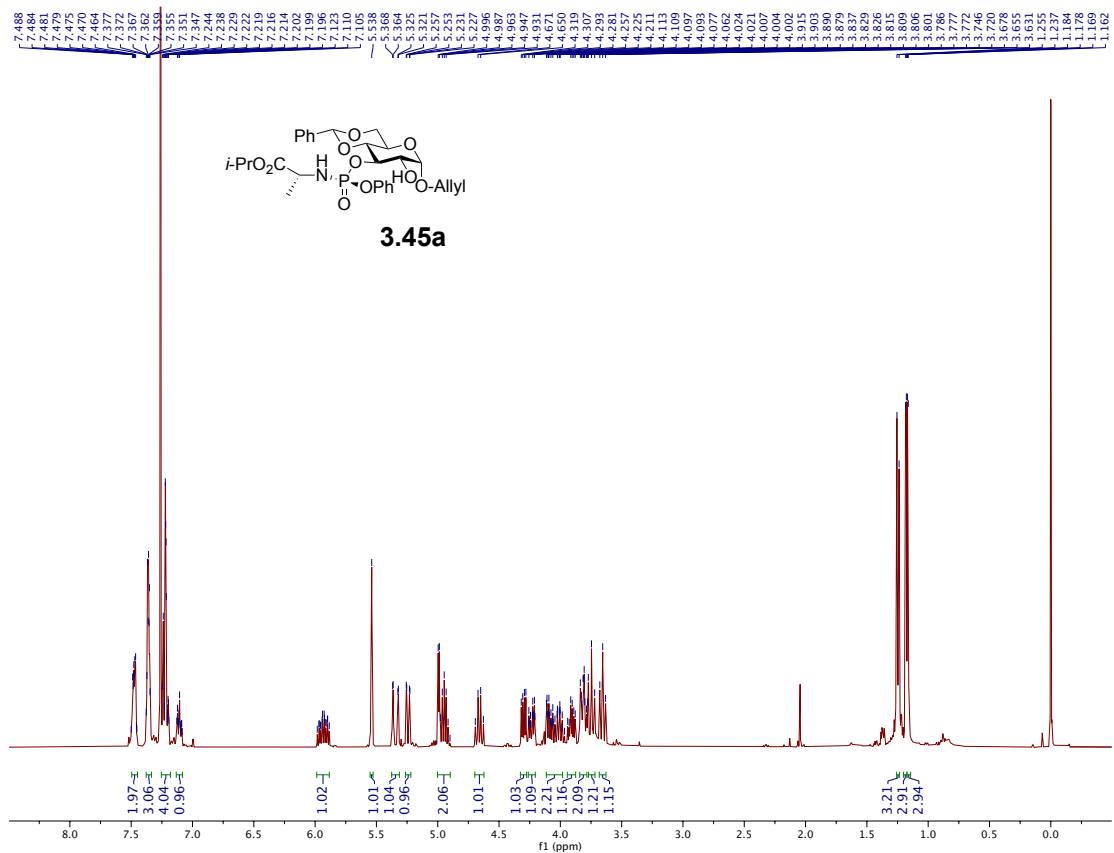
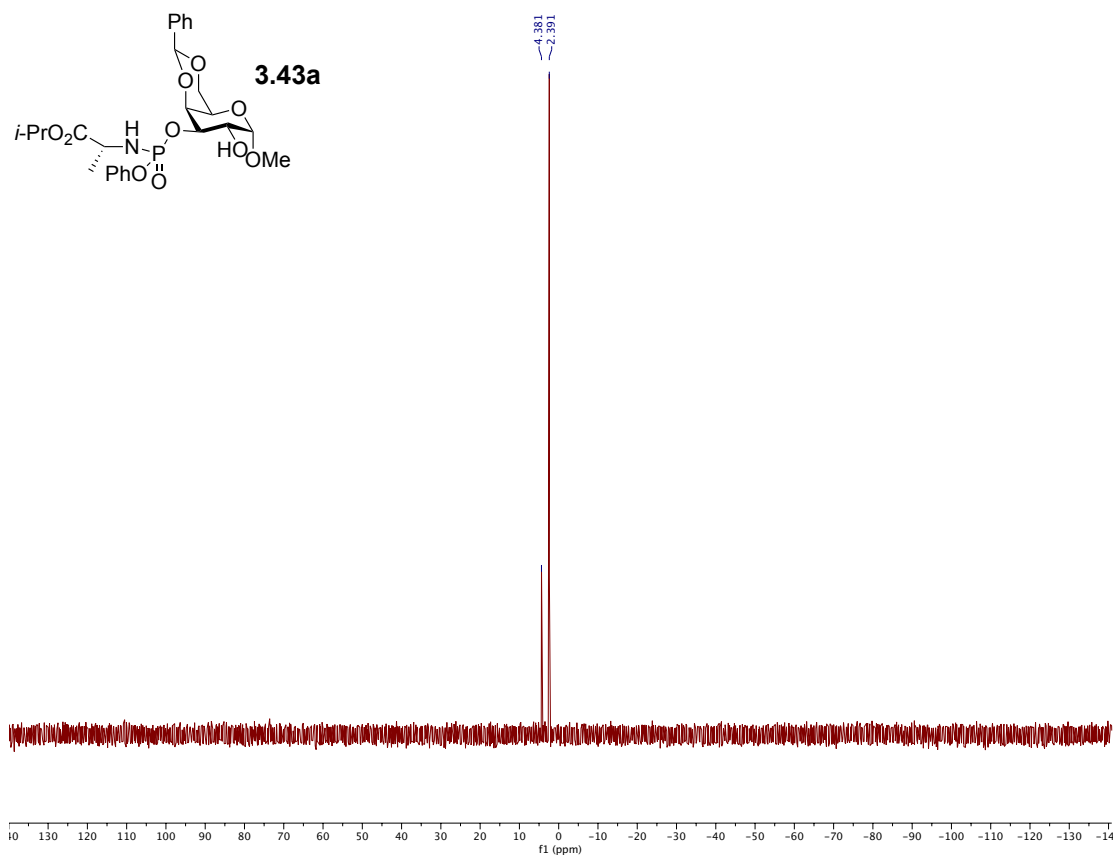


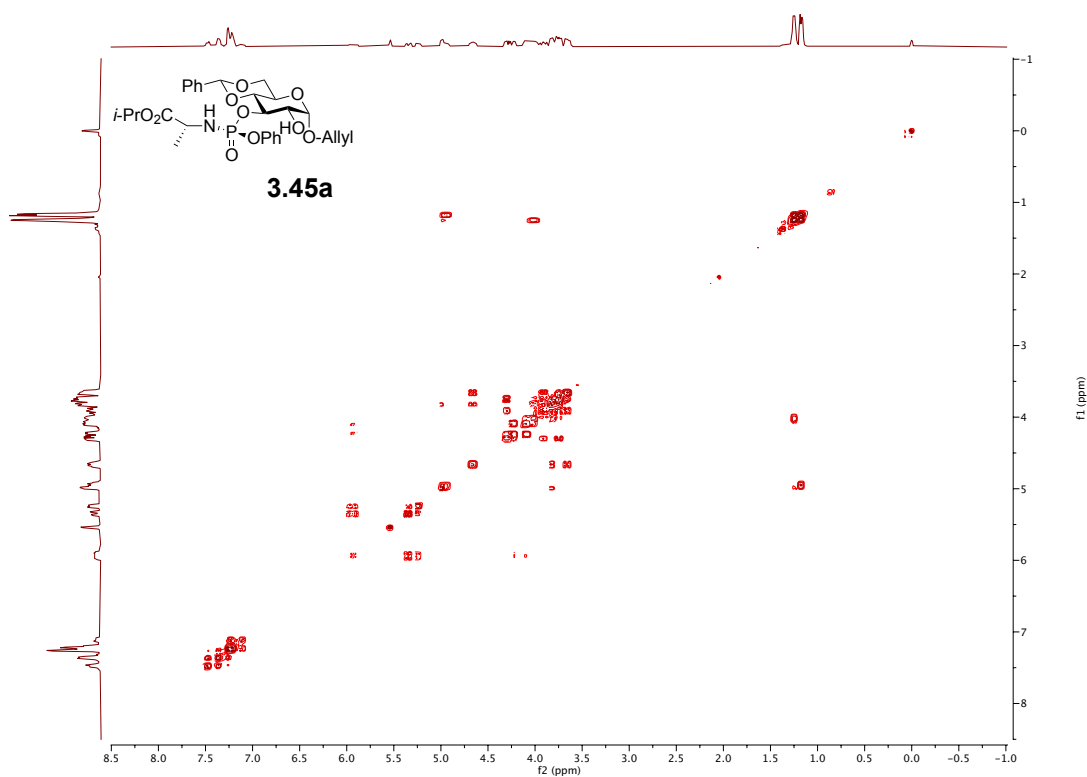
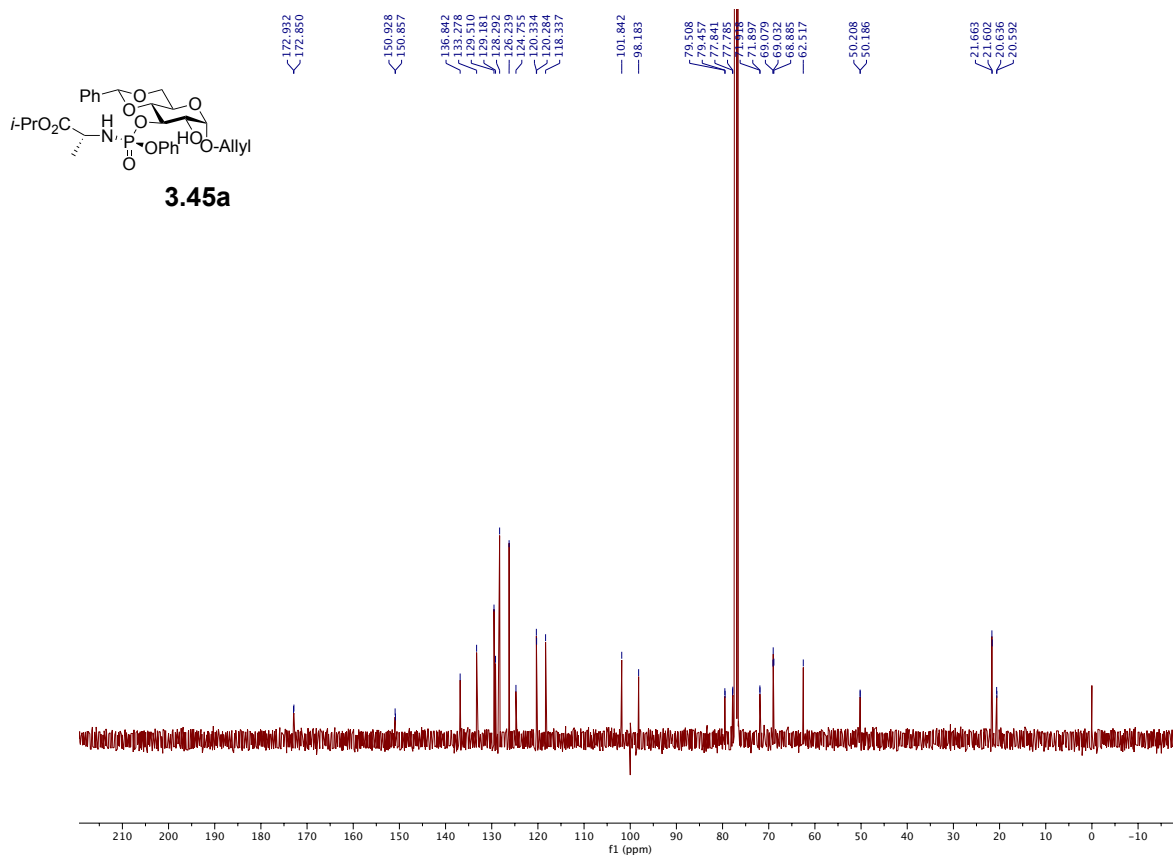


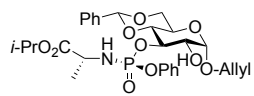




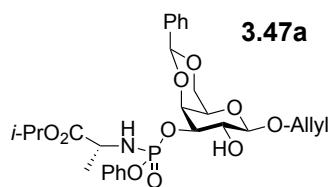
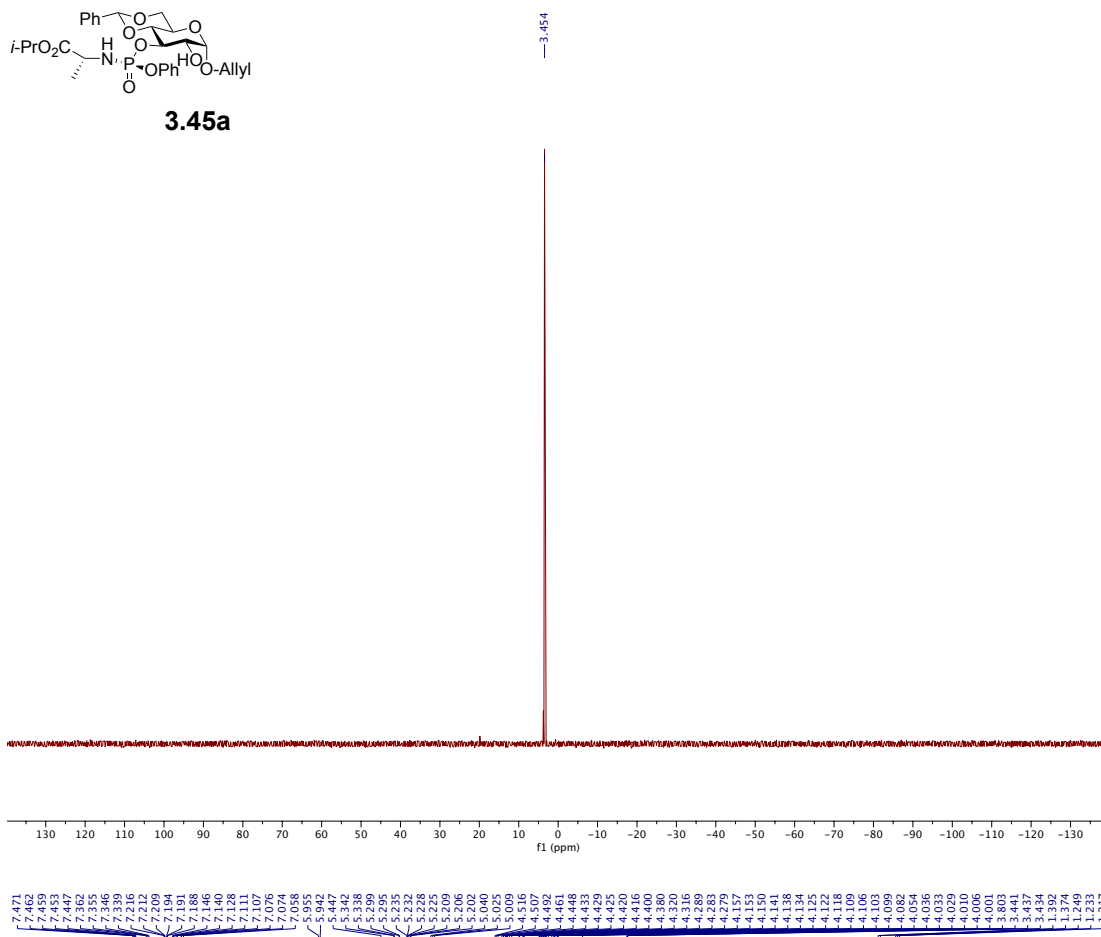




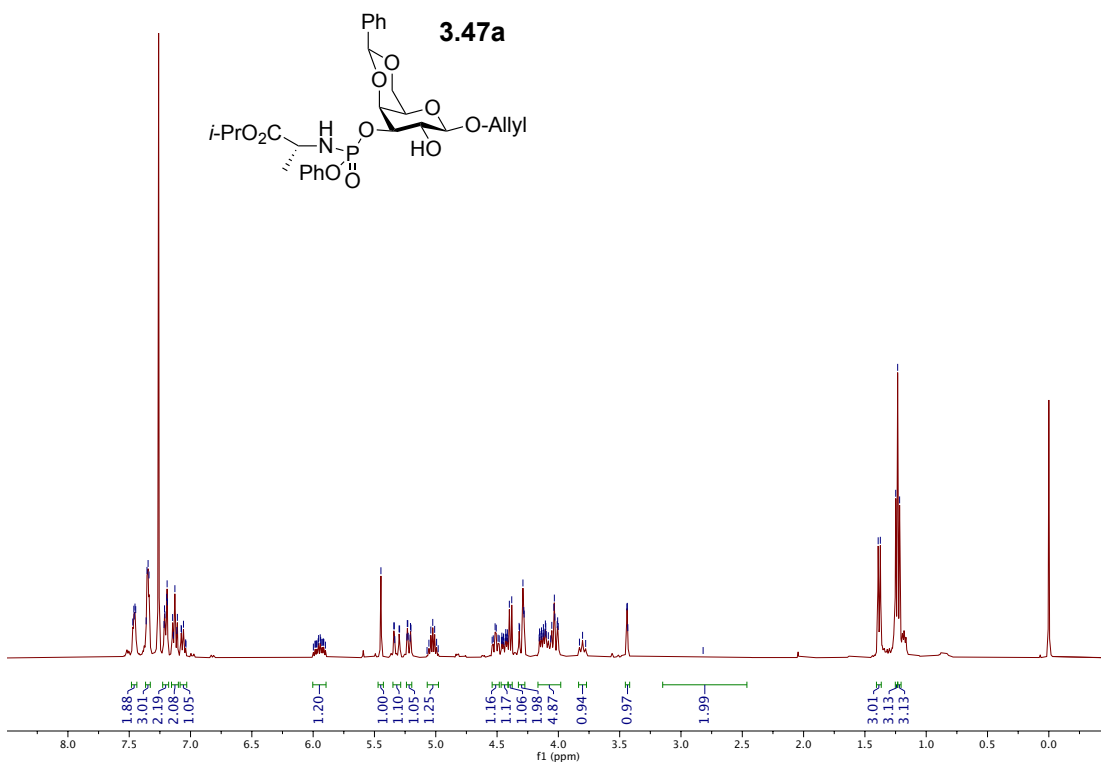


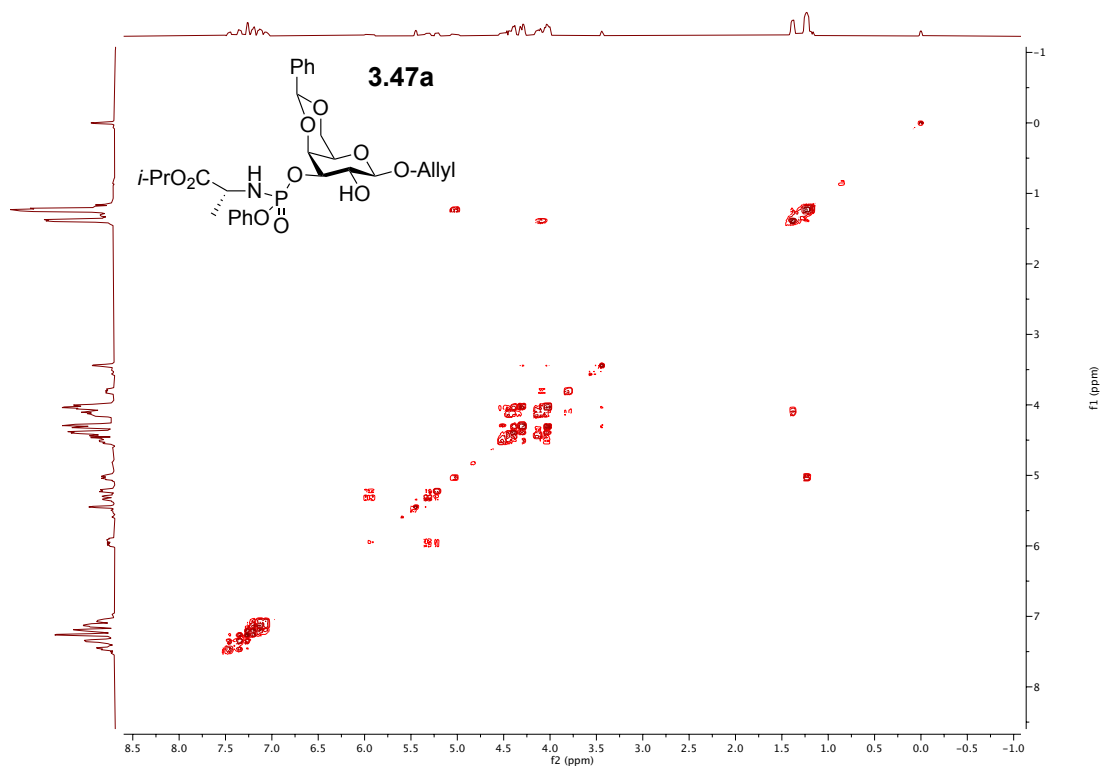
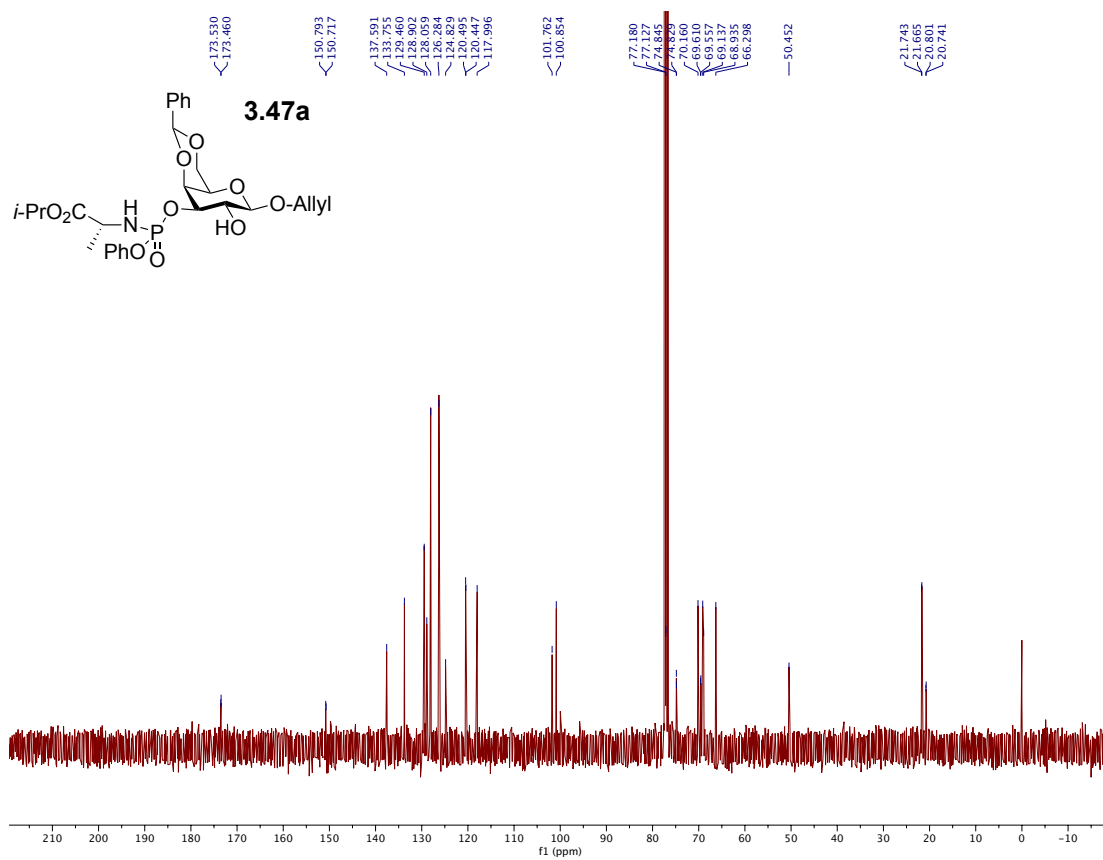


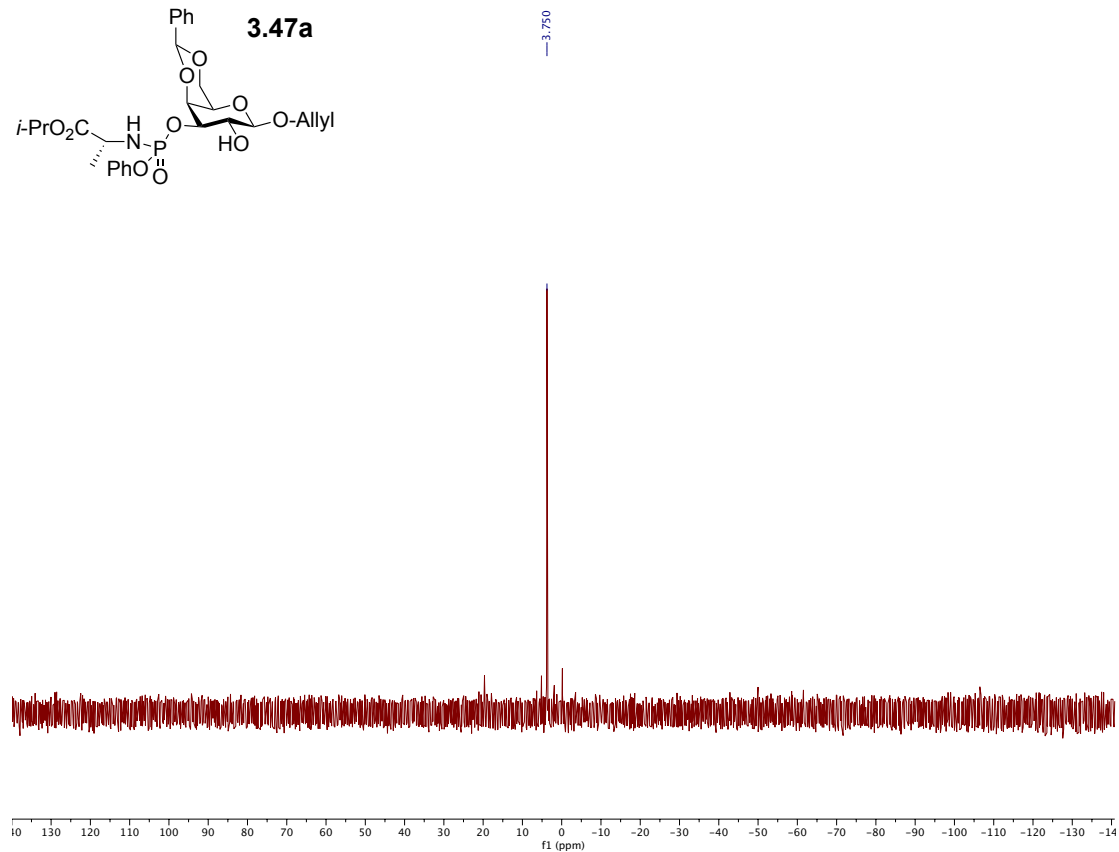
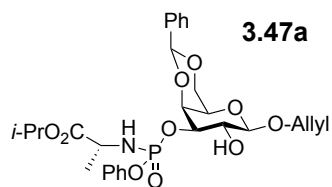
3.45a



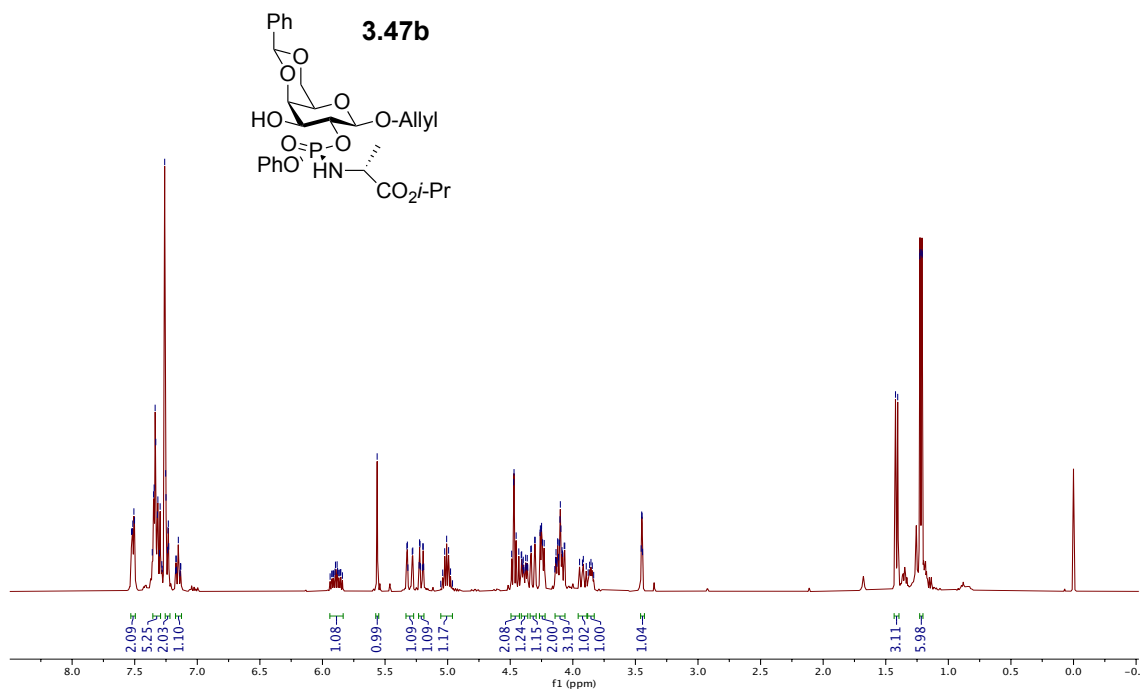
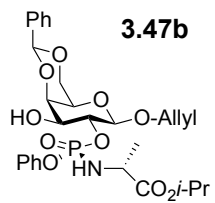
3.47a

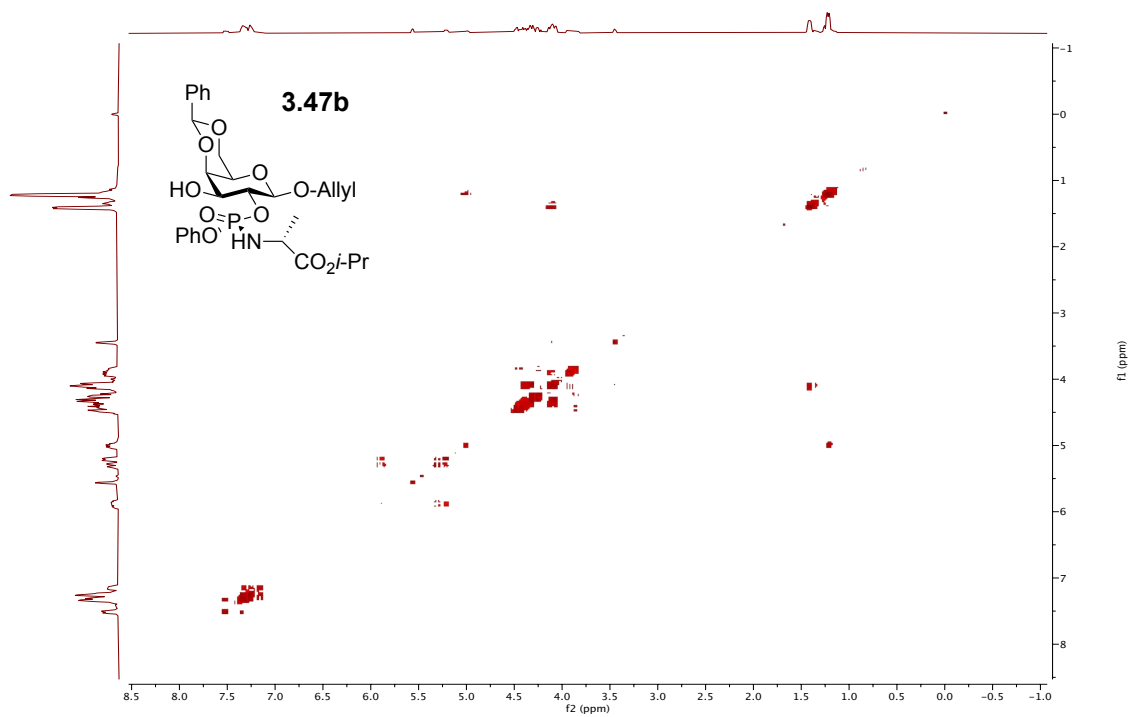
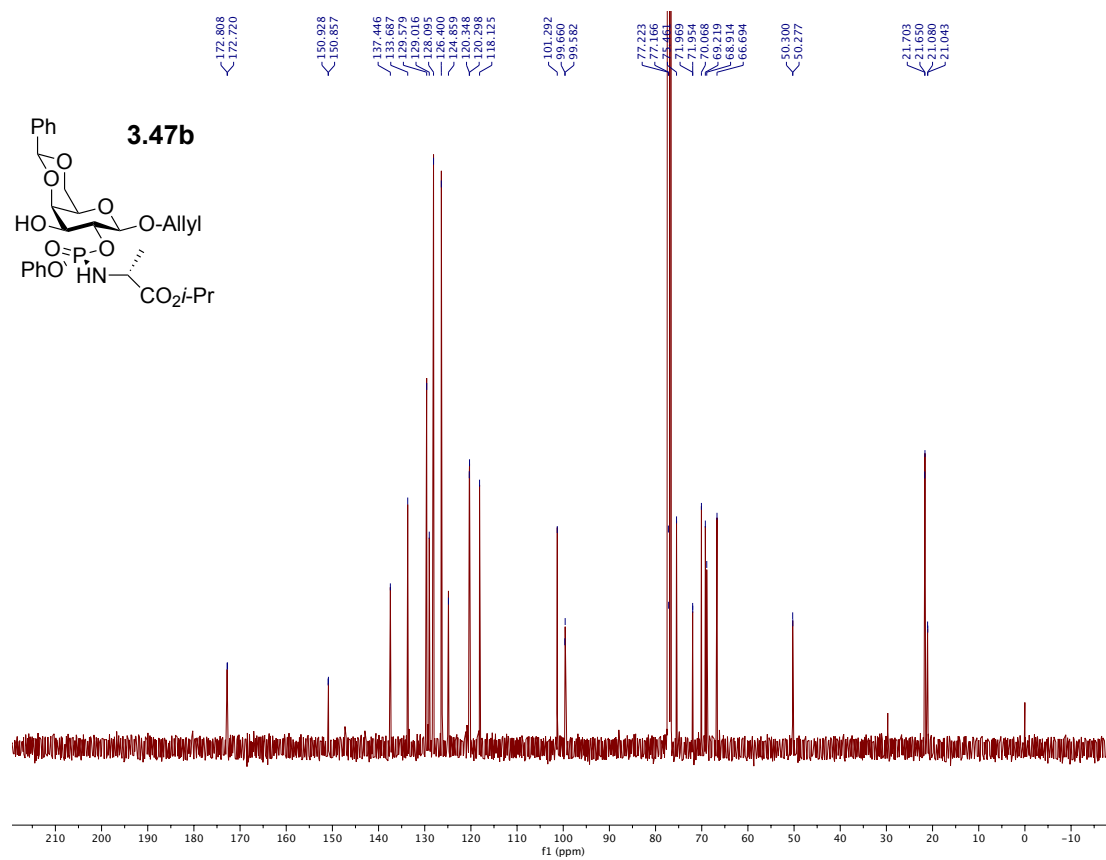


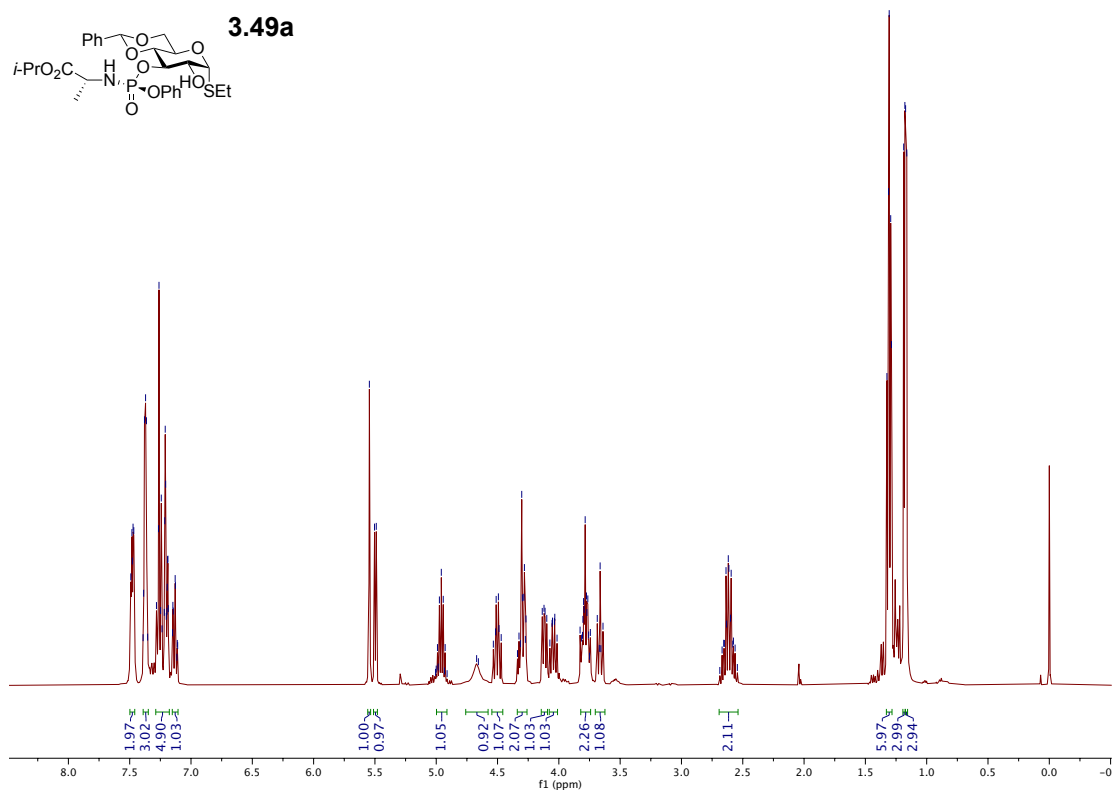
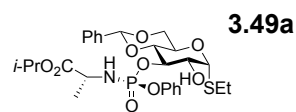
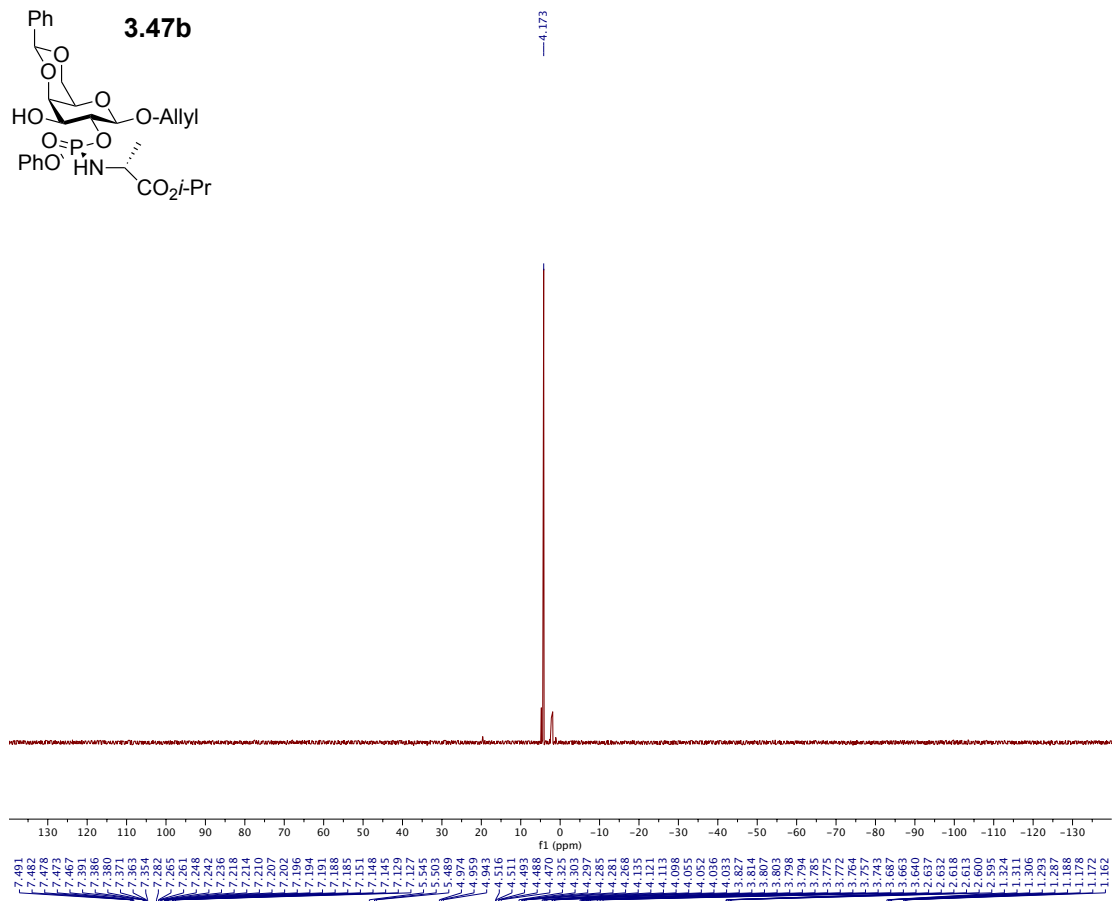
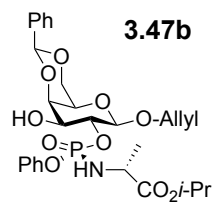


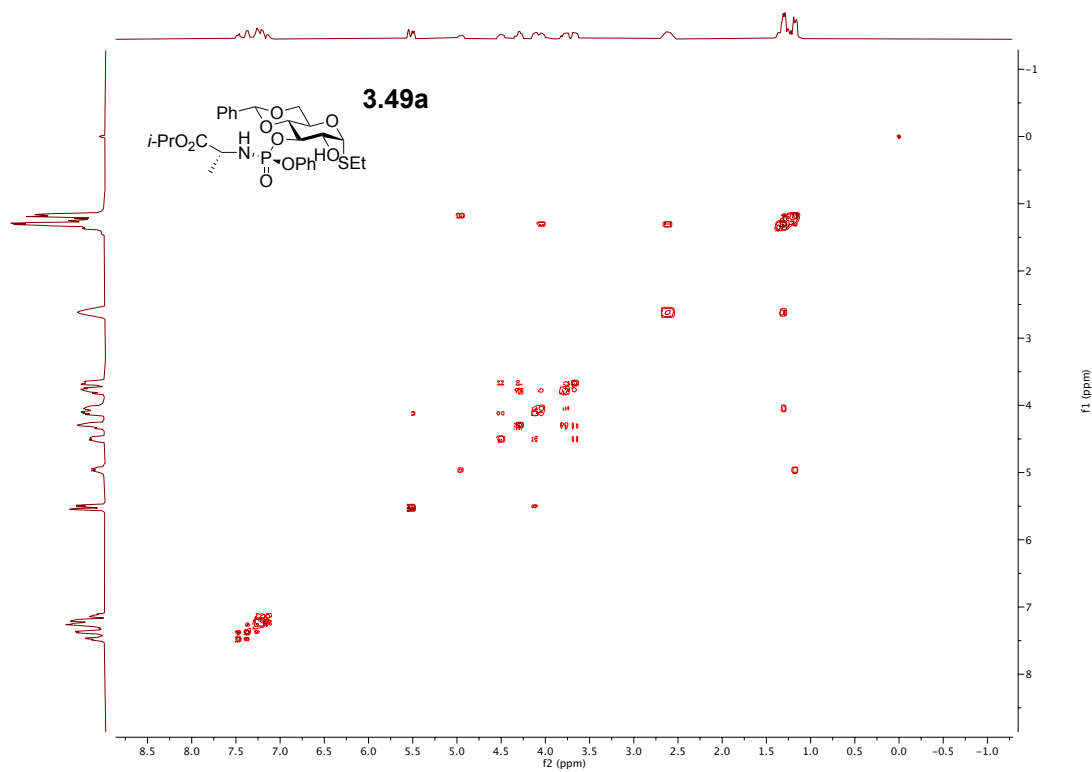
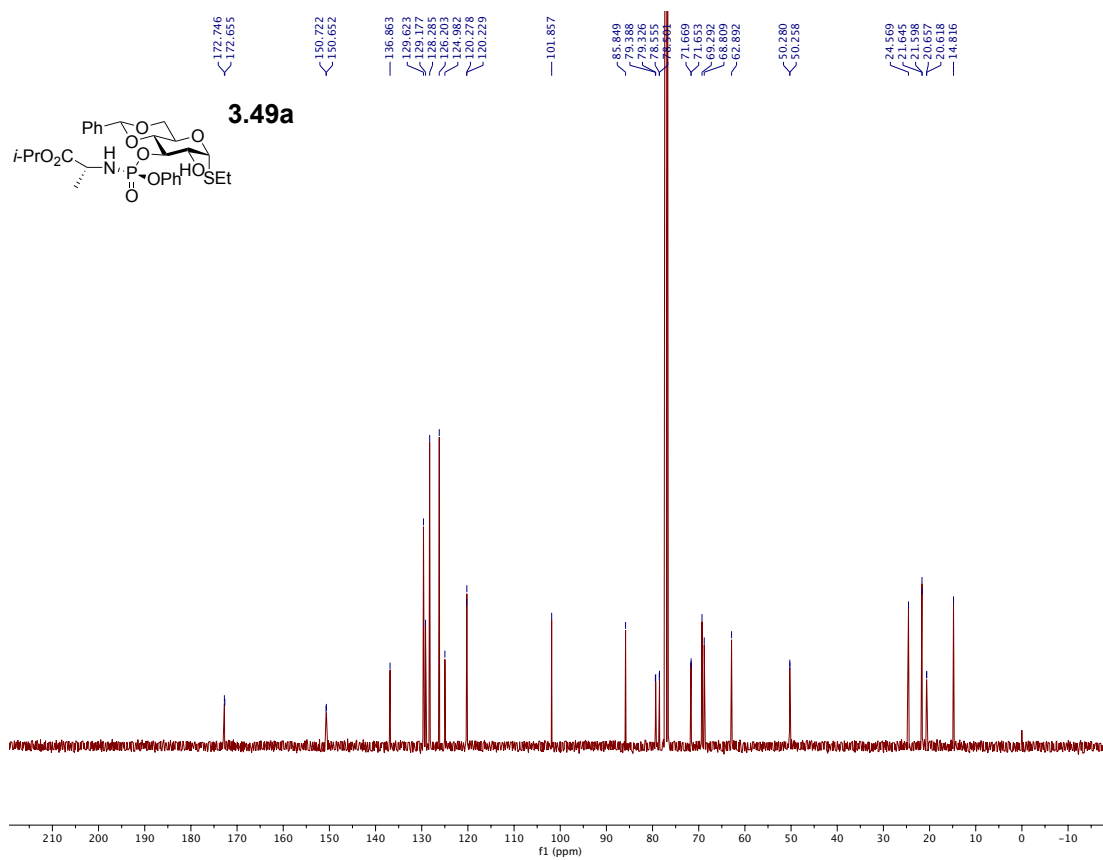


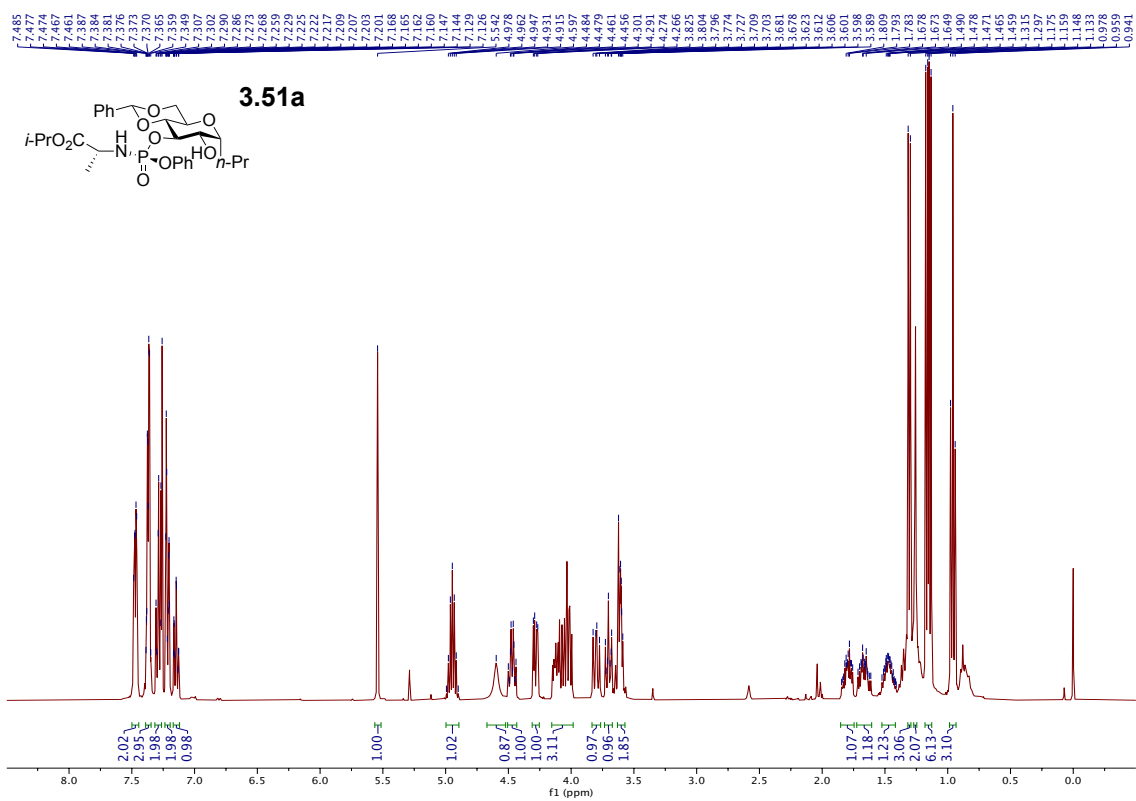
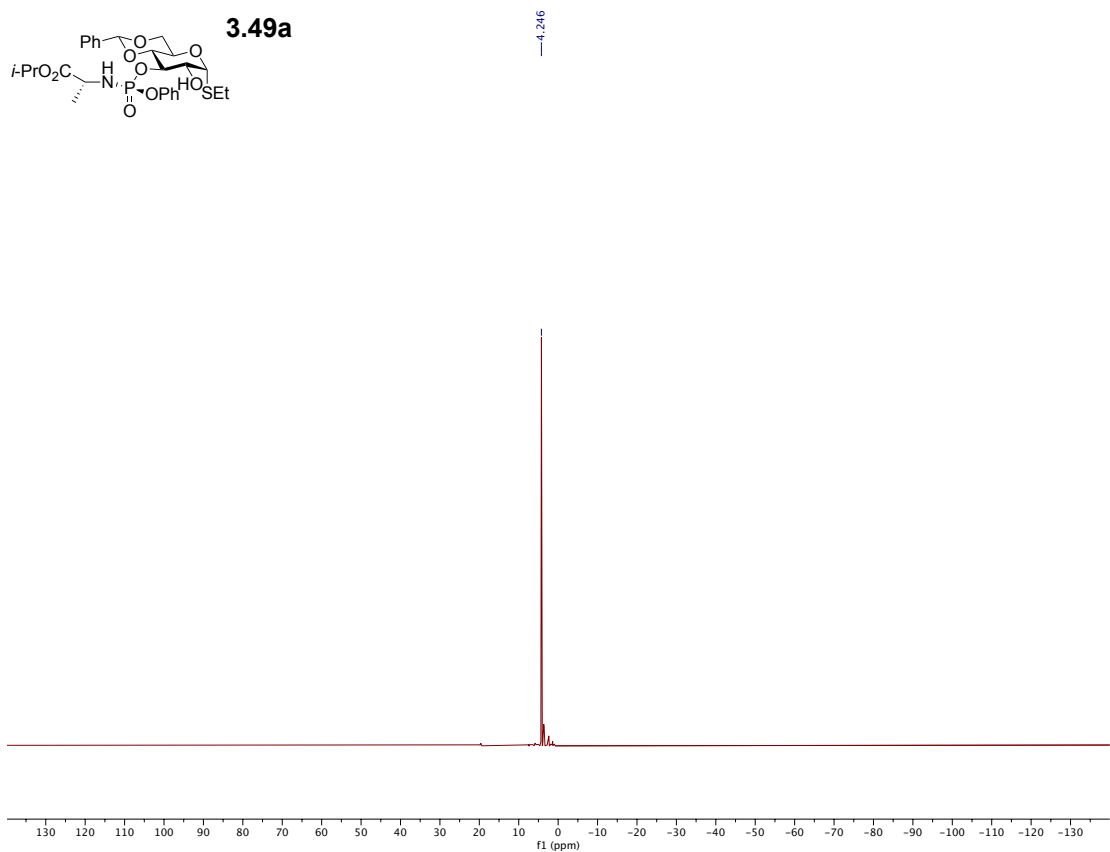
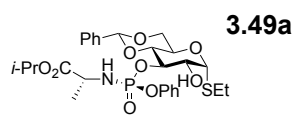
7.526
7.519
7.515
7.507
7.501
7.359
7.349
7.337
7.332
7.319
7.315
7.297
7.283
7.261
7.253
7.253
7.237
7.234
7.231
7.228
7.218
7.168
7.151
5.563
5.526
5.522
5.522
5.278
5.224
5.221
5.198
5.198
5.1024
5.008
4.992
4.489
4.476
4.476
4.453
4.432
4.412
4.405
4.402
4.396
4.377
4.364
4.364
4.335
4.335
4.305
4.301
4.262
4.259
4.259
4.250
4.242
4.229
4.229
4.138
4.138
4.131
4.131
4.126
4.121
4.121
4.118
4.118
4.105
4.105
4.103
4.100
4.100
4.095
4.086
4.086
4.069
4.064
4.064
3.946
3.946
3.912
3.912
3.855
3.855
3.454
3.450
3.447
3.447
1.422
1.405
1.228
1.228
1.275
1.275
1.206
1.206

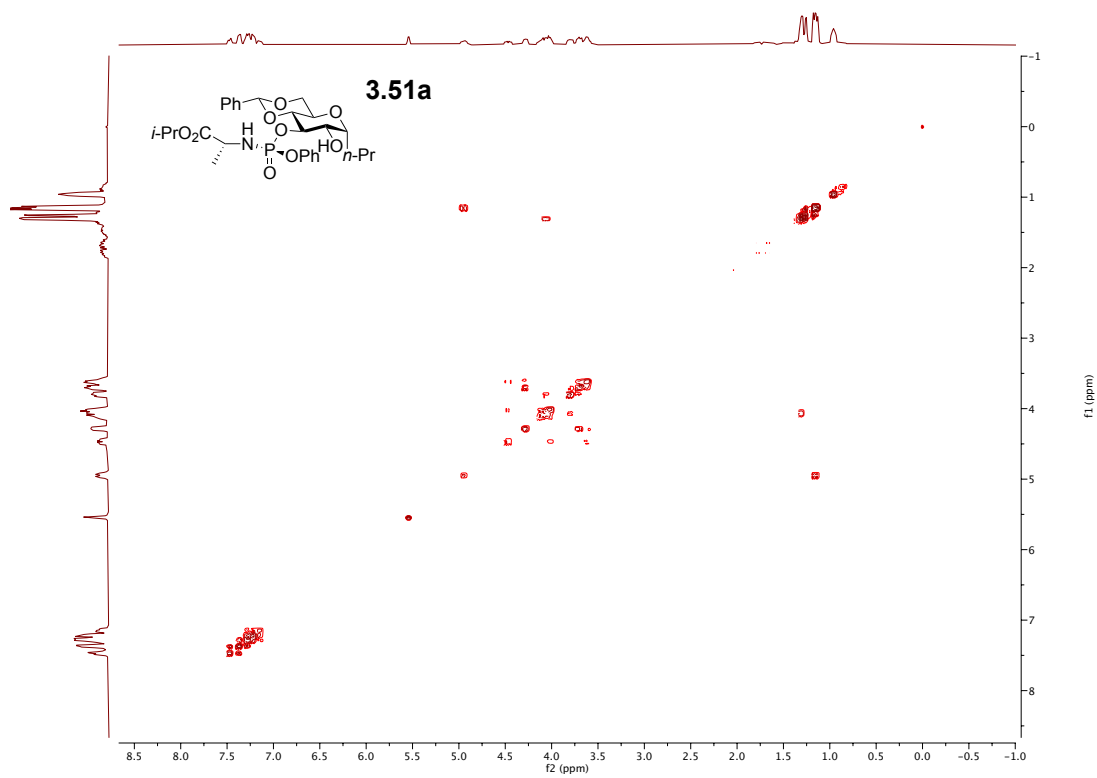
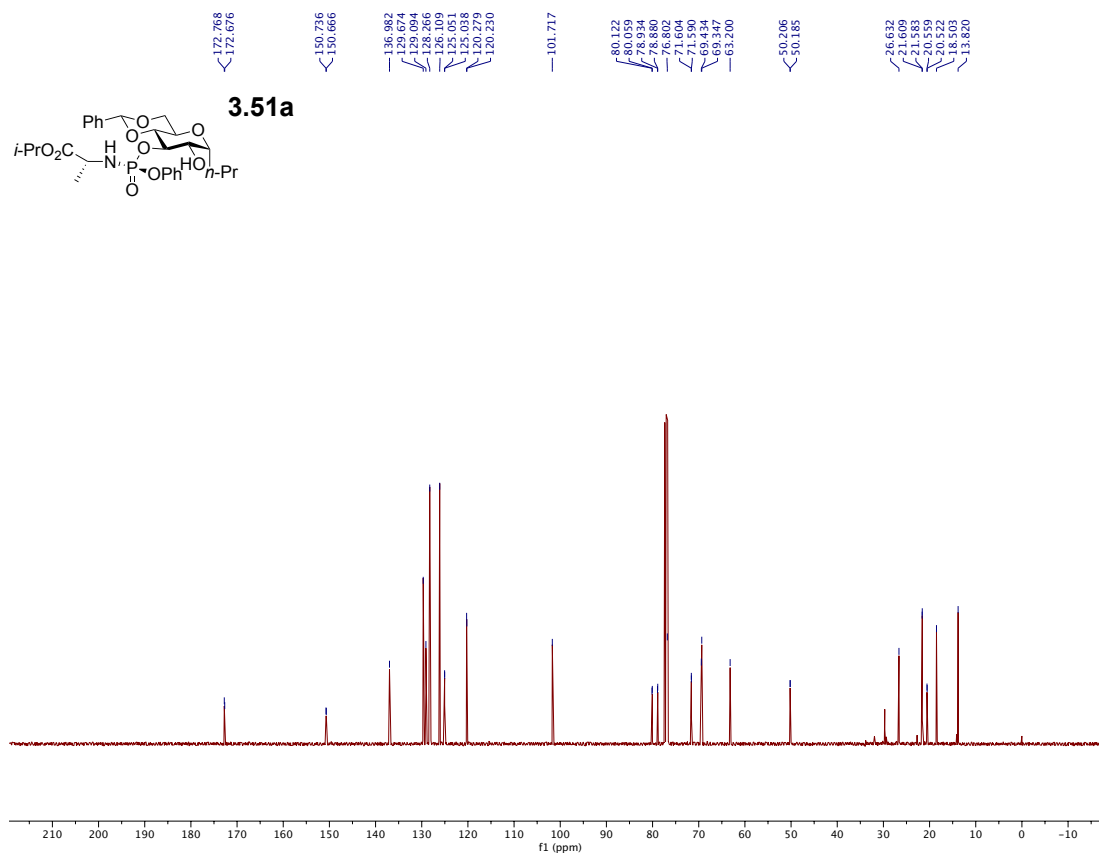


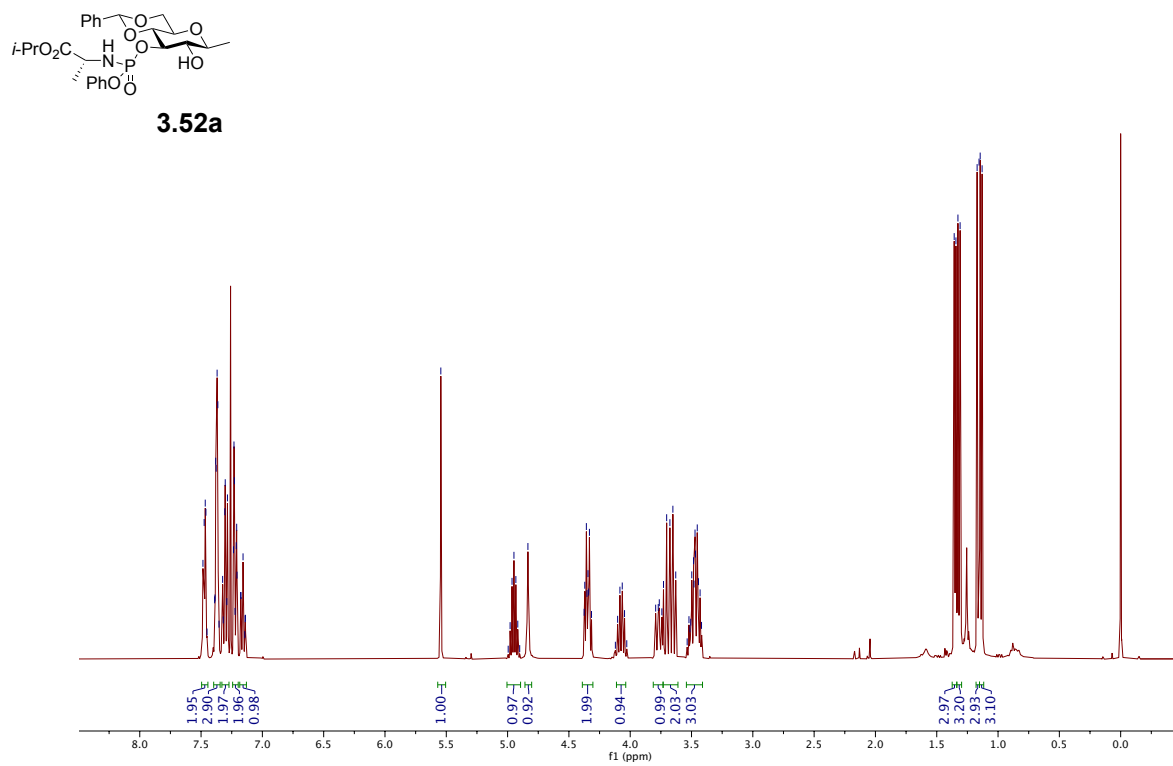
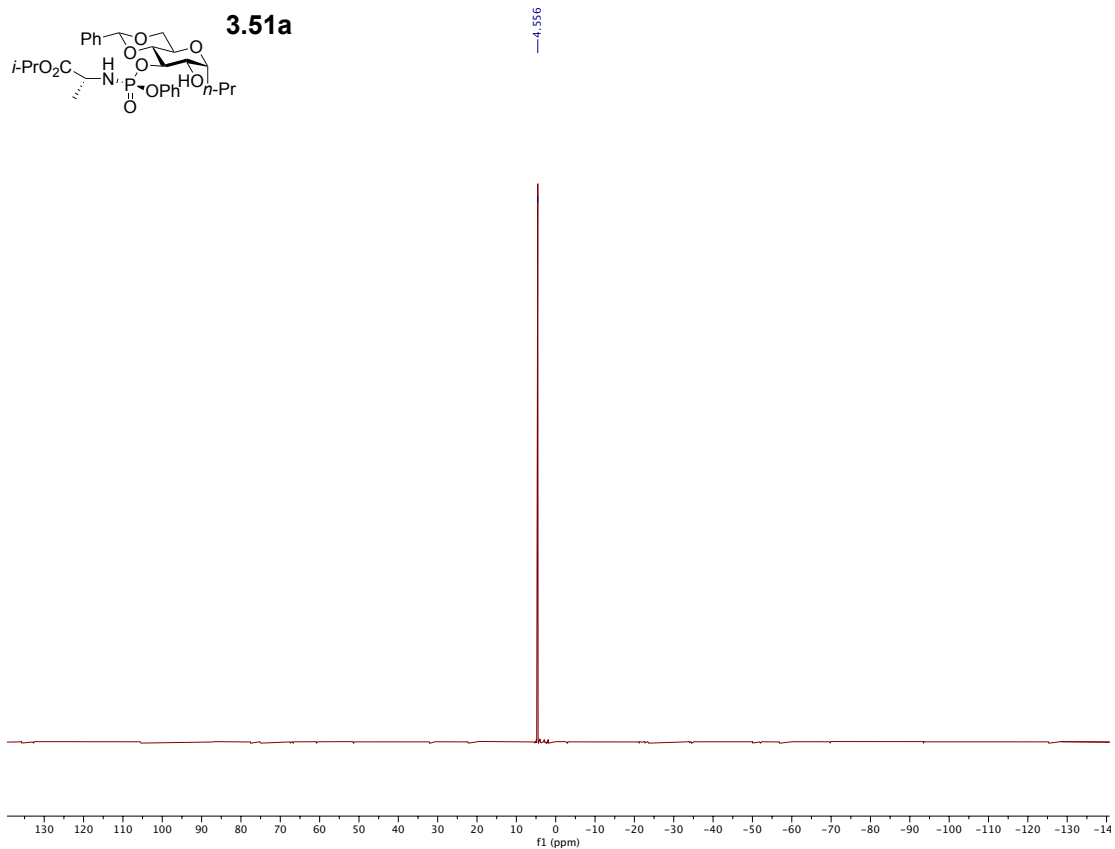


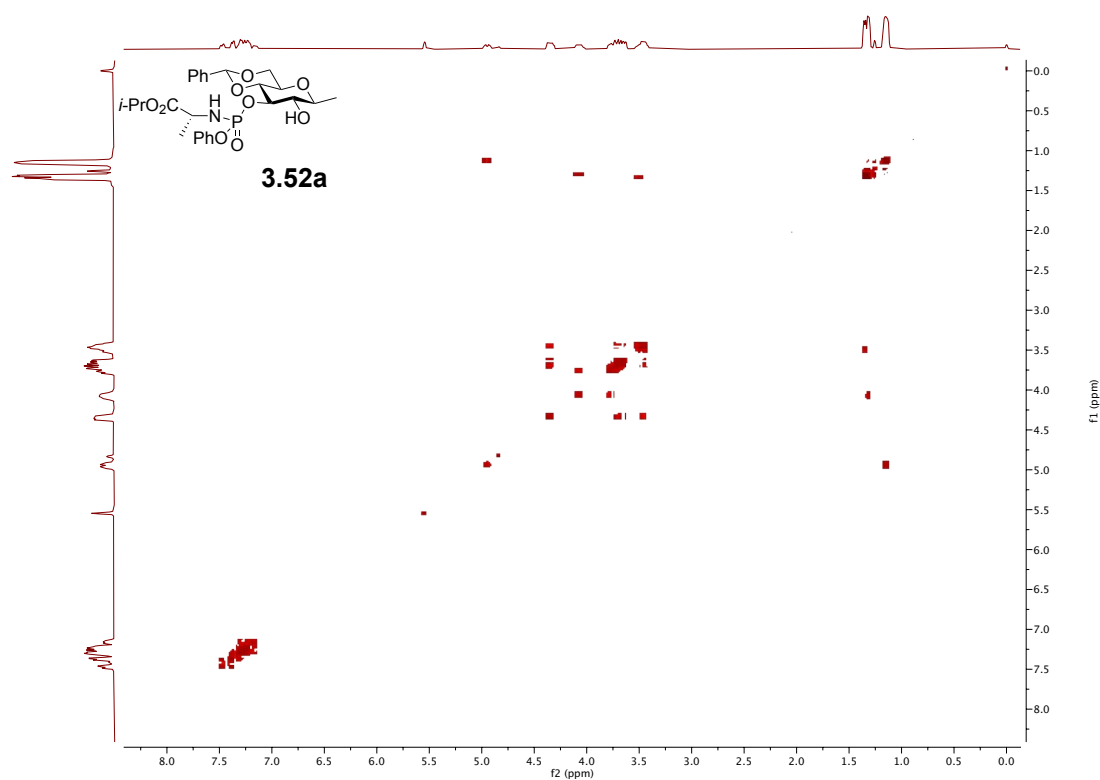
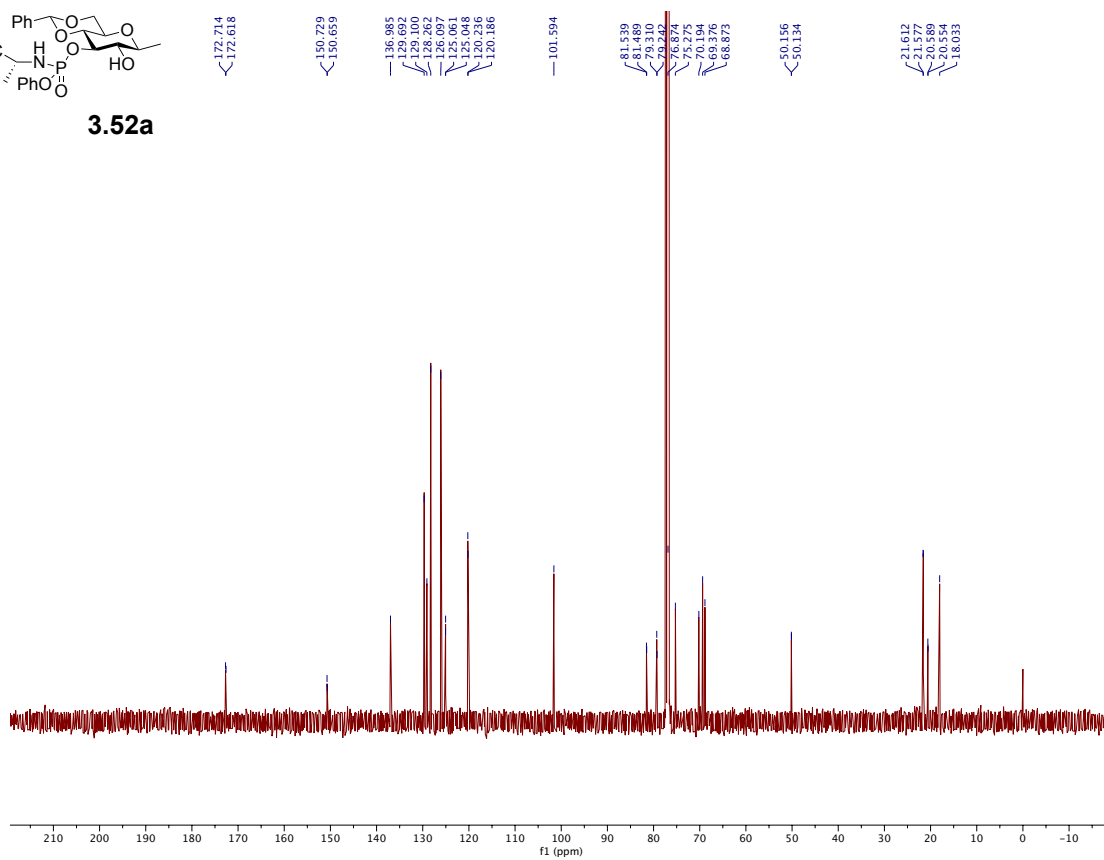
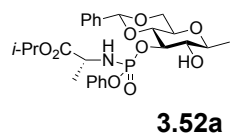


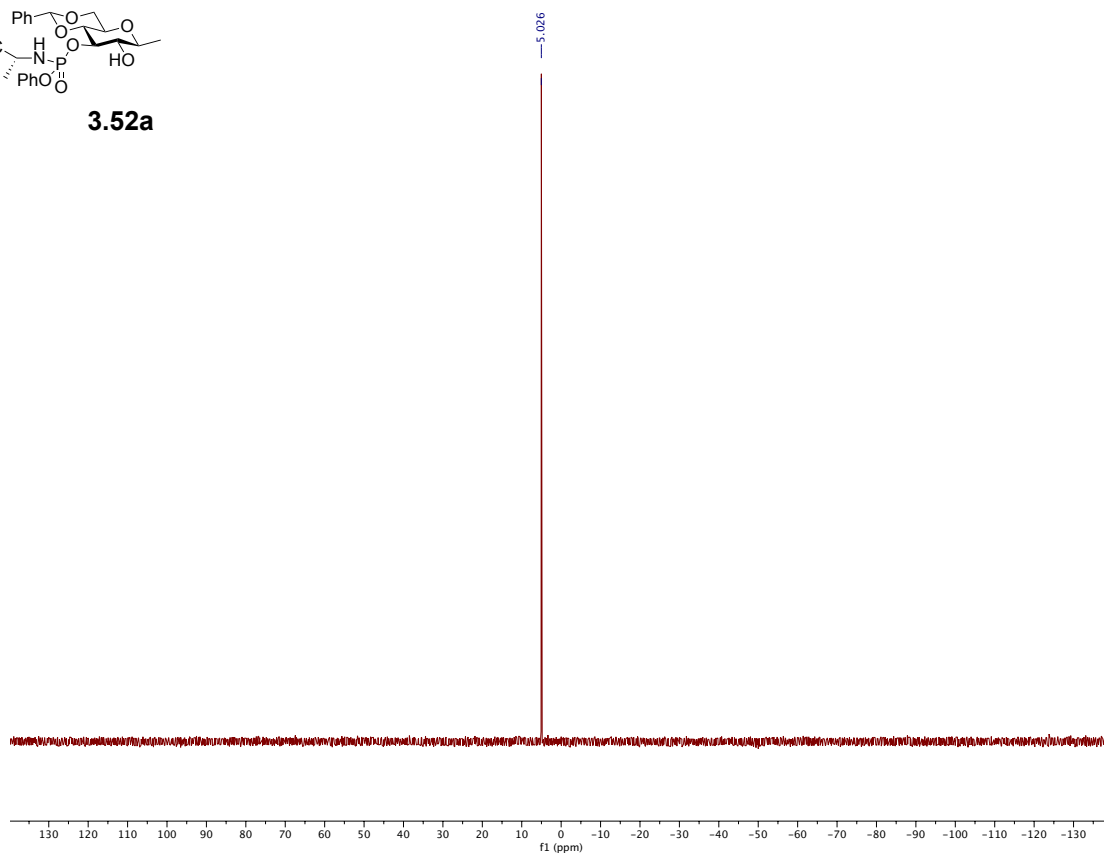
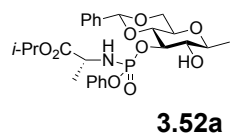










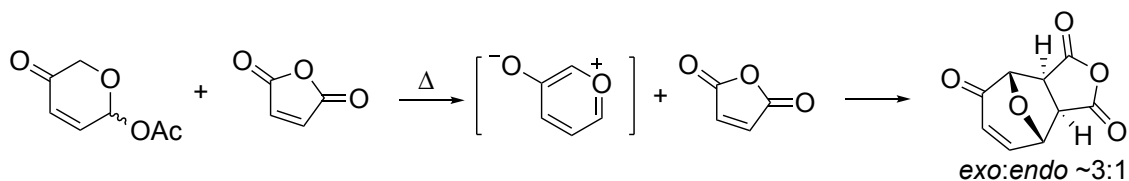


4. Density Functional Theory Investigation of a novel Hetero-[5+2] Cycloaddition of Oxidopyrylium Ylide with Cyclic Imines

Portions of this chapter were previously published in: C. Zhao, D. A. Glazier, D. Yang, D. Yin, Ii. A. Guzei, M. M. Aristov, P. Liu, W. Tang, *Angew. Chemie* **2019**, 131, 897–901.

4.1. Introduction

4.1.1. Oxidopyrylium [5+2] Cycloadditions

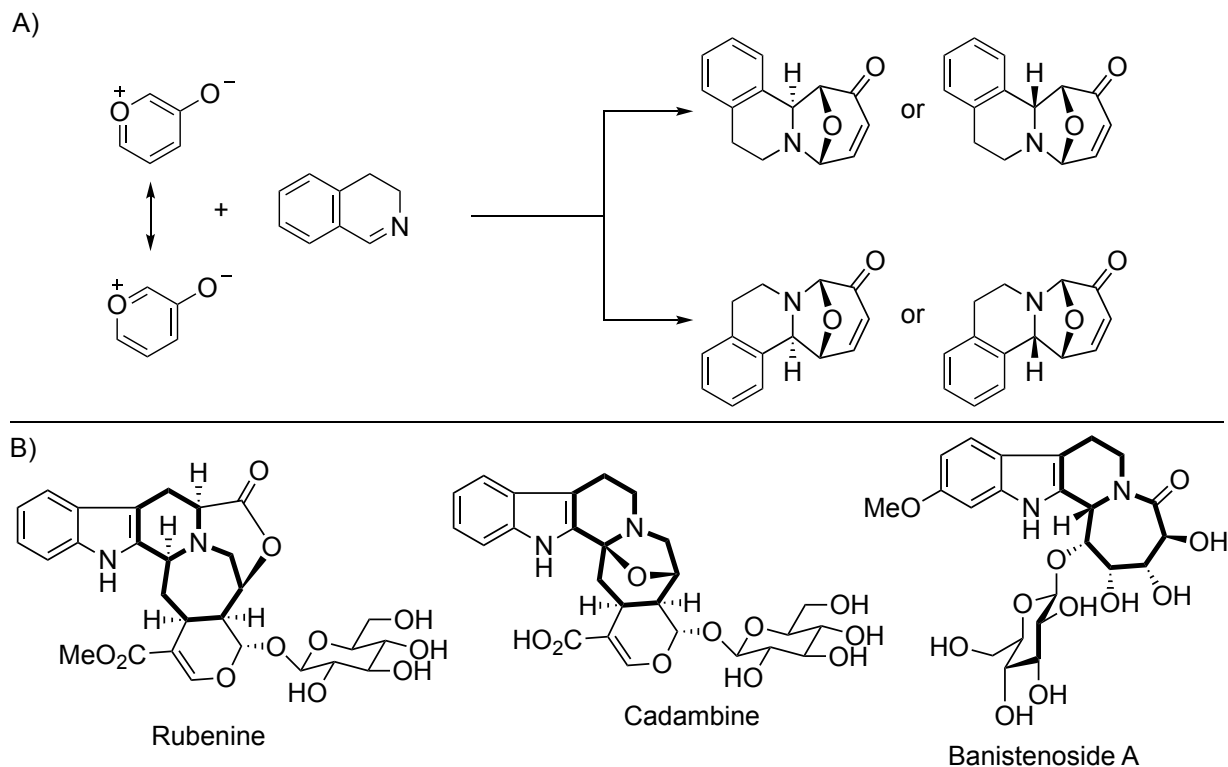


Scheme 4.1. Hendrickson's 1980 report of the first oxidopyrylium [5+2] cycloaddition.

Cycloaddition reactions are powerful and efficient tools used to build complex molecules. Significant efforts have been made to develop efficient stereo- and regio-selective cycloaddition methods for the synthesis of four-, five-, and six-membered rings. However, there has been considerably less effort focused on the synthesis of seven-membered rings.^[1-3] In Hendrickson's 1980^[4] report, an oxidopyrylium [5+2] cycloaddition demonstrated that this strategy is a promising method for the synthesis of seven-membered ring carbocycles (**Scheme 4.1**).^[5] Since Hendrickson's report, numerous methods for oxidopyrylium [5+2] cycloadditions have been developed.^[2,6,7] Most of these studies focused on intramolecular reactions with the alkene 2π component tethered at C2 or C6 position (type I oxidopyrylium–alkene cycloaddition).^[6] In 2015 Li demonstrated type II oxidopyrylium–alkene cycloaddition is possible (alkene 2π component tethered at the C5 position) leading to the formation of highly functionalized bridged seven-membered carbocycles.^[8] Li successfully used this strategy for the synthesis of the carbon skeleton of eurifoloid A^[9] and more recently for the total synthesis of isocyclocitrinol.^[10]

Intermolecular oxidopyrylium–alkene/alkyne cycloadditions are far less studied than the intramolecular reaction. The dimerization of the oxidopyrylium ylide limits the overall yield of the intramolecular reaction unless the alkene 2π component is used in excess.^[5-7] This has resulted in inadequate study of the factors affecting stereo- and regio-selectivity of intermolecular oxidopyrylium [5+2] cycloadditions. Furthermore, both the intra- and intermolecular reactions are limited to the formation of carbocycles, with reports of alkenes, alkynes, indole, dienamines,

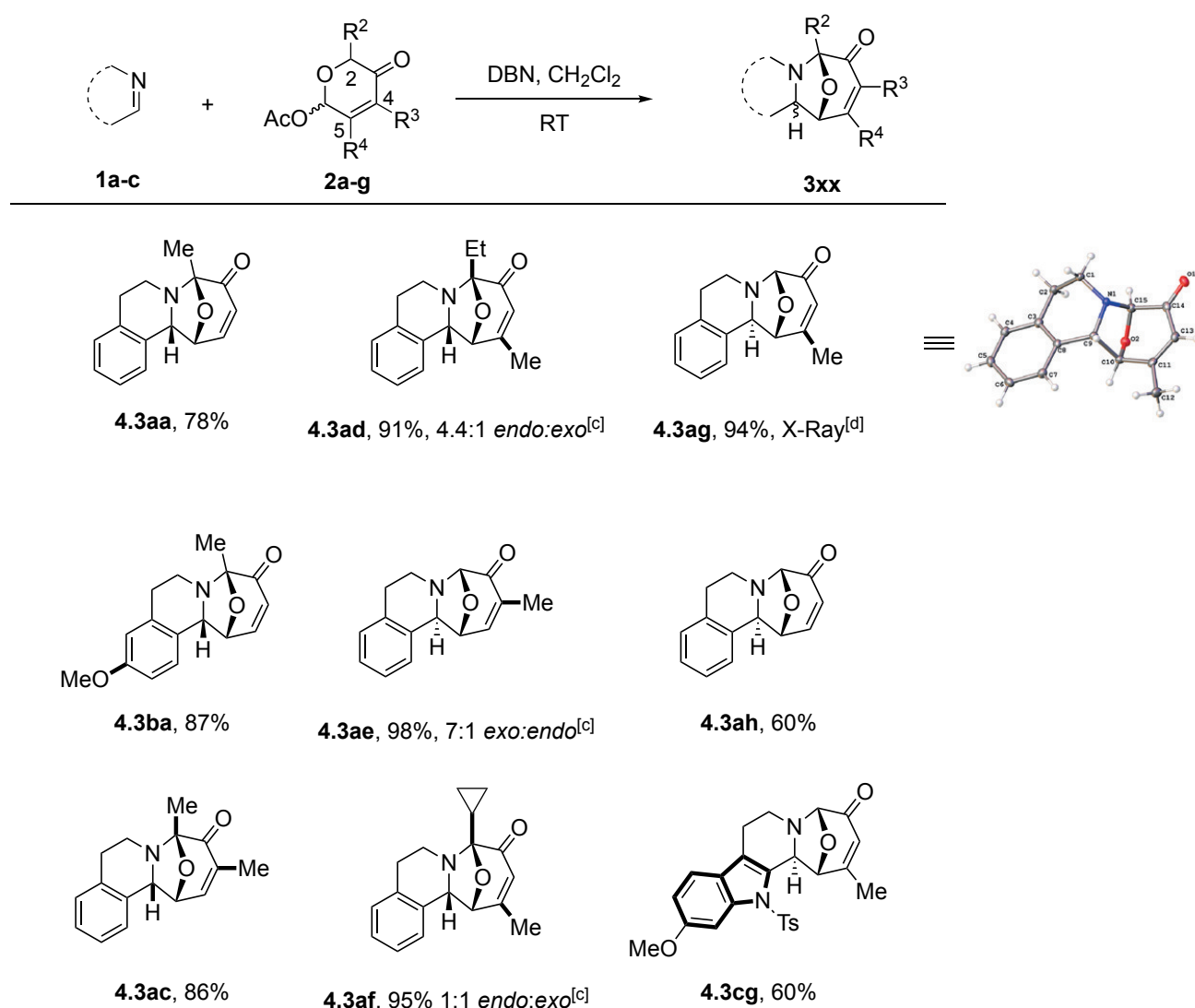
and trienamines being effective coupling partners. No methods for the synthesis of seven-membered heterocycles have been reported using oxidopyrylium [5+2] cycloadditions.



Scheme 4.2. Novel hetero-[5+2] cycloaddition strategy for the synthesis of azepanes and azepane containing natural products.

As part of the Tang lab's continuing effort to develop novel [5+2] cycloaddition reactions,^[11] my labmate, Dr. Changgui Zhao, endeavored to develop a hetero-[5+2] cycloaddition to facilitate the synthesis of various, highly-substituted, azepane-containing, natural products, as shown in **Scheme 4.2A**. Azepane-containing natural products such as rubenine,^[12] cadambine,^[13] and banistenoside^[14] (**Scheme 4.2B**) possess complex penta- and hexa-substituted azepane cores, which are challenging to build due to the core's few retrosynthetic disconnects. The feasibility, regio-, and stereoselectivity of the proposed oxidopyrylium hetero-[5+2] cycloaddition were unknown since there are no previous examples to guide us. Dr. Zhao developed a method for the oxidopyrylium hetero-[5+2] cycloaddition with cyclic imines that gives products in high yields with exceptional regioselectivity and excellent to low diastereo-selectivity for either *endo* or *exo*

products, depending on the substitution pattern of the oxidopyrylium (a representative substrate scope is shown in **table 4.1**). C2-functionalized and C2,4-difunctionalized oxidopyryliums yield exclusively *endo* products (left column in **table 4.1**), while unfunctionalized and C5-functionalized oxidopyryliums yield solely *exo* products (right column in **table 4.1**). Oxidopyryliums with C4-functionalization or C2,5-difunctionalization gives mixtures of *endo* and *exo* products. The substitution pattern dependency of the diastereoselectivity of this cycloaddition is unusual and warrants an investigation of the mechanism of the cycloaddition to determine the origin of the regio- and diastereoselectivity.

Table 4.1. Selected Substrate Scope.

[a] Reaction conditions: under argon atmosphere, 1 (0.2 mmol), 2 (0.4 mmol), base (0.6 mmol), CH₂Cl₂ (2 mL), at room temperature for 8h, *endo/exo* or *exo/endo* >20:1 unless noted otherwise. [b] Yield of isolated products. [c] Isolated ratios. [d] 50% probability ellipsoids.

4.1.2 Computational Investigations of Oxidopyrylium [5+2] Cycloadditions

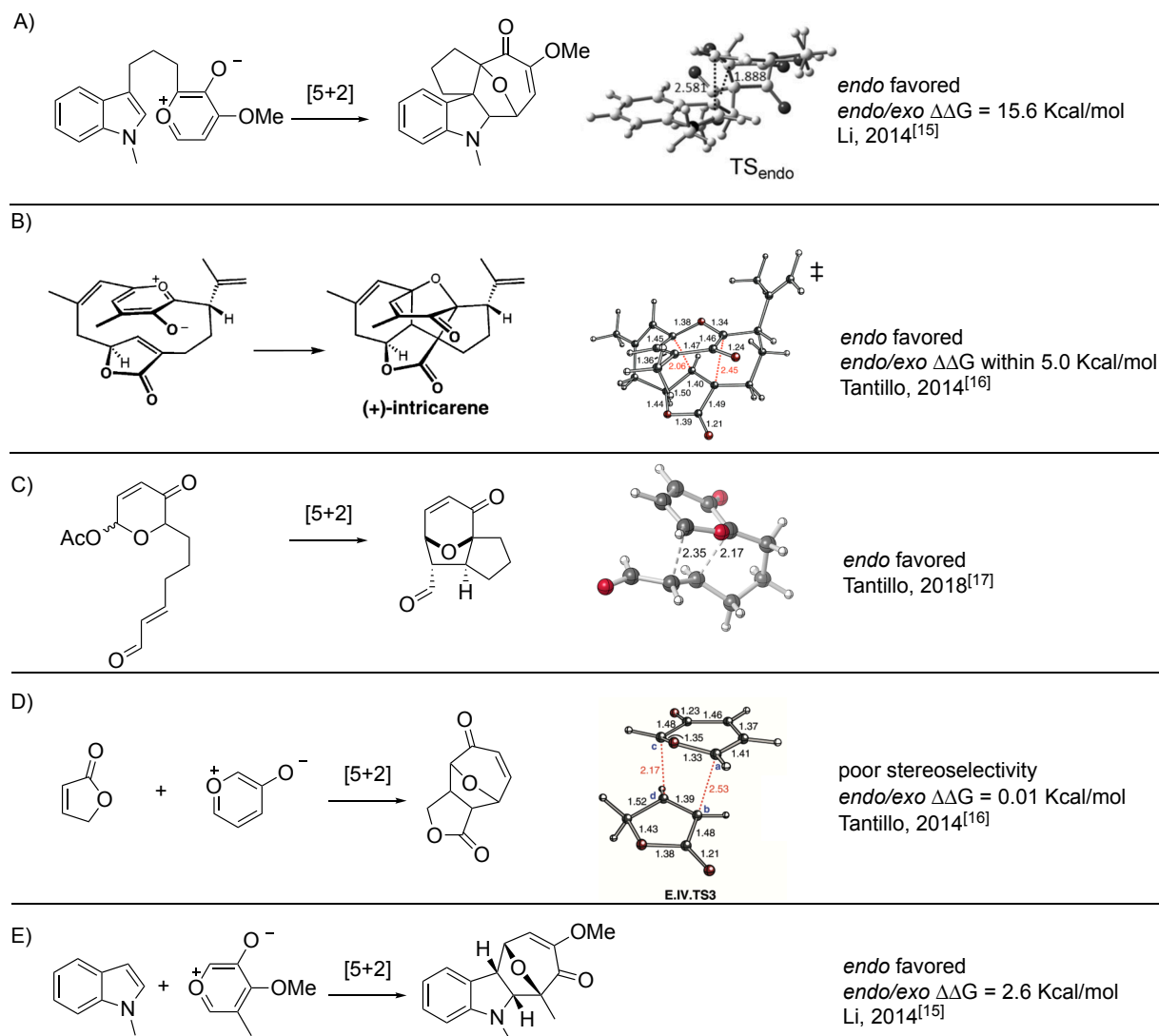
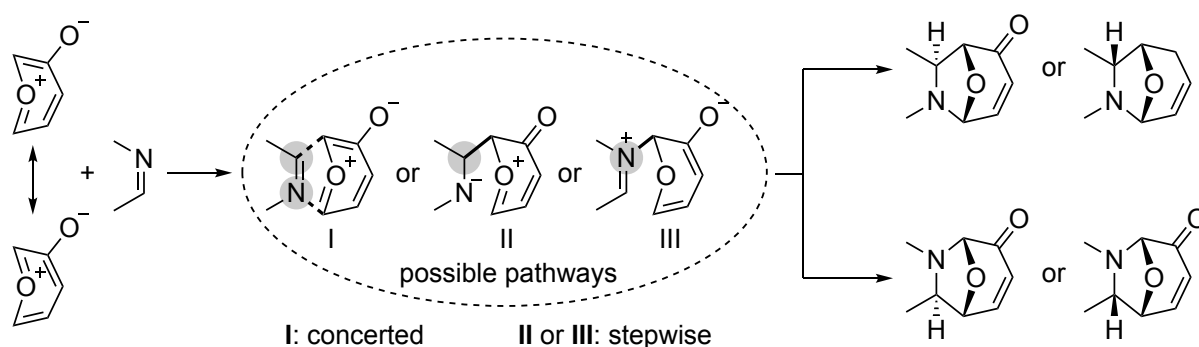


Figure 4.1. Previous DFT investigations of oxidopyrylium [5+2] reactions.

Previous DFT investigations of oxidopyrylium [5+2] cycloadditions by Tantillo and Li uniformly found that the reactions proceed via a concerted mechanism (**Figure 4.1**). Intramolecular mechanisms (**Figure 4.1A-C**) favor *endo* products, but this can be a result of the linker geometry and may not be indicative of intermolecular reactions.^[15-17] Additionally, regioselectivity for intramolecular reactions is also determined by the linker. The studies of intermolecular oxidopyrylium [5+2] cycloaddition from Tantillo and Li provide much more information about the regio- and stereoselectivities of this class of cycloaddition. For the reaction shown in **Figure**

4.1D, Tantillo determined that while the *endo:exo* selectivity of the reaction is poor, it should exhibit high regioselectivity arising from the frontier molecular orbital (FMO) interactions between the HOMO-1 of the oxidopyrylium and the LUMO of the alkene (the HOMO of the oxidopyrylium is a lone-pair type orbital).^[16] Additionally, dipole-dipole interactions favor having the two carbonyl type oxygens as far apart as possible. Li observed, both experimentally and computationally, a complete reversal of regioselectivity between the intra- and intermolecular cycloadditions, but in both cases the reaction gave only *endo* products, presumably because of secondary orbital interactions (**Figure 4.1E**).^[15] Furthermore, calculations show that aza-Diels-Alder reactions between 1,3-butadiene and formimine strongly favor *endo* products due to the unfavorable interaction of the nitrogen sp^2 lone pair and the diene π system in the *exo* transition state.^[18] In light of these findings, our hetero-[5+2] cycloaddition results are unexpected because the diastereoselectivity of the reaction depends on the substitution pattern of the oxidopyrylium and is not uniformly *endo*. If our hetero-[5+2] cycloaddition were to go through a concerted pathway, it would be highly unusual, near impossible to observe >20:1 *exo* selectivity, like compounds **4.3ag**, **4.3ah**, and **4.3cg**, indicating a different pathway may be at play.

Scheme 4.3. Possible mechanisms for our hetero-[5+2] cycloaddition.



There are three possible mechanisms for our hetero-[5+2] cycloaddition: 1) a concerted process where both bonds are formed at the same time, but most likely in a highly asynchronous manner in light of the nitrogen (**Scheme 4.3, I**), 2) nucleophilic attack of the oxidopyrylium ylide onto the imine carbon, followed by ring closure (**Scheme 4.3, II**), or 3) nucleophilic attack from the imine nitrogen on the oxidopyrylium, followed by ring closure (**Scheme 4.3, III**). The high

regioselectivity and the substituent-dependent diastereo-selectivity suggests that a step-wise mechanism (II or III) may be more likely for the hetero-[5+2] cycloaddition. This mechanistic ambiguity prompted me to perform density functional theory (DFT) calculations to explore the reaction mechanisms and the origin of regio- and stereoselectivity. I chose to investigate the reactions that form **4.3ag** and **4.3aa** since they gave high yields of products with completely opposite stereochemistry in >20:1 d.r..

4.2. Methods

4.2.1. A Qualitative Explanation of Density Functional Theory (DFT)

DFT is one of the most powerful and popular methods for the computational study of organic reaction mechanisms because it can provide relatively accurate data in a time-efficient manner. DFT is based on two theorems postulated by Hohenburg and Kohn (HK) in 1964: 1) the ground state properties of a multi-electron system depend only on the electron density of the system $n(x,y,z)$ and 2) the true ground state density of a multi-electron system is the one that minimizes the total energy functional $E[n(x,y,z)]$. The two most important features of DFT follow from these theorems: 1) the degrees of freedom we have to concern ourselves with goes from $3N$, where N is the number of electrons, to 3 when trying to determine the energy of a many electron system, 2) HK DFT does not take quantum mechanical phenomena into account. The first feature drastically cuts down the computational work that must be done to calculate the energy of system when compared to calculating the energy of a system via the Schroedinger equation. The second feature requires significant complications of the simple and elegant theorems above to give useful results.

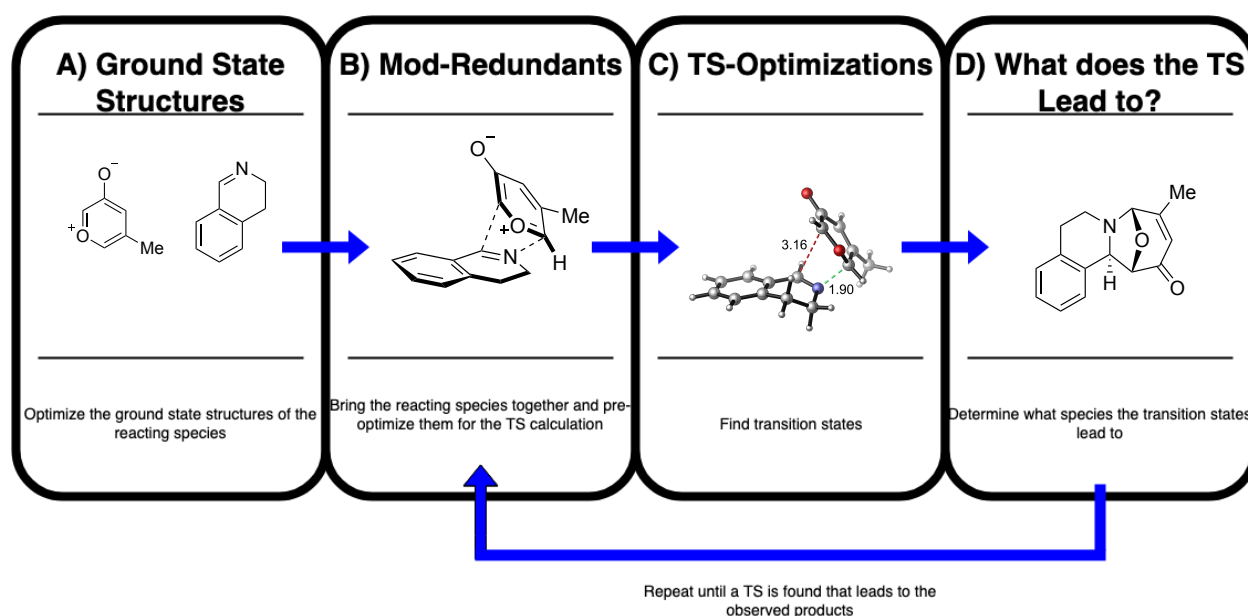
The DFT functional I used most frequently was the Minnesota functional M06-2X. M06-2X is a Kohn-Sham (KS) meta-hybrid-GGA (generalized gradient approximation, explained below) functional. KS-DFT differs from HK-DFT in that KS takes into account the quantum mechanical phenomena of exchange energy (E_x , Pauli repulsion) and correlation energy (E_c , a measure of how the movement of one electron is affected by other electrons) via the local spin-density approximation (LSDA). An approximation is needed because E_x and E_c cannot be known exactly

for any real system. A GGA is a generalized gradient approximation, which means the functional takes into account the derivative of the electron density in addition to the electron density itself which increases the accuracy of the functional. A meta-DFT functional, like the one I used, also includes the second derivative. Finally, a hybrid functional includes the E_x calculated from the Hartree-Fock method. With these modifications to HK-DFT, the Minnesota functionals are accurate enough to be employed in the elucidation of organic reaction mechanisms.

DFT functionals act on functions, or basis sets. Basis sets, at minimum, need one function to describe each atomic orbital (AO), but most basis sets commonly used for DFT calculations are double ζ , which means they use two functions for each AO. A basis set can be split valence where the valence AOs are higher ζ than the core AOs. The ideal function for a basis set to use would be a Slater type orbital (STO), but since they are difficult to calculate, Gaussian type orbitals (GTOs) are used instead and linear combinations of multiple GTOs (CGTOs) are used to mimic an STO. The popular Popel basis sets are a family of split valence based on CGTOs and are what I used as the basis sets for my calculations.

4.2.2 DFT Investigation Work-Flow

Scheme 4.4. Workflow for a DFT investigation of an organic reaction mechanism.



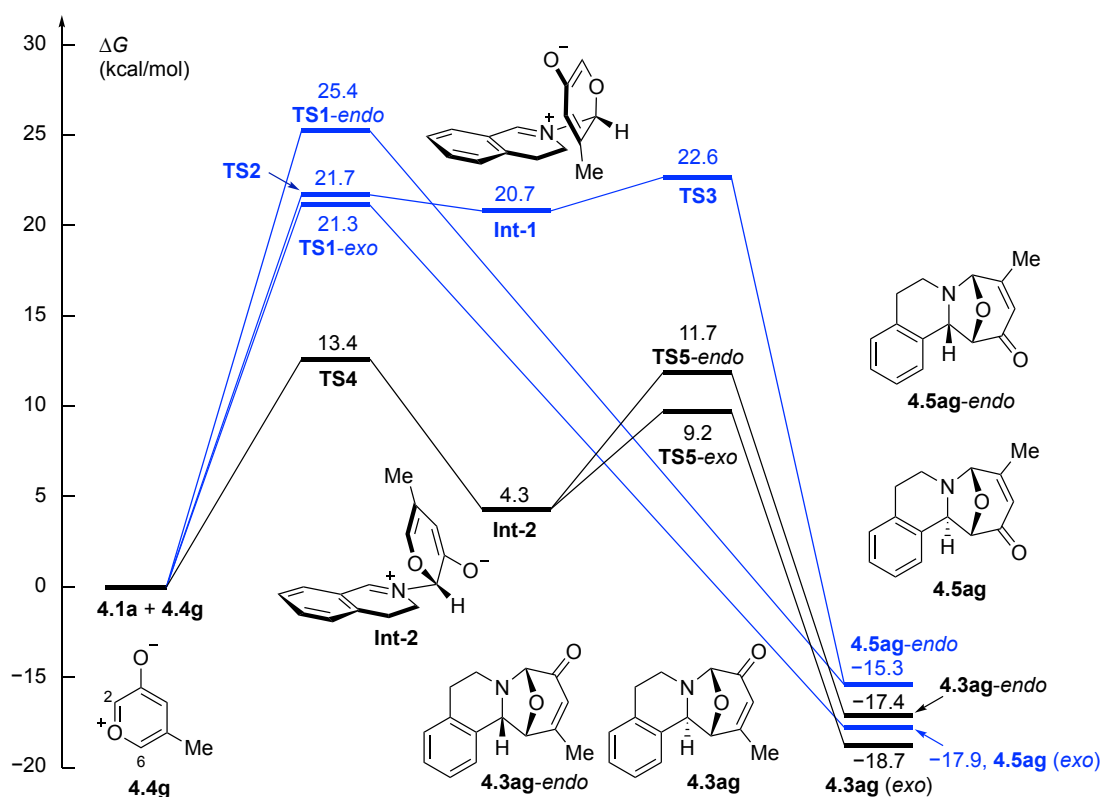
The workflow I used for the investigation of the oxidopyrylium hetero-[5+2] cycloaddition mechanism is shown in **Scheme 4.4**. It starts with identifying the relevant starting species, which are not always the starting materials added to the reaction, and optimizing the ground state structures of those relevant starting species (**Scheme 4.4A**). The second step is performing numerous mod-redundant optimizations of the reacting species (**Scheme 4.4B**). A mod-redundant optimization is a structure optimization calculation where a dimension of the structure is kept constant while the rest of the system is allowed to vary freely to attempt to find an energy minima. When attempting to identify transition-states (TSs) the most common dimension to freeze is the forming bond(s). The lengths I chose for the forming bonds were carefully selected after consulting the literature on calculations concerning similar systems such as oxidopyrylium [5+2] and hetero-Diels-Alder cycloadditions. These mod-redundant calculations are a pre-optimization for the TS-optimization calculation and so one must be very circumspect and ensure that they calculate mod-redundants for every possible pathway and not just the pathway thought to be most likely. This means numerous mod-redundants have to be made for each reaction varying both the forming bond lengths and how the species are brought into contact. Because of the time consuming nature of setting up the mod-redundant structures and the sheer number of them that have to be performed (>200 for this project), this is usually the part of the work-flow that takes the longest.

The next step is to take the optimized mod-redundant structure and use it as the starting point for a TS-optimization calculation (**Scheme 4.4C**). A TS-optimization attempts to find a saddle-point on the potential energy surface (PES) from the mod-redundant structure. This could be the desired TS, but it could also be the TS corresponding to a rotation of a methyl group on the molecule, a ring-flip, or any other myriad of changes in molecular structure. One must check that a completed TS-optimization yielded relevant TS by observing the lowest vibrational mode of the output structure; it should be a negative mode, indicating a TS, and the vibration of the mode must be along the axis of the forming bonds. Finally, the last part of the work-flow is to determine if the TS leads to the desired products, an intermediate, or some other species

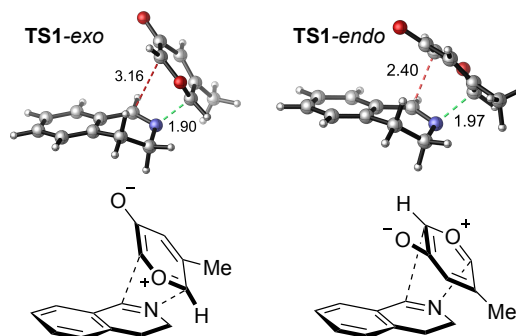
(**Scheme 4.4D**). There are two ways to do this: 1) perform an intrinsic reaction coordinate (IRC) calculation to determine what structure the TS arises from and leads too, 2) shorten the forming bonds by a fraction of an Å and then optimize the structure to see what structure the TS yields. While IRC calculations are a more empirical method than shortening the forming bond lengths, IRCs are computationally very expensive, they do not always properly distinguish between the forward and reverse of the reaction (both directions of the IRC can go towards the same structure), and they can be difficult to set up therefore the bond shortening method is usually preferred. If the structure obtained from either of these methods is not the desired final product, but instead is a plausible intermediate in a pathway leading to the desired product the workflow must be repeated starting at the mod-redundant optimization. If the structure obtained from these methods is the desired final product then the investigation is complete.

4.3 Results

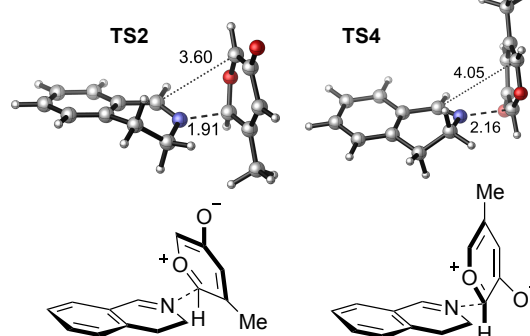
I determined the mechanistic pathways leading to the formation of products **4.3aa** and **4.3ag** using the M06-2X/6-311++G(d,p)/SMD(dichloromethane) level of theory. I started from the oxidopyrylium ylides as they are the relevant species in the stereo- and regio- determining steps of the reaction. The free energy profiles of the reaction of **4.1a** and oxidopyrylium **4.4g** to form **4.3ag** are shown in **Scheme 4.5A** (the free energy profiles for the formation of **4.3aa** is shown in the supporting information).

A) Free energy profiles of the cycloaddition of **4.1a** and **4.4g** to form **4.3ag** (in black) and **4.5ag** (in blue)

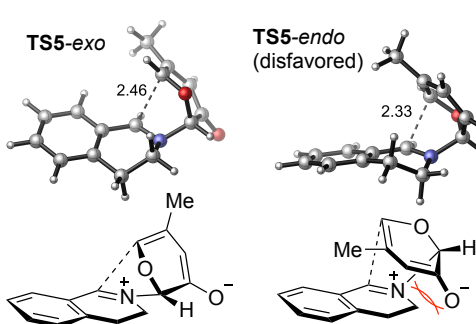
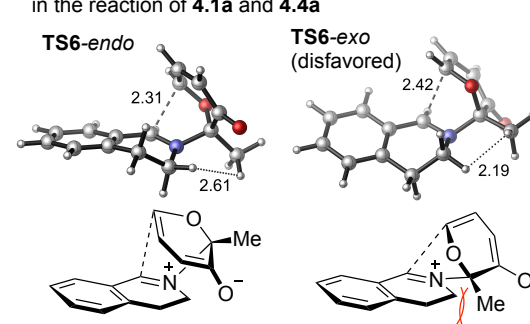
B) Concerted cycloaddition transition states



C) Stepwise transition states (first bond formation)



D) Stepwise transition states (second bond formation)

E) Stereoselectivity-determining transition states in the reaction of **4.1a** and **4.4a**

Scheme 4.5. Density functional theory (DFT) calculations. DFT calculations were performed at the M06-2X/6-311 + + G(d,p)/SMD(dichloro- methane) level of theory .

Two concerted transition states, **TS1-*exo*** and **TS1-*endo***, were located, leading to the *exo* and *endo* isomers of the experimentally unobserved regioisomeric adduct **4.5ag**. Both **TS1-*exo*** and **TS1-*endo*** are highly asynchronous, with a much longer forming C(imine)–C2 bond (3.16 and 2.40 Å, respectively) than the forming N(imine)–C6 bond (1.90 and 1.97 Å). This is consistent with TS structures of inverse-electron-demand hetero-Diels-Alder reactions with imines.^[18] Natural bond orbital (NBO) calculations show that these concerted transition states proceed in an inverse electron manner. The **4.1a**-HOMO/**4.4g**-LUMO gap is 6.41 eV, smaller than the **4.1a**-LUMO/**4.4g**-HOMO gap of 6.68 eV. The stepwise transition state (**TS2**) that forms the N–C6 bond first has a similar barrier compared to that of **TS1-*exo***. This stepwise transition state leads to a zwitterionic intermediate **Int-1**, which then undergoes C(imine)–C2 bond formation via **TS3** to form **4.5ag-*endo***.^[19] After extensive effort to alter the distances of the forming C–N and C–C bonds,^[15-18] all attempts to locate a concerted transition state that leads to **4.3ag** and its diastereomer failed in both solution and vacuum. Most of the failed geometry optimization calculations lead to a stepwise transition state instead. Due to the more favorable FMO interactions between N and C2, these concerted transition states, if they exist, would be even more asynchronous with even longer C(imine)–C6 bond than the C(imine)–C2 bonds in **TS1-*exo*** and **TS1-*endo***.^[18] Instead, I located a stepwise transition state **TS4** in which the imine N lone pair attacks C2 to form zwitterionic intermediate **int-2**. The resonance stabilized cationic-imine and extended enolate present in **int-1** and **int-2** make both zwitterionic structures particularly stable. However, **int-2** is much more stable ($\Delta G = 16.4 \text{ kcal mol}^{-1}$) than **int-1** due to the more effective resonance delocalization of the enolate negative charge via linear conjugation in **int-2** instead of the cross conjugation in **int-1**.^[20] This agrees with the high experimental regioselectivity preference to form **4.3ag**. From **int-2**, C–C bond formation transition states **TS5-*exo*** and **TS5-*endo*** lead to the *exo* and *endo* cycloadducts **4.3ag** and **4.3ag-*endo***, respectively. The steric repulsions between the oxidopyrylium ring and the imine destabilize the *endo* transition state, **TS5-*endo***. The relatively large free energy difference between **TS5-*exo*** and

TS5-endo ($\Delta\Delta G^\ddagger = 2.5 \text{ kcal mol}^{-1}$) is consistent with the high d.r. (>20:1) that favors the less sterically encumbered *exo* products.

The reaction with the C2-substituted oxidopyrylium **4.4a** and imine **4.1a** to form **4.3aa** also occurs via the stepwise mechanism. In the stereoselectivity-determining C - C bond forming step, the *exo*-selective transition state **TS6-*exo*** is destabilized by gauche repulsions between the C2-methyl substituent and the dihydroisoquinoline methylene group (distance of 2.19 Å, see **Scheme 4.5E**). These steric effects make **TS6-*endo*** more stable than **TS6-*exo*** by 1.2 kcal mol⁻¹, thus leading to the reversal of the stereoselectivity to form the *endo* product.

4.4 Conclusion

In summary, the first hetero-[5+2] cycloaddition between oxidopyrylium ylide and cyclic imine was developed, leading to highly substituted azepane scaffolds with excellent regio- and diastereoselectivity. These cycloadducts could be readily transformed into core skeletons of natural products. DFT calculations reveals that the cycloaddition proceeds through an unprecedented, for oxidopyrylium [5+2] cycloadditions, zwitterionic stepwise mechanism which enabled me to rationalize the regio- and substituent-dependent stereoselectivity observed in experiments.

4.5 References

- (1) Selected reviews: a) L. Ghosez in *Stereocontrolled Organic Synthesis* (Ed.: B. M. Trost), Blackwell Science, Oxford, **1994**, pp.193–233; b) *Advances in Cycloaddition, Vols. 1–6*, JAI Press, Greenwich, **1988–1999**; c) *Cycloaddition Reactions in Organic Synthesis* (Eds.: S. Kobayashi, K. A. Jørgensen), Wiley- VCH, Weinheim, **2002**; d) N. Nishiwaki, *Methods and Applications of Cycloaddition Reactions in Organic Syntheses*, Wiley- VCH, Hoboken, **2014**.
- (2) Selected reviews on [5+2] cycloadditions: a) H. Pellissier, *Adv. Synth. Catal.* **2011**, 353, 189; b) K. E. O. Ylijoki, J. M. Stryker, *Chem. Rev.* **2013**, 113, 2244; c) X. Liu, Y.-J. Hu, J.-H. Fan, J. Zhao, S. Li, C.-C. Li, *Org. Chem. Front.* **2018**, 5, 1217; d) H. Pellissier, *Adv. Synth. Catal.* **2018**, 360, 1551.
- (3) Selected examples of hetero-[5+2] cycloadditions involving vinylcyclopropanes, vinyl epoxides, and vinylaziridines: a) E. L. Stogryn, S. J. Brois, *J. Am. Chem. Soc.* **1967**, 89, 605; b) P. A. Wender, T. M. Pedersen, M. J. C. Scanio, *J. Am. Chem. Soc.* **2002**, 124, 15154; c) M.-B. Zhou, R.-J. Song, C.-Y. Wang, J.-H. Li, *Angew. Chem. Int. Ed.* **2013**, 52, 10805; *Angew. Chem.* **2013**, 125, 11005; d) J.-J. Feng, T.-Y. Lin, C.-Z. Zhu, H. Wang, H.-H. Wu, J. Zhang, *J. Am. Chem. Soc.* **2016**, 138, 2178; e) J.-J. Feng, T.-Y. Lin, H.-H. Wu, J. Zhang, *J. Am. Chem. Soc.* **2015**, 137, 3787; f) C. Hu, R.-J. Song, M. Hu, Y. Yang, J.-H. Li, S. Luo, *Angew. Chem. Int. Ed.* **2016**, 55, 10423; *Angew. Chem.* **2016**, 128, 10579; g) J.-J. Feng, T.-Y. Lin, H.-H. Wu, J. Zhang, *Angew. Chem. Int. Ed.* **2015**, 54, 15854; *Angew. Chem.* **2015**, 127, 16080; h) J.-J. Feng, J. Zhang, *J. Am. Chem. Soc.* **2011**, 133, 7304.
- (4) J. B. Hendrickson, J. S. Farina, *J. Org. Chem.* **1980**, 45, 1261.
- (5) Reviews on the oxidopyrylium ylide [5+2] cycloadditions: a) V. Singh, U. M. Krishna, Vikrant, G. K. Trivedi, *Tetrahedron* **2008**, 64, 3405; b) L. P. Bejcek, R. P. Murelli, *Tetrahedron* **2018**, 74, 2501.
- (6) Selected recent examples of acetoxypyranone-based oxidopyrylium ylide [5+2] cycloadditions with alkenes and alkynes: a) N. Z. Burns, M. R. Witten, E. N. Jacobsen, *J. Am. Chem. Soc.* **2011**, 133, 14578; b) G. Mei, H. Yuan, Y. Gu, W. Chen, L. W. Chung, C.-C. Li, *Angew. Chem. Int. Ed.* **2014**, 53, 11051; *Angew. Chem.* **2014**, 126, 11231; c) J. A. Simanis, C. M. Law, E. L. Woodall, C. G. Hamaker, J. R. Goodell, T. A. Mitchell, *Chem. Commun.* **2014**, 50, 9130; d) M. R. W. E. N. Jacobsen, *Angew. Chem. Int. Ed.* **2014**, 53, 5912; *Angew. Chem.* **2014**, 126, 6022; f) A. Orue, U. Uria, E. Reyes, L. Carrillo, J. L. Vicario, *Angew. Chem. Int. Ed.* **2015**, 54, 3043; *Angew. Chem.* **2015**, 127, 3086; e) H. Suga, T. Iwai, M. Shimizu, K. Takahashi, Y. Toda, *Chem. Commun.* **2018**, 54, 1107.
- (7) Selected recent examples on total syntheses of natural products: a) K. C. Nicolaou, Q. Kang, S. Y. Ng, D. Y.-K. Chen, *J. Am. Chem. Soc.* **2010**, 132, 8219; b) M. Zhang, N. Liu, W. Tang, *J. Am. Chem. Soc.* **2013**, 135, 12434; c) B. Chen, X. Liu, Y. J. Hu, D. M. Zhang, L. J. Deng, J. Y. Lu, L. Min, W. C. Ye, C.-C. Li, *Chem. Sci.* **2017**, 8, 4961.
- (8) G. Mei, X. Liu, C. Qiao, W. Chen, C.-C. Li, *Angew. Chem. Int. Ed.* **2015**, 54, 1754; *Angew. Chem.* **2015**, 127, 1774.
- (9) X. Liu, J. Y. Liu, J. Zhao, S. P. Li, C.-C. Li, *Org. Lett.* **2017**, 19, 2742.
- (10) J. Liu, J. Wu, J.-H. Fan, X. Yan, G. Mei, C.-C. Li, *J. Am. Chem. Soc.* **2018**, 140, 5365.
- (11) A review on our Rh-catalyzed [5+2] cycloadditions: a) C. M. Schienebeck, X. Li, X.-Z. Shu, W. Tang, *Pure Appl. Chem.* **2014**, 86, 409; Selected examples of our Rh-catalyzed [5+2] cycloadditions: b) X.-Z. Shu, S. Huang, D. Shu, I. A. Guzei, W. Tang, *Angew. Chem. Int. Ed.* **2011**, 50, 8153; *Angew. Chem.* **2011**, 123, 8303; c) X.-Z. Shu, X. Li, D. Shu, S. Huang, C. M. Schienebeck, X. Zhou, P. J. Robichaux, W. Tang, *J. Am. Chem. Soc.* **2012**, 134, 5211; d) X. Xu, P. Liu, X.-Z. Shu, W. Tang, K. N. Houk, *J. Am. Chem. Soc.* **2013**, 135, 9271; e) X.-Z. Shu, C. M. Schienebeck, W. Song, I. A. Guzei, W. Tang, *Angew. Chem. Int. Ed.* **2013**, 52, 13601; *Angew. Chem.* **2013**, 125, 13846; f) X. z. Shu, C. M. Schienebeck, X. Li, X. Zhou, W. Song, L. Chen, I. A. Guzei, W. Tang, *Org. Lett.* **2015**, 17, 5128.
- (12) R. Brown, A. Charalmbides, *J. Chem. Soc. Chem. Commun.* **1973**, 765.
- (13) M. Lamidi, E. Ollivier, V. Mahiou, R. Faure, L. Debrauwer, L. Nze Ekekang, G. Balansard, *Magn. Reson. Chem.* **2005**, 43, 427.
- (14) a) V. Samoylenko, M. M. Rahman, B. L. Tekwania, L. M. Tripathi, Y.-H. Wang, S. I. Khan, I. A. Khan, L. S. Miller, V. C. Joshi, I. Muhammad, *J. Ethnopharmacol.* **2010**, 127, 357; b) Y.-H. Wang, V. Samoylenko, B. L. Tekwani, I. A. Khan, L. S. Miller, N. D. Chaurasiya, M. M. Rahman, L. M. Tripathi, S. I. Khan, V. C. Joshi, F. T. Wigger, I. Muhammad, *J. Ethnopharmacol.* **2010**, 128, 662.
- (15) G. Mei, H. Yuan, Y. Gu, W. Chen, L. W. Chung, C. Li, *Angew. Chemie Int. Ed.* **2014**, 53, 11051.
- (16) S. C. Wang, D. J. Tantillo, *J. Org. Chem.* **2008**, 73, 1516.
- (17) R. H. Kaufman, C. M. Law, J. A. Simanis, E. L. Woodall, C. R. Zwick, H. B. Wedler, P. Wendelboe, C. G. Hamaker, J. R. Goodell, D. J. Tantillo, T. A. Mitchell, *J. Org. Chem.* **2018**, 83, 9818.

- (18) a) M. A. McCarrick, Y. D. Wu, K. N. Houk, *J. Am. Chem. Soc.* **1992**, 114, 1499; b) M. A. McCarrick, Y. D. Wu, K. N. Houk, *J. Org. Chem.* **1993**, 58, 3330.
- (19) **TS3** leads to **4.5ag-endo**, but I could not find a **TS** from **int1** that leads to **4.5ag**.
- (20) A. Dieckmann, M. Breugst, K. N. Houk, *J. Am. Chem. Soc.* **2013**, 135, 3237.

Supporting Information

Chapter 4: Density Functional Theory Investigation of a novel Hetero-[5+2] Cycloaddition of Oxidopyrylium Ylide with Cyclic Imines

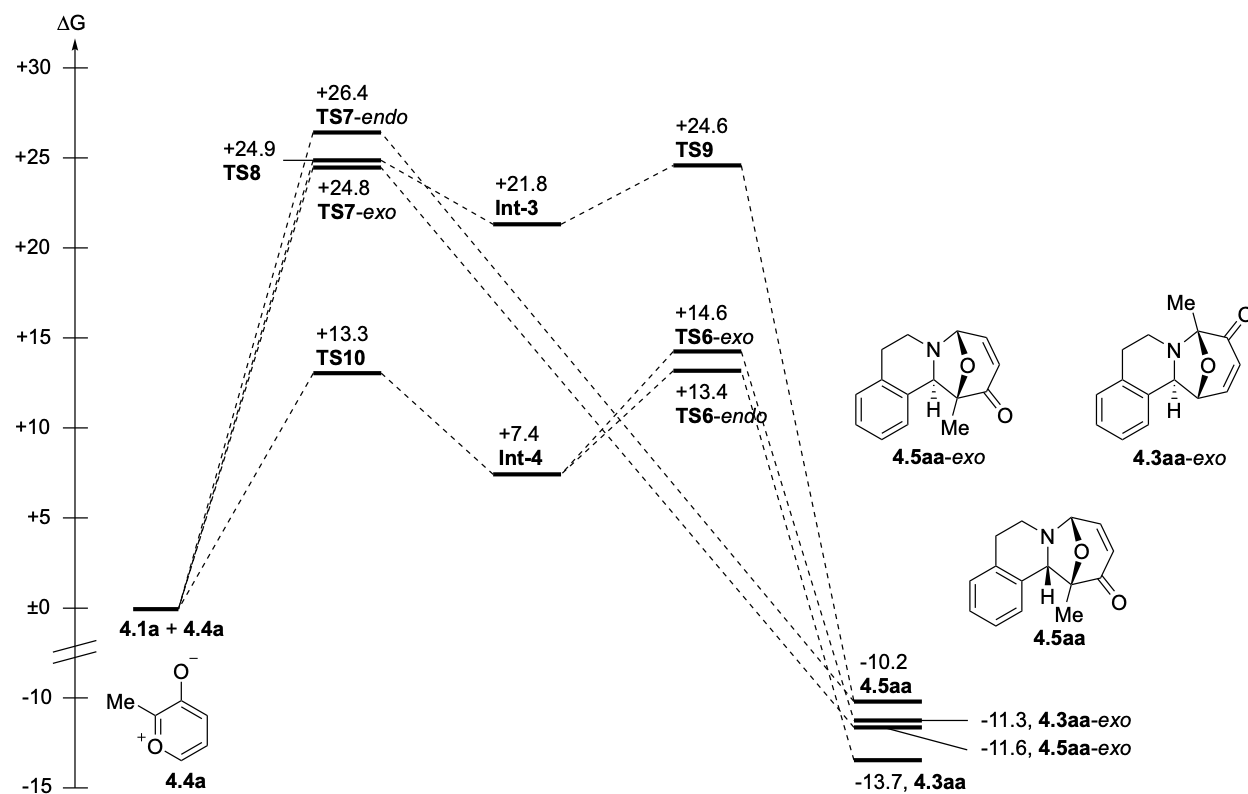
Table of Contents

Computational Details.....	208
References.....	237

Computational Details

All DFT calculations were performed using Gaussian 16.¹ Geometry optimizations were performed using the M06-2X^{2,3} functional and the 6-311++G(d,p) basis set with the SMD⁴ solvation model using dichloromethane solvent.

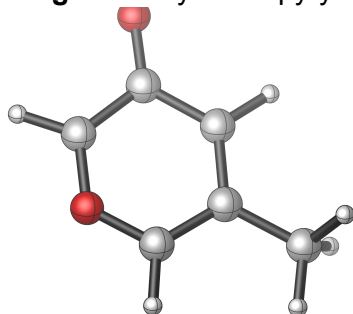
Free Energy Profiles of the Cycloaddition of 4.1a and 4.4a



Energies are in kcal mol⁻¹ with respect to the separate reactants 4.1a and 4.4a.

Cartesian Coordinates of All Optimized Structures

4.4g: 5-methyl-oxidopyrylium ylide



M06-2X/6-311++G(d,p) SCF energy in solution: -382.594290193 a.u.

M06-2X/6-311++G(d,p) enthalpy in solution: -382.478343 a.u.

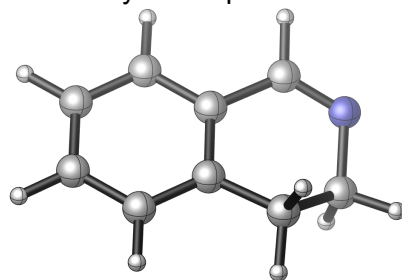
M06-2X/6-311++G(d,p) free energy in solution: -382.519190 a.u.

Three lowest frequencies (cm⁻¹): 16.19, 167.51, 212.29

Cartesian coordinates

ATOM	X	Y	Z
C	-2.523609	0.852313	0.000000
C	-1.150692	0.240485	0.000000
C	-1.007600	-1.132002	-0.000000
O	0.196018	-1.674031	-0.000000
C	1.304998	-0.970084	-0.000000
C	1.318607	0.456835	0.000000
C	0.000000	1.018558	0.000000
H	-0.087329	2.101590	0.000000
O	2.385843	1.111159	0.000000
H	2.198731	-1.580302	-0.000000
H	-1.804542	-1.861164	-0.000000
H	-2.657212	1.480917	0.882533
H	-2.657212	1.480917	-0.882533
H	-3.297542	0.084387	0.000000

4.1a: dihydroisoquinoline



M06-2X/6-311++G(d,p) SCF energy in solution: -403.062689380 a.u.

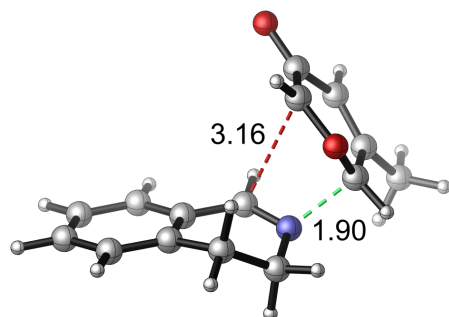
M06-2X/6-311++G(d,p) enthalpy in solution: -402.894942 a.u.

M06-2X/6-311++G(d,p) free energy in solution: -402.935027 a.u.

Three lowest frequencies (cm⁻¹): 137.40, 150.63, 273.82

Cartesian coordinates

ATOM	X	Y	Z
C	2.480947	0.685737	0.110031
C	1.284107	1.387791	0.013514
C	0.077937	0.694912	-0.090430
C	0.060172	-0.706100	-0.114156
C	1.262232	-1.400297	-0.024472
C	2.466625	-0.707533	0.091620
H	-1.172641	2.471193	-0.421119
H	3.420079	1.219454	0.196919
H	1.278748	2.473357	0.023079
C	-1.210952	1.407355	-0.180910
C	-1.282910	-1.364844	-0.288394
H	1.257392	-2.485395	-0.044397
H	3.397846	-1.257850	0.166363
C	-2.364050	-0.538824	0.399235
H	-1.506840	-1.432145	-1.360411
H	-2.237313	-0.585296	1.488670
N	-2.350853	0.881145	0.024802
H	-3.352883	-0.938455	0.173206
H	-1.273060	-2.382059	0.107847

TS1-exo:

M06-2X/6-311++G(d,p) SCF energy in solution: -785.646123143 a.u.

M06-2X/6-311++G(d,p) enthalpy in solution: -785.361320 a.u.

M06-2X/6-311++G(d,p) free energy in solution: -785.420221 a.u.

Three lowest frequencies (cm⁻¹): -355.65, 20.54, 42.25

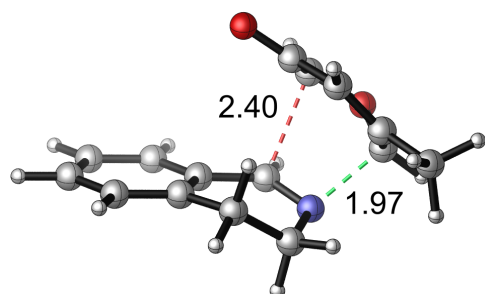
Imaginary frequency(cm⁻¹): -355.65

Cartesian coordinates

ATOM	X	Y	Z
C	-3.608044	1.483461	-0.956955
C	-2.265560	1.240876	-1.222018
C	-1.615802	0.183384	-0.583355
C	-2.294153	-0.627126	0.339786
C	-3.632809	-0.367574	0.604976
C	-4.287760	0.678483	-0.045099
H	0.396125	0.664808	-1.339105
H	-4.121529	2.298460	-1.452794
H	-1.717761	1.862673	-1.922395
C	-0.204112	-0.099133	-0.846276
C	-1.490496	-1.696186	1.031632
H	-4.166241	-0.982469	1.322264

H	-5.334257	0.868172	0.165289
C	-0.451407	-2.265937	0.073916
H	-0.984910	-1.252011	1.897749
H	-0.937494	-2.830228	-0.728902
N	0.355445	-1.222703	-0.577599
H	0.229166	-2.942257	0.592779
H	-2.135922	-2.495810	1.398803
C	2.111593	-1.114793	0.135180
C	1.574737	0.536091	1.691765
C	2.037713	1.581051	0.894294
C	2.761049	1.137062	-0.305435
C	2.802753	-0.156327	-0.697080
O	1.888867	2.811007	1.151442
O	1.818460	-0.779729	1.379915
H	2.348485	-2.169088	0.045867
H	1.144475	0.651456	2.675492
H	3.254014	1.906748	-0.893880
C	3.421968	-0.660452	-1.964295
H	2.653747	-1.107439	-2.604678
H	3.900547	0.152220	-2.510845
H	4.166819	-1.433814	-1.759515

TS1-endo:



M06-2X/6-311++G(d,p) SCF energy in solution: -785.640787289 a.u.

M06-2X/6-311++G(d,p) enthalpy in solution: -785.355759 a.u.

M06-2X/6-311++G(d,p) free energy in solution: -785.413730 a.u.

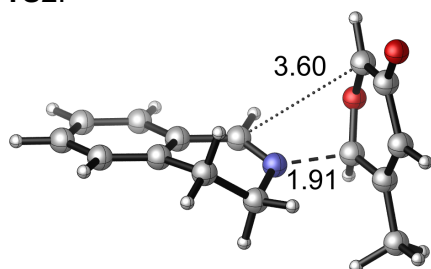
Three lowest frequencies (cm⁻¹): -416.73, 15.01, 44.75

Imaginary frequency(cm⁻¹): -416.73

Cartesian coordinates

ATOM	X	Y	Z
C	3.831981	-0.744719	-0.304105
C	2.609184	-0.963721	-0.925910
C	1.535435	-0.104967	-0.679288
C	1.679671	0.974814	0.199954
C	2.908981	1.187054	0.816647
C	3.981245	0.333601	0.566781
H	0.184911	-1.170860	-2.022964
H	4.665796	-1.409900	-0.495856
H	2.478680	-1.799141	-1.606765
C	0.245536	-0.319703	-1.350277
C	0.466291	1.827523	0.454050
H	3.026162	2.023429	1.498354

H	4.934183	0.508924	1.053164
C	-0.428615	1.881556	-0.786091
H	-0.082147	1.414523	1.305312
H	0.053562	2.504592	-1.547587
N	-0.694321	0.591868	-1.451595
H	-1.379833	2.354563	-0.546715
H	0.763191	2.843312	0.725443
C	-2.382786	-0.308850	-0.975577
C	-1.024683	-1.909806	-0.072844
C	-0.983732	-1.288484	1.206520
C	-1.987284	-0.243194	1.376786
C	-2.659726	0.269665	0.316217
O	-0.174453	-1.612991	2.101028
O	-1.952123	-1.563609	-1.000788
H	-3.012618	-0.074160	-1.824203
H	-0.569809	-2.872001	-0.266154
H	-2.148634	0.140015	2.380443
C	-3.665386	1.380427	0.399949
H	-4.679722	0.970167	0.389710
H	-3.535616	1.955939	1.317020
H	-3.581923	2.053140	-0.456824

TS2:

M06-2X/6-311++G(d,p) SCF energy in solution: -785.644059517 a.u.

M06-2X/6-311++G(d,p) enthalpy in solution: -785.359240 a.u.

M06-2X/6-311++G(d,p) free energy in solution: -785.418976 a.u.

Three lowest frequencies (cm⁻¹): -298.75, 19.64, 25.94

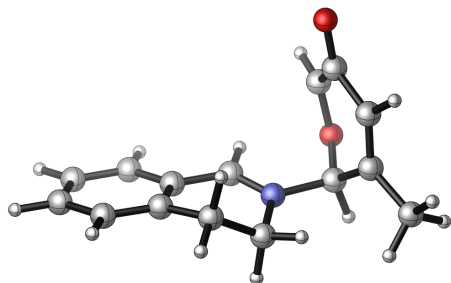
Imaginary frequency(cm⁻¹): -298.75

Cartesian coordinates

ATOM	X	Y	Z
C	4.518962	-0.693152	-0.717764
C	3.232592	-0.736516	-1.241013
C	2.172824	-0.204166	-0.505783
C	2.379293	0.354093	0.764811
C	3.668750	0.379343	1.282383
C	4.732106	-0.134837	0.541305
H	0.565161	-0.901979	-1.852600
H	5.350612	-1.095889	-1.283195
H	3.044198	-1.174739	-2.215523
C	0.804771	-0.234184	-1.023916
C	1.164070	0.834610	1.515184
H	3.843490	0.801174	2.266373
H	5.734816	-0.103523	0.952397

C	0.139575	1.411266	0.547537
H	0.718022	-0.014033	2.047758
H	0.504239	2.343305	0.100739
N	-0.134650	0.480480	-0.549691
H	-0.801921	1.619742	1.056607
H	1.434494	1.586592	2.257719
C	-1.858316	0.183459	-1.313194
C	-2.317698	-1.814466	-0.192226
C	-2.995654	-1.193926	0.841869
C	-3.275660	0.230753	0.599671
C	-2.750819	0.916234	-0.438631
O	-3.400655	-1.762824	1.906377
O	-1.932797	-1.131466	-1.338978
H	-1.624798	0.591872	-2.291424
H	-2.142404	-2.875990	-0.279684
H	-3.941232	0.723817	1.304155
C	-2.957592	2.374022	-0.720389
H	-3.451238	2.520662	-1.685235
H	-3.568599	2.834396	0.056577
H	-1.997901	2.900363	-0.765091

int-1:



M06-2X/6-311++G(d,p) SCF energy in solution: -785.650425529 a.u.

M06-2X/6-311++G(d,p) enthalpy in solution: -785.363263 a.u.

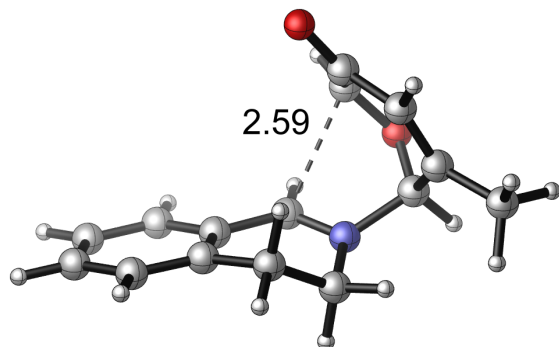
M06-2X/6-311++G(d,p) free energy in solution: -785.421179 a.u.

Three lowest frequencies (cm⁻¹): 27.22, 40.13, 100.57

Cartesian coordinates

ATOM	X	Y	Z
C	4.217619	-1.079746	-0.392544
C	2.913158	-1.204195	-0.848623
C	1.943869	-0.296099	-0.412543
C	2.259483	0.722703	0.499519
C	3.564969	0.825609	0.960061
C	4.537884	-0.065898	0.509263
H	0.259012	-1.323572	-1.386518
H	4.980465	-1.770645	-0.729617
H	2.637812	-1.992137	-1.541264
C	0.574990	-0.421274	-0.875876
C	1.131895	1.599158	0.971533
H	3.823876	1.602456	1.671060
H	5.555764	0.028729	0.870227
C	0.117753	1.810960	-0.140070
H	0.639248	1.117141	1.823999

H	0.537617	2.408517	-0.955091
N	-0.291646	0.517853	-0.729565
H	-0.766096	2.307526	0.246319
H	1.503267	2.568646	1.305643
C	-1.751669	0.294529	-1.171331
C	-1.981115	-1.876362	-0.282189
C	-2.458176	-1.430049	0.925399
C	-2.964267	-0.030965	0.890974
C	-2.690335	0.815225	-0.109977
O	-2.554254	-2.109938	2.005331
O	-1.933943	-1.040222	-1.428235
H	-1.850788	0.837879	-2.113108
H	-1.718710	-2.898214	-0.516068
H	-3.640980	0.258697	1.691542
C	-3.330928	2.157083	-0.314058
H	-4.023106	2.113320	-1.162011
H	-3.895519	2.451416	0.571721
H	-2.605554	2.942470	-0.543876

TS3:

M06-2X/6-311++G(d,p) SCF energy in solution: -785.648351766 a.u.

M06-2X/6-311++G(d,p) enthalpy in solution: -785.418132 a.u.

M06-2X/6-311++G(d,p) free energy in solution: -785.418132 a.u.

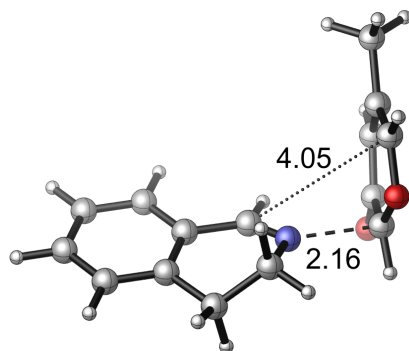
Three lowest frequencies (cm⁻¹): -149.05, 49.76, 67.44

Imaginary frequency (cm⁻¹): -149.05

Cartesian coordinates

ATOM	X	Y	Z
C	-4.031135	0.802602	-0.404344
C	-2.783430	0.944995	-0.994833
C	-1.727998	0.121657	-0.590324
C	-1.908780	-0.836176	0.421286
C	-3.158768	-0.958255	1.013474
C	-4.214722	-0.147202	0.599638
H	-0.215777	1.137394	-1.813071
H	-4.855715	1.431929	-0.716483
H	-2.616701	1.688216	-1.767321
C	-0.405247	0.291736	-1.167637
C	-0.709656	-1.652283	0.825393
H	-3.308978	-1.689914	1.800129
H	-5.187225	-0.256232	1.066173
C	0.168378	-1.899143	-0.392092

H	-0.141424	-1.108665	1.588683
H	-0.368449	-2.505948	-1.126807
N	0.515597	-0.632601	-1.068826
H	1.082410	-2.418290	-0.123769
H	-1.018030	-2.608073	1.252060
C	1.974095	-0.163735	-1.171970
C	1.412158	1.914590	-0.279336
C	1.616043	1.508833	1.035971
C	2.434771	0.278005	1.158537
C	2.668691	-0.533601	0.116510
O	1.208691	2.118856	2.068397
O	1.968985	1.203944	-1.354157
H	2.421908	-0.622193	-2.052626
H	1.061795	2.896888	-0.564032
H	2.889881	0.087523	2.127246
C	3.606289	-1.702800	0.122300
H	3.147960	-2.609551	-0.281644
H	4.473793	-1.483432	-0.509370
H	3.959839	-1.909190	1.133255

TS4:

M06-2X/6-311++G(d,p) SCF energy in solution: -785.656633289 a.u.

M06-2X/6-311++G(d,p) enthalpy in solution: -785.371871 a.u.

M06-2X/6-311++G(d,p) free energy in solution: -785.432841 a.u.

Three lowest frequencies (cm⁻¹): -195.46, 18.22, 22.37

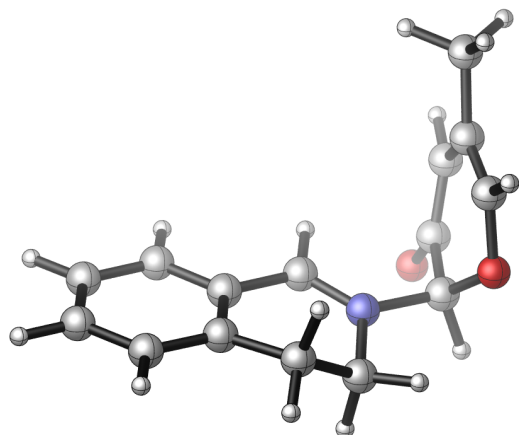
Imaginary frequency(cm⁻¹): -195.46

Cartesian coordinates

ATOM	X	Y	Z
C	3.841738	1.916858	-0.096795
C	2.504645	1.698099	-0.408532
C	1.957473	0.424794	-0.252386
C	2.742473	-0.646040	0.199806
C	4.080741	-0.417677	0.499950
C	4.625329	0.857962	0.357283
H	-0.011280	0.902627	-1.141925
H	4.272610	2.904554	-0.209890
H	1.879852	2.509009	-0.768699
C	0.544536	0.161701	-0.561746
C	2.088953	-2.002531	0.275374

H	4.699930	-1.238362	0.846948
H	5.668877	1.025126	0.599391
C	0.619462	-1.859847	0.655028
H	2.164342	-2.485062	-0.706479
H	0.520166	-1.530143	1.696477
N	-0.076193	-0.874642	-0.173038
H	0.094860	-2.812311	0.560831
H	2.601817	-2.641992	0.995867
C	-2.996272	-0.381802	1.321755
C	-2.149526	-1.231418	-0.657135
C	-2.371262	0.007821	-1.403503
C	-2.876762	1.043568	-0.606668
C	-3.138214	0.851769	0.774595
O	-2.045712	0.039769	-2.618741
O	-2.615003	-1.435886	0.542423
H	-3.228490	-0.680497	2.331999
H	-1.907080	-2.146206	-1.186005
H	-3.051751	2.017441	-1.053411
C	-3.596904	2.002801	1.626867
H	-2.847131	2.797584	1.628203
H	-4.523411	2.422820	1.228034
H	-3.772694	1.690501	2.657110

int-2:



M06-2X/6-311++G(d,p) SCF energy in solution: -785.675880064 a.u.

M06-2X/6-311++G(d,p) enthalpy in solution: -785.388592 a.u.

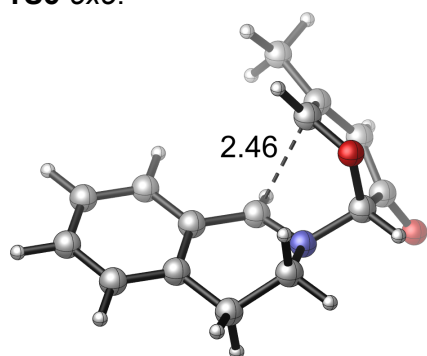
M06-2X/6-311++G(d,p) free energy in solution: -785.447403 a.u.

Three lowest frequencies (cm⁻¹): 20.47, 34.12, 81.39

Cartesian coordinates

ATOM	X	Y	Z
C	3.843609	-1.737351	0.116933
C	2.496812	-1.696160	-0.213113
C	1.808009	-0.481760	-0.134956
C	2.446065	0.692394	0.297812
C	3.790794	0.632672	0.636899
C	4.484369	-0.573216	0.539064
H	-0.170359	-1.348115	-0.579549
H	4.392573	-2.668496	0.050816

H	1.973715	-2.588844	-0.538690
C	0.400518	-0.428828	-0.475016
C	1.604756	1.933137	0.434575
H	4.298989	1.527963	0.977940
H	5.536216	-0.605076	0.799800
C	0.523627	1.964236	-0.630558
H	1.139892	1.937893	1.427244
H	0.946647	2.106454	-1.630116
N	-0.212527	0.683687	-0.667309
H	-0.203989	2.749537	-0.436846
H	2.217869	2.831071	0.351530
C	-2.637126	0.867767	1.116387
C	-1.684465	0.776178	-1.030317
C	-2.257538	-0.627490	-1.263151
C	-2.855348	-1.183771	-0.150692
C	-2.927766	-0.441668	1.093755
O	-2.038096	-1.117686	-2.404873
O	-2.311276	1.542482	-0.058629
H	-2.704810	1.527662	1.969844
H	-1.704570	1.348840	-1.958298
H	-3.234619	-2.199798	-0.192113
C	-3.343236	-1.155535	2.350357
H	-2.648266	-1.967125	2.585137
H	-3.382517	-0.475612	3.203512
H	-4.332591	-1.604164	2.221090

TS5-exo:

M06-2X/6-311++G(d,p) SCF energy in solution: -785.670014742 a.u.

M06-2X/6-311++G(d,p) enthalpy in solution: -785.384064 a.u.

M06-2X/6-311++G(d,p) free energy in solution: -785.439546 a.u.

Three lowest frequencies (cm⁻¹): -237.14, 61.63, 69.29

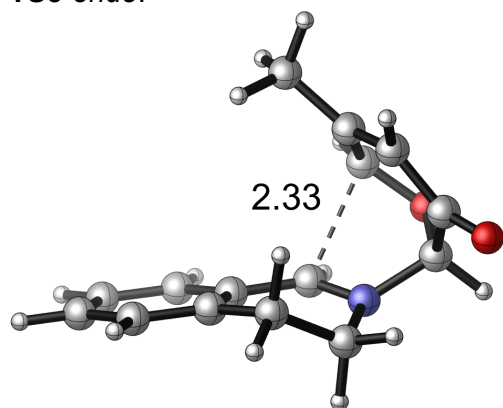
Imaginary frequency (cm⁻¹): -237.14

Cartesian coordinates

ATOM	X	Y	Z
C	3.272721	1.860893	-0.393663
C	1.921076	1.571697	-0.493891
C	1.471907	0.257055	-0.316084
C	2.384170	-0.778246	-0.060245
C	3.739584	-0.475018	0.031895
C	4.181635	0.835020	-0.127653

H	-0.560333	0.584486	-1.072153
H	3.622351	2.878374	-0.521365
H	1.199232	2.356437	-0.696818
C	0.051929	-0.043682	-0.437447
C	1.847241	-2.180268	0.041284
H	4.451237	-1.270471	0.226546
H	5.239385	1.058730	-0.048012
C	0.447399	-2.165654	0.627099
H	1.822816	-2.629619	-0.958074
H	0.472259	-1.815931	1.664990
N	-0.421236	-1.265173	-0.159720
H	-0.005890	-3.156161	0.598501
H	2.495506	-2.797704	0.665006
C	-1.453296	0.756106	1.335535
C	-1.822988	-1.256245	0.291201
C	-2.776194	-0.593245	-0.718346
C	-2.935352	0.806935	-0.562973
C	-2.161988	1.484291	0.390340
O	-3.269085	-1.319800	-1.588022
O	-1.794306	-0.556901	1.524787
H	-0.900047	1.197847	2.153723
H	-2.137159	-2.276640	0.494727
H	-3.514170	1.352230	-1.300602
C	-1.982437	2.973056	0.317340
H	-1.544319	3.262823	-0.642301
H	-2.953891	3.469089	0.391441
H	-1.343641	3.340155	1.121958

TS5-endo:



M06-2X/6-311++G(d,p) SCF energy in solution: -785.666365229 a.u.

M06-2X/6-311++G(d,p) enthalpy in solution: -785.380331 a.u.

M06-2X/6-311++G(d,p) free energy in solution: -785.435559 a.u.

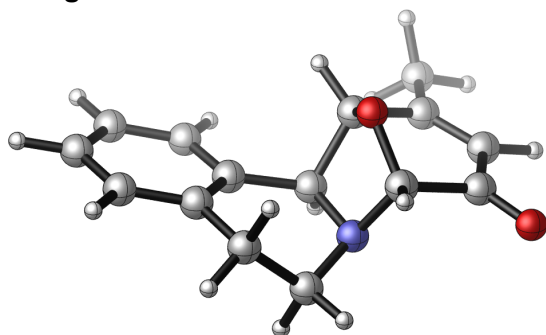
Three lowest frequencies (cm⁻¹): -276.91, 44.60, 72.35

Imaginary frequency (cm⁻¹): -276.91

Cartesian coordinates

ATOM	X	Y	Z
C	-3.830585	0.830817	-0.480805
C	-2.572134	0.905991	-1.061021
C	-1.548882	0.055900	-0.627750

C	-1.783157	-0.878219	0.394488
C	-3.048992	-0.943298	0.966144
C	-4.066868	-0.094587	0.534704
H	-0.087127	0.842247	-2.051656
H	-4.624495	1.487177	-0.816624
H	-2.370179	1.621308	-1.851824
C	-0.221319	0.162371	-1.221307
C	-0.643316	-1.764973	0.833818
H	-3.240822	-1.665850	1.752610
H	-5.048732	-0.159011	0.989670
C	0.300327	-2.033805	-0.331760
H	-0.097013	-1.285729	1.650886
H	-0.192663	-2.673569	-1.069407
N	0.681343	-0.796750	-1.039950
H	1.207482	-2.533741	-0.000621
H	-1.029282	-2.716305	1.206107
C	1.360198	1.739361	-0.544020
C	2.120007	-0.354388	-1.102836
C	2.662340	-0.590569	0.313486
C	2.210623	0.373934	1.240097
C	1.477618	1.490924	0.805336
O	3.323494	-1.617191	0.537576
O	2.120683	0.996275	-1.435671
H	1.004217	2.672120	-0.959290
H	2.674479	-0.902912	-1.861542
H	2.417936	0.228549	2.295274
C	0.788679	2.395213	1.787613
H	-0.029664	1.865155	2.284366
H	1.488239	2.718270	2.562430
H	0.377566	3.278846	1.296916

4.3ag:

M06-2X/6-311++G(d,p) SCF energy in solution: -785.717694180 a.u.

M06-2X/6-311++G(d,p) enthalpy in solution: -785.428940 a.u.

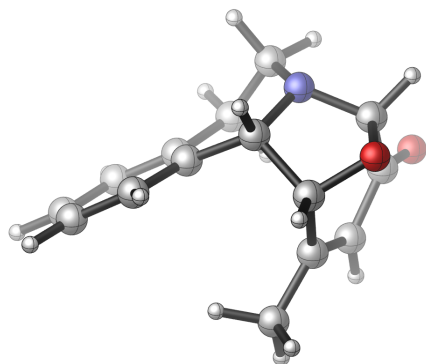
M06-2X/6-311++G(d,p) free energy in solution: -785.483972 a.u.

Three lowest frequencies (cm^{-1}): 43.66, 79.19, 107.01

Cartesian coordinates

ATOM	X	Y	Z
C	-3.532750	1.604391	-0.069078
C	-2.181484	1.546213	-0.381469

C	-1.479532	0.339401	-0.310251
C	-2.150062	-0.830435	0.058337
C	-3.513144	-0.763818	0.363579
C	-4.202047	0.440681	0.309703
H	0.175868	0.920510	-1.538188
H	-4.063964	2.547607	-0.125292
H	-1.655827	2.448434	-0.682663
C	0.006358	0.353026	-0.618453
C	-1.405811	-2.141227	0.073843
H	-4.034530	-1.675158	0.639937
H	-5.258695	0.473055	0.550065
C	-0.275407	-2.092557	-0.950204
H	-0.990049	-2.329797	1.070548
H	-0.690313	-1.972864	-1.954726
N	0.643796	-0.977629	-0.707403
H	0.307175	-3.014874	-0.943627
H	-2.090600	-2.962967	-0.149952
C	0.804482	0.983622	0.558972
C	1.458559	-1.117392	0.504207
C	2.903756	-0.783971	0.124150
C	3.147582	0.650294	-0.099727
C	2.135410	1.514897	0.068556
O	3.737373	-1.651289	-0.037245
O	0.997635	-0.136439	1.414337
H	0.243314	1.748067	1.094049
H	1.393456	-2.109646	0.950886
H	4.130435	0.959946	-0.440060
C	2.205807	2.973756	-0.234353
H	1.417733	3.246663	-0.944457
H	2.026880	3.553688	0.676491
H	3.172173	3.251265	-0.654794

4.3ag-endo:

M06-2X/6-311++G(d,p) SCF energy in solution: -785.716448663 a.u.

M06-2X/6-311++G(d,p) enthalpy in solution: -785.427603 a.u.

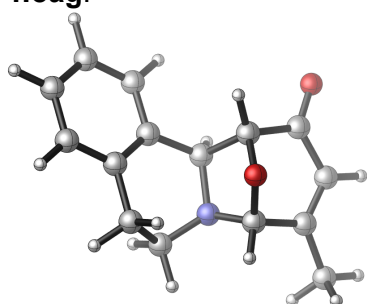
M06-2X/6-311++G(d,p) free energy in solution: -785.481879 a.u.

Three lowest frequencies (cm⁻¹): 63.18, 72.63, 109.33

Cartesian coordinates

ATOM	X	Y	Z
C	-3.566366	0.632187	-0.330246

C	-2.347113	0.802833	-0.971915
C	-1.258795	-0.022403	-0.673586
C	-1.406636	-1.061895	0.250484
C	-2.642555	-1.231840	0.882740
C	-3.712034	-0.389071	0.608395
H	-0.139687	0.470256	-2.415448
H	-4.400405	1.283752	-0.564460
H	-2.227462	1.589565	-1.711683
C	0.058244	0.247030	-1.361828
C	-0.259142	-2.002914	0.520998
H	-2.761422	-2.044457	1.592853
H	-4.661417	-0.536833	1.110615
C	0.637844	-2.113233	-0.715178
H	0.317885	-1.657731	1.383780
H	0.091984	-2.650573	-1.496598
N	1.055880	-0.826113	-1.262855
H	1.536406	-2.692125	-0.492023
H	-0.649884	-2.990871	0.778625
C	0.858779	1.460144	-0.791462
C	2.301045	-0.219112	-0.777556
C	2.395592	-0.260939	0.752232
C	1.561675	0.733527	1.440531
C	0.780023	1.551879	0.716538
O	3.059423	-1.106161	1.321280
O	2.188615	1.122569	-1.185275
H	0.583356	2.402885	-1.262194
H	3.185349	-0.675426	-1.224375
H	1.579015	0.754760	2.525726
C	-0.165360	2.541104	1.312156
H	-1.191503	2.316943	1.003214
H	-0.114961	2.530386	2.401104
H	0.066081	3.547216	0.948991

4.5ag:

M06-2X/6-311++G(d,p) SCF energy in solution: -785.716352515 a.u.

M06-2X/6-311++G(d,p) enthalpy in solution: -785.427542 a.u.

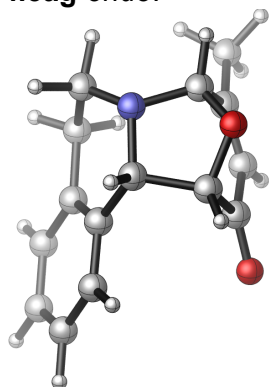
M06-2X/6-311++G(d,p) free energy in solution: -785.482784 a.u.

Three lowest frequencies (cm⁻¹): 33.07, 81.04, 97.12

Cartesian coordinates

ATOM	X	Y	Z
C	3.647345	1.443314	0.343293
C	2.285640	1.427886	0.615558

C	1.519035	0.288326	0.359397
C	2.130238	-0.858059	-0.157319
C	3.502690	-0.836248	-0.419393
C	4.258482	0.305010	-0.181280
H	-0.168693	0.946564	1.494818
H	4.230975	2.334447	0.543977
H	1.803016	2.310232	1.026469
C	0.023148	0.358160	0.593315
C	1.302882	-2.102352	-0.350003
H	3.978130	-1.731520	-0.808011
H	5.322092	0.304970	-0.391220
C	0.214759	-2.126896	0.720344
H	0.842523	-2.111141	-1.344099
H	0.679419	-2.154059	1.709714
N	-0.665590	-0.954173	0.667218
H	-0.414087	-3.014047	0.630594
H	1.936250	-2.989556	-0.273208
C	-1.596680	-0.952984	-0.462878
C	-0.670252	1.031524	-0.639662
C	-1.919128	1.785124	-0.191602
C	-3.078549	0.931487	0.095862
C	-2.933199	-0.400084	0.011881
O	-1.900350	2.988248	-0.022221
O	-1.042278	-0.080102	-1.436174
H	-1.709546	-1.946741	-0.897267
H	-0.010634	1.692028	-1.198349
H	-3.994050	1.401707	0.439667
C	-3.962688	-1.397805	0.415262
H	-3.541839	-2.071722	1.169471
H	-4.853640	-0.919496	0.821304
H	-4.242101	-2.016034	-0.443884

4.5ag-endo:

M06-2X/6-311++G(d,p) SCF energy in solution: -785.713398942 a.u.

M06-2X/6-311++G(d,p) enthalpy in solution: -785.424654 a.u.

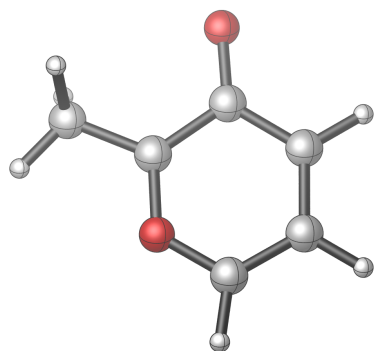
M06-2X/6-311++G(d,p) free energy in solution: -785.478529 a.u.

Three lowest frequencies (cm⁻¹): 54.63, 74.40, 121.91

Cartesian coordinates

ATOM	X	Y	Z
------	---	---	---

C	3.505499	-0.720724	-0.017409
C	2.317393	-0.978022	-0.685456
C	1.253586	-0.071440	-0.634277
C	1.395888	1.125325	0.074766
C	2.603600	1.380386	0.734473
C	3.648331	0.467495	0.699902
H	0.236118	-0.700029	-2.394496
H	4.318071	-1.437029	-0.057800
H	2.202120	-1.898219	-1.250877
C	-0.024576	-0.422555	-1.367853
C	0.275692	2.135496	0.108956
H	2.717657	2.314779	1.275623
H	4.574878	0.682860	1.220047
C	-0.623358	1.988332	-1.120993
H	-0.302868	2.014270	1.029167
H	-0.072067	2.339408	-1.998956
N	-1.056376	0.623957	-1.396130
H	-1.515037	2.613321	-1.030763
H	0.696285	3.144576	0.131688
C	-2.217030	0.080320	-0.683029
C	-0.813383	-1.623990	-0.751571
C	-0.633432	-1.698235	0.761828
C	-1.388033	-0.682983	1.510242
C	-2.140334	0.203289	0.838408
O	0.100202	-2.516013	1.279795
O	-2.167769	-1.286236	-1.033468
H	-3.143619	0.516046	-1.060442
H	-0.570555	-2.580754	-1.208911
H	-1.293647	-0.669423	2.591553
C	-2.915164	1.306283	1.478186
H	-3.985481	1.145168	1.310539
H	-2.726299	1.362646	2.550397
H	-2.668450	2.268798	1.018480

4.4a:

M06-2X/6-311++G(d,p) SCF energy in solution: -382.602662416 a.u.

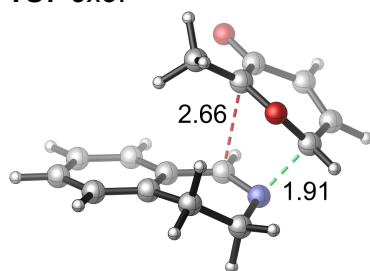
M06-2X/6-311++G(d,p) enthalpy in solution: -382.487030 a.u.

M06-2X/6-311++G(d,p) free energy in solution: -382.525928 a.u.

Three lowest frequencies (cm⁻¹): 112.58, 142.60, 256.49

Cartesian coordinates

ATOM	X	Y	Z
C	1.648420	-0.978069	0.000046
C	-0.636746	-0.509066	0.000152
C	-0.437743	0.918469	0.000573
C	0.935024	1.299342	0.000066
C	1.956000	0.355140	-0.000081
H	2.333579	-1.811652	-0.000034
H	1.169752	2.358586	-0.000187
H	2.997817	0.649765	-0.000293
O	-1.419968	1.696701	-0.000457
O	0.371800	-1.351725	0.000036
C	-1.984034	-1.118354	-0.000057
H	-2.541140	-0.778189	0.877884
H	-2.541113	-0.777636	-0.877802
H	-1.919078	-2.205447	-0.000395

TS7-exo:

M06-2X/6-311++G(d,p) SCF energy in solution: -785.649907874 a.u.

M06-2X/6-311++G(d,p) enthalpy in solution: -785.365043 a.u.

M06-2X/6-311++G(d,p) free energy in solution: -785.421410 a.u.

Three lowest frequencies (cm⁻¹): -438.83, 45.88, 66.39

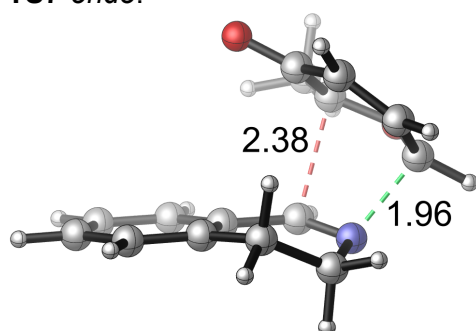
Imaginary frequency (cm⁻¹): -438.83

Cartesian coordinates

ATOM	X	Y	Z
C	-2.289987	1.244673	-0.057275
C	-1.315469	-0.541354	1.050890
C	-1.893005	-1.497957	0.173712
C	-2.941511	-0.966974	-0.694783
C	-3.118842	0.365657	-0.830762
H	-2.558417	2.286494	0.060135
H	-3.535080	-1.681231	-1.256256
H	-3.828639	0.800845	-1.522886
O	-1.541558	-2.701143	0.155113
O	-1.746286	0.743343	1.056147
C	-0.407730	-0.906272	2.166794
H	-0.483440	-0.175910	2.974233
H	-0.661312	-1.898903	2.543306
H	0.637156	-0.942023	1.829296
C	3.139114	-1.546217	-0.764882
C	1.852670	-1.232246	-1.187645
C	1.234677	-0.062521	-0.735825
C	1.897617	0.787403	0.163485
C	3.186451	0.466131	0.574244

C	3.808266	-0.692560	0.110077
H	-0.637090	-0.446112	-1.798091
H	3.619658	-2.451541	-1.116848
H	1.320495	-1.886538	-1.870690
C	-0.118586	0.277485	-1.174603
C	1.132644	1.975629	0.683105
H	3.704689	1.122611	1.266033
H	4.814165	-0.931579	0.436182
C	0.157418	2.491005	-0.374670
H	0.586612	1.679793	1.585017
H	0.716522	2.981490	-1.178643
N	-0.662425	1.459729	-1.039041
H	-0.513764	3.236891	0.053082
H	1.815806	2.778717	0.968165

TS7-endo:



M06-2X/6-311++G(d,p) SCF energy in solution: -785.646789016 a.u.

M06-2X/6-311++G(d,p) enthalpy in solution: -785.362067 a.u.

M06-2X/6-311++G(d,p) free energy in solution: -785.418944 a.u.

Three lowest frequencies (cm⁻¹): -439.26, 31.58, 54.77

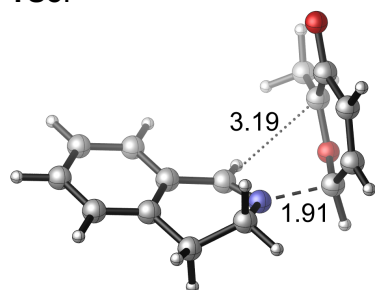
Imaginary frequency (cm⁻¹): -439.26

Cartesian coordinates

ATOM	X	Y	Z
C	2.541514	-0.797372	-0.581769
C	1.661647	1.261729	-0.067700
C	1.251611	0.856897	1.245381
C	1.793657	-0.422397	1.664848
C	2.400022	-1.242176	0.769843
H	3.186625	-1.316674	-1.276454
H	1.661932	-0.711893	2.702283
H	2.746177	-2.234392	1.030949
O	0.517644	1.569857	1.961244
O	2.543681	0.522315	-0.780801
C	1.487785	2.658474	-0.538684
H	2.103026	3.350103	0.046434
H	1.754847	2.746125	-1.592478
H	0.445673	2.955357	-0.396816
C	-3.284177	1.335074	-0.377486
C	-2.019384	1.210256	-0.940459
C	-1.242534	0.078534	-0.679377
C	-1.732566	-0.938184	0.151412

C	-3.002268	-0.806367	0.704276
C	-3.776035	0.323514	0.444529
H	0.386743	0.730037	-1.972605
H	-3.885236	2.213616	-0.581064
H	-1.628326	1.985250	-1.592499
C	0.090032	-0.055962	-1.281732
C	-0.836742	-2.117186	0.431351
H	-3.388468	-1.593866	1.343847
H	-4.763797	0.412747	0.882350
C	0.123956	-2.369161	-0.733702
H	-0.282945	-1.929052	1.354381
H	-0.432368	-2.829061	-1.557874
N	0.771574	-1.182802	-1.321882
H	0.902768	-3.075281	-0.442631
H	-1.437382	-3.014817	0.597418

TS8:



M06-2X/6-311++G(d,p) SCF energy in solution: -785.646735946 a.u.

M06-2X/6-311++G(d,p) enthalpy in solution: -785.361976 a.u.

M06-2X/6-311++G(d,p) free energy in solution: -785.421238 a.u.

Three lowest frequencies (cm⁻¹): -325.54, 19.69, 35.93

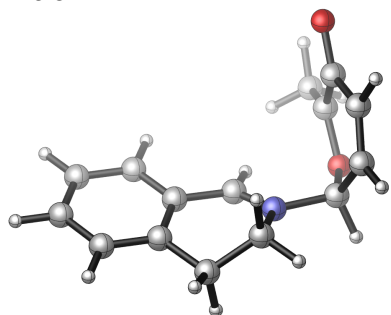
Imaginary frequency (cm⁻¹): -325.54

Cartesian coordinates

ATOM	X	Y	Z
C	1.970972	1.271101	-0.957580
C	2.541956	-0.927390	-0.330026
C	2.769528	-0.586198	0.998917
C	2.812817	0.855745	1.238667
C	2.448355	1.765650	0.305023
H	1.912617	1.928820	-1.815848
H	3.172762	1.175746	2.212376
H	2.475819	2.834182	0.474312
O	2.994237	-1.420386	1.938073
O	2.307564	0.037319	-1.298476
C	2.626033	-2.291057	-0.909139
H	3.351354	-2.329872	-1.728815
H	2.936040	-2.985433	-0.129093
H	1.660067	-2.624825	-1.308770
C	-3.502074	-1.989672	0.136278
C	-2.236289	-1.695063	-0.354636
C	-1.795994	-0.370958	-0.373925
C	-2.618533	0.672302	0.076233

C	-3.886283	0.365681	0.556445
C	-4.322206	-0.958168	0.590199
H	0.081662	-0.769997	-1.464236
H	-3.849803	-3.015223	0.165463
H	-1.582367	-2.483075	-0.713756
C	-0.465189	-0.029353	-0.880631
C	-2.088014	2.077614	-0.045616
H	-4.534665	1.162009	0.906245
H	-5.310666	-1.185911	0.972994
C	-0.580374	2.093364	0.167576
H	-2.319503	2.458066	-1.047595
H	-0.336977	1.854849	1.208771
N	0.086625	1.101884	-0.681302
H	-0.155919	3.072007	-0.063099
H	-2.569429	2.738418	0.676678

int-3:



M06-2X/6-311++G(d,p) SCF energy in solution: -785.679580273 a.u.

M06-2X/6-311++G(d,p) enthalpy in solution: -785.392815 a.u.

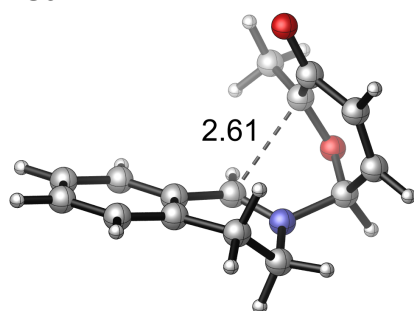
M06-2X/6-311++G(d,p) free energy in solution: -785.449181 a.u.

Three lowest frequencies (cm⁻¹): 35.46, 45.86, 88.97

Cartesian coordinates

ATOM	X	Y	Z
C	-1.623545	-1.280656	-0.850966
C	-2.533157	0.875767	-0.397040
C	-2.850435	0.568587	0.904617
C	-2.831400	-0.881777	1.212264
C	-2.284196	-1.788267	0.395055
H	-1.601973	-2.019372	-1.653080
H	-3.320517	-1.184014	2.134219
H	-2.294678	-2.854146	0.587092
O	-3.198411	1.402115	1.818724
O	-2.196728	-0.134527	-1.337848
C	-2.662181	2.202432	-1.051858
H	-3.377052	2.168990	-1.883304
H	-3.016576	2.925756	-0.317325
H	-1.710700	2.566729	-1.462973
C	3.480072	2.013702	0.243771
C	2.180646	1.752637	-0.166883
C	1.743634	0.428252	-0.259206
C	2.602005	-0.643956	0.029751
C	3.903475	-0.368064	0.427014

C	4.335347	0.952967	0.539334
H	-0.206192	0.911721	-1.164548
H	3.828151	3.035447	0.332271
H	1.496563	2.560697	-0.403016
C	0.386080	0.141034	-0.684922
C	2.070073	-2.036407	-0.180157
H	4.581610	-1.184564	0.649680
H	5.351498	1.156190	0.857818
C	0.590119	-2.100817	0.157382
H	2.222174	-2.320008	-1.227698
H	0.421965	-1.978107	1.230687
N	-0.144403	-1.019532	-0.530517
H	0.150541	-3.046316	-0.160624
H	2.607896	-2.755583	0.438466

TS9:

M06-2X/6-311++G(d,p) SCF energy in solution: -785.652215630 a.u.

M06-2X/6-311++G(d,p) enthalpy in solution: -785.366641 a.u.

M06-2X/6-311++G(d,p) free energy in solution: -785.421705 a.u.

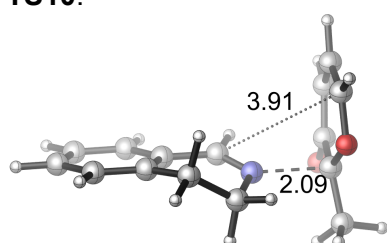
Three lowest frequencies (cm⁻¹): -110.78, 50.89, 73.47

Imaginary frequency (cm⁻¹): -110.78

Cartesian coordinates

ATOM	X	Y	Z
C	-1.987163	1.022491	-1.034155
C	-2.036201	-1.136958	-0.108789
C	-1.984633	-0.670558	1.205936
C	-2.325525	0.759146	1.351471
C	-2.363797	1.588525	0.299732
H	-2.362461	1.586902	-1.884619
H	-2.562679	1.104982	2.353307
H	-2.623235	2.637293	0.376864
O	-1.728436	-1.380991	2.226429
O	-2.405291	-0.285139	-1.160975
C	-2.052109	-2.566572	-0.506121
H	-1.304539	-2.791836	-1.278248
H	-1.845007	-3.181520	0.369247
H	-3.029442	-2.851016	-0.914148
C	3.521486	-1.548467	-0.259313
C	2.253681	-1.404834	-0.805537
C	1.510347	-0.250373	-0.539626
C	2.024292	0.762537	0.288594
C	3.290338	0.600998	0.835163

C	4.036142	-0.545100	0.559929
H	-0.278469	-0.945775	-1.598923
H	4.105169	-2.437513	-0.465143
H	1.830864	-2.177526	-1.439160
C	0.165218	-0.113234	-1.070300
C	1.147380	1.957312	0.566355
H	3.697738	1.373786	1.478326
H	5.025556	-0.655226	0.989134
C	0.275464	2.246370	-0.647034
H	0.516750	1.746462	1.436893
H	0.898004	2.559269	-1.490180
N	-0.450426	1.041003	-1.089290
H	-0.449732	3.031699	-0.446186
H	1.754762	2.834325	0.796405

TS10:

M06-2X/6-311++G(d,p) SCF energy in solution: -785.665338722 a.u.

M06-2X/6-311++G(d,p) enthalpy in solution: -785.380926 a.u.

M06-2X/6-311++G(d,p) free energy in solution: -785.439762 a.u.

Three lowest frequencies (cm⁻¹): -191.83, 24.21, 34.08

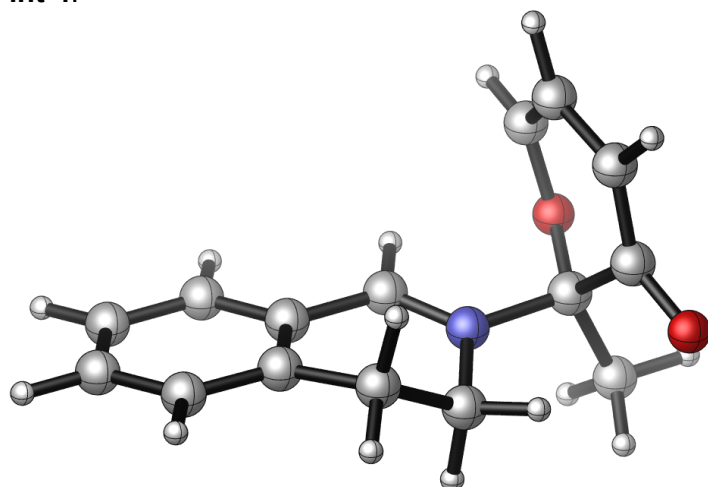
Imaginary frequency (cm⁻¹): -191.83

Cartesian coordinates

ATOM	X	Y	Z
C	-2.692751	0.887811	1.643940
C	-2.391219	0.268459	-0.584728
C	-2.499250	-1.179595	-0.273496
C	-2.628869	-1.457355	1.090019
C	-2.665142	-0.403271	2.037493
H	-2.791188	1.767207	2.260078
H	-2.680961	-2.489981	1.414849
H	-2.697048	-0.614528	3.099704
O	-2.410007	-1.993476	-1.228447
O	-2.701256	1.185732	0.307411
C	-2.531411	0.733262	-1.990780
H	-3.581316	0.630058	-2.283660
H	-2.239725	1.779792	-2.081641
H	-1.934142	0.103812	-2.646750
C	4.084256	-1.505866	0.024583
C	2.704557	-1.635043	-0.087620
C	1.898653	-0.497691	-0.041215
C	2.458386	0.776189	0.135175
C	3.838356	0.892262	0.255860
C	4.646475	-0.242503	0.195387
H	-0.037819	-1.570115	-0.029747

H	4.718385	-2.383399	-0.017103
H	2.247049	-2.610484	-0.216988
C	0.437914	-0.595586	-0.162538
C	1.508741	1.941651	0.242819
H	4.283995	1.871386	0.397122
H	5.722009	-0.139069	0.285089
C	0.291146	1.713591	-0.644836
H	1.181518	2.034866	1.285624
H	0.566229	1.771705	-1.704902
N	-0.307634	0.398652	-0.420654
H	-0.476007	2.467707	-0.457141
H	2.003507	2.874533	-0.032049

int-4:



M06-2X/6-311++G(d,p) SCF energy in solution: -785.679580273 a.u.

M06-2X/6-311++G(d,p) enthalpy in solution: -785.392815 a.u.

M06-2X/6-311++G(d,p) free energy in solution: -785.449181 a.u.

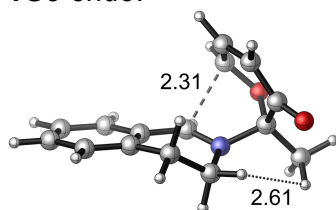
Three lowest frequencies (cm⁻¹): 46.70, 50.44, 102.19

Cartesian coordinates

ATOM	X	Y	Z
C	-1.952832	-2.083650	0.602497
C	-1.928477	-0.109876	-0.711471
C	-2.665575	0.655420	0.434324
C	-2.688947	-0.023384	1.640962
C	-2.238116	-1.387106	1.711983
H	-1.689475	-3.129604	0.539965
H	-3.110820	0.461636	2.513222
H	-2.159760	-1.893227	2.667550
O	-3.096173	1.803840	0.161466
O	-2.083548	-1.493328	-0.649987
C	-2.337313	0.342021	-2.094655
H	-1.777119	-0.221644	-2.843399
H	-3.405025	0.158099	-2.219530
H	-2.156214	1.408788	-2.216691
C	4.148233	-1.139549	-0.220058
C	2.813489	-1.416868	-0.478736

C	1.846301	-0.438149	-0.230659
C	2.199582	0.813310	0.298483
C	3.537671	1.072271	0.564365
C	4.505131	0.103645	0.300631
H	0.134373	-1.741377	-0.686819
H	4.907549	-1.886471	-0.416377
H	2.511902	-2.379944	-0.876518
C	0.446401	-0.722701	-0.490493
C	1.085181	1.779358	0.597047
H	3.825673	2.032607	0.978026
H	5.547203	0.320116	0.506921
C	-0.035493	1.625837	-0.416277
H	0.697006	1.582686	1.602841
H	0.292977	1.928446	-1.415535
N	-0.446443	0.205413	-0.529435
H	-0.913479	2.206196	-0.142624
H	1.446657	2.808232	0.575522

TS6-endo:



M06-2X/6-311++G(d,p) SCF energy in solution: -785.670753633 a.u.

M06-2X/6-311++G(d,p) enthalpy in solution: -785.385270 a.u.

M06-2X/6-311++G(d,p) free energy in solution: -785.439572 a.u.

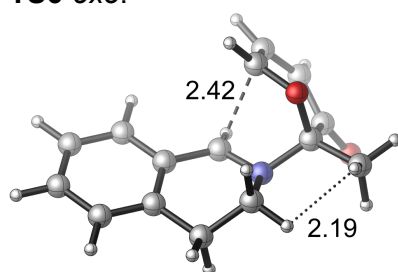
Three lowest frequencies (cm⁻¹): -291.14, 49.94, 80.00

Imaginary frequency (cm⁻¹): -291.14

Cartesian coordinates

ATOM	X	Y	Z
C	-1.108787	-1.881766	0.812438
C	-2.070705	-0.300607	-0.582289
C	-2.477838	0.564816	0.632988
C	-1.869741	0.153503	1.847162
C	-1.133583	-1.030098	1.893724
H	-0.744685	-2.898826	0.844276
H	-1.980442	0.784207	2.721443
H	-0.566510	-1.302907	2.776961
O	-3.173507	1.573215	0.454115
O	-2.001764	-1.652628	-0.220946
C	-2.955742	-0.154808	-1.789372
H	-2.576433	-0.784337	-2.596020
H	-3.973351	-0.454737	-1.533798
H	-2.971953	0.886160	-2.111870
C	3.996194	-1.002277	-0.170852
C	2.689652	-1.355876	-0.478568
C	1.663038	-0.412418	-0.367797
C	1.943413	0.897930	0.051273
C	3.256882	1.239690	0.353907

C	4.278133	0.297166	0.247409
H	0.122301	-1.783751	-1.089365
H	4.791818	-1.732755	-0.256865
H	2.452994	-2.363624	-0.804620
C	0.288584	-0.799170	-0.672706
C	0.800452	1.877076	0.162339
H	3.483156	2.252032	0.672339
H	5.297115	0.579271	0.486819
C	-0.275522	1.556279	-0.867664
H	0.374097	1.832627	1.168251
H	0.093388	1.776907	-1.873739
N	-0.647554	0.129362	-0.857395
H	-1.172859	2.147619	-0.698357
H	1.159813	2.895238	-0.001000

TS6-exo:

M06-2X/6-311++G(d,p) SCF energy in solution: -785.669224337 a.u.

M06-2X/6-311++G(d,p) enthalpy in solution: -785.383698 a.u.

M06-2X/6-311++G(d,p) free energy in solution: -785.437764 a.u.

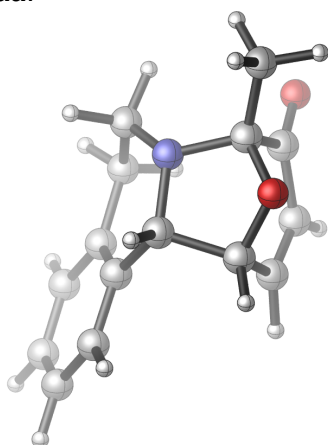
Three lowest frequencies (cm⁻¹): -267.12, 62.78, 73.87

Imaginary frequency (cm⁻¹): -267.12

Cartesian coordinates

ATOM	X	Y	Z
C	1.160471	-1.219268	1.443182
C	1.968552	0.559672	0.190114
C	2.688281	-0.443049	-0.757081
C	2.566966	-1.823027	-0.420477
C	1.707395	-2.185889	0.611398
H	0.543736	-1.431504	2.305623
H	3.005008	-2.555162	-1.087678
H	1.372967	-3.212871	0.722153
O	3.274748	0.024776	-1.733870
O	1.789104	-0.004469	1.487066
C	2.784123	1.821640	0.344752
H	2.406883	2.426178	1.169069
H	3.815950	1.543161	0.560064
H	2.766657	2.394847	-0.581608
C	-3.649149	-1.585412	-0.168841
C	-2.268348	-1.563516	-0.286245
C	-1.583501	-0.341832	-0.263338
C	-2.288464	0.863851	-0.145891
C	-3.675553	0.829578	-0.032379
C	-4.352426	-0.386186	-0.037547

H	0.338276	-1.118370	-0.962053
H	-4.180522	-2.529579	-0.176851
H	-1.705536	-2.486622	-0.381609
C	-0.132056	-0.322610	-0.400317
C	-1.498344	2.140050	-0.214984
H	-4.226162	1.760165	0.057198
H	-5.432124	-0.401280	0.058363
C	-0.113449	1.951267	0.378978
H	-1.405708	2.448082	-1.262878
H	-0.177993	1.763570	1.456891
N	0.572266	0.811471	-0.268347
H	0.485472	2.842632	0.209599
H	-2.010566	2.942380	0.318637

4.3aa:

M06-2X/6-311++G(d,p) SCF energy in solution: -785.716970858 a.u.

M06-2X/6-311++G(d,p) enthalpy in solution: -785.428841 a.u.

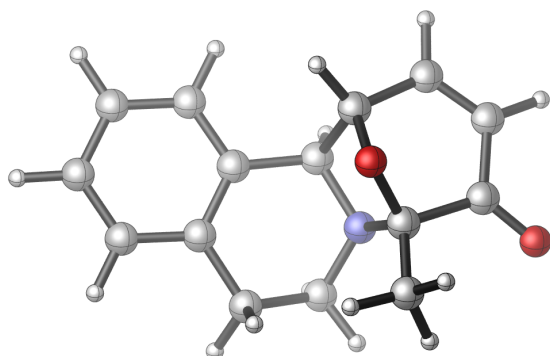
M06-2X/6-311++G(d,p) free energy in solution: -785.482718 a.u.

Three lowest frequencies (cm⁻¹): 53.52, 91.60, 104.62

Cartesian coordinates

ATOM	X	Y	Z
C	-0.82958700	-1.93661200	0.36892200
C	-2.11736000	-0.23386800	-0.41311100
C	-2.08093400	0.47949000	0.95076600
C	-1.21782400	-0.15007200	1.95152800
C	-0.57650200	-1.29596300	1.64359900
H	-0.58634300	-2.98659700	0.25470600
H	-1.08562100	0.36089400	2.89856400
H	0.15792500	-1.73615700	2.30973200
O	-2.64497200	1.54698600	1.12152100
O	-2.05472800	-1.62240900	-0.20407500
C	-3.34558600	0.08880800	-1.22286700
H	-3.31135100	-0.47736900	-2.15438300
H	-4.24327300	-0.17637400	-0.66097300
H	-3.38304300	1.15478200	-1.44679600
C	3.83919600	-0.90603600	-0.09594800
C	2.58604200	-1.28525500	-0.55293500

C	1.51254300	-0.38631300	-0.52748500
C	1.71070500	0.92154000	-0.06448400
C	2.98043800	1.29426100	0.38334000
C	4.03665000	0.39155300	0.37907400
H	0.20741900	-1.61871200	-1.74348000
H	4.66138000	-1.61220800	-0.11377900
H	2.42245500	-2.29086000	-0.92908600
C	0.17776400	-0.84954200	-0.97158700
C	0.57183700	1.91277900	-0.09507100
H	3.13746800	2.31078200	0.73089900
H	5.01442400	0.69980700	0.73155300
C	-0.44322900	1.52667300	-1.17000300
H	0.08978500	1.96713200	0.88453400
H	-0.00544700	1.71285300	-2.15498600
N	-0.84680100	0.11593500	-1.13227100
H	-1.33811800	2.14414400	-1.09237500
H	0.96264200	2.91105400	-0.31023100

4.3aa-exo:

M06-2X/6-311++G(d,p) SCF energy in solution: -785.713206012 a.u.

M06-2X/6-311++G(d,p) enthalpy in solution: -785.424717 a.u.

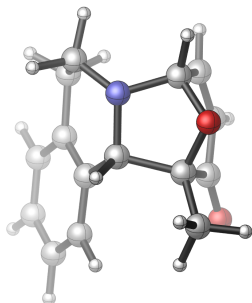
M06-2X/6-311++G(d,p) free energy in solution: -785.478914 a.u.

Three lowest frequencies (cm⁻¹): 40.70, 81.75, 110.45

Cartesian coordinates

ATOM	X	Y	Z
C	0.70108100	-1.13840500	-1.12220100
C	1.83021400	0.58080100	-0.17753400
C	2.88283900	-0.41466800	0.38215100
C	2.73544600	-1.82416900	-0.00221400
C	1.63599300	-2.18370900	-0.68722300
H	-0.06307700	-1.39713400	-1.84646100
H	3.46513600	-2.53156600	0.37400000
H	1.38708000	-3.22455900	-0.86871400
O	3.74865600	-0.01921300	1.13532800
O	1.32427200	0.05856100	-1.41247000
C	2.49193200	1.90814900	-0.46833900
H	3.37581800	1.72960100	-1.08202100
H	1.81038400	2.55767200	-1.01785000
H	2.80533500	2.39167300	0.45596400
C	-3.78512400	-1.37993300	0.36227000

C	-2.42611800	-1.47795000	0.63456400
C	-1.57205800	-0.39965000	0.38423600
C	-2.09395700	0.79734500	-0.12785900
C	-3.45971900	0.88796500	-0.38932600
C	-4.30373300	-0.19432300	-0.15597300
H	0.15644300	-1.37354700	1.25414700
H	-4.43935200	-2.22161500	0.55876300
H	-2.01510900	-2.39706800	1.04108100
C	-0.11152700	-0.55831200	0.58539700
C	-1.14939000	1.95811100	-0.30633900
H	-3.86428700	1.81993600	-0.77174300
H	-5.36410800	-0.10914600	-0.36479300
C	-0.09061600	1.87516300	0.79146700
H	-0.66837400	1.92126600	-1.28959000
H	-0.58896100	1.90852600	1.76413100
N	0.68706700	0.62463000	0.75285800
H	0.59417300	2.71825800	0.75828000
H	-1.69558600	2.90201400	-0.23653500

4.5aa:

M06-2X/6-311++G(d,p) SCF energy in solution: -785.711858693 a.u.

M06-2X/6-311++G(d,p) enthalpy in solution: -785.423524 a.u.

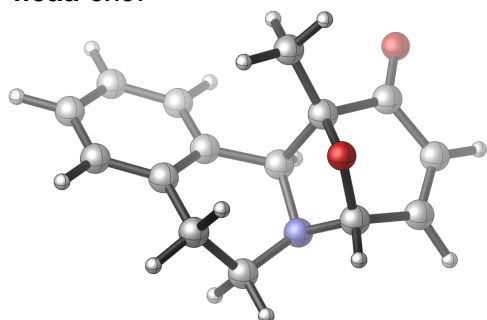
M06-2X/6-311++G(d,p) free energy in solution: -785.477264 a.u.

Three lowest frequencies (cm⁻¹): 47.39, 73.71, 126.70

Cartesian coordinates

ATOM	X	Y	Z
C	1.98454000	-1.32107900	0.00316900
C	1.80840900	0.91240400	-0.28089600
C	1.19319600	1.15442600	1.05355600
C	1.12924200	-0.03245000	1.92544400
C	1.48570900	-1.22005700	1.42556900
H	2.64574000	-2.17631700	-0.12888300
H	0.74831800	0.09832100	2.93236300
H	1.39820800	-2.13436000	2.00367500
O	0.70817200	2.23222800	1.35614800
O	2.69496300	-0.15570400	-0.32273800
C	2.26427000	2.09230300	-1.07264100
H	2.53208500	1.78497100	-2.08420500
H	1.47405400	2.84181900	-1.11354200
H	3.13980700	2.54586300	-0.59661500
C	-2.89208100	1.71096300	-0.36092000
C	-1.62943300	1.42349100	-0.85704500

C	-1.05191600	0.16173900	-0.66366400
C	-1.76872800	-0.83266200	0.01711600
C	-3.04403800	-0.53284100	0.50304900
C	-3.60339300	0.72651700	0.32614600
H	0.46880400	0.31629000	-2.19442400
H	-3.32352100	2.69422900	-0.50935300
H	-1.06916500	2.18157400	-1.39619900
C	0.30668300	-0.09638500	-1.19765100
C	-1.18262800	-2.21287500	0.19611900
H	-3.60435500	-1.30651700	1.01944600
H	-4.59392100	0.93888100	0.71226200
C	-0.07150700	-2.48623900	-0.82179500
H	-0.80971400	-2.32322500	1.21755500
H	-0.52718400	-2.67387000	-1.79811400
N	0.88666000	-1.39148500	-1.00392000
H	0.49054000	-3.38276400	-0.54851900
H	-1.97134600	-2.96022900	0.07137300

4.5aa-exo:

M06-2X/6-311++G(d,p) SCF energy in solution: -785.713833649 a.u.

M06-2X/6-311++G(d,p) enthalpy in solution: -785.425183 a.u.

M06-2X/6-311++G(d,p) free energy in solution: -785.479489 a.u.

Three lowest frequencies (cm⁻¹): 30.84, 84.34, 98.85

Cartesian coordinates

ATOM	X	Y	Z
C	-1.90190500	1.42849900	-0.01577700
C	-1.19207500	-0.56255300	0.78937000
C	-2.24960300	-1.35952800	0.09890000
C	-3.23013500	-0.54760900	-0.66389900
C	-3.03725900	0.76890900	-0.76239600
H	-2.15656300	2.44731000	0.26949200
H	-4.02952800	-1.07063000	-1.17714900
H	-3.66226600	1.39969000	-1.38585000
O	-2.24310900	-2.57695900	0.06702600
O	-1.63989900	0.69086200	1.17986100
C	-0.34556200	-1.25209000	1.80713500
H	-0.94529100	-1.51844000	2.68315600
H	0.07239400	-2.16800200	1.38706100
H	0.47100500	-0.60030900	2.12357200
C	3.17198800	-1.63005700	-0.75703300
C	1.84227500	-1.35323200	-1.05418800

C	1.24072700	-0.18362700	-0.58188900
C	1.98267600	0.71836900	0.19491900
C	3.31820900	0.43890500	0.47450800
C	3.91245900	-0.73123900	0.00806100
H	-0.61050400	-0.54376700	-1.62998200
H	3.63135400	-2.53971700	-1.12641500
H	1.25937900	-2.04601700	-1.65342800
C	-0.19728200	0.05709600	-0.82198700
C	1.28651900	1.96630100	0.67001900
H	3.89556000	1.14459600	1.06366000
H	4.95203900	-0.93810500	0.23562500
C	0.31543600	2.43003000	-0.41615600
H	0.73739300	1.76487100	1.59565800
H	0.88835600	2.69216500	-1.30987200
N	-0.67449100	1.40905800	-0.80625300
H	-0.23183500	3.31946600	-0.10296400
H	2.01520100	2.75323400	0.87858300

References

- (1) Gaussian 16, Revision B.01, M. J. Frisch, G. W. Trucks, H. B. Schlegel, G. E. Scuseria, M. A. Robb, J. R. Cheeseman, G. Scalmani, V. Barone, G. A. Petersson, H. Nakatsuji, X. Li, M. Caricato, A. V. Marenich, J. Bloino, B. G. Janesko, R. Gomperts, B. Mennucci, H. P. Hratchian, J. V. Ortiz, A. F. Izmaylov, J. L. Sonnenberg, D. Williams-Young, F. Ding, F. Lipparini, F. Egidi, J. Goings, B. Peng, A. Petrone, T. Henderson, D. Ranasinghe, V. G. Zakrzewski, J. Gao, N. Rega, G. Zheng, W. Liang, M. Hada, M. Ehara, K. Toyota, R. Fukuda, J. Hasegawa, M. Ishida, T. Nakajima, Y. Honda, O. Kitao, H. Nakai, T. Vreven, K. Throssell, J. A. Montgomery, Jr., J. E. Peralta, F. Ogliaro, M. J. Bearpark, J. J. Heyd, E. N. Brothers, K. N. Kudin, V. N. Staroverov, T. A. Keith, R. Kobayashi, J. Normand, K. Raghavachari, A. P. Rendell, J. C. Burant, S. S. Iyengar, J. Tomasi, M. Cossi, J. M. Millam, M. Klene, C. Adamo, R. Cammi, J. W. Ochterski, R. L. Martin, K. Morokuma, O. Farkas, J. B. Foresman, and D. J. Fox, Gaussian, Inc., Wallingford CT, 2016.
- (2) Grimme, S., Antony, J., Ehrlich, S., Krieg, H. *J. Chem. Phys.* **2010**, *132*, 154104.
- (3) Grimme, S. *J. Comput. Chem.* **2006**, *27*, 1787.
- (4) Marenich, A. V., Cramer, C. J., Truhlar, D. G. *J. Phys. Chem. B*, **2009**, *113*, 6378.